THE CLEVELAND MUSEUM OF NATURAL HISTORY NUMBER 57

KIRTLANDIA®

NOVEMBER 2010

KIRTLANDIA

The Scientific Publication of The Cleveland Museum of Natural History

Joseph T. Hannibal, Editor

Proofreaders: Kathleen Farago, Douglas Dunn, and Wendy Wasman

Brief History and Purpose

Kirtlandia, a publication of The Cleveland Museum of Natural History, is named in honor of Jared Potter Kirtland, a noted nineteenth-century naturalist who lived in the Cleveland, Ohio area. It began publication in 1967 and is a continuation of the earlier series *Scientific Publications* volumes 1 to 10 (1928–1950), and new series volumes 1 to 4 (1962–1965).

Supported by the Kirtlandia Society of The Cleveland Museum of Natural History, *Kirtlandia* is devoted to the publication of scientific papers in the various fields of inquiry within the Museum's sphere of interest: Cultural and Physical Anthropology; Archaeology; Botany; Geology; Paleobotany; Invertebrate and Vertebrate Paleontology; Systematics; Ecology; and Invertebrate and Vertebrate Zoology. Issues will vary from single monographs to collections of short papers, review articles, and brief research notes.

Kirtlandia is abstracted in *Biological Abstracts* and indexed in *GeoRef* and *Zoological Record*. An index to *Kirtlandia* numbers 1–52 was published in *Kirtlandia* number 52 (2001).

Kirtlandia No. 57
ISSN 0075-6245

Cover: *Cladoselache* specimen, CMNH 5408, from the Cleveland Member. Specimen is about 62 cm long.

Copies of *Kirtlandia*, and many issues of the *Scientific Publications* series of
The Cleveland Museum of Natural History, are available for sale.
Write to: Library, The Cleveland Museum of Natural History, 1 Wade Oval Drive,
University Circle, Cleveland, Ohio 44106-1767 (library@cmnh.org) for a current price list.

KIRTLANDIA
The Cleveland Museum of Natural History

November 2010 *Number 57:1–2*

MICHAEL E. WILLIAMS (1940–2003)

Michael E. Williams, known to all of his colleagues as "Mike," was the curator of vertebrate paleontology at The Cleveland Museum of Natural History for 28 years. During that time he supervised the Museum's extensive collection of vertebrate fossils, including one of the world's largest and most important collections of Devonian sharks and placoderms. He also authored or co-authored a number of important scientific papers on fossil sharks, dinosaurs, and dinosaur extinction.

Mike was born in Ina, a little town in south-central Illinois, and spent his childhood in St. Louis. He attended the Missouri School of Mines and Metallurgy (now the Missouri University of Science and Technology) in Rolla, Missouri, and received a bachelor's degree in geology in 1963. While at Missouri, he exhibited a sense of adventure, being a member of the caving club for four years. There he mastered the art of rappelling under the guidance of the club advisor, a geologist who had been a mountain climber.

After graduation, Mike joined the Quartermaster Corps of the U.S. Army. His first assignment was in Crailsheim, in south-central Germany. Mike's posting in Germany led to a number of key events in his life. Here he acquired a life-long love of German culture. And because he lived off base in Crailsheim he was able to pursue his interests in fossil hunting and mountain climbing. With American and German friends, he practiced climbing techniques in the nearby Jura Mountains. The highpoint, both literally and figuratively, of Mike's climbing pursuits was the scaling of the Matterhorn in October of 1965. The climb was done with a colleague from the military and two local guides. They made the climb very late in the year (most climbs of the Matterhorn were—and are—made in the summer), when a considerable amount of snow had built up. Mike's unpublished manuscript, "A Matterhorn diary," recounts the details of this climb.

Mike met a young German woman, Ortrud Pappenscheller, in Crailsheim. After four years of service in Germany and Viet Nam, Mike left the army, and he and Ortrud married and moved to Lawrence, Kansas, so that Mike could do graduate work at the University of Kansas. The university was by that time world-famous as a center of paleontological research and training, primarily because of the prodigious output of paleontologist Raymond C. Moore. Mike and his spouse lived on the second floor of Moore's house in return for Ortrud's culinary skills (Moore especially loved steak and potatoes). Ortrud also helped with collecting.

While working on his master's degree, Mike had Standard Oil and Pratt fellowships as well as teaching assistantships. He also participated in summer field parties. Mike received his master's degree in the spring of 1972. His thesis was a study of spiral coprolites. This well written, excellently illustrated work was published in the *University of Kansas Paleontological Contributions* (Williams, 1972).

Mike joined The Cleveland Museum of Natural History in July of 1975. At the Museum he was known for his general intellect as well as his expertise in geology, dinosaurs, and fossil fish. He supervised a small department at the Museum, overseeing the collecting and, particularly, the preparation of fossil fish from the Cleveland Member of the Ohio Shale. He led field teams to local outcrops (as seen in the accompanying photograph), as well as to dinosaur localities in North Dakota. During Mike's tenure at the Museum, he supervised trimming of the Cleveland Member concretions that had been collected in the 1960s so that they took up a more manageable space. Mike also supervised the expansion of the fossil-preparation stations at the Museum to make additional space for the preparators and volunteers who put in countless hours in preparation time. He also instituted the department's casting program so that casts could be produced continually. Mike continued work on his dissertation while

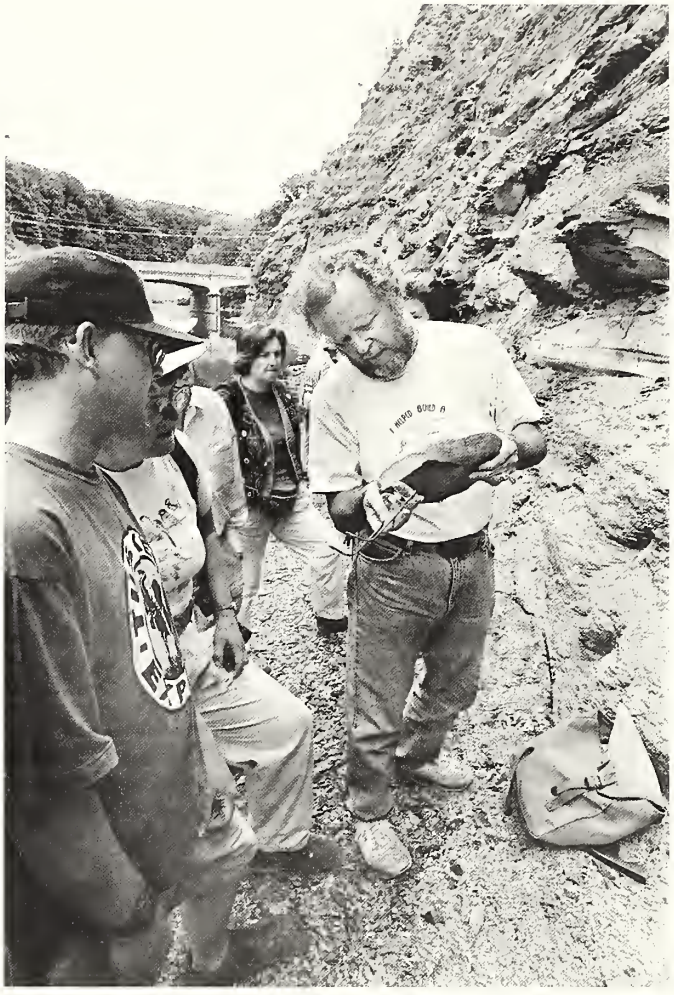

employed by the Museum, receiving his Ph.D. in Geology from the University of Kansas in 1979. His dissertation, "The 'cladodont level' sharks of the Pennsylvanian black shales of central North America," was later (Williams, 1985) published in *Palaeontographica.*

Mike was not prodigious in his publication output, but what he wrote was well reasoned, meticulously prepared, finely crafted, and beautifully illustrated. Mike had a very methodical mind and must have carefully thought out his ideas before putting pencil to paper, for he typically began writing a scientific paper, or even a nontechnical article, at the beginning and then carefully proceeded, point by point, to the end.

Mike, in collaboration with several well-known dinosaur workers, described two dinosaur taxa based on Cleveland Museum of Natural History specimens. One was the sauropod *Haplocauthosaurus delfsi* which John McIntosh and Mike described in this journal (McIntosh and Williams, 1988); the other was *Nanotyrannus*, described by Robert Bakker, Mike, and Philip Currie (Bakker, Williams, and Currie, 1988). It was Mike who coined the apt name *Nanotyrannus* for this small tyrannosaurid. The genus *Nanotyrannus* would become well known, in part because of the announcement of its identification as a new genus on the front page of the *New York Times*, and in part because of the subsequent controversy over its generic assignment (*Nanotyrannus* vs. *Tyrannosaurus*). Mike's most provocative technical article, however, was "Catastrophic versus noncatastrophic extinction of the dinosaurs: testing, falsifiability, and the burden of proof" (Williams, 1994), which he published in the *Journal of Paleoutology*. This article ran contrary to the dominant position on dinosaur extinction as Mike found key arguments for the instantaneous extinction of the dinosaurs to be flawed. Needless-to-say, Mike found that it was difficult to get his view published, but the fair-minded editors of the *Journal of Paleontology* not only accepted his paper but placed it as the lead article in the March, 1994, issue. The paper included cogent, well-reasoned arguments as well as a set of simple, yet elegant explanatory illustrations. The arguments given in this paper were taken seriously, and this paper became one of Mike's most cited works. Mike's work on this paper eventually led him to probe the basis for scientific reasoning, resulting in a thought-provoking paper (Williams, 1998b) on this topic published in the *Journal of Recreational Mathematics.*

But it is fossil fish, subjects of Mike's master's thesis and Ph.D. dissertation, in which Mike's true expertise lay. His papers on fish included "Feeding behavior in Cleveland Shale fishes" (Williams, 1990), a study which included a host of observations and inferences, notably a list of shark and placoderm specimens from the Cleveland Member that were associated with prey. This paper contains the best evidence for the food sources of the vertebrate predators of the Cleveland Member and is one of the best such studies of the prey of Devonian fish to date. Mike liked to refer to these fossil fish, with their identifiable stomach contents, as the first fossil collectors in the area. His paper on *Tamiobatis vetustus* (Williams, 1998a) described a well-preserved braincase from the Cleveland Member, and associated other material of this species. This paper included a review and analysis of a number of other fossil shark braincases. A 2001 paper by Mike reported on cladodont sharks retaining their teeth rather than shedding them as do modern sharks. In this paper he demonstrated his extensive knowledge of extant and extinct shark tooth mechanisms and mechanics. In the course of his career, Mike also co-authored papers on fossil fish with the well-known fossil fish workers Rainer Zangerl and Bobb Schaeffer.

Mike co-authored one technical paper on mammals, a posthumous work (Williams and Domning, 2004) describing Pleistocene or Holocene manatees in the Mississippi and Ohio river valleys, including the first marine mammal to be reported from the state of Ohio. Mike also wrote, upon occasion, for the Museum's nontechnical publications. The most important of these was an excellent article (Williams, 1992) on fossil shark jaws and teeth entitled "Jaws: the early years."

On a personal level, Mike was basically a quiet man. But once he realized that you were really interested in his favorite paleontological subjects he would open up and share his knowledge in great detail. He enjoyed gardening, beer, barbeque, chili, and wine, and had a large collection of movies, serials, and comic books. Mike also liked old-time music. He played bluegrass, country-folk, and old western music on the banjo which he built himself. He and his musically inclined colleagues would play at lunchtime in the paleontology preparation room at the Cleveland Museum. This group included his preparator, the Museum's chief financial officer, and an ever-changing array of other Museum staff and volunteers. This musical tradition has continued to this day.

J. Hannibal

References

Bakker, R. T., M. Williams, and P. Currie. 1988. *Nanotyrannus*, a new genus of pygmy Tyrannosaur, from the latest Cretaceous of Montana. Hunteria, 1(5):1–30.

McIntosh, J. S., and M. E. Williams. 1988. A new species of sauropod dinosaur, *Haplocauthosaurus delfsi* sp. nov., from the Upper Jurassic Morrison Fm. of Colorado. Kirtlandia, 43:3–26.

Williams, M. E. 1972. The origin of "spiral coprolites." University of Kansas Paleontological Contributions, 59:1–19.

Williams, M. E. 1985. The "cladodont level" sharks of the Pennsylvanian black shales of central North America. Palaeontographica. Abteilung A: Palaeozoologie-Stratigraphie, 190:83–158, plus 18 plates.

Williams, M. E. 1990. Feeding behavior in Cleveland Shale fishes, p. 273–287. *In* A. J. Boucot, Evolutionary Paleobiology of Behavior and Coevolution. Elsevier, Amsterdam.

Williams, M. E. 1992. Jaws: the early years. Explorer, 34(2):4–8.

Williams, M. E. 1994. Catastrophie versus non-catastrophic extinction of the dinosaurs: testing, falsifiability, and the burden of proof. Journal of Paleontology, 68:183–190.

Williams, M. E. 1998a. A new specimen *of Tamiobatis vetustus* (Chondrichthyes, Ctenacanthoidea) from the Late Devonian Cleveland Shale of Ohio. Journal of Vertebrate Paleontology, 18:251–260.

Williams, M. E. 1998b. Truth, science, and the liar's paradox. Journal of Recreational Mathematics, 29:205–208.

Williams, M. E. 2001. Tooth retention in cladodont sharks: with a comparison between primitive grasping and swallowing, and modern cutting and gouging feeding mechanisms. Journal of Vertebrate Paleontology, 21:214–226.

Williams, M. E., and D. P. Domning. 2004. Pleistocene or post-Pleistocene manatees in the Mississippi and Ohio River Valleys. Marine Mammal Science, 20:167–175.

KIRTLANDIA
The Cleveland Museum of Natural History

November 2010 *Number 57:3–12*

GEOCHEMISTRY OF THE CLEVELAND MEMBER OF THE OHIO SHALE, APPALACHIAN BASIN: INDICATORS OF DEPOSITIONAL ENVIRONMENT DURING SEDIMENT ACCUMULATION

SUSAN M. RIMMER
Department of Geology
Southern Illinois University Carbondale, 1259 Lincoln Drive, MC 4324, Carbondale, Illinois 62901
srimmer@geo.siu.edu

HAROLD D. ROWE
Department of Earth and Environmental Sciences, University of Texas at Arlington, Arlington, Texas 76019

SARAH J. HAWKINS
Pioneer Natural Resources, Denver, Colorado 80202

AND **HENRY FRANCIS**
Kentucky Geological Survey, University of Kentucky, Lexington, Kentucky 40506

ABSTRACT

Conditions that existed during accumulation of the Devonian Ohio Shale of the Appalachian Basin, and in particular the degree of anoxia, have been debated widely. In this study, two spatial transects that include the Cleveland Member of the Ohio Shale (Famennian, Upper Devonian) are investigated using geochemical proxies (C, S, and trace-elements) to elucidate paleo-depositional environments. One transect extends from the south-central section to the northeastern section of the Kentucky Devonian outcrop belt, and the other extends from central Kentucky northwards into central and northern Ohio. The transect approach defines spatial variability in the redox characteristics that existed across the Appalachian Basin during a unique episode in Earth history.

Results indicate that for these very organic-carbon rich shales (which contain up to 15% organic carbon), redox conditions likely varied both spatially and temporally. The upper Cleveland contains more organic carbon than does the lower Cleveland, and the overall carbon content decreases toward the northernmost part of our study area (northern Ohio). Associated with these variations in organic carbon are redox differences, in that conditions during accumulation of the lower part of the Cleveland Shale Member may have been slightly better oxygenated (dysoxic) compared with those that existed during accumulation of the upper parts of the unit (anoxic). This is demonstrated by vertical variations in DOP_T, V/Cr, and Ni/Co. Redox conditions also vary from core to core, suggesting local fluctuations may have been important; data for the northernmost (or most proximal) core suggest the least reducing conditions.

Mo contents are generally high in these cores (averaging between 80 and 125 ppm for various cores). Some cores demonstrate a decrease in Mo content in the upper part of the Cleveland Shale Member whereas others do not, suggesting local control on Mo content rather than a global or basin-wide drawdown of seawater Mo levels during accumulation of the upper Cleveland.

Introduction

Devonian organic-rich black shales of the Appalachian Basin have been studied extensively in terms of depositional environments, stratigraphy, and tectonics (for example, Ettensohn et al., 1979; Ettensohn and Barron, 1981; Ettensohn, 1985 a,b; Schieber, 1998; Murphy, Sageman, and Hollander, 2000; Murphy, Sageman, Hollander, Lyons, and Brett, 2000; Murphy, Sageman, Hollander, and Ver Straeten, 2000; Werne et al., 2002; Sageman et al., 2003; Rimmer, 2004; Rimmer et al., 2004). However, the reasons for extensive OM (organic material) accumulation and preservation in these sediments have been debated; in particular there have been different interpretations regarding bottom-water

conditions during sediment accumulation. Ettensohn (1998) proposed accumulation under conditions of sediment starvation and widespread water-column anoxia beneath a permanent pycnocline for high organic-carbon (> 10%) black shales which he considered to be transgressive shales, and which include the Late Devonian lower and upper Huron Member and the Cleveland Member of the Ohio Shale, along with the Early Mississippian Sunbury Shale. For lower organic-carbon (< 10%) shales, which he considered regressive black shales and which include the middle Huron Member of the Ohio Shale, the Three Lick Bed, and the Bedford Shale, Ettensohn (1998) suggested that organic matter accumulation was driven by productivity, possibly enhanced by the influx of terrestrially derived nutrients, but in the absence of widespread water-column anoxic conditions.

A detailed analysis of paleo-redox trace metal indicators by Rimmer (2004) suggested that, at least for Devonian shales in the outcrop belt of Kentucky, bottom-water conditions may have been quite variable. Whereas anoxic conditions may have prevailed during accumulation of some intervals in the upper part of the Cleveland Member, bottom-water conditions may have been intermittently anoxic and dysoxic during deposition of the lower Cleveland. During accumulation of the underlying Huron Member, it is likely that conditions ranged from anoxic to dysoxic to marginally oxic, possibly being close to normal marine conditions at times during accumulation of the lowermost Huron sediments.

Further north in the Appalachian Basin in New York, models have been proposed that invoke only seasonal water-column stratification during deposition of Middle Devonian black shales, such as the Oatka Creek Formation and the Geneseo Shale, and that emphasize the importance of nutrient cycling under variable bottom-water conditions that in turn enhances productivity in surface waters following periodic deep-water overturn (Murphy, Sageman, and Hollander, 2000; Murphy, Sageman, Hollander, Lyons, and Brett, 2000; Murphy, Sageman, Hollander, and Ver Straeten, 2000; Werne et al., 2002; Sageman et al., 2003). An analysis of several black shale units from the same core in New York demonstrated that very few of the black shale units were deposited under persistently anoxic or euxinic conditions, and that most accumulated under seasonally stratified water columns (Sageman et al., 2003).

As a major area of debate has been the extent to which these black-shale basins were anoxic or euxinic, and that their redox characteristics potentially varied depending on location within the basin, the purpose of this study is to evaluate redox indicators in the Cleveland Member of the Ohio Shale (Famennian, Upper Devonian) across two transects. One of these transverses the outcrop belt of east-central Kentucky, the other passes from central Kentucky into central and northern Ohio. The transect approach allows comparison of redox conditions in the distal areas of the basin (central Kentucky) with those in closer proximity to the Catskill Delta sediment source to the north (i.e., the central and northern Ohio cores).

Sampling and Methods

Stratigraphy

Within the Devonian outcrop belt of east-central Kentucky, the New Albany/Ohio Shale thins onto the Cincinnati Arch to around 40–45 m (130–150 ft) thick. In this area, U.S. Geological Survey 7.5-minute geologic quadrangle maps use both New Albany Shale (cores D-6, D-10, and T-16) and Ohio Shale (core KEP-5) terminology. From the outcrop belt, the Devonian shales increase in thickness toward southeastern Kentucky (up to ~ 455m, 1500 ft thick) as they dip down into the subsurface in the Appalachian Basin. Present-day burial depths for the shale increase toward the southeast, reaching ~ 730m (2400 ft) in southeastern Kentucky. Even greater thicknesses and burial depths are seen in West Virginia (Provo, 1977). From Kentucky, the outcrop belt continues northwards into Ohio where in central Ohio, the Ohio Shale averages 140 m (460 ft) thick and increases to over 400 m (1312 ft) thick in the northeastern part of the state (Hellstrom and Babcock, 2000).

In central Kentucky, the Ohio Shale/New Albany Shale consists of the Cleveland and the Huron members, separated by the Three Lick Bed (a number of interbedded siltstones and shales). In this area, the upper part of the Cleveland Member is typically a black (N1) or grayish-black (N2) laminated shale, with occasional olive black laminae (5Y 2/1), whereas the lower part of the Cleveland is typically olive black (5Y 2/1) to brownish gray (5YR 2/1) (Pollock et al., 1982). Within the unit, pyrite nodules occur as do phosphate nodules and cone-in-cone limestone. The unit, bounded by the Bedford Shale and the Three Lick Bed, increases in thickness across transect A–A′ (Figure 1), from approximately 7.6 m (25 ft) in the south (core T-16) to over 15 m (50 ft) in the north (KEP-5) (Figure 2). The Three Lick Bed is identifiable into central Ohio, but toward northern Ohio, the Cleveland Member is separated from the Huron Member by the Chagrin Shale Member, thought to be, in part, correlative with the Three Lick Bed observed to the south (Hellstrom and Babcock, 2000). In the northern part of Ohio, the Cleveland Member is a dark grey (N3 to N5) shale, typically microlaminated, and with occasional cone-in-cone limestone. In the area studied, the Cleveland is approximately 23 m (75 ft) thick. Stratigraphic correlation was based on driller's logs, input from state survey personnel, and comparison of gamma logs to those in the literature (for example, Hellstrom and Babcock, 2000).

Sampling

For the central Kentucky transect (A–A′), four cores were selected to represent a SW–NE transect along the eastern Devonian shale outcrop belt (Figure 1). These included the T-16 (Madison Co., KY), D-10 (Estill Co., KY), D-6 (Montgomery Co., KY), and KEP-5 (Fleming Co., KY) cores. For these and other cores in the outcrop belt, we have an extensive data base (UK Devonian Shale Database) that includes carbon, sulfur, major and minor elements, and trace-element data for Ohio Shale cores which were generated as part of an evaluation of oil-shale resources in Kentucky in the 1980s at the University of Kentucky's Center for Applied Energy Research (CAER), formerly the Kentucky Center for Energy Research Laboratory (KCERL). These data are being used to evaluate depositional conditions for the black shales in central Kentucky (Rimmer, 2004; Rimmer et al., 2004; Rimmer and Rowe, in preparation). For the four A–A′ transect cores, the data were collected on composite samples of the Cleveland Member representing ~ 0.6 m (2 ft) intervals for organic-carbon-rich intervals, or 1.5 m (5 ft) intervals for lean zones.

The second transect (B–B′) is defined by one core from central Kentucky (D-4, Bath Co.), one from central Ohio (OHRS-5, Ross Co.), and one from northern Ohio (OHLO-2, Lorain Co.) (Figure 1). For these cores, a different sampling approach was taken, whereby 10 cm (3–4 in) intervals were selected. For each

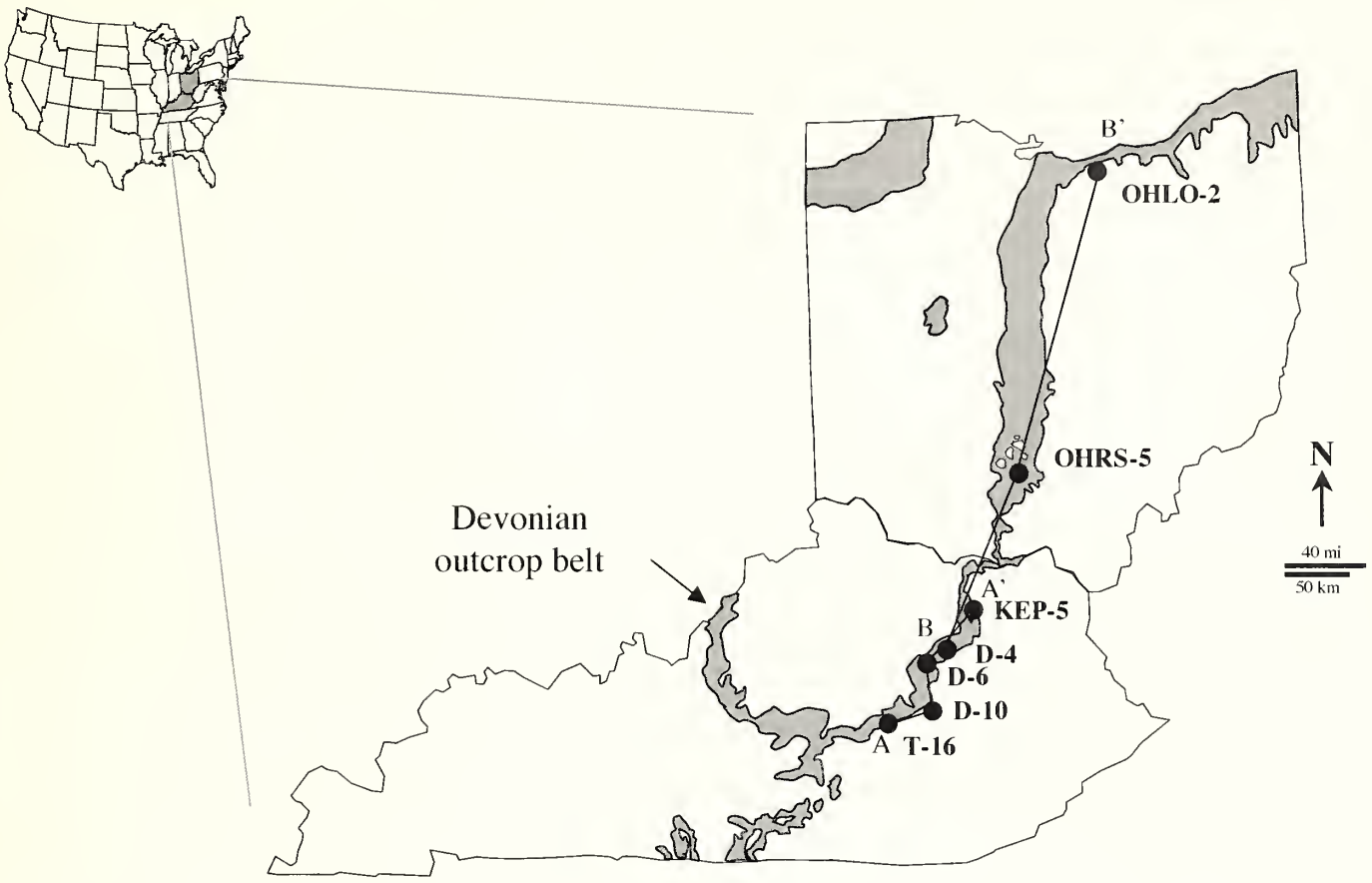

Figure 1. Map showing location of cores used in this study. Transect A–A′ is based on data for four cores (T-16, D-10, D-6, and KEP-5) from the UK Devonian Shale Database; transect B–B′ includes three cores (D-4, OHRS-5, and OHLO-2) sampled for the purpose of this investigation.

interval, an attempt was made to sample only homogeneous intervals, thus encapsulating more of the small-scale geochemical variability than could be assessed using the larger intervals for data used for transect A–A′.

Analytical methods

Results for cores from transect A–A′ were obtained from the UK Devonian Shale Database. Carbon and sulfur analyses were performed previously based on standard methods (Robl et al., 1983), using a Carlo-Erba Model 1106 elemental analyzer (for carbon) and a Fisher Model 470 sulfur analyzer. Coefficient of variation (100 × standard deviation/mean) for replicate analyses was 0.5% for carbon and 2% for sulfur (Robl et al., 1983). Trace elements were determined by x-ray fluorescence, using a Philips AXS automated spectrometer. For samples from transect B–B′, organic carbon was determined using a Costech 5010 elemental analyzer following multiple treatments with 50 μL H_2SO_3 to remove carbonate. Sulfur was determined using a Leco sulfur analyzer. Standard deviations for analyses were 0.05% and 0.01% for carbon and sulfur, respectively. Trace elements were determined by x-ray fluorescence using a Brucker S4 Pioneer, housed at the Kentucky Geological Survey.

For the purposes of calculating the degree of pyritization (DOP), S_T was assumed to approximate pyritic sulfur (S_{pyr}) as little organic sulfur is thought to be present. Analysis of kerogen concentrates has shown that S_{org} constitutes less than 2% of the organic matter (Taulbee et al., 1990). DOP is defined as pyritic iron/(pyritic iron plus HCl-soluble iron) (Berner, 1970). In this study, DOP_T was determined from pyritic iron/total iron (Raiswell and Berner, 1986), and pyritic iron was calculated from total sulfur, assuming all of the sulfur was in the form of pyrite.

Redox terms used here—oxic, dysoxic, and anoxic—refer to bottom-water oxygen levels (8.0 to 2.0, 2.0 to 0.2, and 0.0 ml O_2/l, respectively) (Tyson and Pearson, 1991). Euxinic environments are those in which free H_2S is present in the water column (Raiswell and Berner, 1985).

Results and Discussion

Carbon-sulfur-iron relationships

Along the Kentucky transect (A–A′), organic carbon contents of the Cleveland Member range from approximately 5% in the lower part of the unit to 12–15% in the upper Cleveland with very similar patterns exhibited in all four cores (Figure 2). These unusually high organic carbon contents suggest that conditions during sediment accumulation were not those encountered under normal marine conditions. The relationship between carbon and sulfur may provide clues as to whether conditions at the time of sediment accumulation were normal marine or euxinic. For

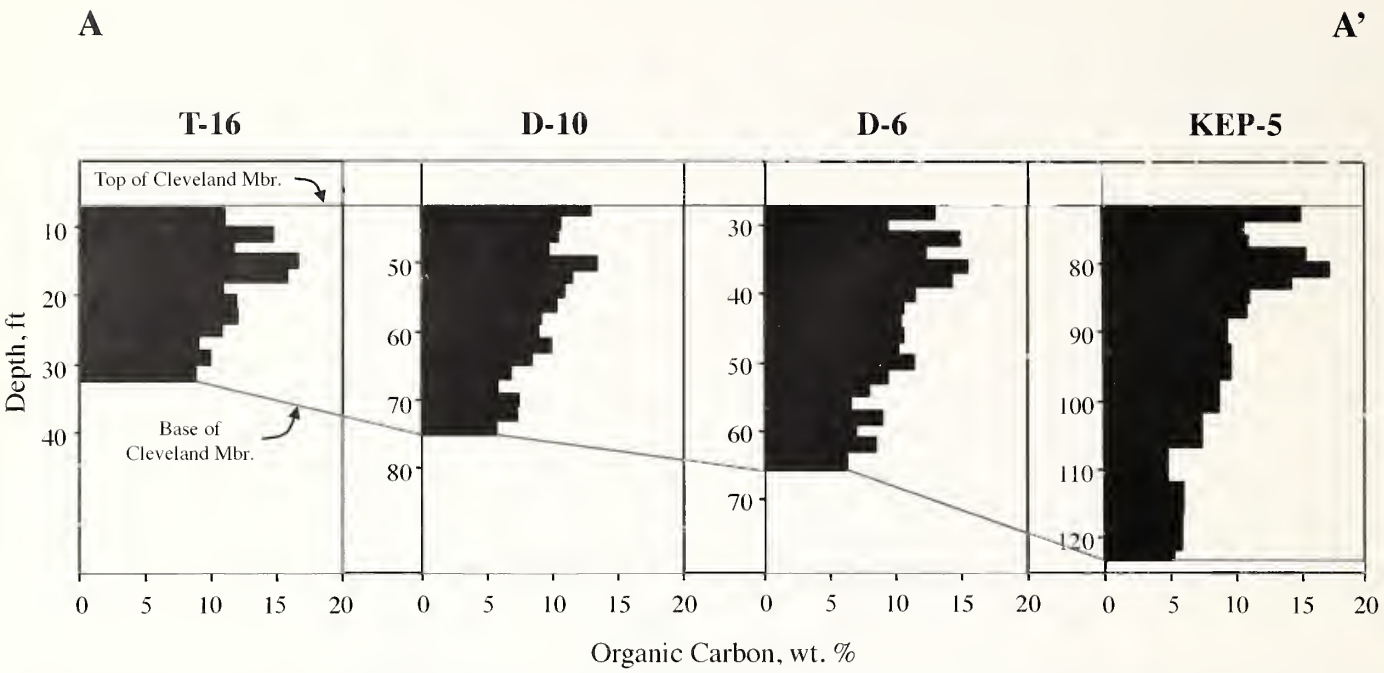

Figure 2. Variation in thickness and organic carbon content (wt. %) of the Cleveland Member of the Ohio Shale across transect A–A′ in central Kentucky.

sediments that accumulated under oxygenated conditions (normal marine), a crossplot for organic carbon and pyritic sulfur should show a strong positive correlation with the trend line through the data having a zero intercept (Berner and Raiswell, 1983). This is because pyrite formation in normal marine sediments is controlled by OM availability. In contrast, in euxinic environments, pyrite formation is primarily controlled by iron availability and a plot of C_{org} versus S_{pyr} shows a non-zero sulfur intercept (thus higher S_{pyr} contents are associated with low C_{org} contents) and may or may not show any correlation between the two variables (Berner and Raiswell, 1983). Interpretations based on C-S plots could be compromised if there has been a significant loss of carbon accompanying thermal maturity (as discussed by Raiswell and Berner, 1987). However, the black shales in this part of the Appalachian Basin are relatively immature ($R_o \sim 0.5\%$) (Rimmer et al., 1993; Curtis and Faure, 1997), and therefore C-S plots may be used to evaluate original depositional environment.

For the four cores along transect A–A′, a C-S crossplot shows no correlation between the two variables (Figure 3), suggesting that conditions during sediment accumulation were not normal marine, and possibly anoxic. Further evidence for non-normal marine conditions is provided by the DOP_T values determined for these samples. Degree of pyritization (DOP_T) reflects redox conditions during sediment accumulation: DOP values less than 0.42 indicate oxic (normal marine) conditions, and values in excess of 0.75 indicate conditions with no oxygen present (anoxic) and possibly H_2S present (euxinic) (Raiswell et al., 1988) (Figure 4). Values between 0.42 and 0.75 indicate dysoxic conditions although there may be some overlap for values associated with dysoxic and anoxic environments. Raiswell et al. (1988) originally referred to conditions associated with DOP values > 0.75 as inhospitable, and those associated with values between 0.42 and 0.75 as restricted. Hatch and Leventhal (1992) suggested that values between 0.67 and 0.75 represent a less strongly stratified water column, whereas values greater than 0.75 represent a strongly stratified, anoxic water column.

DOP_T values for the four cores along transect A–A′ suggest a fairly wide range of conditions, from dysoxic to anoxic, but with the majority of the values falling into the dysoxic range (Figure 5). Very few values are consistent with anoxic conditions using the Raiswell et al. (1988) threshold of 0.75; however, if the Hatch and Leventhal's (1992) threshold of 0.67 is used, several

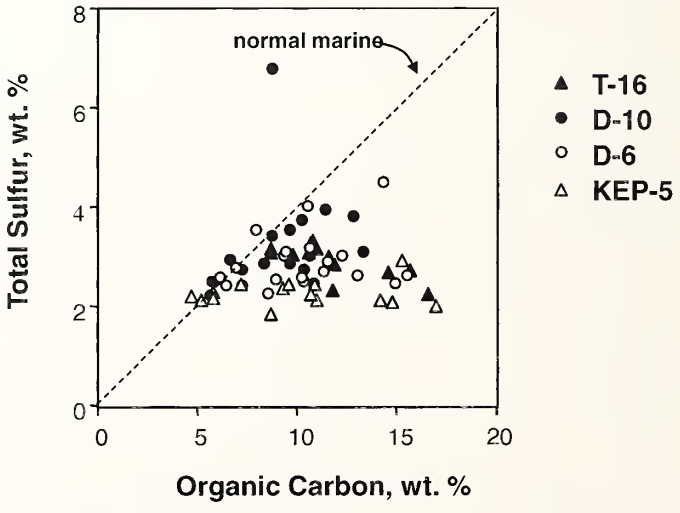

Figure 3. Carbon-sulfur relationships for the Cleveland Member in transect A–A′. The dashed line shows the typical S-C relationship for normal marine sediments (based on Berner and Raiswell, 1983).

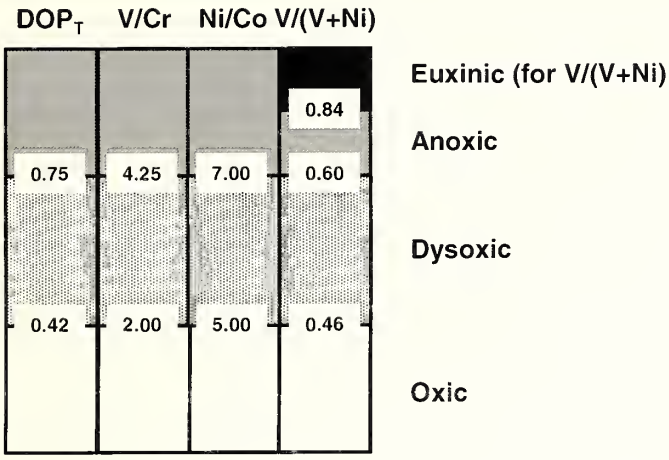

Figure 4. Correlation of redox proxies used in this study (modified from Jones and Manning (1994); based on thresholds reported in Raiswell et al. (1988), Hatch and Leventhal (1992), and Jones and Manning (1994).

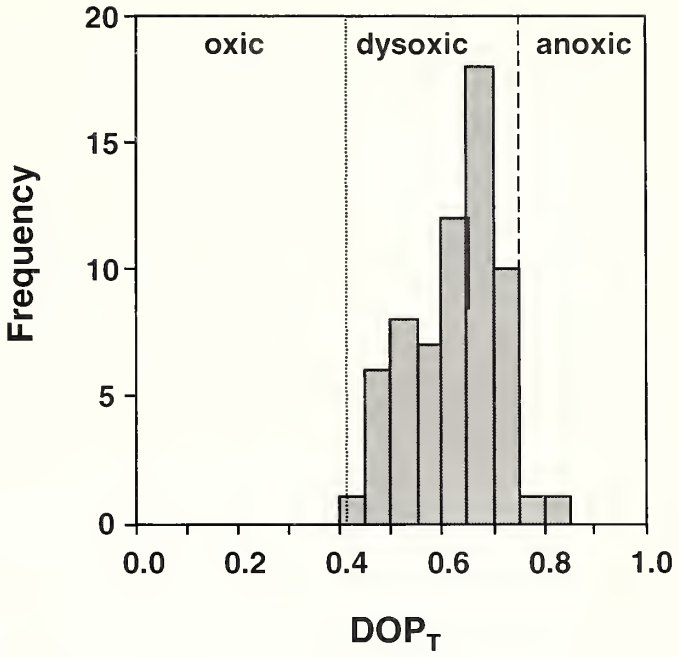

Figure 5. Histogram showing the distribution of DOP_T values determined for cores in transect A–A′.

intervals have values that are high enough to indicate anoxic conditions. Analysis of results for individual cores suggests that evidence exists for lateral variability in DOP_T: for example, DOP_T values determined for core T-16 are higher than those observed in core KEP-5 (Figure 6). In both cores, somewhat lower values are observed in the bottom part of the Cleveland Member.

Thus, it appears that C-S-Fe relationships for cores along transect A–A′ indicate somewhat variable conditions during deposition of the Cleveland Member. C-S plots suggest that conditions were not normal marine, and may even have been anoxic to euxinic. However, the degree of pyritization suggests dysoxic conditions may have been prevalent, with possibly more anoxic conditions emerging during deposition of some intervals in the upper part of the Cleveland. This is consistent with observations made by Rimmer (2004) and Rimmer et al. (2004) who analyzed results for several cores from the outcrop belt, and those of Robl and Barron (1987) who evaluated C-S relationships for the Cleveland.

Moving north from central Kentucky into central Ohio along transect B–B′, organic carbon contents appear to be relatively consistent, ranging from approximately 5% to over 15% in cores D-4 and OHRS-5, and also showing higher organic carbon levels in the upper part of the unit (Figure 7). However, in core OHLO-2 at the northernmost part of our transect, carbon contents throughout the unit are generally lower, ranging from less than 5% up to 10% (Figure 7). The C-S crossplot for transect B–B′ shows no relationship between the variables, again suggesting that conditions were not normal marine. DOP_T values for the D4 core are similar to those determined for the other cores from Kentucky, with most of the values plotting in the dysoxic field and a few in the anoxic field (Figure 7). DOP_T values for OHRS-5 and OHLO-2 are also mostly dysoxic, but generally lower than those for D-4; several values for these two cores plot in the oxic field. Thus, it appears that based on C-S-Fe relationships, there are differences in redox conditions moving along transect B–B′ towards the north: conditions appear to become slightly more oxygenated in northern Ohio than they are in central Kentucky.

Trace-metal enrichment factors and ratios

Trace-metal concentrations and ratios can also be used to evaluate depositional environments (for example, Breit and Wanty, 1991; Hatch and Leventhal, 1992; Jones and Manning, 1994; Tribovillard et al., 1994). In this study, we focus on a few indices that have been used previously to elucidate depositional environment of organic-rich shales, specifically Mo, V/(V+Ni), V/Cr, and Ni/Co. Thresholds for several of these have been suggested as a means of differentiating between oxic, dysoxic, and anoxic conditions (Hatch and Leventhal, 1992; Jones and Manning, 1994) (Figure 4) and have been applied previously to the Devonian shales of Kentucky (Rimmer, 2004; Rimmer et al., 2004).

Trace metals in general are enriched in these shales. The enrichment factor (EF) for an element is equal to (Element/Al)/(Element/Al)$_{shale}$, where the ratio in the numerator is that for the shale in question, and the ratio in the denominator is that for a "typical" shale (based on averages reported by Wedepohl, 1971). In these shales we see a significant level of enrichment in some trace metals (Table 1), in particular Mo. Overall, enrichment levels relative to an average shale are similar in the two transects: Mo > V > Zn > Cu > Ni > Cr > Co, although in transect B–B′, Cu and Ni are in reversed order in terms of enrichment. Some of the differences observed in the enrichment factors for transects A–A′ and B–B′ may be due to the different sampling approach used for these two transects, thus we limit our comparisons to within each transect. High Mo contents are associated typically with anoxic and euxinic conditions (Dean et al., 1977; Crusius et al., 1996), although some workers have suggested Mo contents as high as 150 ppm may be associated with dysoxic environments (Schultz and Coveney, 1992). Mo data indicate a decrease along transect B–B′ suggesting changing conditions toward the north; conditions were at least dysoxic and possibly anoxic (based on Mo levels that average 80 to 100 ppm), but a slight decrease in OHLO-2 suggests less reducing conditions for this most northerly core. At individual

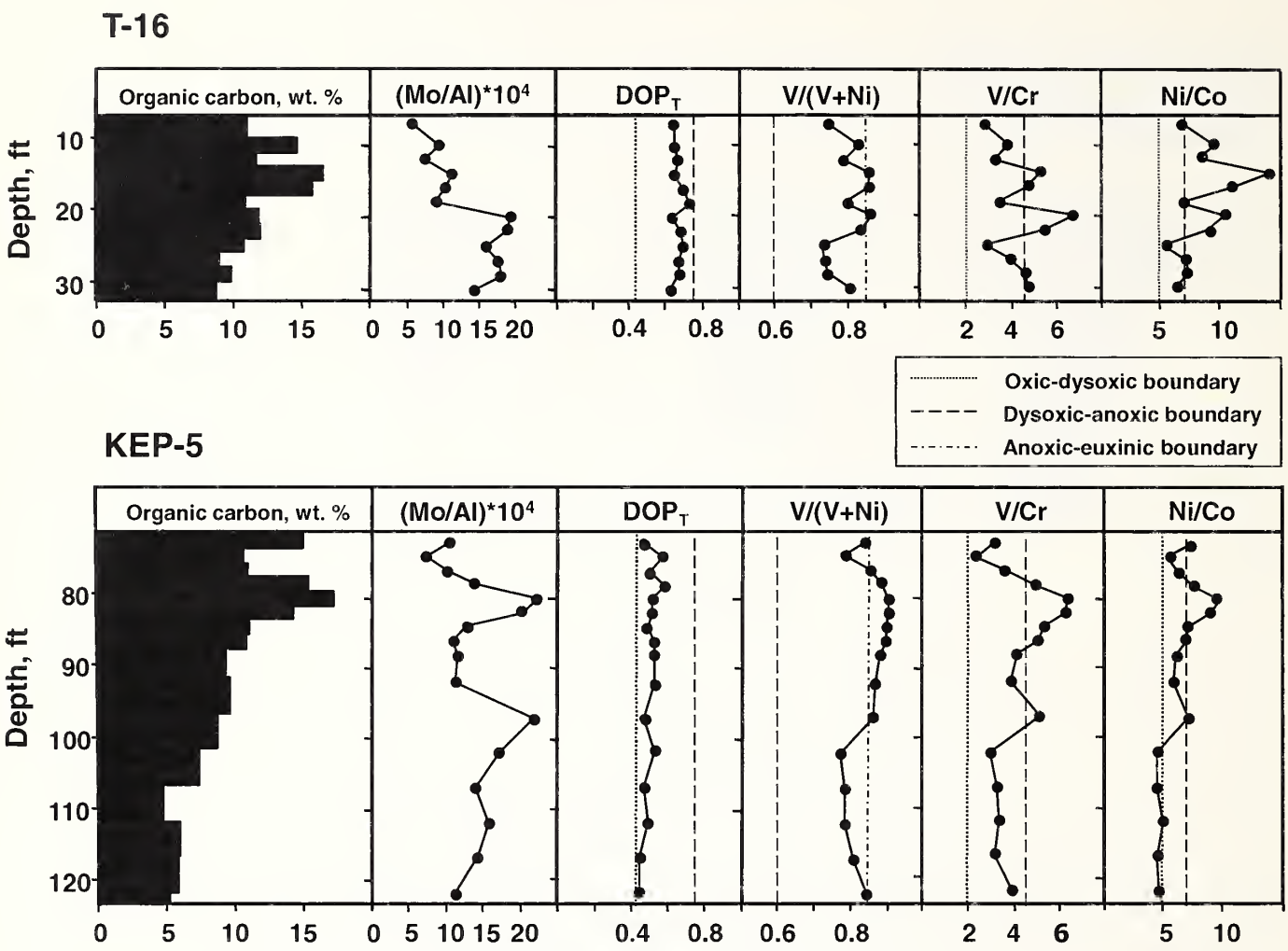

Figure 6. Stratigraphic variations in organic carbon (wt. %) and redox proxies for two cores (T-16 and KEP-5) in transect A–A′. Redox thresholds based on values in Figure 4.

loeations, there are some apparent vertical changes in Mo content: results for cores D-4 and T-16 show a decrease in Mo in the upper Cleveland. However, this does not appear to be a trend seen throughout the basin: no decrease is observed in KEP-5, OHRS-5, or OHLO-2 and in fact some of the highest Mo levels are observed in the upper part of both KEP-5 and OHRS-5.

Based on thresholds shown in Figure 4, V/Cr and Ni/Co ratios suggest oxic to dysoxic conditions for the lower part of the Cleveland Member for cores T-16 and KEP-5 (transect A–A′), with dysoxic to anoxic conditions for the upper Cleveland. V/(V+Ni) ratios suggest anoxic conditions for the base and euxinic conditions for the upper part of the section. The discrepancy in redox conditions indicated by these trace-element proxies is consistent with observations by Rimmer (2004) who cautioned against strict use of redox thresholds developed in previous studies and suggested that these ratios should be used in a relative sense. At the very least, using a cautious approach, it is reasonable to suggest that there were differences in redox conditions at the time of sediment accumulation between the lower and upper parts of the Cleveland Member.

For transect B–B′, similar values are seen for D-4 and OHRS-5, with differences apparent between the upper and lower parts of the unit: V/Cr and Ni/Co indicate primarily dysoxic conditions in the lower Cleveland Member, but anoxic conditions in the top of the unit, although the results for OHRS-5 indicate only a slight increase in Ni/Co values in the top of the section. As in the case of the A–A′ transect, V/(V+Ni) values indicate more reducing conditions than do V/Cr and Ni/Co. In this transect, trace elements ratios for core OHLO-2 suggest less reducing conditions overall, although they follow similar trends to the two more southerly cores: V/Cr suggests dysoxic (bottom) to anoxic (top) conditions, but most Ni/Co values straddle the range for dysoxic conditions with even a few intervals that fall in the oxic range. V/(V+Ni) are in the anoxic range, but rarely are high enough to be indicative of euxinic conditions.

Redox conditions during accumulation of the Cleveland Member

A much-debated issue surrounding Devonian black shales of the Appalachian Basin is the extent to which a stratified water column persisted leading to anoxic to euxinic bottom waters. The very high organic carbon contents observed in these shales (as high as 15% in some intervals) suggest non-normal marine conditions. The organic matter in these shales is typically Type II, predominated by bituminite (altered algal and bacterial matter)

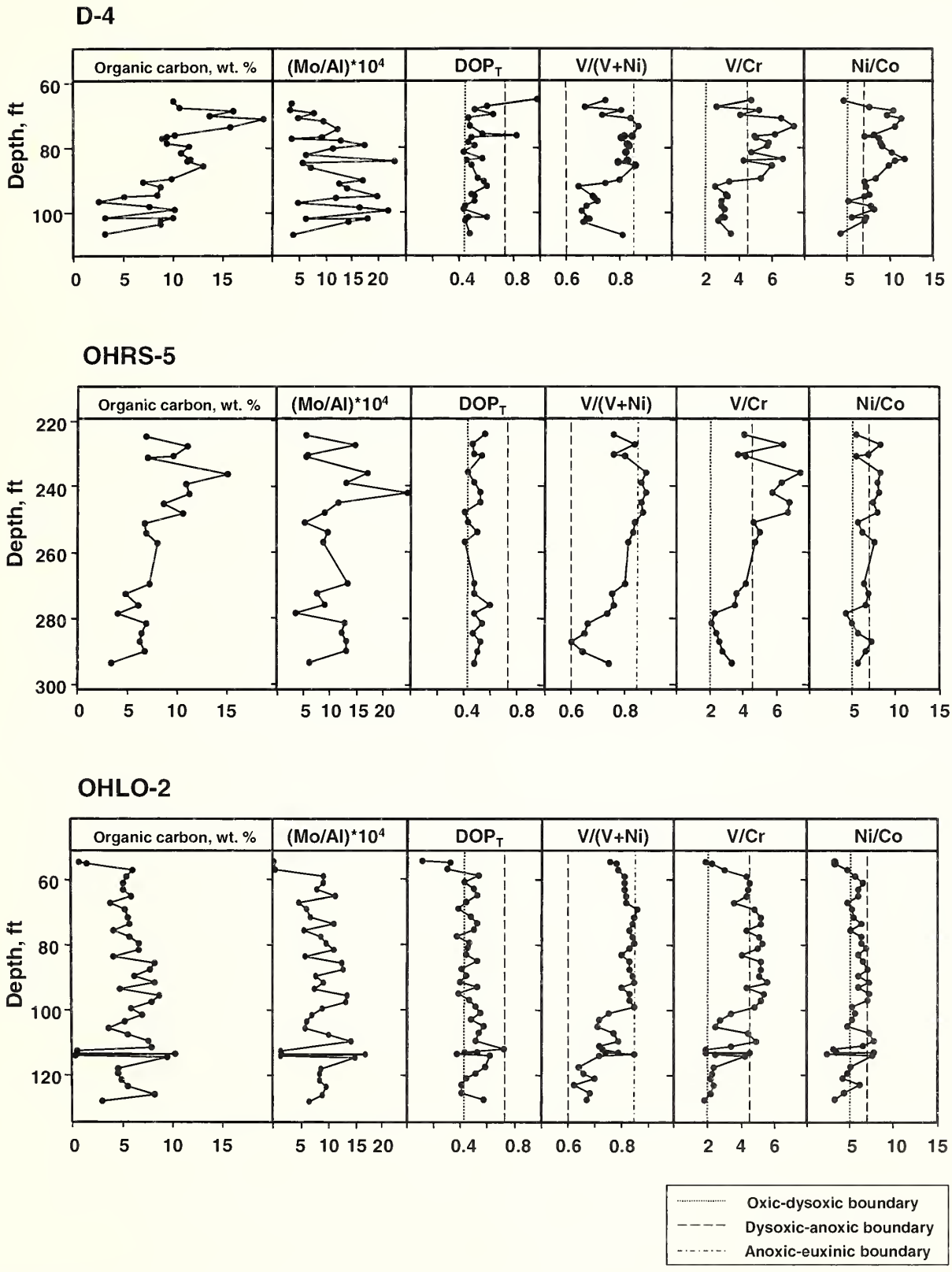

Figure 7. Stratigraphic variations in organic carbon (wt. %) and redox proxies for the three cores in transect B–B′ (D-4, OHRS-5, and OHLO-2). Redox thresholds based on values in Figure 4.

Table 1. Enrichment factors (EF) for selected trace elements for samples from cores through the Cleveland Shale Member along transects A–A′ and B–B′.

			Transect A–A′					Transect B–B′	
Element	Average* Shale	Average** Black Shale	T-16 (n = 12)	D-10 (n = 17)	D-6 (n =19)	KEP-5 (n = 16)	D-4 (n = 28)	OHRS-5 (n = 21)	OHLO-2 (n = 40)
Co (ppm)	19	10	20	20	19	22	17	18	18
(Co/Al) *10^4	2.1	1.4	2.6	2.5	2.4	2.5	2.2	1.8	2.0
EF		0.7	1.2	1.2	1.1	1.2	1.1	0.9	0.9
Cr (ppm)	90	100	164	160	167	198	104	107	97
(Cr/Al) *10^4	10.2	14.3	21.6	19.8	20.6	22.5	13.7	11.1	11.0
EF		1.4	2.1	1.9	2.0	2.2	1.0	1.1	1.1
Cu (ppm)	45	70	124	104	103	99	79	60	46
(Cu/Al) *10^4	5.1	10.0	16.4	12.9	12.7	11.3	10.4	6.2	5.2
EF		2.0	3.2	2.5	2.5	2.2	2.0	1.2	1.0
Mo (ppm)	2.6	10	101	100	114	125	82	87	71
(Mo/Al) *10^4	0.3	1.4	13.3	12.4	14.1	14.2	10.9	9.0	8.0
EF		4.9	44.5	41.3	46.9	47.3	36.2	29.9	26.7
Ni (ppm)	68	50	162	132	138	138	134	116	99
(Ni/Al) *10^4	7.7	7.1	21.4	16.3	16.9	15.7	17.7	12.1	11.2
EF		0.9	2.8	2.1	2.2	2.0	2.3	1.6	1.4
V (ppm)	130	150	713	654	740	883	483	506	391
(V/Al) *10^4	14.7	21.4	94.2	80.7	91.2	100.5	63.7	52.5	44.2
EF		1.5	6.4	5.5	6.2	6.8	4.3	3.6	3.0
Zn (ppm)	95	300	527	369	478	503	294	278	368
(Zn/Al) *10^4	10.7	42.9	69.6	45.5	58.9	57.2	38.7	28.9	41.6
EF		4.0	6.5	4.3	5.5	5.3	3.6	2.7	3.9

* Average shale data from Wedepohl (1971); ** Average black shale data from Vine and Tourtelot (1970).

with lesser amounts of alginite (preserved algal matter), vitrinite (preserved woody tissue from terrestrial sources), and inertinite (oxidized organic matter of both marine and terrestrial origin) (Rimmer et al., 1993; 2004). Within the Devonian shales, the amount and type of organic matter varies stratigraphically and geographically. For example, increased amounts of terrestrial organic matter are observed in the Cleveland Member as compared to the Huron Member which is lower in the section (Rimmer et al., 2004) and there is also thought to be an increase in terrestrial organic matter toward the north (approaching the deltaic source) as suggested by carbon isotopic data (Maynard, 1981).

For such large amounts of organic matter to accumulate, either productivity had to be very high, or preservation had to occur under optimal conditions (i.e., low oxygen conditions), or both. Based on the C-S-Fe relationships observed in these two transects, it is likely that conditions during accumulation of the Cleveland Member of the Ohio Shale were at least dysoxic and probably anoxic to some degree. The lack of a correlation between carbon and sulfur observed for data from all seven cores (Figures 3 and 8) indicates that conditions were not normal marine, and were possibly anoxic; degree-of-pyritization data for these cores plots mostly in the dysoxic range (Figures 5–7). The trace element data also point to at least dysoxic and possibly anoxic conditions. The data also suggest slightly more reducing conditions in the upper part of the unit than in the lower part, and slightly more oxidizing conditions to the north (OHLO-2).

These observations are consistent with those made previously by Rimmer et al. (2004) who suggested that conditions during accumulation of the Cleveland Member were initially dysoxic to anoxic, but became predominantly anoxic during accumulation of the upper part of the unit. Additional data in that study suggested that productivity was also high, driven by land-derived nutrients and by phosphorous that was regenerated due to a productivity-anoxia feedback mechanism (a decoupling of organic carbon and phosphorus under anoxic conditions).

There are indications from this study that conditions were fairly constant (dysoxic for the lower Cleveland, anoxic for the upper Cleveland) in the more distal parts of the basin (i.e., central Kentucky and southern Ohio), but that conditions may have become less extreme towards the north, approaching more proximal facies. In particular, results for core OHLO-2 suggest less reducing conditions, with dysoxic conditions being more prevalent. As these are preliminary data, our future work will focus on additional cores in the northern outcrop belt of Ohio to determine the extent to which trends seen in OHLO-2 are typical.

Another area of interest is the relatively high Mo content of these shales. Recent work by Algeo (2004) using our data for the D-4 core from the UK Devonian Shale Database called upon a drawdown of dissolved Mo in Late Devonian seawater (at the time of accumulation of the upper part of the Cleveland Member) to explain the depletion in Mo at the top of the D-4 core. Further analysis of our core data (for example, KEP-5) and the new data we have collected (for example, OHRS-5) suggest that this trend is not widespread across the entire basin. Thus, whatever the cause of the lower Mo levels seen in the upper Cleveland in some of the cores in the UK Devonian Shale Database, also commented on by Rimmer (2004), it may not be a global or even a basin-wide phenomenon but a situation arising from local conditions.

Conclusions

Geochemical proxies allow us to infer conditions that existed during accumulation of the Cleveland Member. Based on the data

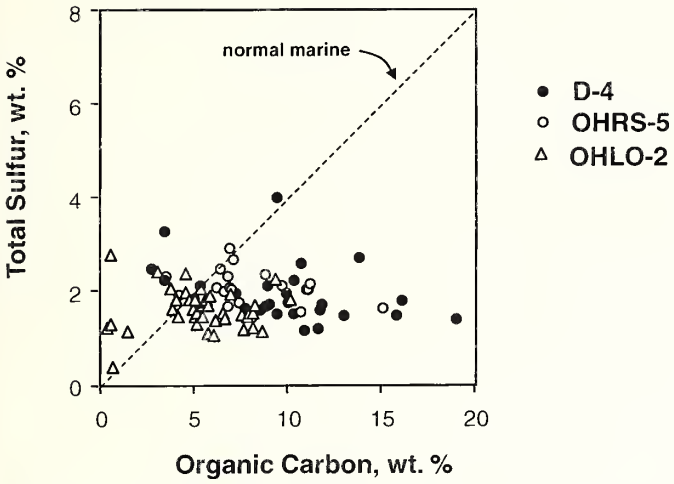

Figure 8. Carbon-sulfur relationships for the Cleveland Member in transect B–B′. The dashed line shows the typical S-C relationship for normal marine sediments (based on Berner and Raiswell, 1983).

from seven cores across the Devonian outcrop belt of the Appalachian Basin, we present the following salient conclusions:

1. Our results indicate stratigraphic and geographic variations in organic carbon content. Within the outcrop belt of Kentucky, the lower Cleveland contains less than 10% organic carbon, with the lower part of the KEP-5 core containing approximately 5%. The upper Cleveland is richer, containing 10 to 15% organic carbon. Moving north into Ohio, organic carbon contents decrease to 10% or less, with no discernable stratigraphic trends in OHLO-2.
2. Conditions during accumulation of the lower part of the Cleveland may have been slightly better oxygenated (dysoxic) compared with the upper parts of the unit (anoxic). This is demonstrated by vertical variations in DOP_T, V/Cr, and Ni/Co. V/(V+Ni) ratios indicate more reducing conditions for all cores, but are not necessarily consistent with the other redox indicators.
3. Redox conditions also vary from core to core, suggesting local fluctuations may have been important. Overall, more prevalent anoxie conditions are indicated for the T-16 core than for the KEP-5 core; results for the OHLO-2 core suggest that there were more prevalent periods of dysoxic or, at times, even oxic conditions.
4. Mo contents, while generally high, are not inconsistent with levels previously ascribed to dysoxic conditions. A decrease in Mo content is seen in the upper part of the Cleveland Member in some cores but not others, suggesting local control on Mo content rather than a global or a basin-wide drawdown of seawater Mo levels during accumulation of the upper Cleveland.

Acknowledgments

This material is based, in part, on work supported by the National Science Foundation under grant no. 0310072. We thank Tom Robl of the University of Kentucky's Center for Applied Energy Research for allowing unlimited use of the Devonian shale geochemical database in our research. We also thank the Kentucky Geological Survey (Well Sample and Core Library) and the Ohio Geological Survey (Ohio Geological Sample Repository) for access to cores; we especially thank Patrick Gooding (KGS) and Gregory Schumaker (OGS) for allowing us to borrow cores for study and sampling. Thanks also go to Ron Riley of the Ohio Geological Survey for his assistance with the stratigraphy of core OHLO-2, and the many members of the Ohio Geological Survey who helped with our requests for core logs and well records. In addition, we thank Rachael Von Mann and Shannon Daugherty for their assistance with sampling and processing. This paper was reviewed by P. O. Banks and an anonymous reviewer.

References

Algeo, T. J. 2004. Can marine anoxic events draw down the trace element inventory of seawater? Geology, 32:1057–1060.

Berner, R. A. 1970. Sedimentary pyrite formation. American Journal of Science, 268:1–23.

Berner, R. A., and R. Raiswell. 1983. Burial of organic carbon and pyrite sulphur in sediments over Phanerozoic time: a new theory. Geochimica et Cosmochimica Acta, 47:855–862.

Breit, G. N., and R. B. Wanty. 1991. Vanadium accumulation in carbonaceous rocks: a review of geochemical controls during deposition and diagenesis. Chemical Geology, 91:83–97.

Crusius, J., S. Calvert, T. Pedersen, and D. Sage. 1996. Rhenium and molybdenum enrichments in sediments as indicators of oxic, suboxic and sulfidic conditions of deposition. Earth and Planetary Science Letters, 145:65–78.

Curtis, J. B., and G. Faure. 1997. Accumulation of organic matter in the Rome Trough of the Appalachian Basin and its subsequent thermal history. American Association of Petroleum Geologists Bulletin, 81:424–437.

Dean, W. E., J. V. Gardner, and D. Z. Piper. 1997. Inorganic geochemical indicators of glacial-interglacial changes in productivity and anoxia on the California continental margin. Geochimica et Cosmochimica Acta, 61:4507–4518.

Ettensohn, F. R. 1985a. The Catskill delta complex and the Acadian orogeny: a model, p. 39–49. *In* D. L. Woodrow and W. D. Sevon (eds.), The Catskill Delta. Geological Society of America Special Paper 201.

Ettensohn, F. R. 1985b. Controls on development of Catskill delta complex basin-facies, p. 65–77. *In* D. L. Woodrow and W. D. Sevon (eds.), The Catskill Delta. Geological Society of America Special Paper 201.

Ettensohn, F. R. 1998. Compressional tectonic controls on epicontinental black-shale deposition: Devonian-Mississippian examples from North America, p. 109–128. *In* J. Schieber, W. Zimmerle, and P. Sethi (eds.), Shales and Mudstones. I. E. Schweizerbart'sche Verlagsbuchhadlung (Nagele u. Obermiller), D-70176, Stuttgart.

Ettensohn, F. R., and L. S. Barron. 1981. Depositional model for the Devonian-Mississippian black shales of North America: a paleoclimatic-paleogeographic approach, p. 344–361. *In* T. C. Roberts (ed.), Geological Society of America Cincinnati '81 Field Trip Guidebooks, Volume II: Economic Geology, Structure. American Geological Institute.

Ettensohn, F. R., L. P. Fulton, and R. C. Kepferle. 1979. Use of scintillometer and gamma-ray logs for correlation and stratigraphy in homogeneous black shales. Geological Society America Bulletin, 90:421–423, 828–849.

Hatch, J. R., and J. S. Leventhal. 1992. Relationship between inferred redox potential of the depositional environment and geochemistry of the Upper Pennsylvanian (Missourian) Stark Shale Member of the Dennis Limestone, Wabaunsee County, Kansas, U.S.A. Chemical Geology, 99:65–82.

Hellstrom, L. W., and L. E. Babcock. 2000. High-resolution stratigraphy of the Ohio Shale (Upper Devonian), central Ohio. Northeastern Geology and Environmental Sciences, 22(3):202–226.

Jones, B., and D. A. C. Manning. 1994. Comparison of geochemical indices used for the interpretation of palaeoredox conditions in ancient mudstones. Chemical Geology, 111: 111–129.

Maynard, J. B. 1981. Carbon isotopes as indicators of dispersal patterns in Devonian-Mississippian shales of the Appalachian Basin. Geology, 9:262–265.

Murphy, A. E., B. B. Sageman, and D. J. Hollander. 2000. Eutrophication by decoupling of the marine biogeochemical cycles of C, N, and P: a mechanism for the Late Devonian mass extinction. Geology, 28(5):427–430.

Murphy, A. E., B. B. Sageman, D. J. Hollander, T. W. Lyons, and C. E. Brett. 2000. Black shale deposition and faunal overturn in the Devonian Appalachian Basin: clastic starvation, seasonal water-column mixing, and efficient biolimiting nutrient recycling. Paleoceanography, 15(3):280–291.

Murphy, A. E., B. B. Sageman, D. J. Hollander, and C. A. Ver Straeten. 2000. Organic carbon burial and faunal dynamics in the Appalachian Basin during the Devonian (Givetian-Famennian) greenhouse: an integrated paleoecological/biochemical approach, p. 351–385. *In* B. Huber, K. MacLeod, and S. Wing (eds.), Warm Climates of Earth History. Cambridge University Press, Cambridge, England.

Pollock, D., L. Barron, and J. Beard. 1982. Stratigraphy and resource assessment of the oil shales of east central Kentucky. Proceedings of the Eastern Oil Shale Symposium, IMMR-University of Kentucky, Lexington, Kentucky. p. 195–212.

Provo, L. J. 1977. Stratigraphy and sedimentology of radioactive Devonian-Mississippian shales of the Central Appalachian Basin. Unpublished Ph.D. dissertation, University of Cincinnati. 177 p.

Raiswell, R., and R. A. Berner. 1985. Pyrite formation in euxinic and semi-euxinic sediments. American Journal of Science, 285:710–724.

Raiswell, R., and R. A. Berner. 1986. Pyrite and organic matter in Phanerozoic normal marine shales. Geochimica et Cosmochimica Acta, 50:1967–1976.

Raiswell, R., and R. A. Berner. 1987. Organic carbon losses during burial and thermal maturation of normal marine shales. Geology, 15:853–856.

Raiswell, R., F. Buckley, R. A. Berber, and T. F. Anderson. 1988. Degree of pyritization of iron as a paleoenvironmental indicator of bottom-water oxygenation. Journal of Sedimentary Petrology, 58:812–819.

Rimmer, S. M. 2004. Geochemical paleoredox indicators in Devonian-Mississippian black shales, central Appalachian Basin (U.S.A.). Chemical Geology, 206:373–391.

Rimmer, S. M., D. J. Cantrell, and P. J. Gooding. 1993. Rock-eval pyrolysis and vitrinite reflectance trends in the Cleveland Shale Member of the Ohio Shale, eastern Kentucky. Organic Geochemistry, 20:735–745.

Rimmer, S. M., and H. D. Rowe. In preparation. Comparative analysis of redox conditions assoeiated with black shale accumulation in the Appalachian and Illinois basins during the Late Devonian.

Rimmer, S. M., J. A. Thompson, S. A. Goodnight, and T. Robl. 2004. Multiple controls on the preservation of organic matter in Devonian-Mississippian marine black shales: geochemical and petrographic evidence. Palaeogeography, Palaeoclimatology, and Palaeoecology, 215:125–154.

Robl, T. L., and L. S. Barron. 1987. The geochemistry of black shales in central Kentucky and its relationship to inter-basinal correlation and depositional environment, p. 377–396. *In* N. J. McMillan, A. F. Embry, and D. G. Glass (eds.), Devonian of the World, Vol. II: sedimentation. Canadian Society of Petroleum Geologists Memoir 14.

Robl, T. L., L. Barron, A. Bland, D. Koppenaal, A. Rubel, T. Coburn, D. Pollaek, G. Thomas, J. Beard, and R. Kepferle. 1983. The commercial feasibility of Mississippian and Devonian oil shales of Kentucky. Final Report to U.S. Department of Energy, Grant No. DEFG44-80R-410-195, IMMR83/081, IMMR, Lexington, Kentucky.

Sageman, B. B., A. E. Murphy, J. P. Werne, C. A. Ver Straeten, D. J. Hollander, and T. W. Lyons. 2003. A tale of shales: the relative roles of production, decomposition, and dilution in the accumulation of organic-rich strata, Middle-Upper Devonian, Appalachian Basin. Chemical Geology, 195:229–273.

Schultz, R. B., and R. M. Coveney, Jr. 1992. Time-dependent changes for Midcontinent Pennsylvanian black shales, U.S.A. Chemical Geology, 99:83–100.

Schieber, J. 1998. Sedimentary features indicating erosion, condensation, and hiatuses in the Chattanooga Shale of central Tennessee: Relevance for sedimentary and stratigraphic evolution, p. 187–215. *In* J. Schieber, W. Zimmerle, and P. Sethi (eds.), Shales and Mudstones. I. E. Schweizerbart'sche Verlagsbuchhadlung (Nagele und Obermiller), D-70176, Stuttgart.

Taulbee, D. N., E. D. Seibert, L. S. Barron, and T. L. Robl. 1990. Comparison of maceral group chemistries for a New Albany and an Ohio Shale kerogen. Energy Fuels, 4:254–263.

Tribovillard, N.-P., A. Desprairies, E. Lallier-Verges, P. Bertrand, N. Moureau, A. Ramdani, and L. Ramanampisoa. 1994. Geochemical study of organic-matter rich cycles from the Kimmeridge Clay Formation of Yorkshire (UK): productivity versus anoxia. Palaeogeography, Palaeoclimatology. Palaeoecology, 108:165–181.

Tyson, R. V., and T. H. Pearson. 1991. Modern and ancient continental shelf anoxia: an overview, p. 1–24. *In* R. V. Tyson and T. H. Pearson (eds.), Modern and Ancient Continental Shelf Anoxia. Geological Society Special Publication 58.

Vine, J. D., and E. B. Tourtelot. 1970. Geochemistry of black shale deposits - a summary report. Economic Geology, 65:253–272.

Wedepohl, K. H. 1971. Environmental influences on the chemical composition of shales and clays. *In* L. H. Ahrens, F. Press, S. K. Runcorn, and H. C. Urey (eds.), Physics and Chemistry of the Earth. Oxford, Pergamon, 8:307–331.

Werne, J. P., B. B. Sageman, T. W. Lyons, and D. J. Hollander. 2002. An integrated assessment of a "type euxinic" deposit: evidence for multiple controls on black shale deposition in the Middle Devonian Oatka Creek Formation. American Journal of Science, 302:110–143.

KIRTLANDIA
The Cleveland Museum of Natural History

November 2010 *Number 57:13–21*

HESLERODIDAE (CHONDRICHTHYES, ELASMOBRANCHII), A NEW FAMILY OF PALEOZOIC PHALACANTHOUS SHARKS

JOHN G. MAISEY
Division of Paleontology
American Museum of Natural History, Central Park West & 79th Street
New York, New York 10024-5192
maisey@amnh.org

ABSTRACT

A new family of extinct chondrichthyans (Heslerodidae) is created, containing the Paleozoic phalacanthous (fin-spine-bearing) shark *Heslerodus divergens* (known from fairly complete skeletal remains), plus two genera known only from isolated dorsal-fin spines, *Bythiacanthus* St. John and Worthen, 1875, and *Avonacanthus* gen. nov. Two species are retained in the genus *Bythiacanthus* (*B. vanhornei*, *B. siderius*), and *Glymmatacanthus* is synonymized with *Bythiacanthus*. *Avonacanthus* is probably a cladistically primitive member of the Heslerodidae.

Introduction

Many examples of isolated Paleozoic shark-fin spines have been described in the literature, but in most cases the kinds of sharks that possessed them are unknown. Bilaterally symmetrical spines are located at the dorsal midline in front of the dorsal fins in various extant sharks (e.g., *Squalus*, *Heterodontus*) and in some articulated fossil sharks (e.g., *Hybodus*; Maisey, 1978, 1979). In the past, many of these Paleozoic fossil spines were simply lumped together as an ill-defined assemblage of "ctenacanths," characterized by the presenee of two dorsal-fin spines but supposedly lacking the apomorphic characters of hybodonts or neoselachians (Maisey, 1975). Collectively, "ctenaeanths," hybodonts and neoselachians have been characterized as phalacanthous sharks (Zangerl, 1973) although it is unlikely that these are monophyletic when modern anacanthous (spineless) taxa are excluded. Furthermore, the phylogenetic relationships of Paleozoic phalacanths to their contemporary anacanthous relatives (e.g., symmoriids) or to Paleozoic sharks in which only a single dorsal spine is present (e.g., stethacanthids, xenacanths, some cladoselachians), are unresolved. The type species of *Ctenacanthus* (*C. major* Agassiz, 1837, p. 10) is still known only from isolated fin spines with ridges (costae) ornamented with fine pectinations (as are all the nominal species still referred to this genus; Maisey, 1981), although two Upper Devonian phalacanthous sharks from the Cleveland Shale (*C. compressus*; Dean, 1909; Maisey, 1981, 1984; "*Tamiobatis vetustus*" Williams, 1998) possess dorsal-fin spines very similar to those of *C. major*. As an additional complication, some Paleozoic sharks appear to have paired pectoral-fin spines with *Ctenacanthus*-like pectinate ornament (e.g., *Doliodus* and perhaps *Antarctilamna*), although it is still unclear whether such forms also possessed dorsal spines.

It would clearly help resolve this systematic and phylogenetic conundrum if different kinds of Paleozoic fin spines could be reliably associated with other skeletal remains. Among extant sharks, many aspects of fin-spine morphology (including shape, curvature, depth of insertion, internal structure, histology, ornament pattern, and presence or absence of posterior and posterolateral denticles) are often highly conserved, and it can be difficult (or impossible) to distinguish between the fin spines of certain modern genera. For example, the enameloid layer forming the mantle in fin spines of both *Squalus* and *Centroscymnus* is smooth and continuous, but in both *Etmopterus* and *Deania* it is restricted to three narrow costae (one anteriorly plus a pair posterolaterally), and in some forms there is no ornamented mantle whatsoever, for example in adult fin spines of extant *Oxynotus*, *Euprotomicrus*, and some Jurassic batoids (e.g., *Belemnobatis*, *Spathobatis*; Schweizer, 1964; Maisey, 1976, 1979). In Mesozoic hybodonts, fin-spine morphology is often highly conserved; those of *Hybodus*, *Egertonodus*, *Acrodus*, *Tribodus*, *Palaeobates*, and even the Pennsylvanian *Hamiltonichthys* are practically indistinguishable from each other. Exceptionally, an unusual fin-spine ornament pattern seems to characterize a single genus. For example, there is only a single narrow anterior costa in the extant neoselachian *Centrophorus*, and fin spines in the Mesozoic hybodont *Asteracanthus* are ornamented with longitudinal rows of large tubercles instead of continuous ribs (although intermediate morphologies blur even this distinction; e.g., *A. verrucosus*, representing a rare case of an ornament pattern which changes disto-proximally from ribs to tubercles; Egerton, 1854; Woodward, 1916).

Morphological and ontogenetic studies of modern shark-fin spines show that sclerogenetic tissues forming the spine mantle occur only at the base of the ornamented area, where they are deposited directly on the external surface of the underlying spine trunk, and investigation of fossil spines supports a similar developmental interpretation (Markert, 1896; Maisey, 1978, 1979). Elasmobranch fin-spine ornament therefore always seems to have been deposited sequentially and in a distal-proximal

direction. More importantly, the ornament in modern elasmobranch fin spines does not develop by secondary fusion of previously-formed mantle hard tissues, and does not involve the addition of secondary-mantle hard tissue between pre-existing ornament. Instead, the different ornament patterns (tubercles, costae, continuous mantle deposits) result from different (and fluctuating) rates and periodicities of mantle scleroblast activity, and do not involve the secondary deposition or re-working of mantle hard tissues. An identical mode of growth and enlargement can be postulated for fossil elasmobranch fin spines, where curved "growth lines" representing periodic pauses in scleroblastic activity are often observed passing across the ornamented mantle region and more or less parallel to the proximal margin of the ornament. Such indicators of periodic disto-proximal ornament accretion would be obliterated if there was secondary growth of mantle hard tissues between pre-existing areas. Even in spines with a tuberculate ornament, individual tubercles are frequently aligned in curved series running across the spine rather than longitudinally. Where tubercle formation is temporarily interrupted or suspended during spine growth, a space may form across the longitudinal tubercle rows (e.g., near the base of the ornament in the *Bythiacanthus* spine shown in Figure 1F–G). Thus, as in modern shark fin spines, mantle sclerogenesis in the fossils was (a) confined to the mantle base, (b) independent of proximal extension of the fin spine, and (c) coordinated across the entire ornament field throughout life irrespective of whether the ornament is broad, linear, or consists of individual tubercles.

One important systematic consequence of this morphological conservatism is that isolated fossil spines can often be assigned fairly reliably to already-established families or other suprageneric taxa, but rarely to genus or species. Although different fin-spine morphologies are certainly recognizable, the vast majority of extinct species founded on isolated fin spines probably do not represent equivalent or consistent operational taxonomic units (OTU's) and should not be considered valid without corroborative morphological data from other sources (e.g., teeth or skeletons).

This paper attempts to define a previously unrecognized higher taxon of extinct phalacanthous sharks that was first known only from isolated (but very distinctive) fin spines described under the generic name *Bythiacanthus* (St. John and Worthen, 1875, p. 445). The inspiration for this paper comes from Alexander Ivanov's and Michal Ginter's seminal work on phoebodontid and cladodont teeth, particularly the recognition (first noted by Ivanov during the mid-1990s; see Ginter, 2002, p. 554) that the teeth of the Pennsylvanian phalacanthous shark described by Williams (1985, p. 124) as *Phoebodus heslerorum* are identical to those described more than a century earlier under the name *Cladodus divergens* (Trautschold, 1879, p. 51). Ginter (2002) documented differences between the teeth of "*Phoebodus*" *heslerorum* and *Phoebodus* sensu stricto, and recommended that the former should not be referred to that genus (or even to the Family Phoebodontidae as defined by Williams, 1985, p. 124). Instead, Ginter (2002) erected a new genus (*Heslerodus*) and synonymized *P. heslerorum* with *H. divergens*. He retained *Phoebodus* in the Family Phoebodontidae, but removed *Heslerodus* as *incertae familiae*.

It has been noted elsewhere that the fin spines of this shark closely resemble those of *Bythiacanthus* (Maisey, 1982, p. 7). Recently, after examining specimens of *P. heslerorum* and *Bythiacanthus* in the Field Museum of Natural History (April 2004), I was able to confirm this similarity and concluded that these taxa are related. Furthermore, after examining the holotype of "*Oracanthus*" *lineatus* Newberry, 1897 (also in the Field Museum collection), I concluded that it is really an incomplete *Bythiacanthus* fin spine (a revision of *Oracanthus* is long overdue but is beyond the scope of this work).

On face value, this represents a simple taxonomic exercise; *Bythiacanthus* should take priority over *Heslerodus*, and the shark described by Williams (1985, p. 124) should be renamed *Bythiacanthus divergens*, sinking both the genus *Heslerodus* and the species *heslerorum*. Alternatively, we could go further and regard *Heslerodus divergens* as a synonym of *Bythiacanthus vanhornei*, thereby sinking all the names previously attached to William's (1985, p. 124) shark. Either conclusion might be justified if we were dealing with entire specimens of all the taxa involved and could compare spines, teeth, and other features. However, given the fragmentary nature of the critical type specimens, in this case all we would create is a chimeric taxon known from complete individuals but bearing the name of an isolated fin spine, while burying the somewhat more useful species name *divergens* (founded on isolated but distinctive teeth). In my opinion this is not progress but confusion, because we know nothing about the dentition and skeletal features in the type species of *Bythiacanthus* (*B. vanhornei* St. John and Worthen, 1875, p. 445). Consequently, there seems to be no empirical basis or practical justification for making *Heslerodus divergens* a synonym of *Bythiacanthus vanhornei*. On the other hand, Ginter's (2002) argument for synonymizing *heslerorum* with *divergens* is based on observed dental similarities, a reasonable proposal since most modern shark teeth are identifiable to genus if not species. Thus, the preferred course of action here is to retain *Heslerodus* and *Bythiacanthus* as distinct genera, with revised generic-level diagnoses, and to place both of them into a new Family Heslerodidae. In addition, some nominal species previously referred to *Bythiacanthus* (Maisey, 1982) are removed here to a new genus, which is also referred to the Heslerodidae. By taking this course, *Heslerodus* is retained as a valid taxon (a useful attribute in future phylogenetie analyses, because many aspects of its skeletal morphology are known) while recognizing its similarity to other Paleozoic taxa founded on less satisfactory, fragmentary material.

Systematic Paleontology

Class Chondrichthyes Huxley, 1880
Subclass Elasmobranchii Bonaparte, 1838
Family Heslerodidae new family

Diagnosis

Extinct elasmobranchs possessing two dorsal-fin spines with a stout rhomboidal profile, often though not invariably compressed laterally, posterior wall convex apically (sometimes exaggerated by diagenetic compression of fossil) and extremely short (level of posterior closure 75–95 percent of spine height), spine mantle consists of longitudinal rows of large rounded tubercles bearing radial striations (frequently abraded apically), tubercle rows increase proximally by primary bifurcation anteriorly and by insertion between other rows marginally, spines lack retrorse posterior and/or posterolateral denticle rows.

Included genera

Heslerodus Ginter, 2002; *Bythiacanthus* St. John and Worthen, 1875; *Glyumatacanthus* St. John and Worthen, 1875; *Avonacanthus* new genus.

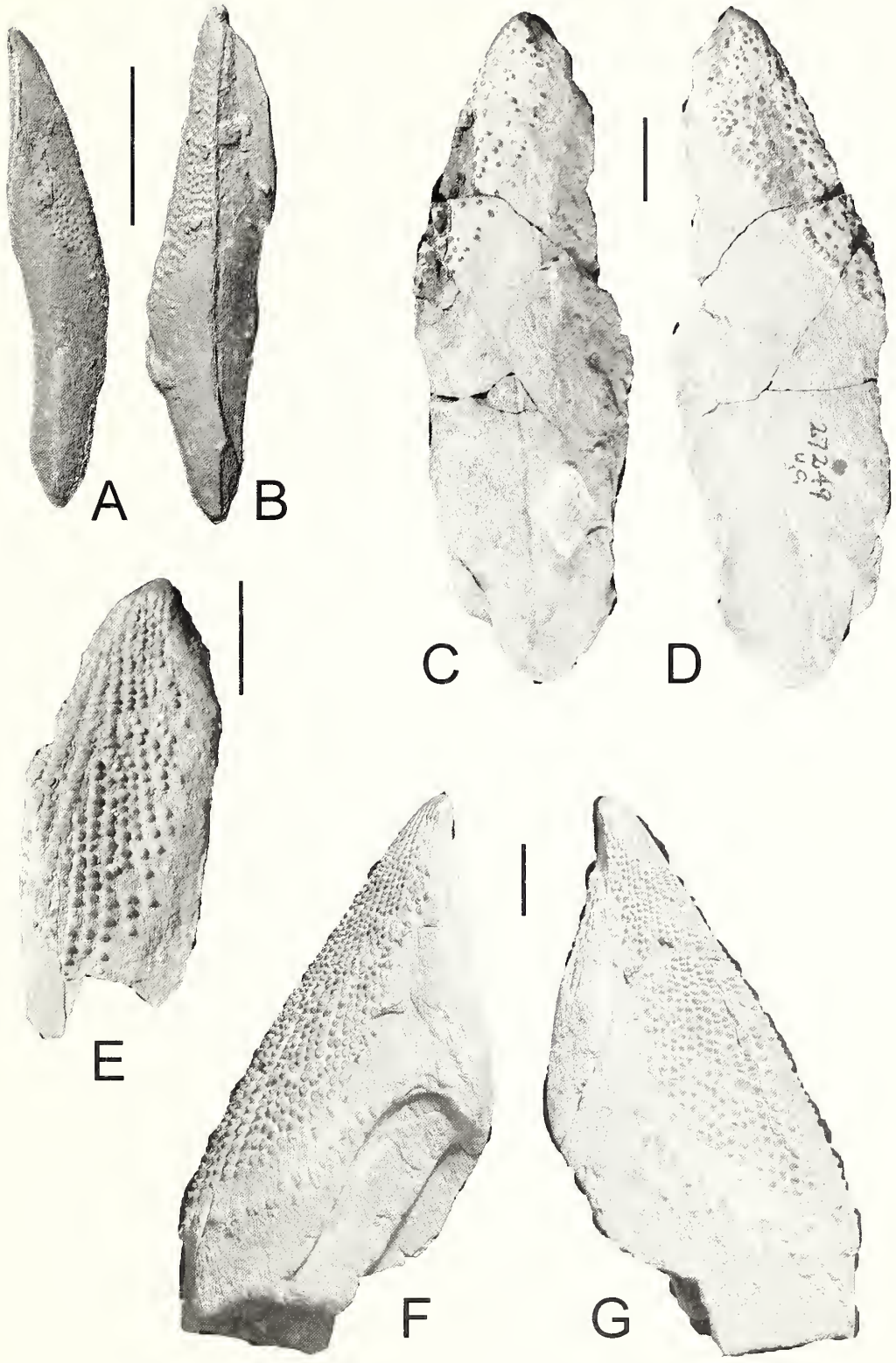

Figure 1. A–B, *Heslerodus divergens* (Trautschold), Middle Pennsylvanian, Parke County, Indiana. A, FMNH PF 8171, complete isolated anterior dorsal-fin spine, Mecca Quarry, right lateral view. B, FMNH PF2473, complete isolated anterior dorsal-fin spine, Logan Quarry, left lateral view. C–D, *Bythiacanthus vanhornei* St John and Worthen, genoholotype FMNH UC 27249, Middle Mississippian, Meramec Group, Upper St. Louis Limestone, Alton, Madison Co., Illinois, complete but inadequately prepared dorsal-fin spine in left and right lateral views. E, fragmentary holotype (only the apical region is preserved) of *Oracanthus lineatus* Newberry, synonymized here with *Bythiacanthus siderius* (Leidy, 1873), FMNH UC 9918, Meramac Group, St. Louis Limestone, Washington County, Indiana, left lateral view. F–G, *Bythiacanthus vanhornei*, lateral views of dorsal-fin spine lacking a small part of its base, previously misidentified as *Oracanthus* sp., FMNH UC 2197, Mississippian, Hardin County, Kentucky; note the gap in tubercles near the base of the ornamented region, indicating a pause in tubercle formation late in spine development. All scale bars equal 20 mm.

Comments

Collectively, the high level of posterior closure, massive unornamented spine trunk, and prominent anterior saddle suggest that heslerodid fin spines were deeply inserted in the body of the shark, and that most were probably inclined strongly backwards. As with all fossil fin spines, the shape of the posterior spine wall is commonly distorted by post-mortem deformation, because isolated spines are frequently subject to lateral compression after burial, causing the posterior wall (which is usually thinner than the adjacent lateral and anterior walls) to buckle outward. A spine with an originally flat or weakly convex posterior wall may therefore appear to have pronounced convexity following taphonomic and diagenetic distortion (involving localized plastic and/or brittle failure of spine hard tissues), although this can usually be detected by careful inspection.

Genus *Heslerodus* Ginter, 2002

Emended diagnosis

Heslerodid with fin spines strongly flattened laterally, tubercles slightly elongated and usually not contacting each other, distributed erratically on spine surface and exposing the outer vascularized surface of the underlying spine trunk, ornament extending over half the fin-spine height, level of posterior closure 70–75 percent of spine height; teeth with crown composed of three long, recurved main cusps, and usually two intermediate, smaller cusplets. Median cusp slightly larger than or equal to lateral main cusps in size, lateral cusps sigmoidal, strongly divergent mesiodistally (around 80–90°), tooth base rounded, with a distinct labial concavity and a lingual torus usually with two buttons on its apical surface.

Type species

Heslerodus divergens (Trautschold, 1879, p. 51).

Comments

Ginter and Ivanov (1992) noted that teeth in the phalacanthous shark named *Phoebodus heslerorum* by Williams (1985, p. 124) differ from those in the type species *P. sophiae* St. John and Worthen (1875), in which the median cusp is always slightly shorter than the lateral main cusps and the tooth base bears only a single median button on its apical surface. Ginter (2002) subsequently placed "*P.*" *heslerorum* in a new genus *Heslerodus*, and also recognized that its teeth are identical with those named *Cladodus divergens* by Trautschold (1879), which Ginter considered are distinct from *Cladodus* sensu stricto. However, Ginter's (2002) diagnosis of *Heslerodus* was limited to dental characters, whereas in the present work the diagnosis is expanded to include additional features involving fin spines (it could also include features of the endoskeleton, but that is beyond the scope of this work). The concave labial margin of *Heslerodus* teeth is an especially important feature that has not been observed in teeth referred to *Phoebodus* (M. Ginter, personal communication, 2004). Williams (1985, p. 124–131, plates 16–17) illustrated several fin spines of *H. divergens*, and two specimens are illustrated here (Figure 1A–B).

Heslerodus divergens (Trautschold, 1879)

Figure 1A–C

Cladodus divergens Trautschold, 1879, p. 51, Pl. 6, no. 11.

Phoebodus sp. Case, 1973, fig. 47.

Phoebodus n. sp. Zangerl, 1981, figs. 56–58.

"*Cladodus*" sp. Schultze, 1985, fig. 3.5.

Phoebodus heslerorum sp. n. Williams, 1985, p. 124–131, figs. 22–23, Pl. 16–17.

"*Cladodus*" *divergens* Trautschold Ivanov, 1999, p. 276–277, fig. 3, Pl. 7.1.

Heslerodus divergens (Trautschold) Ginter, 2002, p. 548–551, fig. 1A–C, 2.

Diagnosis

As for genus.

Holotype

Institute of Zoology, Wroclaw University, Wroclaw, Poland, Pch/617, the largest and most complete of three teeth catalogued under this number (Ginter, 2002), described and figured by Trautschold (1879, p. 51, Pl. 6, no. 11).

Comments

The holotype of *Phoebodus heslerorum* Williams, 1985 is reposited in the Field Museum of Natural History (PF 8170, Pennsylvanian, Westphalian Upper C, Des Moines Series, Linton Fm., Liverpool Cyclothem, Mecca Quarry Shale, Parke County, Indiana). It consists of a disarticulated skull, a partial pectoral fin, and both dorsal-fin spines. *Heslerodus divergens* is the only heslerodid known from skeletal remains. According to Ginter (2002), *Heslerodus divergens* teeth have a stratigraphie range from the Late Carboniferous (Bashkirian–Gzhelian) probably through the Lower Permian (Asselian). The species is recorded from Russia (Upper Carboniferous of the Moseow region and the Pechora Sea region of Arctic Russia) and North America (Pennsylvanian of Indiana, Nebraska, Ohio, Pennsylvania, and Wyoming; Lower Permian of Kansas). No teeth referable to *Heslerodus* are known from the Lower Carboniferous. Thus, if the Lower Carboniferous taxa discussed below are correctly referred to the Family Heslerodidae, their teeth were probably different from those of *Heslerodus*.

Bythiacanthus St. John and Worthen, 1875
(= *Glyptacanthus* St. John and Worthen, 1875)

Emended diagnosis

Heslerodid with fin spines strongly compressed laterally, producing a very deep cross-section so that the anteroposterior dimension is 3 to 4 times the spine width; spine ornamented with large round tubercles with radial striations (often lost by abrasion), tubercle bases sometimes separate and sometimes distributed erratically but more commonly united, especially in longitudinal rows, revealing little of the underlying trunk surface; very high level of posterior closure (85–95 percent of spine length).

Type species

Bythiacanthus vanhornei St. John and Worthen, 1875, p. 445.

Comments

Maisey (1982) referred several nominal species founded on isolated fin spines to the genus *Bythiacanthus* in addition to the type species. However, some of those fin spines differ from the type species in not being strongly compressed laterally and are removed here to another genus (see below).

Bythiacanthus vanhornei St. John and Worthen, 1875
Figures 1D, 1F–G, 2A

Bythiacanthus vanhornei St. John and Worthen, 1875, p. 445, Pl. 17, no. 1; Maisey, 1982, p. 3, fig. 1A–I.

Diagnosis

Bythiacanthus with fin spines ornamented with sparse, scattered tubercles arranged in disorganized fashion, and confined to the apicalmost part of the spine.

Holotype

Field Museum of Natural History UC 27249, Middle Mississippian, Meramec Group, Upper St. Louis Limestone, Alton, Madison Co., Illinois. Complete fin spine, approximately 16.5 cm total length.

Comments

While it is possible that the type specimen of *Bythiacanthus vanhornei* represents an abnormally developed fin spine in which the regular deposition of tubercles had become disrupted, it is retained here as a distinct species. It is not uncommon for fossil fin spines to display irregularities in their ornament (e.g., in hybodonts; Maisey, 1978), but this is usually quite local in extent. Comparison of St. John and Worthen's (1875) original figure with the photographs here show that although the specimen is sparsely ornamented, matrix still covers much of its surface and may obscure smaller tubercles (cf. Figure 1C–D).

Bythiacanthus siderius (Leidy, 1873)
Figures 1E, 2B–J

Asteracanthus siderius Leidy, 1873, p. 313, Pl. 32, no. 59.
Glyptmatacanthus irishi St. John and Worthen, 1875, p. 447, Pl. 17, no. 2.
Oracanthus lineatus Newberry, 1897, p. 289, Pl. 22, fig. 5.
Ctenacanthus solidus Eastman, 1902, p. 313; Eastman, 1903, Pl. 7, no. 3.
Ctenacanthus ianishevskyi Khabakov, 1928, p. 23, Pl. 3, nos. 5–10.
Bythiacanthus ianishevskyi (Khabakov) Maisey, 1982, p. 5, figs. 2G–K.
Bythiacanthus solidus (Eastman) Maisey, 1982, p. 5, figs. 3A–B.
Bythiacanthus siderius (Leidy) Maisey, 1982, p. 6, figs. 1J–L.

Diagnosis

Bythiacanthus with fin spines ornamented with numerous large tubercle rows commonly arising at or near anterior midline and passing obliquely across spine upper lateral surface, sometimes also arising by bifurcation farther laterally, posterior rows considerably shorter and more recurved than those farther anteriorly, forming a very oblique level of insertion.

Holotype

The whereabouts of the holotype is presently unknown. According to Leidy (1873, p. 313) the specimen was reputed to be from the "Sub-Carboniferous" of Glasgow, Tennessee. If that age is correct, this is by far the earliest known *Bythiacanthus*. However, its age has clearly always been problematic and could be Mississippian.

Comments

It is not an entirely satisfactory situation that the holotype was not available at the time of this revision, since several nominal species are synonymized here with *Bythiacanthus siderius*. It is nevertheless clear from the original description and figure that the holotype should not be referred to *Asteracanthus* (Maisey, 1982). St. John and Worthen (1875, p. 477) suggested that Leidy's (1873, p. 313) species *siderius* may be conspecific with *Bythiacanthus vanhornei*. However, the tubercles in Leidy's very fragmentary type specimen are better organized into vertical rows than in the holotype of *B. vanhornei*. Orderly tubercle rows are also present in AMNH 1826, a fairly complete fin spine referred to *Bythiacanthus siderius* by Maisey (1982, Figure 1J–K).

Two additional examples of *Bythiacanthus* fin spines are reposited in the Field Museum collection. One of them is the holotype of *Oracanthus lineatus* Newberry, 1897 (FMNH UC 9918; Figure 1E), from the Meramac Group, St. Louis Limestone of Washington County, Indiana. The other example is a very large fin spine previously misidentified as *Oracanthus* sp. (FMNH UC 2197; Figure 1F–G), from the Mississippian of Hardin County, Kentucky. The ornament and shape of these two spines is completely different from the type species of *Oracanthus* (*O. milleri*; Agassiz, 1837, p. 13), and they do not pertain to that genus. However, FMNH UC 9918 is very close in size, shape and ornament to AMNH 1826, and it is concluded that *Oracanthus lineatus* is synonymous with *B. siderius*.

Glyptmatacanthus irishii (the type species of the genus) is also considered synonymous with *Bythiacanthus siderius* (*Glyptmatacanthus* was already regarded as a junior subjective synonym of *Bythiacanthus*; Maisey, 1982). Other species referred to *Glyptmatacanthus* (e.g., *G. rudis*, *G. petrodoides*; St. John and Worthen, 1875) could also pertain to *Bythiacanthus*, but are founded on specimens that are too fragmentary to present any diagnosable features.

Eastman's (1903) *Ctenacanthus solidus* and Khabakov's (1928) *Ctenacanthus ianishevskyi* were both referred to *Bythiacanthus* by Maisey (1982), but were retained as separate species. However, in the absence of any unique features, there seems little reason to continue separating them from *B. siderius*, and they are here placed into synonymy with that species. Two species formerly included in *Ctenacanthus* (*C. peregrinus*; Khabakov, 1928; *C. lucasi*; Eastman, 1902) were reassigned by Maisey (1982) to *Bythiacanthus*, but are now removed to a new genus (see below).

Fin spines referred here to *Bythiacanthus siderius* can be categorized into two distinct forms, distinguishable by their shape and profile. One form has a strongly rhombic profile and a massive anterior saddle, below which the leading edge of the trunk slopes at an angle of almost 80° away from the leading edge of the ornamented mantle region. Examples of this form include the specimens referred to *B. ianishevskyi* by Khabakov (1928) and Maisey (1982), as well as the paratype of *B. solidus* (Eastman, 1903, Pl. 7, no. 3: also see Maisey, 1982, fig. 3B). The other form is less rhombic and has a much smaller anterior saddle, below which the trunk slopes less abruptly away from the leading edge of the ornamented region (ca. 170°). Examples of this form include AMNH 1826 and FMNH UC 2197 (Figure 1F–G). The holotype of *B. solidus* may also represent this form, although its saddle is not preserved (see Maisey, 1982, fig. 2A). Unfortunately, the type specimens of *Bythiacanthus siderius*, *Glyptmatacanthus irishii*, and "*Oracanthus*" *lineatus* are not sufficiently complete to determine their original outline or the extent of the saddle.

It is possible that these two forms represent different taxa, but this is considered unlikely because in *H. divergens* the posterior fin spine is more rhombic in profile and has a more extensive saddle than the anterior one (e.g., FMNH PF 8170; Williams, 1985, Pl.

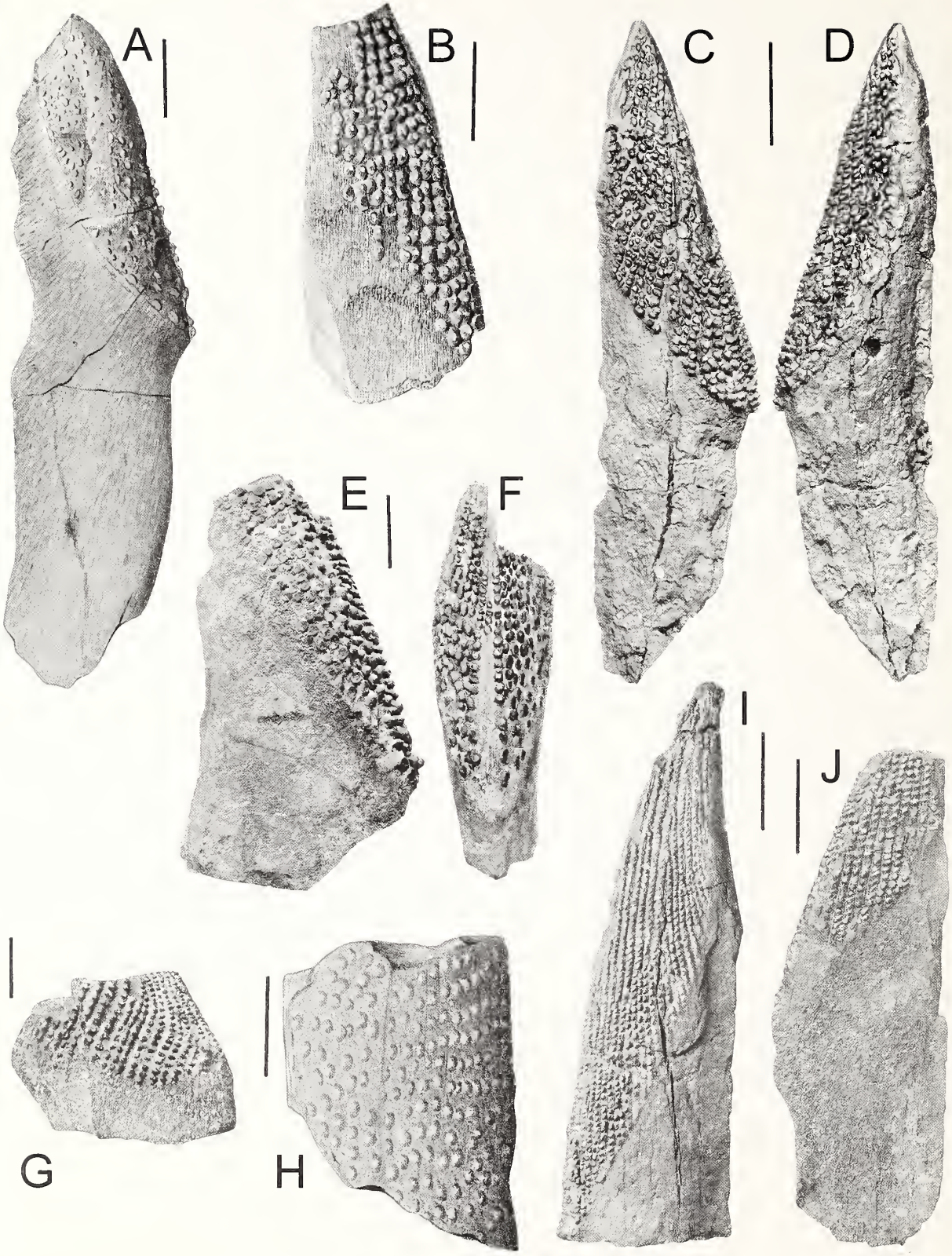

Figure 2. A, *Bythiacanthus vanhornei* St. John and Worthen; genoholotype FMNH UC 27249, complete dorsal-fin spine in right lateral view (from St. John and Worthen 1875, Pl. 17, no. 1). B, *B. siderius* (Leidy); holotype PAN S22:13 7835, dorsal-fin spine lacking apical and basal regions, right lateral view (from Leidy, 1873, Pl. 32, no. 59). C–D, *Bythiacanthus siderius* (Leidy), AMNH 1826, St. Louis Limestone, Alton, Illinois, right and left lateral views of complete dorsal-fin spine (from Maisey, 1982, Figure 1J–K). E–F, *Bythiacanthus siderius* (Leidy), AMNH 9594, dorsal-fin spine lacking apical region and part of base, right lateral and anterior views (from Maisey, 1982, fig. 1M, N). G, fragmentary holotype of *Ctenacanthus ianishevskyi* Khabakob (synonymized here with

16, figs. 5–6), although the difference is not as great as in the spines referred to *B. siderius*. Corresponding differences in anterior and posterior fin-spine morphology are also found in articulated skeletons of *Hybodus hauffianus*, where the posterior dorsal-fin spine has a well-developed saddle and is more erect, while the anterior spine has a relatively inconspicuous saddle and is inserted more obliquely (Maisey, 1978, p. 664). Collectively, these observations suggest that more rhombic *Bythiacanthus* fin spines are from the posterior dorsal fin while the less rhombic ones are from the anterior fin, and that their insertion angles relative to the main body axis were profoundly different. These shape differences are therefore not considered taxonomically significant.

HESLERODIDAE?
AVONACANTHUS new genus

Diagnosis

Heslerodid? with fin spines not strongly compressed laterally, C-shaped cross section widening below the ornament base; moderately high level of posterior closure; ornament with numerous closely-spaced and well-defined longitudinal rows of large tubercles extending more than half length of fin spine.

Type species

Ctenacanthus brevis Agassiz, 1837, p. 11.

Comments

The fin spines included here are distinguished from those referred to *Heslerodus* or *Bythiacanthus* in being more rounded in cross section and less rhombic in profile (Figure 3). However, they have a high level of posterior closure and are ornamented with large tubercles, as in *Heslerodus* and *Bythiacanthus*. *Avonacanthus* fin spines therefore share some but not all the specialized features of those genera. If *Avonacanthus* is a heslerodid, it may represent a cladistically primitive member of the group, since its fin spines are comparatively generalized except for the features just noted.

AVONACANTHUS BREVIS (Agassiz, 1837)
Figure 3A–G

Ctenacanthus brevis AGASSIZ, 1837, p. 11, Pl. 2, no. 2; DAVIS, 1883, p. 337, Pl. 43, fig. 3.
Ctenacanthus lucasi EASTMAN, 1902, p. 80, Pl. 6, no. 3.
Ctenacanthus peregrinus KHABAKOV, 1928, p. 25, Pl. 3, nos. 1–4.
Bythiacanthus brevis (Agassiz) MAISEY, 1982, p. 5, fig. 2A–F.
Bythiacanthus lucasi (Eastman) MAISEY, 1982, p. 5, fig. 3G.
Bythiacanthusperegrinus (Khabakov) MAISEY, 1982, p. 5, figs. 3C–F.

Holotype

Bristol City Museum and Art Gallery C 4154, Lower Carboniferous, Carboniferous Limestone, Avon Gorge, near Bristol, England. Isolated fin spine lacking the proximal part of the inserted region (Figure 3A–C).

Comments

The original figure of the holotype in Agassiz (1837, Pl. 2, no. 2) was not drawn from the specimen but was based instead on an earlier drawing made by William Buckland (see Figure 3A). Subsequent photographs of the specimen (Figure 3B–C) suggest that it was more complete in Buckland's time (the Bristol City Museum's paleontological collections were extensively damaged during the Second World War). Other fin spines resembling those of *Avonacanthus brevis* include the holotypes of *Ctenacanthus lucasi* Eastman, 1902, and *C. peregrinus* Khabakob, 1928 (Figure 3D–H). These species were referred to *Bythiacanthus* by Maisey (1982) and are regarded here as synonymous with *A. brevis*, based on general similarities in spine transverse sections and ornament pattern.

Discussion

The systematic arrangement adopted here is admittedly a compromise solution to an all-too-common problem in paleontology, namely how to maintain the individuality of a recently-described taxon known from fairly complete fossil remains, and to propose a higher-level relationship with other previously-named taxa known only from similar but extremely fragmentary fossils, even though the latter probably represent essentially undiagnosable species (and possibly genera). In fact, the present case is comparatively straightforward because the fin spines involved are highly distinctive, increasing the probability that they represent a monophyletic group of phalacanthous sharks. The fortuitous discovery of complete *Heslerodus* fossils (Williams, 1985) shows that teeth previously referred to *Cladodus divergens* are from a phalacanthous shark whose fin spines closely resemble those of *Bythiacanthus* in their distinctive shape and ornament.

The diagnostic features distinguishing *Heslerodus* and *Bythiacanthus* are admittedly subjective, because they are limited to features of the fin spines such as differences in the density, shape, and spacing of tubercles, the level of posterior closure, and the degree to which the spine profile approaches a rhombic shape. The absence of *divergens* teeth in the Lower Carboniferous provides additional biostratigraphic support for continued separation of *Heslerodus* and *Bythiacanthus*. The systematic importance of the slightly different tubercle arrangements noted in *B. vanhornei* and *B. siderius* is unclear; both taxa are retained as separate species here, but given the lack of systematically informative characters they could represent different genera, or variants of a single species (in which case *B. vanhornei* would become a junior subjective synonym of *B. siderius*).

Acknowledgments

I miss the discussions about early sharks I had with Mike Williams, and I regret he is not here to enjoy the ongoing

←

Bythiacanthus siderius), CNIGR 2421/2, Leningrad; Carboniferous Limestone C, Kuznetsk Basin, Siberia, right lateral view of dorsal-fin spine lacking apical and basal regions (from Khabakob, 1928, Pl. 3, no. 5). H, fragmentary holotype of *Glyptotatacanthus irishii* St. John and Worthen (synonymized here with *Bythiacanthus siderius*), USNM 13537, Kinderhook Formation, Marshall Co., Iowa (from St. John and Worthen, 1875, Pl. 17, no. 2a), from an undetermined part of the spine mid-region, right lateral view. I, holotype of *Ctenacanthus solidus* Eastman (synonymized here with *Bythiacanthus siderius*), USNM 3383, Kinderhook Formation, Iowa, dorsal-fin spine lacking basal region, left lateral view (from Maisey, 1982, fig. 3A). J, paratype of *Ctenacanthus solidus* Eastman, USNM 4843, Kinderhook Formation, Iowa, dorsal-fin spine lacking basal region, left lateral view (from Eastman, 1903, Pl. 7, no. 3). All scale bars equal 20 mm.

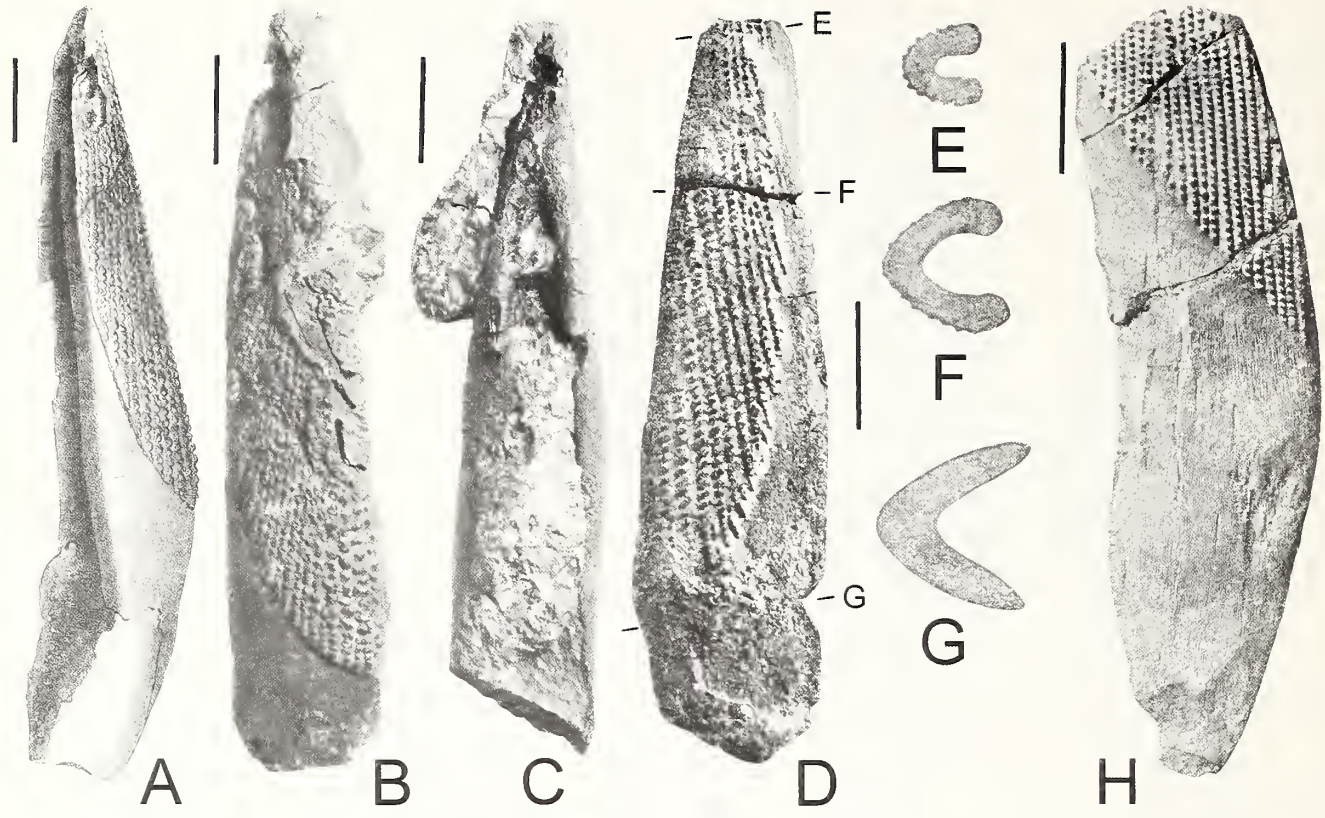

Figure 3. *Avonacanthus*, new genus. A–C, *Avonacanthus brevis* (Agassiz), genoholotype, C4154, Bristol City Museum and Art Gallery, U.K., Carboniferous Limestone (Avonian Z2 fish beds), Clifton, near Bristol. A, original figure (from Agassiz, 1837, Pl. 2, no. 2), right lateral view (slightly oblique) showing dorsal-fin spine with most of basal region. B–C, photographs of same specimen in lateral (B) and posterior (C) views, with less of the basal region preserved (from Maisey, 1982, fig. 2A–D; photos courtesy of BCMAG). D–G, *Ctenacanthus peregrinus* Khabakob (synonymized here with *Avonacanthus brevis*), holotype, CNIGR 2421/3, Leningrad, Carboniferous Limestone (Tournaisian C1), Roika Village, Tom River, Siberia, dorsal-fin spine lacking parts of apical and basal regions. D, right lateral view, E–G, transverse sections at levels indicated (from Khabakob, 1928, Pl. 3, nos. 1–4). H, *Ctenacanthus hicasi* Eastman (synonymized here with *Avonacanthus brevis*), holotype, USNM 4686, Kinderhook Formation, Iowa, dorsal-fin spine lacking much of its apical region, right lateral view (from Eastman, 1902, Pl. 6, no. 1). All scale bars equal 20 mm.

developments in our shared field of interest. Mike's untimely passing came just a few months before that of Bobb Schaeffer, so I have lost two good friends and colleagues in close succession. I am extremely grateful to M. Ginter for useful discussions about phoebodontid teeth and the distinctions between *Phoebodus* and *Heslerodus*. I thank him and an anonymous reviewer for providing many helpful comments and suggestions. I also thank L. Grande for permitting me to work in the fossil fish collection at the Field Museum of Natural History, the Bass Visiting Scientist Scholarship Committee for funding part of this investigation, and the support of the American Museum of Natural History in completing this work, and thank L. Meeker for creating additional illustrations for this paper at short notice.

References

Agassiz, L. 1837–44. Recherches sur les Poissons fossiles, 5 vols. Neuchatel, 1420 p.

Bonaparte, C. L. 1838. Synopsis vertebratorum systematis. Nuovi Annali della Scienze Naturali, Bologna, 11:105–133.

Case, G. R. 1973. Fossil sharks: a pictorial review. Pioneer Litho Co., New York. 64 p.

Davis, J. W. 1883. On the fossil fishes of the Carboniferous Limestone series of Great Britain. Transactions of the Royal Society of Dublin, 1:327–600.

Dean, B. 1909. Studies on fossil fishes (sharks, chimaeroids and arthrodires). Memoirs of the American Museum of Natural History, 5:211–287.

Eastman, C. R. 1902. Some Carboniferous cestraciont and acanthodian sharks. Bulletin of the Museum of Comparative Zoology, 39:55–99.

Eastman, C. R. 1903. Carboniferous fishes from the central western states. Bulletin of the Museum of Comparative Zoology, 39:163–226.

Egerton, P. M. G. 1854. On some new genera and species of fossil fishes. Annals and Magazine of Natural History, 13:433–436.

Ginter, M. 2002. Taxonomic notes on "*Phoebodus heslerorum*" and *Symmorium reniforme* (Chondrichthyes, Elasmobranchii). Acta Palaeontographica Polonica, 47:547–555.

Ginter, M., and A. Ivanov. 1992. Relationships of *Phoebodus*. Modern Geology, 20:263–274.

Huxley, T. H. 1880. On the application of the laws of evolution to the arrangement of the Vertebrata and more particularly the Mammalia. Proceedings of the Zoological Society of London, 1880:649–662.

Ivanov, A. 1999. Late Devonian-early Permian chondrichthyans of the Russian Arctic. Acta Palaeontographica Polonica, 49:267–285.

Khabakov, A. V. 1928. Description of new species of ichthyodorulites of the genus *Ctenacanthus* Ag. from Carboniferous deposits in the USSR. Bulletin du Comité Géologique, Leningrad, 47:23–31 (In Russian with English summary).

Leidy, J. 1873. Contributions to the extinct vertebrate fauna of the western territories. Governmental Printing Office, Washington, D.C. 358 p.

Maisey, J. G. 1975. The interrelationships of phalacanthous selachians. Neues Jahrbuch für Geologie und Paläontologie Monatsheft, 9:553–567.

Maisey, J. G. 1976. The Jurassic selachian fish *Protospinax* Woodward. Palaeontology, 19:733–747.

Maisey, J. G. 1978. Growth and form of finspines in hybodont sharks. Palaeontology, 21:657–666.

Maisey, J. G. 1979. Finspine morphogenesis in squalid and heterodontid sharks. Zoological Journal of the Linnean Society, 66:161–183.

Maisey, J. G. 1981. Studies on the Paleozoic selachian genus *Ctenacanthus* Agassiz. No. 1. Historical review and revised diagnosis of *Ctenacanthus*, with a list of referred taxa. American Museum Novitates, 2718:1–22.

Maisey, J. G. 1982. Studies on the Paleozoic selachian genus *Ctenacanthus* Agassiz. No. 2. *Bythiacanthus* St. John and Worthen, *Amelacanthus*, new genus, *Eunemacanthus* St. John and Worthen, *Sphenacanthus* Agassiz, and *Wodnika* Münster. American Museum Novitates, 2722:1–24.

Maisey, J. G. 1984. Studies on the Paleozoic selachian genus *Ctenacanthus* Agassiz. No. 3. Nominal species referred to *Ctenacanthus*. American Museum Novitates, 2774:1–20.

Markert, F. 1896. Die Flossenstacheln von *Acanthias*; ein Beitrag zur Kenntniss der Hartsubstanzgebilde der Elasmobranchier. Zoologische Jahrbüche, Anatomie, 9:665–730.

Newberry, J. S. 1897. New species and a new genus of American Palaeozoic fishes, together with notes on the genera *Oracanthus*, *Dactylodus*, *Polyrhizodus*, *Sandalodus*, *Deltodus*. Transactions of the New York Academy of Sciences, 16:282–304.

Schultze, H.-P. 1985. Marine to onshore vertebrates in the Lower Permian of Kansas and their paleoenvironmental implications. University of Kansas Paleontological Contributions, Paper, 113:1–18.

Schweizer, R. 1964. Die Elasmobranchier und Holocephalen aus den Nusplinger Plattenkalken. Palaeontographica, A 123:58–110.

St. John, O., and A. H. Worthen. 1875. Descriptions of fossil fishes. Geological Survey of Illinois, 2:9–134.

Trautschold, H. 1879. Die Kalchbrüche von Mjatschkowa. Eine Monographie des oberen Bergkalks. Nouveau Mémoires de la Société Impériale des Naturalistes de Moscou, 14:3–82.

Williams, M. E. 1985. The "cladodont level" sharks of the Pennsylvanian black shales of North America. Palaeontographica, A 190:83–158.

Williams, M. E. 1998. A new specimen of *Tamiobatis vetustus* (Chondrichthyes, Ctenacanthoidea) from the late Devonian Cleveland Shale of Ohio. Journal of Vertebrate Paleontology, 18:251–260.

Woodward, A. S. 1916. The Wealden and Purbeck fishes. Part 1. Palaeontographical Society Monograph, 59:1–48.

Zangerl, R. 1973. Interrelationships of early chondrichthyans, p. 1–14. *In* P. H. Greenwood, R. S. Miles, and C. Patterson (eds.), Interrelationships of Fishes. Academic Press, London.

Zangerl, R. 1981. Chondrichthyes 1: Paleozoic Elasmobranchii. *In* H.-P. Schultze (ed.), Handbook of Paleoichthyology, 3A. Gustav Fischer, Stuttgart. 115 p.

KIRTLANDIA
The Cleveland Museum of Natural History

November 2010 *Number 57:22–35*

A NEW SPECIES OF *BRYANTOLEPIS* CAMP, WELLES, AND GREEN, 1949 (PLACODERMI, ARTHRODIRA) FROM THE EARLY DEVONIAN WATER CANYON FORMATION OF NORTHERN UTAH AND SOUTHERN IDAHO, WITH COMMENTS ON THE ENDOCRANIUM

DAVID K. ELLIOTT
Department of Geology
Northern Arizona University, Flagstaff, Arizona 86011-4099
David.Elliott@nau.edu

AND **ROBERT K. CARR**
Department of Biological Sciences
Ohio University, Athens, Ohio 45701

ABSTRACT

A new species of the actinolepidoid arthrodire *Bryantolepis* Camp, Welles, and Green, 1949, is described from the Water Canyon Formation of northern Utah and southern Idaho, where it is characteristic of the uppermost part of the Lower Devonian in the Grassy Flat Member. *Bryantolepis williamsi* n. sp. is about 60% larger than the only other previously recognized species, *B. brachycephala* (Bryant, 1932), from the Early Devonian Beartooth Butte Formation of Wyoming, but is otherwise very similar to it. The new material provides information on the endocranial morphology showing that it is very similar to that of *Kujdanowiaspis* Stensiö, 1942 and *Lehmanosteus* Goujet, 1984, the only other actinolepidoids for which the endocranium is known. The parasphenoid is described for the first time in this genus, as is the anterior superognathal. The superognathal is only the second to be definitely attributed to an actinolepidoid and is shown to be a crushing rather than a shearing element.

Introduction

Placoderms are early, jawed fishes that are almost exclusively Devonian in age. Within the Placodermi M'Coy, 1848, the major group is the Arthrodira Woodward, 1891, the most basal members of which are the Actinolepidoidei Miles, 1973 (now thought to be a paraphyletic group [Dupret, 2004; Dupret et al., 2009; Figure 1]). Five genera and six species of actinolepidoids have been described previously from the Beartooth Butte and Water Canyon Formations and the Sevy Dolomite of the western United States (Bryant, 1932, 1934, 1935; Denison, 1958; Johnson et al., 2000), and in this paper an additional species of the actinolepidoid *Bryantolepis* Camp, Welles, and Green, 1949, *Bryantolepis williamsi* n. sp., is described from the Water Canyon Formation of northern Utah and southern Idaho. As the genus had previously only been known from the Beartooth Butte Formation of Wyoming the new species extends the range of the genus and supports the correlation between the Beartooth Butte Formation and the Grassy Flat Member of the Water Canyon Formation that had previously been proposed (Elliott and Johnson, 1997).

Despite their age, the morphology of placoderms is known in considerable detail. This is particularly true of the cranial anatomy, which was minutely studied by Stensiö who used serial-grinding techniques to determine the shape of the cranial cavities and the position of canals and foramina for nerves and vessels (Stensiö, 1963a, b; Stensiö, 1969). Serial grinding provides remarkable detail but it is destructive of the specimen and also extremely time consuming so it was not until the advent of preparation using acetic acid that additional information started to be obtained from well-preserved arthrodire endocrania. More recent studies by Young (1979, 1981), Goujet (1984), and Dupret (2010) have provided additional information on arthrodire cranial morphology, particularly on the structures surrounding the orbit (Young, 1979). However, the only actinolepidoids for which detailed information is available remain *Kujdanowiaspis* Stensiö, 1942, described in detail by Stensiö (1963b, with an update by Dupret, 2010), and *Lehmanosteus* Goujet, 1984. Thus the presence of a well-preserved endocranium in one specimen of *Bryantolepis williamsi* n. sp. helps to improve knowledge of variation in the cranial anatomy of this group of early, jawed fishes.

Geological Setting

The material described here was collected from the lower part of the Grassy Flat Member of the Water Canyon Formation at

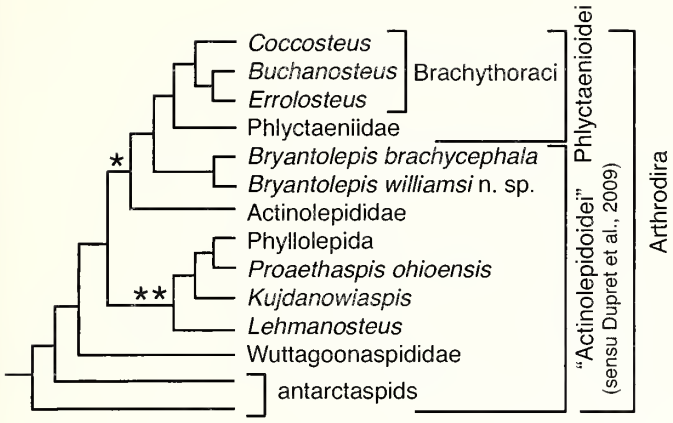

Figure 1. Hypothesis of relationships for arthrodiran taxa used in the text. Based on strict concensus tree of Dupret et al., 2009, fig. 3, with the addition of *Errolosteus* and *Bryantolepis williamsi* n. sp. *, **, nodes 20 and 8, respectively, of the Dupret et al. tree.

Green Canyon, east of Logan, northern Utah, and near St. Charles Creek, southern Idaho. Although only a few specimens are known, this species appears to be characteristic of the uppermost part of the Lower Devonian portion of the section. The Water Canyon Formation of northern Utah and southeastern Idaho consists of dolomites, dolomicrites, and dolomicritic quartz-arenites deposited within a restricted coastal embayment along the northwest coast of Euramerica (the Old Red Sandstone continent). It lies above the Silurian (Ludlovian–earliest Pridolian) Laketown Dolomite, which consists of mottled, dark grey to black, fossiliferous dolostone, and forms prominent cliffs in the study area.

The Water Canyon Formation is divided into the lower Card Member and the upper Grassy Flat Member (Williams and Taylor, 1964). The Card Member is unfossiliferous and is characterized by mottled, grey, thick- to very thick-bedded, dolomicrite at the base to light blue-grey, thinly bedded dolomicrite in the upper part. Near the top of the Card Member, the argillaceous content increases until the dolomite becomes arenaceous. The first occurrence of sand in the formation defines the base of the Grassy Flat Member (Williams and Taylor, 1964).

The lithologically more varied Grassy Flat Member is characterized by very thin- to medium-bedded laminated dolomicrite, laminated to massive argillaceous and arenaceous dolomicrite, and massive to planar trough cross-bedded dolomicritic and dolomitic quartz-arenite. The upper part of the member is more arenaceous and is capped by an intraformational breccia that forms prominent rounded cliffs at the top of the section, above which the Hyrum Dolomite occurs. Vertebrates occur throughout the lower part of the Grassy Flat Member but are largely limited to the argillaceous and arenaceous dolomicrite and dolomitic quartz-arenites (Reed, 1997). The new species of *Bryantolepis* described here occurs just below the more arenaceous upper part of the Grassy Flat Member in thick- to very thick-bedded silty dolostones. It occurs with *Allocryptaspis utahensis* Denison, 1953, and acanthodian spines in Green Canyon, but in St. Charles Creek it is associated with an extensive but undescribed fauna including a species of *Cardipeltis* Branson and Mehl, 1931, at least two species of pteraspid, another arthrodire, and a species of *Uranolophus* Denison, 1968.

The Water Canyon Formation was deposited within a restricted coastal embayment along the northwest coast of the Old Red Sandstone continent. Restrictive conditions are thought to be the result of paleogeographic features such as the orientation of the basin, the position of the Tooele Arch, which flanked the southern margin of the basin, and the probable existence of a barrier along the basin's oceanward margin. The Card Member represents hypersaline, peritidal deposition and includes mainly subtidal to intertidal lithologies, although some supratidal lithologies are recognized. The Grassy Flat Member records fluvial influences and hyposaline conditions such as prodelta, delta, marginal delta basin, distributary channel, and estuarine sediments many of which record tidal influences (Reed, 1997).

Due to the lack of age-diagnostic invertebrates the Water Canyon Formation has been assigned a variety of ages, from the Upper Silurian to the Middle Devonian, since its initial description (Williams and Taylor, 1964; Johnson and Sandberg, 1977; Johnson et al., 1988; Elliott and Ilyes, 1996; Elliott and Johnson, 1997; Elliott et al., 2000). Temporal control was placed on the formation by Elliott and Johnson (1997), who correlated the vertebrate fauna at the base of the Grassy Flat Member to the basal Lippincot Member of the Lost Burro Formation of Death Valley, California, the Sandy Member of the Sevy Dolomite in east-central Nevada (Davis, 1983), and the Beartooth Butte Formation of Beartooth Butte in northern Wyoming (Dehler, 1995). The Beartooth Butte Formation has a spore determination of middle to late Emsian (Tanner, 1983) and thus provides the basis for an Emsian date for the lower part of the Grassy Flat Member. Reed (1997) has confirmed this age by the correlation of transgressive-regressive cycles through the Water Canyon Formation to those established for the Devonian of Euramerica by Johnson et al. (1985). In addition to placing more accurate temporal constraints on the formation as a whole the eustatic data suggests that the Card Member may be Pragian, although there is no supporting paleontological evidence, and that the upper part of the Grassy Flat Member is Eifelian to possibly earliest Givetian. The latter is supported by the presence of a species of *Asterolepis* Eichwald, 1840, osteolepids, *Holoptychius* Agassiz, 1839, and the pteraspid *Psephaspis williamsi* Ørvig, 1961, all of which are indicators of the Middle Devonian (Elliott and Johnson 1997; Elliott et al., 2000). The overlying Hyrum Dolomite provides an upper age constraint as it is dated to the early Givetian based on the presence of the *Stringocephalus* biozone near its base (Stokes, 1986; Johnson et al., 1988).

Materials and Methods

The material consists of disarticulated cranial and post-cranial material preserved in a silty dolostone. The specimens were prepared mechanically using a vibrotool with a tungsten-carbide bit. The specimens are deposited in the collections of the University of Kansas Museum of Natural History, and bear their catalog numbers (prefixed KUVP). Phylogenetic analyses were conducted using PAUP* (v.4.0b10, Swofford, 2002). Data was based on the published matrix of Dupret et al. (2009) with the addition of *Bryantolepis williamsi* n. sp. and new scoring for their characters 1–4. Characters were considered unordered with a heuristic search conducted using a random-addition sequence with ten repetitions (holding 100 trees).

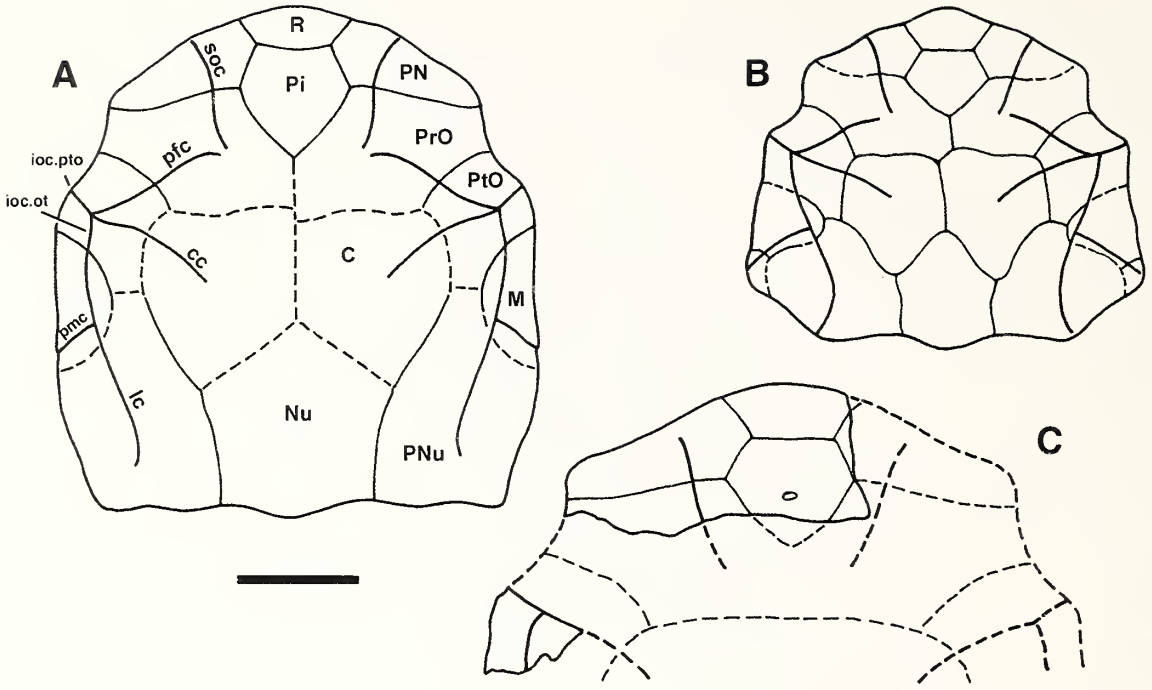

Figure 2. Reconstructions of the skulls of *Bryantolepis* species drawn to the same scale. A, *Bryantolepis williamsi* n. sp. B, *Bryantolepis brachicephala*. C, *Bryantolepis* sp. (B and C redrawn from Denison, 1958). Key: cc, central-canal groove; C, central plate; ioc.ot, otic branch of the infraorbital-canal groove; ioc.pto, postorbital branch of the infraorbital-canal groove; lc, lateral-canal groove; M, marginal plate; Nu, nuchal plate; PNu, paranuchal plate; pfc, profundus-canal groove; P, pineal plate; PN, postnasal plate; pmc, postmarginal-canal groove; PrO, preorbital plate; PtO, postorbital plate; R, rostral plate; soc, supraorbital-canal groove. Scale bar equals 1 cm.

Systematic Paleontology

Class Placodermi M'Coy, 1848
Order Arthrodira Woodward, 1891
Suborder "Actinolepidoidei" Miles, 1973
UNNAMED FAMILY
Genus *Bryantolepis* Camp, Welles, and Green, 1949

Diagnosis

Preorbital plates wide, deeply notched anteriorly by a very large pentagonal pineal plate. Postnasal plates large and together with rostral and pineal plates fused to the rest of the cranial roof. Distinct profundus sensory-canal grooves extend from the preorbital to the postorbital plates.

Type species

Bryantolepis brachycephala (Bryant, 1932).

Remarks

Bryantolepis was originally named *Euryaspis* Bryant, 1932, and described from material from the Lower Devonian Beartooth Butte Formation at Beartooth Butte, Wyoming. *Bryantolepis brachycephala*, the type species (Figure 2B), was considered by Denison (1958, 1978) to be the only valid species, as *B. obscurus* Bryant, 1934, and *B. cristata* Bryant, 1934, are doubtfully distinct and are considered to be conspecific with *B. brachycephala*; and *B. major* Bryant, 1935, was based on a specimen that was considered to be cranial but is probably an imperfectly preserved median dorsal of *Anarthraspis* Bryant, 1934 (Denison, 1958). The only other *Bryantolepis* specimen reported comes from the Water Canyon Formation at Green Canyon near Logan, Utah (Denison, 1958, p. 492–493; Figure 2C). This specimen is the poorly preserved anterior part of a skull roof showing the rostral, pineal, and postnasal plates, and parts of the preorbital and postorbital plates. The large five-sided pineal plate and the large and wide postnasal plate show that this is *Bryantolepis*, but it is considerably larger than the type species (Figure 2B) and so was attributed only to *Bryantolepis* sp. by Denison (1958).

Bryantolepis williamsi n. sp.
Figures 2A, 3–7, 9–10

Diagnosis

Large species of *Bryantolepis* in which the nuchal and paranuchal plates are longer than broad resulting in a cranial roof that is also longer than broad.

Remarks

The incomplete anterior part of a *Bryantolepis* skull roof also collected from Green Canyon and described as *Bryantolepis* sp. by Denison (1958) is close in size and proportions to the type skull described here. Although slightly larger, it is assumed that this specimen is also an example of *Bryantolepis williamsi* n. sp.

Etymology

Named after Michael E. Williams, in recognition of his important contributions to our understanding of early vertebrates.

Holotype

University of Kansas Natural History Museum No. KUVP 141304 is a complete skull roof (Figure 3).

Horizon

All specimens are from the lower part of the Grassy Flat Member of the Water Canyon Formation, Green Canyon, northern Utah, and St. Charles, southern Idaho.

Additional material

KUVP 141305, the rostral part of a skull roof (Figure 2) associated with the type specimen; KUVP 141307, a right suborbital plate (Figure 4); KUVP 141308, a skull roof preserving the endocranium (Figures 5–7, 9); KUVP 141306, a right anterior-lateral plate with attached anterior ventral, interolateral, and spinal plates (Figure 10).

Description

Skull roof

The skull is represented by one complete skull roof preserved in dorsal view and associated with the incomplete rostral area of a separate skull (Figures 2A, 3), and a skull with endocranium preserved in ventral view (Figures 5–7, 9). The skull roof is broad and rounded anteriorly and the two complete skull roofs are both 40 mm in length and 36 mm in width. The dermal plates of the skull roof can be identified in much of the type specimen (Figures 2A, 3A) although the central part of this skull roof is weathered, making it difficult to delineate the plate margins in that area.

The rostral part of the skull is fused to the rest of the cranial roof, as is characteristic of *Bryantolepis*. Slight etching of this area due to weathering in the type specimen and the associated fragment has picked out marginal bands around the rostral, pineal, and postnasal plates that presumably relate to slight differences in composition as the plates grew marginally (Figure 3A). This complex of plates is essentially as in *B. brachycephala* and the pineal plate shows the pentagonal shape that is characteristic of the genus, although it appears to be a little more elongated than in the type species. The post-pineal part of the skull is clearly more elongated than in the type species, however, with the nuchal and paranuchal plates being proportionally much more elongated (Figures 2A, 3A; contrast with Figure 2B).

As is characteristic of the genus, distinct profundus sensory-canal grooves (pfc) extend from the preorbital to the postorbital plates. Grooves for the supraorbital canals (soc) traverse the postnasal plate and terminate at the ossification center of the preorbital plates. Four sensory grooves radiate from the ossification center of the postorbital plates: profundus sensory canal (pfc), postorbital (ioc.pto) and otic (ioc.ot) branches of the infraorbital canals, and central canals (cc). The otic branches of the infraorbital canals terminate at the ossification center of the marginal plates. From this point, grooves for the postmarginal canals (pmc) extend to the skull roof margin. The lateral-line canals (lc) extend posteriorly and terminate within the paranuchal plates rather than transecting the posterior margin as in the type species (Figures 2A, B, 3B).

Suborbital plate

A single right suborbital plate, incomplete anteriorly and preserved with the internal face visible, is included within the material of the new species (Figure 4). It shows a slight notch in the dorsal margin near its anterior edge that represents the position of the infraorbital canal that runs from this point below the orbital notch on the external surface. A postocular crista (cr.po) is present. Posteriorly, there is a contact face for the postsuborbital plate (cf.PSO). The overall shape for the suborbital plate accords well with that of *B. brachycephala* (Denison, 1958, fig. 106C).

Parasphenoid

A partial parasphenoid showing the ventral surface is still attached to the endocranium on KUVP 141308 (Figures 5–7). As preserved it shows the left side and is irregularly ovate in outline and gently concave. The entire surface of the bone is covered with small closely packed tubercles. It would be expected that the buccohypophysial duct should perforate the center of the bone as in other described examples; however, although there is a depression near the posterior median margin it appears to be floored with tubercles, and damage to the midline of the bone has destroyed other possible sites for this feature. An attempted reconstruction of the endocranium and associated features, accomplished by mirror-imaging the left side, shows the parasphenoid to be ovate, wider than long and gently concave (Figure 7). No paired lateral indentations or grooves are present although this feature is reported in other parasphenoids (Dennis-Bryan, 1995). In comparison to other described parasphenoids this is a large bone in relation to the size of the skull.

Dennis-Bryan (1995) noted descriptions of the parasphenoid in 33 arthrodire genera but pointed out that the number of specimens is small with only one or two examples for each species. This paucity of information is particularly true for actinolepidoids with parasphenoids having been described from only two genera. Stensiö (1963b) described *Kujdanowiaspis* as having a parasphenoid whose ventral surface is entirely covered by tubercles and with a large undivided median buccohypophysial foramen. The parasphenoid outline is oblong and longer than wide with a median notch on each side; however, the outline is uncertain (indicated by Stensiö's use of a dashed line for the reconstructed margin, e.g., Stensiö, 1963b, fig. 10A). The parasphenoid of *Lehmanosteus hyperboreus* Goujet, 1984 (fig. 107), is similar to that of *Kujdanowiaspis* in that the ventral surface is covered by tubercles and has a single buccohypophysial foramen at its center. It is wider than long, however, and has a pentagonal outline. Dennis-Bryan (1995) concluded that parasphenoids are species specific and show no feature or character that is specific to a higher taxon. However, she also noted that "primitive" and "advanced" parasphenoid types had been recognized in the past (Gardiner and Miles, 1990). The "primitive" type is usually flat and without notches or grooves; the ventral surface is covered with tubercles and there is a large medial buccohypophysial foramen, which may be single or paired. The "advanced" type is thicker, with lateral notches and grooves and the buccohypophysial foramina reduced; tubercles are reduced or absent, and a well-developed median crest is developed.

This specimen adds a third actinolepidoid species to those for which the parasphenoid is known. It appears to be "primitive" in structure, despite the lack of a recognizable buccohypophysial foramen, but it provides no new characters that indicate taxonomic value beyond the species level.

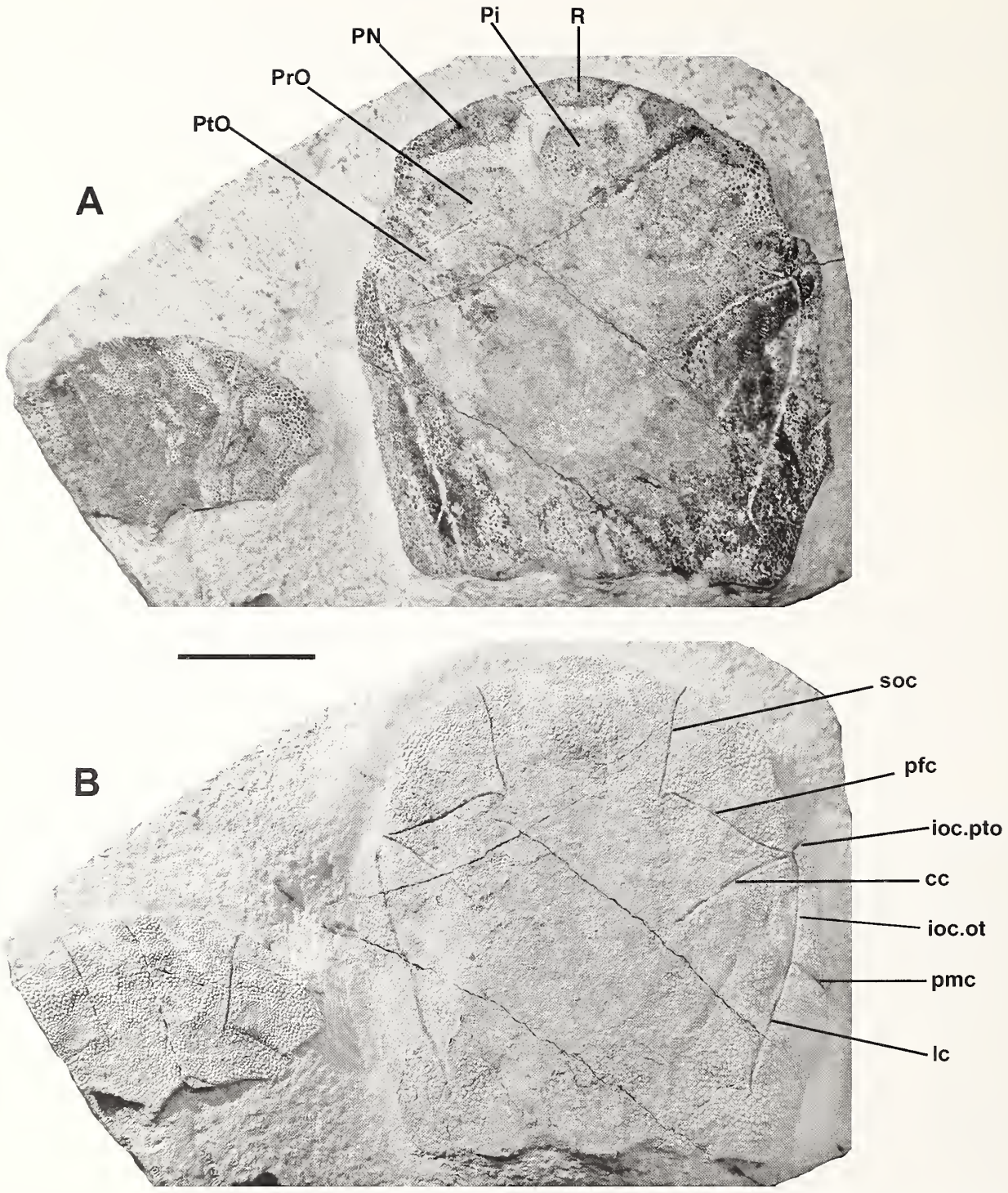

Figure 3. *Bryantolepis williamsi* n. sp. Holotype skull roof, KUVP 141304, and rostral area of a second skull, KUVP 141305. A, uncoated to show the plates of the anterior part of the skull; B, coated with ammonium chloride to show the sensory canals. Key as in Figure 1. Scale bar equals 1 cm.

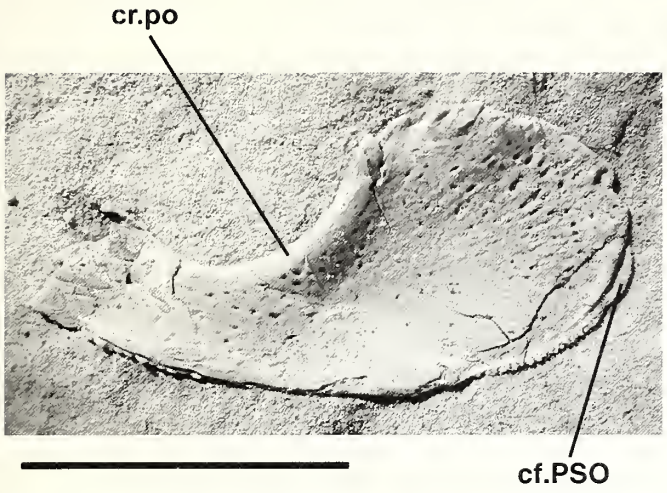

Figure 4. *Bryantolepis williamsi* n. sp. Right suborbital plate, KUVP 141307, in visceral view. Key: cr.po, postocular crista; cf.PSO, contact face for postsuborbital plate. Scale bar equals 1 cm.

Gnathal element

The left anterior superognathal is attached to the anterior part of a ridge developed on the ethmoid region of the endocranium (Figures 5–7). The posterior superognathal is unfortunately missing but would have occupied a position posterior to the anterior superognathal (supported by the autopalatine portion of the palatoquadrate). The anterior superognathal is oval, and 2.0 mm long by 1.5 mm broad. It is covered by small tubercles similar in size and shape to those present over the anterior part of the parasphenoid. Tubercles become larger and taller around the anterior and medial edges of the plate, forming a raised edge. The ossification center is indicated by a cluster of the smallest tubercles. Greatest amount of growth is in the direction of the larger anterior and medial tubercles. The occlusal surface of the element is not parallel to the endocranial surface but slopes steeply dorso-medially, thus there is a thickened face anterolaterally. A few tubercles are found on this vertical face.

The superognathals are poorly known in actinolepidoids. Denison (1958) described from the Water Canyon Formation a broad elongated plate with a smooth occlusal surface and with a group of tubercles on one side. He identified this as a posterior superognathal and noted that it may have belonged to an actinolepidoid although he was not able to positively identify it. He also described an additional and smaller plate that was also smooth on its occlusal surface and that may have been an anterior superognathal (Miles, 1969). Denison (1960) identified a small gnathal plate of uncertain position from the Holland Quarry Shale where it occurs with *Proaethaspis ohioensis* (Denison, 1960). It is a broad element with a few blunt ridges and worn teeth, identified as a crushing dentition (Denison, 1960). Stensiö (1963b) described an anterior superognathal in place in a specimen of *Kujdanowiaspis* as a "comparatively high but rostro-caudally fairly thin bone" oriented transversely in the skull and with a series of small ventral tubercles along its edge. However, the condition described by Stensiö is a byproduct of weathering (D. Goujet, personal communication, 2010). Dupret (2010, p. 30) describes the anterior superognathal as a wider than long flat structure with tubercles confined to the anterior portion that he equates with a non-shearing primitive character state. This

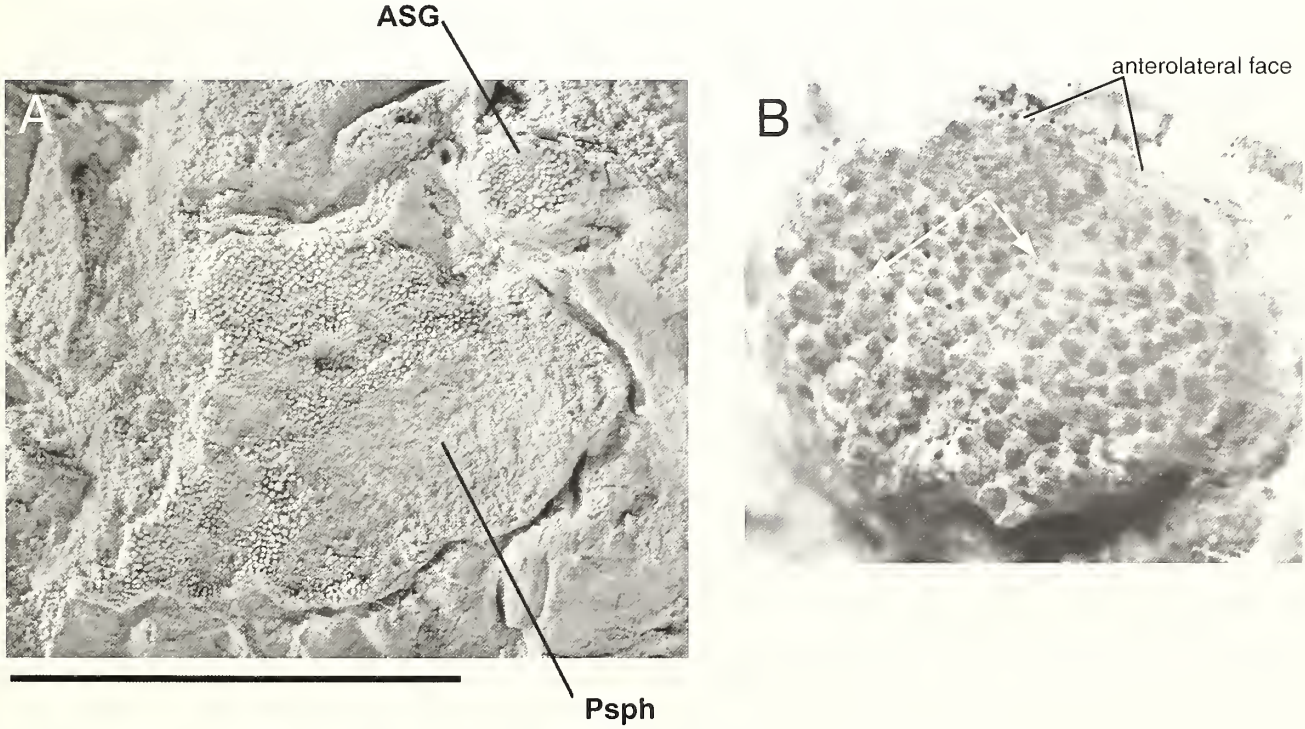

Figure 5. *Bryantolepis williamsi* n. sp. A, detail of endocranium KUVP 141308 to show the parasphenoid and anterior superognathal; B, close-up of the anterior superognathal. Arrows indicate the direction of growth from the ossification center. Additional tubercles are located on the anterolateral face. Key: ASG, anterior superognathal; Psph, parasphenoid. A, scale bar equals 5 mm.

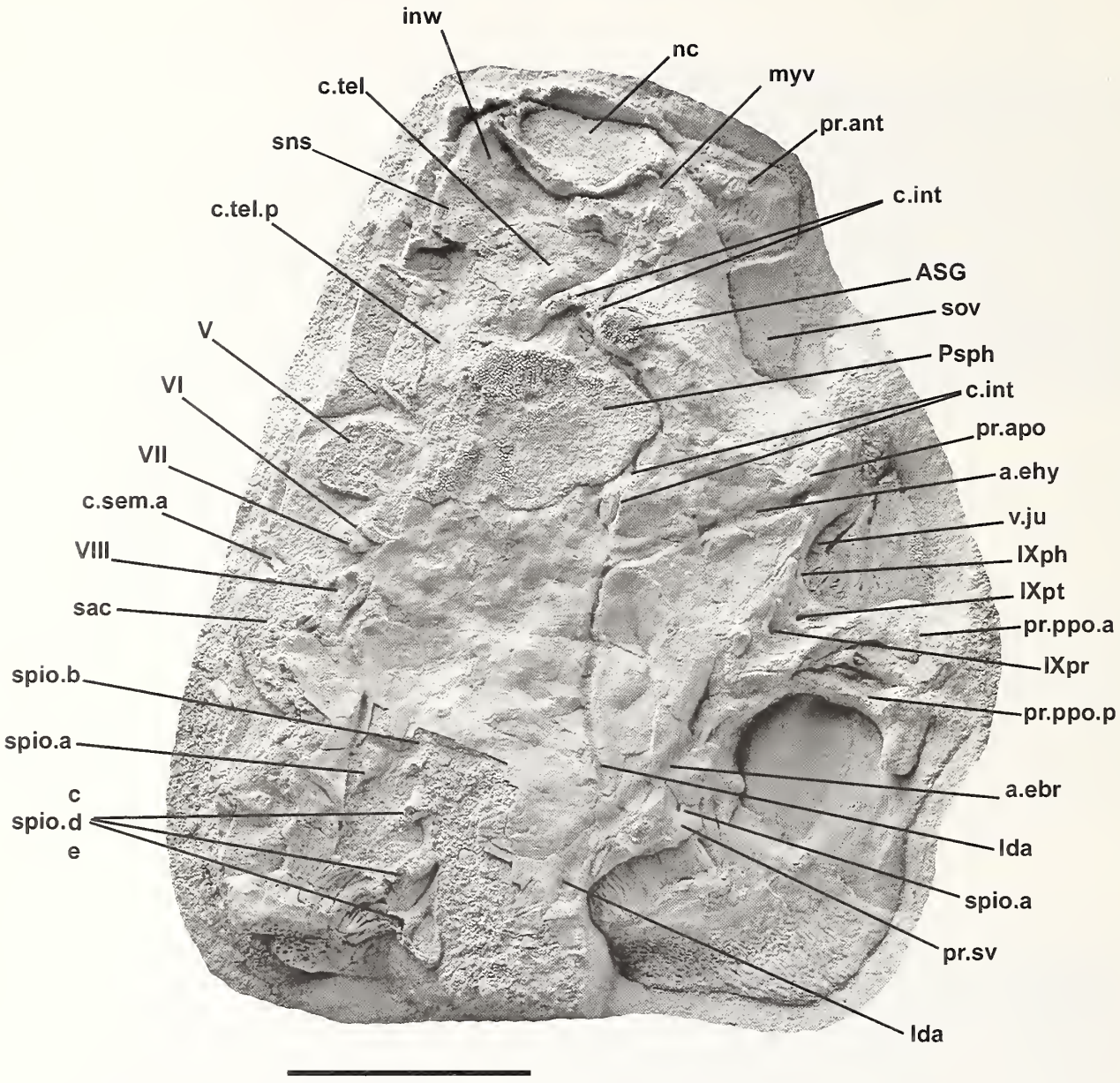

Figure 6. *Bryantolepis williamsi* n. sp. Endocranium KUVP 141308 in ventral view. Key: a.ehy, efferent hyoid artery; a.ebr, efferent branchial artery; ASG, anterior superognathal; c.int, internal carotid; c.sem.a, anterior semicircular canal; c.tel., cavity for the telencephalon; c.tel.p, cavity for posterior part of the telencephalon; inw, internasal wall; lda, lateral dorsal aorta; myv, ventral myodome of the orbit; nc, nasal capsule; pr.ant, antorbital process; pr.apo, anterior postorbital process; pr.ppo.a, anterior branch of the posterior postorbital process; pr.ppo.p, posterior branch of the posterior postorbital process; pr.sv, supravagal process; Psph, parasphenoid; sac, sacculus; sns, subnasal shelf; sov, supraorbital vault; spio.a–e, spino-occipital nerves; V, maxillary and mandibular branches of trigeminal nerve; VI, abducens nerve; VII, facial nerve; VIII, acoustic nerve; v.ju, canal for jugular vein; IXph, glossopharyngeal nerve, pharyngeal branch; IXpr, glossopharyngeal nerve, pretrematic branch; IXpt, glossopharyngeal nerve, posttrematic branch. Scale bar equals 1 cm.

appears to be the condition described here from *Bryantolepis*, although the entire plate surface is tuberculated.

The anterior superognathal of *Bryantolepis* is only the second for an actinolepidoid that is positively identified due to being attached to a skull. In contrast with that seen in more advanced forms such as *Coccosteus*, which is a shearing plate, the plate in *Bryantolepis* is clearly adapted for crushing and indicates an early development of this specialization.

Endocranium

Specimen KUVP 141308 is a skull roof exposed in ventral view and preserving the endocranium (Figure 6). Much of the right side and part of the anterior was removed by weathering prior to collection and the perichondral laminae lining the cavities and canals within the endocranium were exposed in that area. Preparation has further exposed these structures and the ventral surface of the left side of the endocranium allowing identification

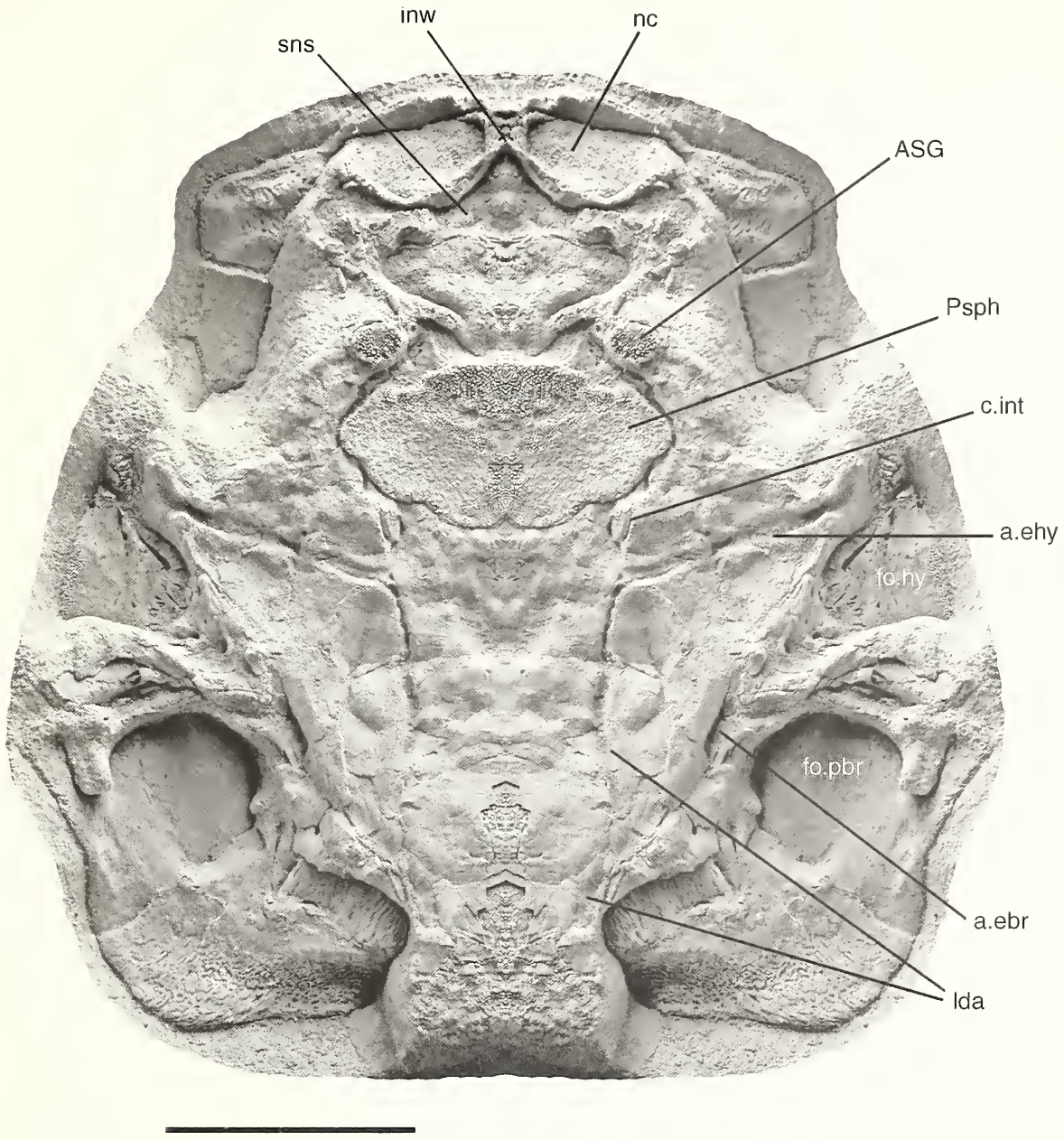

Figure 7. *Bryantolepis williamsi* n. sp. Reconstruction of the endocranium in ventral view, made by mirror-imaging the left side of the specimen as preserved. Key, as for Figure 6, plus fo.hy, hyoid muscle fossa; fo.pbr, parabranchial fossa. Scale bar equals 1 cm.

of the major features. Although generally well-preserved, the bone forming the ventral surface of the endocranium is very thin and has been crushed or distorted in some areas. An overall reconstruction has been attempted by mirror-imaging the more complete left side (Figure 7). Identification of the major features is based on the reconstructions of the endocranial cavities and canals in *Kujdanowiaspis* (Stensiö, 1963b; Dupret, 2010), and *Lehmanosteus* (Goujet, 1984) as these are the only other actinolepidoids for which such information is available. Additional information has been taken from the work of Young (1979, 1981) on *Buchanosteus* Stensiö, 1945, and *Errolosteus* Young, 1981.

The lateral wall of the endocranium is fused to the ventral surface of the dermal skull roof and forms a series of processes and embayments. The interpretation of homology for these processes and fossae and the subsequent nomenclature applied has varied (contrast Young, 1980, with Goujet, 1984, and Dupret, 2010). Interpretations by Goujet and Young (Figure 8) have differed in their interpretation of bounding foramina, differing in their identification of the foramen in the posterior part of the anterior parajugular fossa (pr.pja) in *Macropetalichthys*. Goujet (personal communication, 2010) interprets this as the glossopharyngeal foramen (IX, Figure 8B) while Young places this foramen in the posterior parajugular fossa (fo.pjp, Figure 8A). While using similar defining characteristics for the processes, it is the difference in cranial nerve sequence that leads to alternative process identifications. Although beyond the scope of the current study, resolution of these questions is important for resolving the

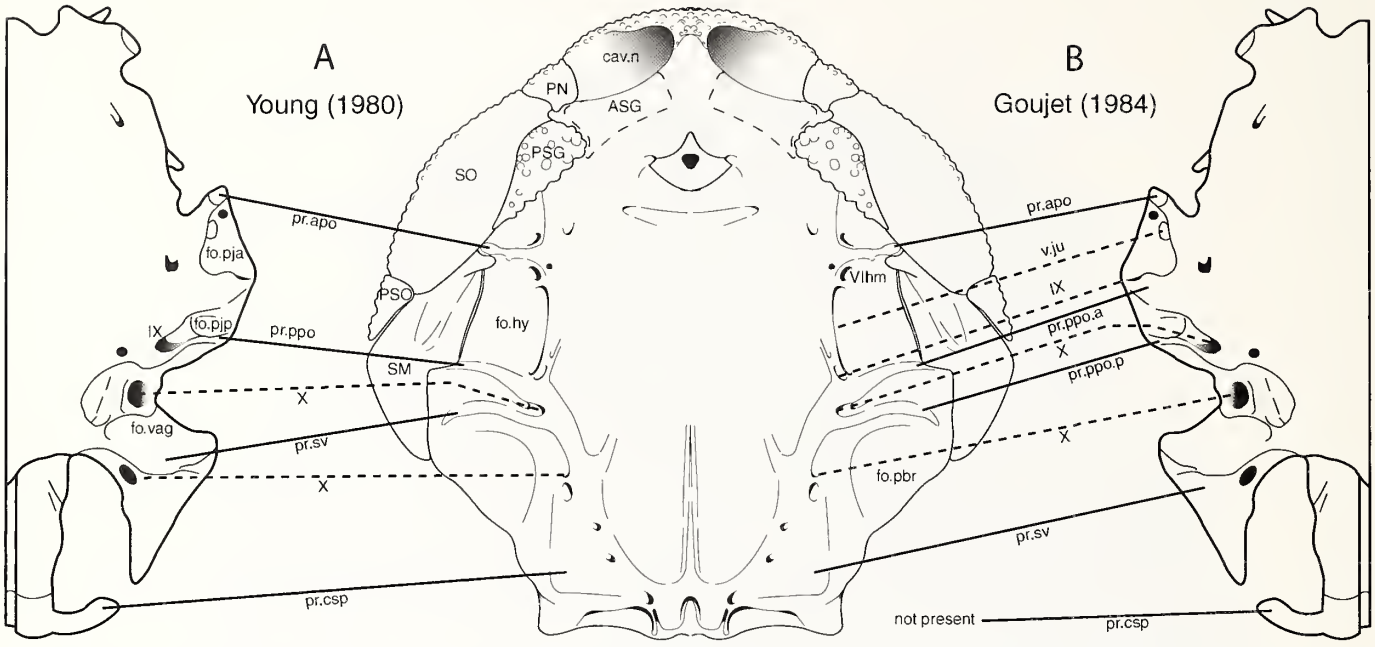

Figure 8. Proposed homologies of the processes and fossae between *Dicksonosteus* (center; after Goujet, 1984) and *Macropetalichthys* (right and left; after Young, 1980). A, interpretation after Young (1980). B, interpretation after Goujet (1984). Solid lines for processes, dashed lines for foramina. Key: as for Figure 6, plus fo.pja, anterior parajugular fossa; fo.pjp, posterior parajugular fossa; fo.vag, vagus fossa; PN, postnasal plate; pr.csp, craniospinal process; pr.ppo, posterior postorbital process; PSG, posterior superognathal plate; PSO, postsuborbital plate; SM, submarginal plate; SO, suborbital plate; VIIhm, hyomandibular branch of the facial nerve foramen.

content and function for the processes and bounded fossae (viseeral arch attachments, muscle insertions, and branchial and parabranchial chambers). Nomenclature in this study follows that of Goujet (1984) and Dupret (2010) (both interpretations are presented, without favor, to permit comparison of the condition in *Bryantolepis williamsi* n. sp. to other described taxa). An interpretive reconstruction of the endocranial cavities and canals is provided (Figure 9). Posteriorly the supravagal process (pr.sv, Figures 6, 9) has been somewhat crushed and little detail can be seen. Its posterior limits can be discerned on the right side. The surface of the endocranium and the skull roof in this area is roughened and pitted presumably for muscle attachment. Anterior to this a broad parabranchial fossa (sensu Carr et al., 2009; cucullaris fossa sensu Goujet, 1984) is recessed into the endocranial wall and is delimited anteriorly by the posterior postorbital process, which forms a conspicuous lateral feature. This process is bifid (pr.ppo.a, pr.ppo.p) as in the actinolepidoids *Kujdanowiaspis* (Stensiö, 1963b, fig. 41) and *Lehmanosteus* (Goujet, 1984, fig. 107), but unlike the brachythoracid *Buchanosteus* (Young, 1979, fig. 2), which has a single process only. Young (1979, p. 315–316) has suggested that the anterior branch of this process is homologous to the postorbital process in *Buchanosteus* and that the posterior branch is homologous to the supravagal process in *Macropetalichthys* Norwood and Owen, 1846 (Stensiö, 1969, fig. 22A). Based on this he concludes that the fossa enclosed by the branches is homologous to the paravagal fossa of *Macropetalichthys* (Figure 8A), that it contained muscles controlling the operculum, and that its presence may be associated with the presence of a large submarginal plate, considered to be a primitive feature. Although the submarginal plate is not known in *Bryantolepis williamsi* n. sp. it is reconstructed as a large plate in the only other species *B. brachycephala* (Denison, 1962, fig. 57; Denison, 1978, fig. 34; apparently based on a composite reconstruction using cheek plates identified as "Arctolepida indet.," Denison, 1958, fig. 103C, D). The presence of an internal groove, suggestive of a groove for the epihyal, implies that the submarginal as reconstructed by Denison, 1978, fig. 34, is anteroposteriorly reversed. Following Young (1980), the reduced vagal fossa (fo.vag, Figure 8) in *Bryantolepis williamsi* n. sp. implies a reduced musculature for a relatively large operculum.

Between the posterior (pr.ppo) and anterior (pr.apo) postorbital processes is a short hyoid muscle fossa (fo.hy, Figure 8). The lateral wall of this fossa contains foramina for the pharyngeal, pre-, and posttrematic branches of the glossopharyngeal nerve (IXph, IXpt, IXpr, Figures 6, 9). A foramen and short groove in this area probably represents the position of the canal that bore the jugular vein (v.ju, Figure 6). Anterior to the anterior postorbital process the endocranium is crushed and the mandibular fossa cannot be recognized, however, there is a deep orbital cavity roofed by the dermal bone of the skull roof.

The ventral surface of the endocranium is marked by a series of branching grooves, best seen on the left side (Figures 6, 7). These represent the position of the two lateral vessels of the dorsal aorta (lda) and its branches, which proceed anteriorly. That on the left can be followed to the level of the supravagal process at which point the lateral aorta continues anteriorly while the efferent branchial artery (a.ebr) branches off laterally and runs parallel to the margin of the parabranchial fossa (fo.pbr). The anterior portion of the lateral dorsal aorta divides again at the level of the hyoid muscle fossa. At this point the efferent hyoid artery (a.ehy) branches laterally and continues along the ventral surface of the anterior postorbital process, while the internal carotid artery

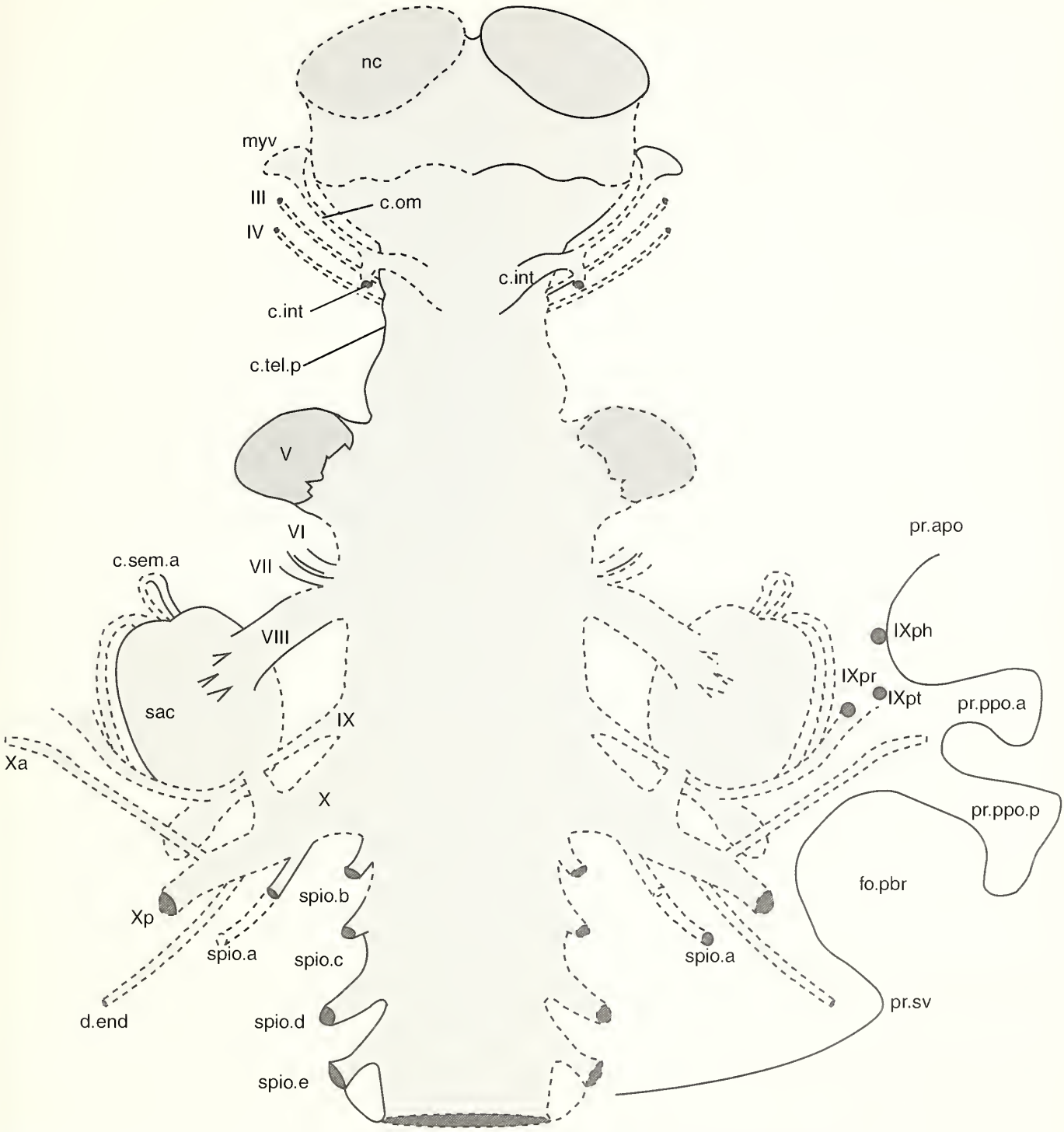

Figure 9. Proposed reconstruction of the cranial endocast in *Bryantolepis williamsi* n. sp. Based on the endocranium in KUVP 141308 (Figure 6). Solid lines represent preserved structures. Dashed lines represent hypothesized features. Reconstruction of hypothetical features are based on *Kujdanowiaspis* (Goujet, 1984, fig. 29). Known structures, limited to the right or left, are reconstructed on the opposite side as mirror-images. The posterolateral outline of the neurocranium is shown for the left side to provide a reference for known foramina. The posterior extent of the supravagal process is based on its fragmented presence on the right side and on impressions of the process on the internal face of the dermal skull roof. Key: as for Figure 6, plus III, occulomotor nerve; IV, trochlear nerve; c.om, canal for the opthalmica-magna artery; Xa, anterior branch of the vagus nerve; Xp, posterior branch of the vagus nerve; d.end, endolymphatic duct.

(c.int) runs anteriorly before entering a foramen and running a short distance in a canal which vanishes dorsal to the lateral margin of the parasphenoid (Psph). In *Lehmanosteus* (Goujet, 1984, fig. 107) and *Kujdanowiaspis* (Stensiö, 1963b, fig. 14) the internal carotid apparently continued in a groove lateral to the parasphenoid, however, the parasphenoid in *Bryantolepis williamsi* n. sp. is a large plate leaving no lateral space for this to happen.

Other structures on the ventral surface of the endocranium include the previously described parasphenoid and left anterior superognathal (Figure 6, Psph, ASG) and anterior to them the left nasal capsule (nc). Although partly removed by weathering it shows an oval cavity walled by the dermal rostral bone anteriorly but posteriorly by a thin wall of perichondral bone. Medially part of the internasal wall is preserved (inw). This rises medially suggesting the presence of a median ridge (Figure 7) and where exposed laterally by weathering it is seen to lie ventral to the dermal rostral bone. Posterior to the nasal capsule the subnasal shelf (sns) appears to meet the ossification surrounding the telencephalon (c.tel) along a sinuous margin. The connection between this and the nasal capsule is through the olfactory tract and bulb, neither of which is visible here. A crushed area posterolateral to the nasal capsule and triangular in shape may represent the position of the ventral myodome in the orbit (myv, Figures 6, 9). On the posterolateral surface of the telencephalon and anterior to the parasphenoid a canal rises and continues anterolaterally. This is the canal for the internal carotid artery (c.int), which subsequently divides in *Kujdanowiaspis* (Stensiö, 1963b; fig. 30) to form the canal for the opthalmica-magna artery (Young, 1979, p. 329; c.om, Figure 9), which then leads into the ventral myodome. Unfortunately this area has been crushed and weathered so that the canal cannot be traced into the myodome, however, a small foramen just anteromedial to the anterior superognathal leading into a canal that lies medial to the superognathal may be the branch of the internal carotid that connects posteriorly, dorsal to the lateral margin of the parasphenoid.

The right side of the endocranium was weathered obliquely, almost to the midline anteriorly, and a little less posteriorly, exposing the perichondral laminae lining the cavities and canals within the endocranium (Figures 6, 9). Posteriorly five canals in series can be seen projecting from within the endocranium and these appear to be canals surrounding five spino-occipital nerves (spio.a–e). The foramina for these nerves should be visible in the surface of the supravagal process on the left side but crushing and loss has obscured all but one (spio.a). The canal for the anterior spino-occipital nerve on the right side is in close-proximity to the vagal recess (not preserved). This position could imply that the anterior spino-occipital nerve may be associated with the vagus nerve, possibly a posterior lateral-line nerve. On the left side the foramina for the pretrematic and posttrematic branches of the glossopharyngeal nerve can be seen on the anterior surface of the base of the posterior postorbital process (IXpr, IXpt). The foramen for the pharyngeal branch is present in the lateral wall of the hyoid muscle fossa (IXph). At the level of the posterior postorbital process, on the right side, a part of the labyrinth cavities is preserved. This is an oval structure that represents the cavity for the sacculus (sac). The external semicircular canal has been eroded but a short section of canal that leads anterolaterally from the sacculus probably represents part of the anterior semicircular canal (c.sem.a), which would then continue dorsally. The canal for the acoustic nerve (VIII, Figures 6, 9) is visible and has a branching connection to the sacculus. None of the ampullae have been preserved.

The canals for the facial and abducens nerves (VII, VI, Figures 6, 9) can be traced just anterior to that for the acoustic nerve. Anterior to these and lateral to the posterior part of the parasphenoid is a large canal preserved at its branch from the cranial cavity which from its position is most likely to be the canal for the maxillary and mandibular branches of the trigeminal nerve (V). The canal for the pituitary vein is a large ossified structure in *Buchanosteus* (Young, 1979, fig. 6) but appears to be much smaller in actinolepidoids such as *Kujdanowiaspis* (Stensiö, 1963b, fig. 30) where it is not carried in an ossified canal. Canals for the oculomotor (III) and trochlear (IV) nerves should be present at the level of the anterior part of the parasphenoid but cannot be seen here (reconstructed in Figure 9). In this region the lateral portion of the posterior part of the telencephalon (c.tel.p) can be seen.

The endocranium of actinolepidoids is well known from the work of Stensiö (1963b) in which specimens of *Kujdanowiaspis* were serially sectioned to provide an immense amount of information on the shape of the cranial cavity and the position of canals and foramina for the cranial nerves and vessels. The only additional information on the eranial anatomy of an actinolepidoid comes from specimens of *Lehmanosteus* (Goujet, 1984, fig. 107) in which the ventral surface of the endocranium was preserved. The endocranium of *Bryantolepis williamsi* n. sp. is in accord with the information known for the other actinolepidoids, differing only in the greater clarity of the grooves and canals for blood vessels on the ventral surface of the endocranium, which allows a more complete pieture of their distribution to be seen and shows that the internal carotid is present in a canal dorsal to the lateral margin of the parasphenoid in this species.

Trunk shield

The only trunk shield material (KUVP 141306) consists of a single specimen found in association with the type skull and comprising the right anterior ventrolateral, anterior-ventral, interolateral, and spinal plates (Figure 10). These are essentially as in the described species *B. brachycephala* (Denison, 1958, fig. 112G) with the only important difference being that the new specimen is almost twice as large.

Actinolepidoid Relationships

The order Arthrodira has been divided into two main complexes, the "dolichothoracids" with a long trunk armor and the "brachythoracids" with a short armor (Stensiö, 1944). The dolichothoracids are now considered not to be a natural group but one that represents an evolutionary grade (Goujet, 1984) and that consists of two subgroups, the Actinolepidoidei Miles, 1973, and the Phlyctaenii Miles, 1973. The actinolepidoids have been considered a clade by some workers (Long, 1984, his Actinolepidi + Wuttagoonaspidi + Phyllolepidi), and this was assumed by Johnson et al. (2000) in their first cladistic analysis of the group. Although they selected the Petalichthyida as the outgroup they had only the actinolepidoids as the ingroup making it impossible to test actinolepidoid monophyly (Dupret, 2004). Analyses by Dupret and Dupret and others incorporated characters from a new description of *Kujdanowiaspis* (Dupret, 2004) and a basal member of the Actinolepidoidei (Dupret et al., 2009), as well as the best-known actinolepidoids together with phlyctaeniids and brachythoracids. These analyses showed that the "Actinolepidoi-

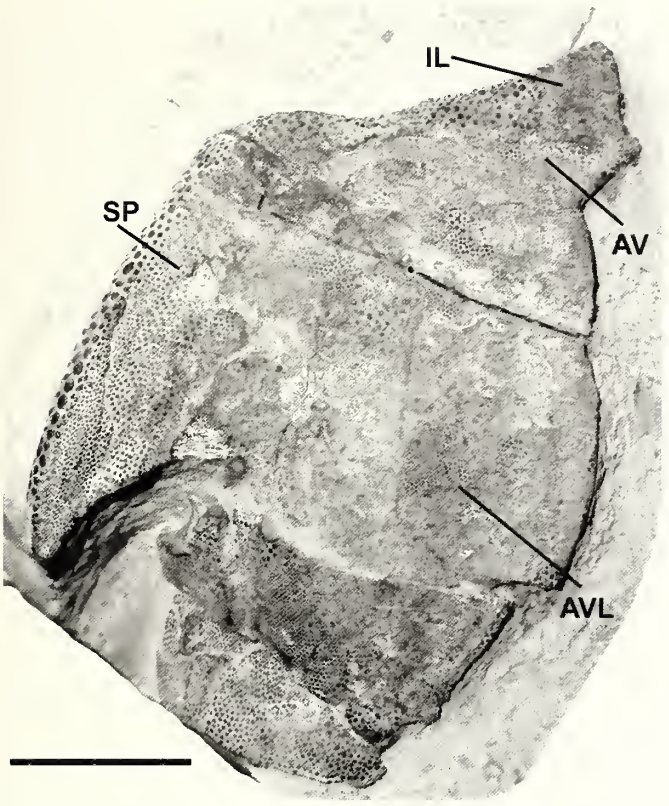

Figure 10. *Bryantolepis williamsi* n. sp. Right anterior part of ventral armor, KUVP 141306. Key: AV, anterior-ventral plate; AVL, anterior ventrolateral plate; IL, interolateral plate; SP, spinal plate. Scale bar equals 1 cm.

dei" is a paraphyletic group (with or without *Wuttagoonaspis* and/or the phyllolepids) and that the Wuttagoonaspididae and the paraphyletic antarctaspids represent the basal-most members of the Arthrodira (Dupret, 2009, fig. 3; Figure 1).

Bryantolepis brachycephala, the previously only known species, is shown in the latter analysis to be an isolated taxon forming a sister group to the Phlyctaenioidei (Dupret, 2009, fig. 3; Figure 1). The new species of *Bryantolepis* described here adds nothing to knowledge of the external morphology of the genus, however; Dupret (2004) developed four characters for the endocranium that could not be scored for *Bryantolepis* at the time of the analysis but can be assessed now.

Character 1 is "Connection between endocranial ethmoid and postethmoid components. 0: no connection; 1: connection produced by osseous trabecules or fusion." It is noted (Dupret, 2004) that no connection is observed in all major groups of arthrodires, and preservation is not complete enough to show what the situation is in *Bryantolepis williamsi* n. sp. (scored as ?). Character 2 is "Anterior postorbital process. 0: massive; 1: thin." The description of this character was clarified by Dupret et al. (2009) to note the position of the hyomandibular branch of the facial nerve ("0: foramen in the distal part of the anterior postorbital process" and "1: foramen in a proximal and posterior position"). It is the position of this nerve that correlates with a massive process (D. Goujet, personal communication, 2010; compare Goujet, 1984, figs. 51 and 52, *Dicksonosteus* and *Kujdanowiaspis*, respectively). The new specimen is preserved in ventral view and the anterior postorbital process does appear to be massive based on its similarity in size to that of *Kujdanowiaspis* (Stensiö, 1963b, fig. 25) (scored as 0). Character 3 is "Supraorbital process. 0: absent; 1: present." This process is present only in actinolepidoids (Goujet, 1984) but is not exposed in the new specimen (scored as ?). Character 4 is "Basal process. 0: absent; 1: present." This process is again only present in actinolepidoids and can be seen in the new specimen (scored as 1).

Adding the new scoring to the matrix of Dupret et al. (2009) for *B. brachycephala* (assuming that characters 2 and 4 of *Bryantolepis williamsi* n. sp. are consistent within the genus) and running the analysis does not result in any change to the position of *Bryantolepis* in the published tree (Dupret et al., 2009, fig. 3; Figure 1). Due to missing data for *Bryantolepis williamsi* n. sp. (characters 17, 18, 29, 30, 36, 42, 43, 46–48, 51–54, 59–62, and 64–65; most related to incomplete knowledge of the trunk shield), addition of this taxon to the analysis reduces the resolution of tree topology only in the case of *Bryantolepis* (individual species form a polytomy with the Phlyctaenioidei, Actinolepididae, and node "**" of Figure 1 [node 8 of Dupret et al., 2009, fig. 3]).

Acknowledgments

We would like to thank Daniel Goujet for his early and final reviews, the anonymous reviewer, and Sandy Swift for doing the photography and assembling the plates.

References

Agassiz, L. J. R. 1839. Fishes of the Old Red Sandstone, p. 589–602. *In* R. I. Murchison, The Silurian System, Part II. John Murray, London.

Branson, E. B., and M. G. Mehl. 1931. Fishes of the Jefferson Formation of Utah. Journal of Geology, 39:509–531.

Bryant, W. L. 1932. Lower Devonian fishes of Bear Tooth Butte, Wyoming. Proceedings of the American Philosophical Society, 71:225–254.

Bryant, W. L. 1934. The fish fauna of Beartooth Butte, Wyoming: Parts II and III. Proceedings of the American Philosophical Society, 73:127–162.

Bryant, W. L. 1935. *Cryptaspis* and other Lower Devonian fossil fishes from Beartooth Butte, Wyoming. Proceedings of the American Philosophical Society, 75:111–128.

Camp, C. L., S. P. Welles, and M. Green. 1949. Bibliography of fossil vertebrates, 1939–1943. Geological Society of America Memoir 37. 371 p.

Carr, R. K., Z. Johanson, and A. Ritchie. 2009. The phyllolepid placoderm *Cowralepis mclachlani*: insights into the evolution of feeding mechanisms in jawed vertebrates. Journal of Morphology, 270:775–804.

Davis, R. L. 1983. Geology of the Dog Valley-Red Ridge area, southwest Pavant Mountains, Millard County, Utah. Brigham Young University Geology Studies, 30:19–36.

Dehler, C. M. 1995. Paleoenvironmental and stratigraphic analysis of Lower Devonian Beartooth Butte Formation and associated strata, central-eastern Idaho. Unpublished master's thesis, Northern Arizona University, Flagstaff. 157 p.

Denison, R. H. 1953. Early Devonian fishes from Utah. Part II. Heterostraci. Fieldiana: Geology, 11:199–355.

Denison, R. H. 1958. Early Devonian fishes from Utah, Part III, Arthrodira. Fieldiana: Geology, 11:461–551.

Denison, R. H. 1960. Fishes of the Devonian Holland Quarry Shale of Ohio. Fieldiana: Geology, 11:555–613.

Denison, R. H. 1962. A reconstruction of the shield of the arthrodire, *Bryantolepis brachycephalus* (Bryant). Fieldiana: Geology, 14:99–104.

Denison, R. H. 1968. Early Devonian lungfishes from Wyoming, Utah, and Idaho. Fieldiana: Geology, 17:353–413.

Denison, R. H. 1978. Handbook of Paleoichthyology 2, Placodermi. H-P. Schultze (ed.), Gustav Fischer Verlag, Stuttgart. 128 p.

Dennis-Bryan, K. 1995. Some comments on the placoderm parasphenoid. Bulletin du Muséum National d'Histoire Naturelle, 17:127–142.

Dupret, V. 2004. The phylogenetic relationships between actinolepids (Placodermi: Arthrodira) and other arthrodires (phlyctaeniids and brachythoracids). Fossils and Strata, 50:44–55.

Dupret, V. 2010. Revision of the genus *Kujdanowiapis* Stensiö, 1942 (Placodermi, Arthrodira, "Actinolepida") from the Lower Devonian of Podolia (Ukraine). Geodiversitas, 32:5–63.

Dupret, V., Z. Min, and J.-Q. Wang. 2009. The morphology of *Yujiangolepis liujingensis* (Placodermi, Arthrodira) from the Pragian of Guangxi (south China) and its phylogenetic significance. Zoological Journal of the Linnean Society, 157:70–82.

Eichwald, C. E. von. 1840. Die Their- und Pflanzenreste des alten rothen Sandsteins und Bergkalks im Novgorodschen Gouvernement. Bulletin de l'Académie Impériale des Sciences de Saint Pétersbourg, 7:78–91.

Elliott, D. K., and R. R. Ilyes. 1996. New Early Devonian pteraspidids (Agnatha, Heterostraci) from Death Valley National Monument, southeastern California. Journal of Paleontology, 70:152–161.

Elliott, D. K., and H. G. Johnson. 1997. Use of vertebrates to solve biostratigraphic problems: examples from the Lower and Middle Devonian of Western North America, p. 179–188. *In* G. Klapper, M. A. Murphy, and J. A. Talent (eds.), Paleozoic Sequence Stratigraphy, Biostratigraphy, and Biogeography: Studies in Honor of J. Granville ("Jess") Johnson. Geological Society of America Special Paper 321.

Elliott, D. K., H. G. Johnson, R. Cloutier, R. K. Carr, and E. B. Daeschler. 2000. Middle and Late Devonian vertebrates of the western Old Red Sandstone Continent, p. 291–308. *In* A. Blieck and S. Turner (eds.), Palaeozoic Vertebrate Biochronology and Global Marine/Non-Marine Correlation. Frankfurt am Main, Courier Forschungsinstitut Senckenberg, 223.

Gardiner, B. G., and R. S. Miles. 1990. A new genus of eubrachythoracid arthrodire from Gogo, western Australia. Zoological Journal of the Linnean Society of London, 99:159–204.

Goujet, D. 1984. Les poissons placodermes du Spitsberg: Arthrodires Dolichothoraci de la Formation de Wood Bay (Dévonien inférieur). Cahiers de Paléontologie, CNRS. 284 p.

Johnson, H. G., D. K. Elliott, and J. H. Wittke. 2000. A new actinolepid arthrodire (Class Placodermi) from the Lower Devonian Sevy Dolomite, east-central Nevada. Zoological Journal of the Linnean Society of London, 129:241–266.

Johnson, J. G., G. Klapper, and C. A. Sandberg. 1985. Devonian eustatic fluctuations in Euramerica. Geological Society of America Bulletin, 96:567–587.

Johnson, J. G., and C. A. Sandberg. 1977. Lower and Middle Devonian continental-shelf rocks of the western United States, p. 121–143, *In* M. A. Murphy, W. B. N. Berry, and C. A. Sandberg (eds.), Western North America: Devonian. University of California, Riverside Campus Museum Contribution 4.

Johnson, J. G., C. A. Sandberg, and F. G. Poole. 1988. Early and Middle Devonian paleogeography of western United States, p. 161–182. *In* N. J. McMillan, A. F. Embry, and D. G. Glass (eds.), Devonian of the World. Canadian Society of Petroleum Geologists Memoir 14.

Long, J. A. 1984. New phyllolepids from Victoria and the relationships of the group. Proceedings of the Linnean Society of New South Wales, 107:263–308.

M'Coy, F. 1848. On some new fossil fish of the Carboniferous period. Annals and Magazine of Natural History, 2:1–10, 115–133.

Miles, R. S. 1969. Features of placoderm diversification and the evolution of the arthrodire feeding mechanism. Transactions of the Royal Society of Edinburgh, 68:123–170.

Miles, R. S. 1973. An actinolepid arthrodire from the Lower Devonian Peel Sound Formation, Prince of Wales Island. Palaeontographica, Abteilung A, 143:109–118.

Norwood, J. G., and D. D. Owen. 1846. Description of a new fossil fish from the Palaeozoic rocks of Indiana. American Journal of Science, 2:367–371.

Ørvig, T. 1961. Notes on some early representatives of the Drepanaspida (Pteraspidomorphi, Heterostraci). Arkiv för Zoologi, 2:515–535.

Reed, R. C. 1997. Stratigraphy and sedimentology of the Lower and Middle Devonian Water Canyon Formation, northern Utah. Unpublished master's thesis, Northern Arizona University, Flagstaff. 322 p.

Stensiö, E. A. 1942. On the head of certain Arthrodires. Kungliga Svenska Vetenskapsakademiens Handlingar, 20:1–32.

Stensiö, E. A. 1944. Contributions to the knowledge of the vertebrate fauna of the Silurian and Devonian of Podolia II: notes on two arthrodires from the Downtonian of Podolia. Arkiv för Zoologi, 35A(9):1–83.

Stensiö, E. A. 1945. On the head of certain arthrodires. II. On the cranium and cervical joint of the Dolichothoraci (Acanthaspida). Kungliga Svenska Vetenskapsakademiens Handlingar, 22:1–70.

Stensiö, E. A. 1963a. The brain and cranial nerves in fossil, lower craniate vertebrates. Skrifter utgitt av Det Norske Videnskaps-Akademi i Oslo. I. Matematisk-naturvidenskapelig klasse. New Series, 13:1–20.

Stensiö, E. A. 1963b. Anatomical studies on the arthrodiran head. Part I. Preface, geological and geographical distribution, the organization of the head in the Dolichothoraci, Coccosteomorphi and Pachyosteomorphi. Taxonomic appendix. Kungliga Svenska Ventenskapsakademiens Handlingar, (4)9: 1–419.

Stensiö, E. A. 1969. Elasmobranchiomorphi Placodermata Arthrodires, p. 71–692. *In* J. Piveteau (ed.), Traité de Paléontologie, 4(2). Masson, Paris.

Stokes, W. L. 1986. Geology of Utah. Utah Museum of Natural History and Utah Geological and Mineral Survey, Salt Lake City. 280 p.

Swofford, D. L. 2002. PAUP* Phylogenetic Analysis Using Parsimony (*and other methods), Version 4. Sinauer Associates, Sunerland.

Tanner, W. 1983. A fossil flora from the Beartooth Butte Formation of northern Wyoming. Unpublished Ph.D. thesis, Southern Illinois University, Carbondale. 208 p.

Williams, J. S., and M. E. Taylor. 1964. The Lower Devonian Water Canyon Formation of northern Utah. Contributions to Geology of the University of Wyoming, 3: 38–53.

Woodward, A. S. 1891. Catalogue of the fossil fishes in the British Museum (Natural History), 2. British Museum (Natural History), London. 567 p.

Young, G. C. 1979. New information on the structure and relationship of *Buchanosteus* (Placodermi: Euarthrodira) from the Early Devonian of New South Wales. Zoological Journal of the Linnean Society, 66:309–352.

Young, G. C. 1980. A new Early Devonian placoderm from New South Wales, Australia, with a discussion of placoderm phylogeny. Palaeontographica. Abteilung A, Paläozoologie, Stratigraphie, 167:10–76.

Young, G. C. 1981. New early Devonian brachythoracids (placoderm fishes) from the Taemas-Wee Jasper region of New South Wales. Alcheringa, 5:245–271.

KIRTLANDIA
The Cleveland Museum of Natural History

November 2010 *Number 57:36–45*

PALEOECOLOGY OF *DUNKLEOSTEUS TERRELLI* (PLACODERMI: ARTHRODIRA)

ROBERT K. CARR
Department of Biological Sciences
Ohio University, Athens, Ohio 45701-2979
carrr1@ohio.edu

ABSTRACT

The Cleveland Member (Late Famennian) fish fauna represents one of the most speciose and well-collected faunas from the Late Devonian; however, our understanding of the fauna's paleoecology is limited. Published interpretations of placoderm paleoecology typically suggest that most species are obligate bottom-living forms or are tied closely to life on the bottom. *Dunkleosteus terrelli* (Newberry, 1873) (Placodermi, Arthrodira), however, was a pelagic organism. This interpretation is based on an analysis of the nature of the distal Appalachian Basin depositional habitat and the distribution of this species' remains within the basin. The species presence as fossils represents the remains of organisms that lived within the water column in the basin rather than an allochthonous accumulation of floating carcasses. Thus, the disarticulation seen in specimens of *Dunkleosteus terrelli* is a result of local post-mortem flotation and possible scavenging within the water column. This hypothesis is supported by a Chi-squared statistical analysis for the geographic distribution of *Dunkleosteus terrelli* fossil remains. Finally, estimates of dry and wet weights for *Dunkleosteus terrelli* suggest (1) an inability to rest on the bottom given the physical properties of the sediments and (2) the presence of a mechanism for static buoyancy, which would account for post-mortem flotation in a basin with published estimated depths of 30 to 100 meters.

Introduction

Our understanding of the paleoecology of Late Devonian fish faunas is limited by the lack of high diversity faunas available for analysis. The Cleveland Member (Late Famennian) fauna is one of the best known, possessing 66 species (Hlavin, 1976; Denison, 1979; Williams, 1990; Carr, 1996; Carr and Jackson, 2010) consisting of sharks (33), placoderms (28), and osteichthyans (5).

Paleoecological interpretations of the fauna historically were based on analogy to putatively similar taxa from other faunas. *Coccosteus* (Miles and Westoll, 1968), for example, is often used as an analogue to interpret other arthrodires (e.g., Heintz, 1932, p. 202, used the form of *Coccosteus* to interpret "*Dinichthys*" or *Dunkleosteus*, a comparison across subordinal-level distinct taxa). These analogies often involve the comparison of taxa from dissimilar facies and faunal compositions.

Hlavin (1976) reviewed sedimentological-depositional models to interpret the Catskill Delta and the distal black shales (the Cleveland Member of the Ohio Shale along with other regional shales and their biostratigraphic relationships) and provided an up-to-date faunal analysis for the Cleveland Member. However, he did not consider the impact of sedimentological interpretations on the potential lifestyles of the fishes associated with the depositional habitat of the Cleveland Member.

Williams (1990) provided the first comprehensive predator-prey analysis of the Cleveland Member fish fauna. His analysis centered on chondrichthyans due to their unusually complete preservation including stomach contents (53 specimens reported with identifiable gastric contents, Williams, 1990, p. 280). Evaluation of non-chondrichthyans was limited to a few cases of associated remains possibly suggesting predator-prey relationships (the presence of a shark spine imbedded in the oral region of an arthrodire; associated arthrodire and shark remains suggesting a possible predator-prey interaction; and a palaeoniscid with shark and arthrodire stomach contents; Williams, 1990, p. 286–287).

Despite the vast amount of effort dedicated to the sedimentological history of the Appalachian Basin (e.g., Woodrow and Sevon, 1985) and the long history of vertebrate paleontology in the region, little work has addressed the paleoecology of the vertebrate fauna associated with these sediments. The placoderms, which represent the most speciose Devonian clade (Carr, 1995) and numerically the largest part of regional collections, represent the least known clade in terms of their paleoecology.

As seen in the examples above, estimates concerning the paleoecology of Paleozoic fishes are based on evidence such as stomach contents, body form, or indirectly on facies analyses. Little is known concerning placoderm stomach contents, although Dennis and Miles (1981) and Miles and Westoll (1968, p. 462) have evaluated stomach contents in *Incisoscutum* and *Coccosteus*, respectively. The interpretation of gnathal-plate morphology is

used to suggest specializations for various feeding strategies such as durophagy or piscivory (Denison, 1978, p. 17). However, the feeding strategies of generalized forms or forms without recent analogues are difficult, if not impossible, to interpret without additional supporting evidence.

Lindsey (1978) and Webb (1982) used body form to interpret locomotor styles among extant fishes. Among placoderms this approach has found limited application being applied primarily to laterally and dorsoventrally compressed forms. Miles (1969, p. 129; see also Moy-Thomas and Miles, 1971, p. 175) suggested a nektonic lifestyle for the laterally compressed brachydeirid arthrodires, while several authors (Stensiö, 1963, p. 13; Miles, 1969, p. 129; Moy-Thomas and Miles, 1971, p. 185, 197–198) interpreted dorsoventrally compressed forms, such as the raylike rhenanids, as bottom living. Between these extremes, a vast number of taxa are interpreted generally as bottom living (Stensiö, 1963, p. 13) or specialized for "life just above the bottom" (Moy-Thomas and Miles, 1971, p. 197).

Finally, analysis of the facies in which placoderm fossils are found has provided an additional source of information, but relies on the assumption that fishes lived in a habitat on or above the accumulating sediments. The utility of this approach is difficult to evaluate when post-mortem transport is involved and the fishes lived outside the area of deposition.

Of the methods that have been used to determine aspects of placoderm paleoecology, none individually can provide a complete picture, and thus far, few attempts have been made to combine analyses. Ideal preservation, having complete organisms preserved with soft tissue and stomach contents, is an exceedingly rare occurrence. Within the Devonian, this ideal is achieved among the chondrichthyan remains found in carbonate concretions from the Cleveland Member (Williams, 1990). For placoderms, researchers have retrieved some of the best-preserved fossil material from the Hunsrückschiefer of Germany (Lower Emsian) and the acid-prepared concretions from the Gogo Formation of Western Australia (Frasnian). Even in these conservation Lagerstätten (*sensu* Seilacher, 1990) information is lost. However, a total-evidence approach including, e.g., sedimentology, geochemistry, and taphonomic mechanisms, may recover sufficient information to reconstruct details of life history and paleoecology (Tasch, 1965; Elder and Smith, 1988).

The Catskill Delta and its associated foreland basin (Appalachian Basin, Figure 1C) provide a unique opportunity to analyze the paleoecology of fishes in the region. The black-shale facies found within the distal basin (Figure 1D) represent an anoxic depositional environment, potentially inhospitable to benthic organisms or capable only of supporting a low-diversity fauna (see Discussion below). Fossil fishes found in these shales represent either fishes living and dying within the region, post-mortem allochthonous accumulations of floating carcasses, or a mixture (Brett and Baird, 1993, p. 254).

Historically, most placoderms have been seen as obligate benthic organisms, which accessed the water column only to feed (Stensiö, 1963, p. 13; Moy-Thomas and Miles, 1971, p. 197; Denison, 1978, p. 17), suggesting that the presence of carcasses within the low-diversity deep basin represents an accumulation of remains originating in the established benthic communities of the aerated shallow regions of the basin. To evaluate this hypothesis in one species, the current study analyses the distribution of gnathal elements from *Dunkleosteus terrelli* (Newberry, 1873) within the Appalachian Basin. *Dunkleostens terrelli* (Figure 2A–C) is a large arthrodire (4.5–6 m in length) found within the Appalachian Basin. This species is oval in cross-section and possesses a well-developed dermal skeleton (Figure 2B, C) with individual bones up to 5–7.5 cm thick along the lateral and occipital thickenings of the head shield. The gnathal elements (IG, ASG, PSG, Figure 2B, C) in this species represent bones that detach relatively early in the disarticulation process (see Schäfer, 1972, p. 49–91, and Elder, 1985, for a discussion of disarticulation patterns) and would be expected to accumulate close to the site of death (secondary transport after these remains settle is discussed below). The geographic distribution of the gnathal elements for *Dunkleosteus terrelli* does not support a hypothesis where remains of this arthrodire represent long-distance floating of carcasses.

Methods and Materials

Dunkleosteus terrelli specimens from the Cleveland Member (Upper Famennian; *postera* to late *expansa*–early *praesulcata* conodont zones, Zagger, 1995) of the Ohio Shale analyzed in this study are housed within the collections of the Cleveland Museum of Natural History. Data were retrieved from the Museum vertebrate paleontology catalog using those specimens with entries providing detailed locality information. The presence or absence of individual plates indicated in the catalog was confirmed from the actual specimens. The specimen localities included seven north-south river or creek basins and the excavation site for Interstate-71 in northern Ohio near Cleveland (Figure 3). These localities were grouped into five drainage systems representing five north-south transects in northern Ohio paralleling the ancient Catskill shoreline (from west-to-east: 1, Huron and Vermillion Rivers and Chance Creek; 2, Beaver Creek; 3, Black River; 4, Rocky River; 5, Big Creek and Interstate-71). These drainage basins expose the black shales (Cleveland Member) of the distal foreland basin. Recorded specimens included those with and without gnathal elements and isolated gnathal elements. The relative abundance of specimens with and without gnathal elements was evaluated for the localities listed above.

A Chi-squared nonparametric analysis for k independent samples (Equation 1; Siegel and Castellan, 1988) was conducted to test the null hypothesis (H_0) that the proportion of specimens with and without gnathal elements was statistically the same in each geographic sample (i.e., there was no geographic trend and the distribution of fossils was random). The research hypothesis, based on published interpretations of placoderm paleoecology (e.g., Stensiö, 1963; Denison, 1978), was that the proportions differ across samples (an increased concentration of gnathal elements shoreward, suggesting an allochthonous accumulation of fossils within the distal basin from an eastward shallower source). A significance level of alpha = 0.05 was chosen with a sample size of $n = 199$.

$$X^2 = \sum_{i=1}^{r} \sum_{j=1}^{k} \frac{n_{ij}^2}{E_{ij}} - N \qquad (1)$$

E_{ij} = number of expected cases in the ith row of the jth column when the null hypothesis is true
i = variables within the $r \times k$ contingency table
j = groups within the $r \times k$ contingency table
n_{ij} = number of observed cases categorized in the ith row of the jth column (Siegel and Castellan, 1988, p. 191)

Dry weight represents the weight of a living specimen out of water, while wet weight is its weight in water. Body mass (wet weight) is an important factor influencing buoyancy (static or

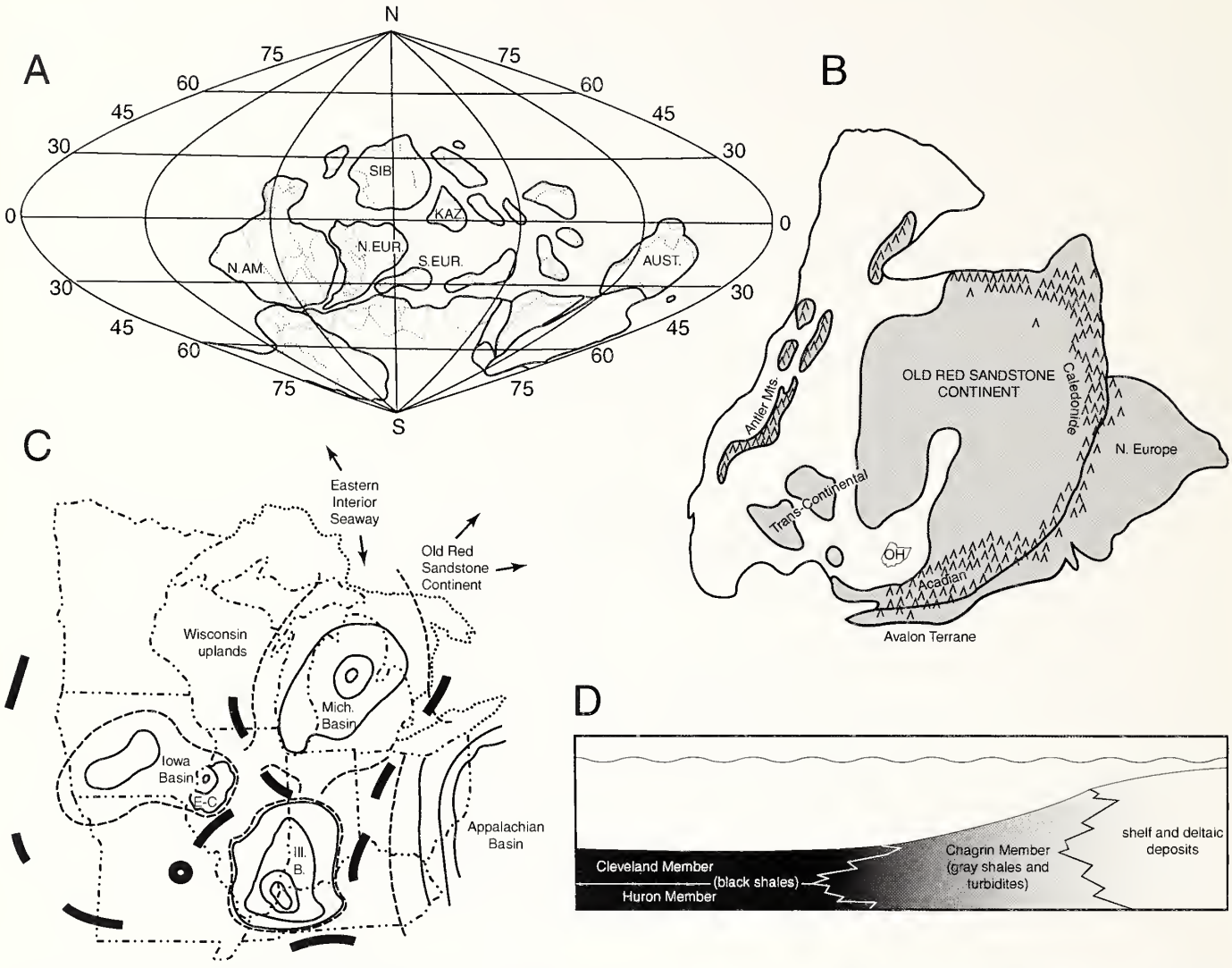

Figure 1. A, paleogeographic reconstruction with paleolatitudes based on Middle Devonian map of Streel et al., 2000. B, detailed reconstruction of North American and northern European blocks after Ettensohn (1985, fig. 2).The position of Ohio (OH) is indicated and probable landmasses are shaded (Λ Λ = mountains). C, close-up of the western Appalachian Basin in Ohio and other regional basins (from Elliot et al., 2000, fig. 2). States (dash, double-dotted lines), Great Lakes' boundaries (dotted lines), basin depositional contours (solid thin lines), hypothesized basin boundaries (dashed lines), and regional geographic highs (solid thick lines) are indicated. D, schematic cross-section of the Ohio Shale (Cleveland and Huron Members) and the laterally equivalent shoreward (eastward) sediments.

dynamic) in active swimmers, equally important to benthic forms when considering an unstable substrate, and an important consideration in the post-mortem transport of carcasses. To evaluate locomotor patterns in *Dunkleosteus terrelli*, estimates of its wet and dry weight were calculated based on a conservative comparison to extant Western Atlantic sharks and ten Pacific examples for three species with limited or no Atlantic weight data. A total of 59 length-weight examples from 18 species were used (Bigelow and Schroeder, 1948, all of their reported length-weights were included in this analysis). Bigelow and Schroeder (1948) provided a conversion factor for dry to wet weight in sharks (5.5% for noncontinuous and 2.6% for continuous swimmers) that was applied to *Dunkleosteus terrelli*. The lack of bone in sharks gives a conservative estimate for dry and wet weight in *D. terrelli*; however, the purpose of this estimate was to evaluate its impact on potential settling in bottom sediments and buoyancy (static or dynamic).

After Allison et al. (1995, p. 98), the root *aerobic* is used here to refer to "modes of life or biofaces," while *oxic* refers to oxygen levels within the environment. The specimen-number prefix CMNH denotes specimens from the Cleveland Museum of Natural History Department of Vertebrate Paleontology.

Results

The raw data of specimens with or without gnathal plates are summarized in an $r \times k$ contingency table (Table 1). A Chi-squared analysis for the five independent samples gives a Chi-square of 6.1 with four degrees of freedom. The critical Chi-square value for alpha = 0.05 is 9.49, thus the null hypothesis (H_0)

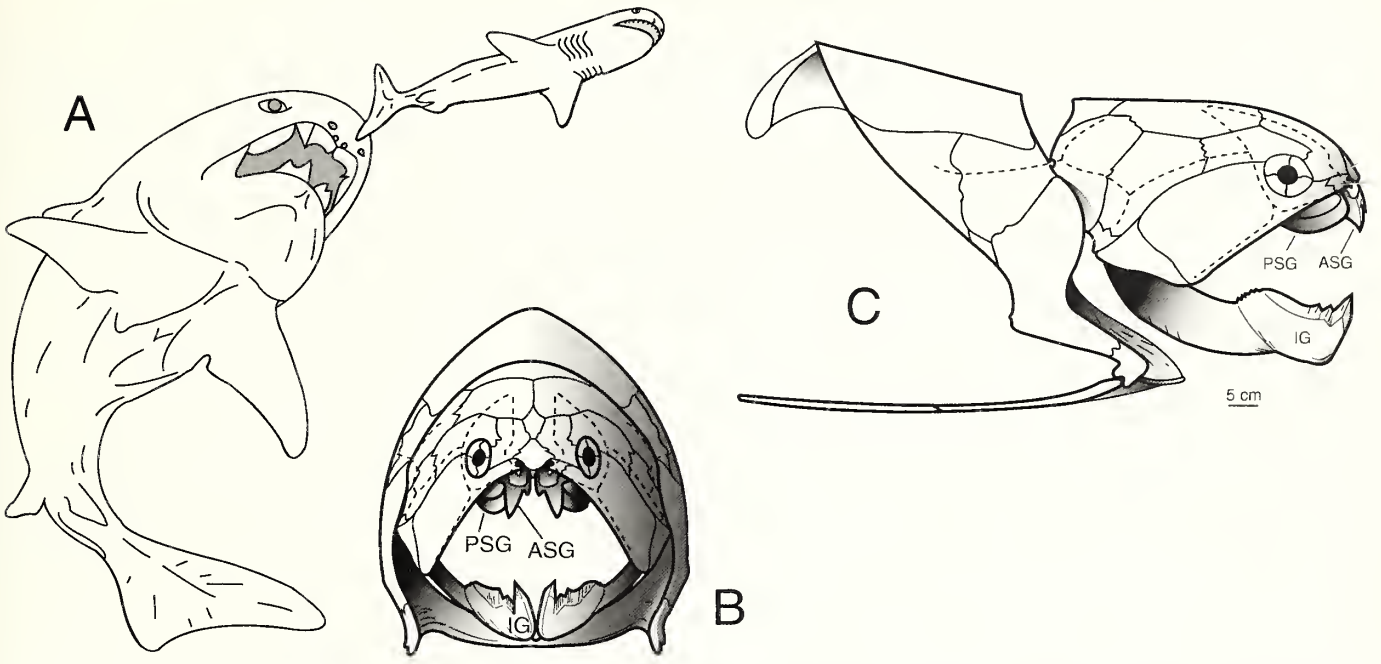

Figure 2. A, life reconstruction of *Dunkleosteus terrelli* in pursuit of *Cladoselache*. Redrawn from Carr (1995, fig. 17). B and C, anterior and right lateral views of *D. terrelli* ossified skeleton (composite after Heintz, 1932 and 1968). ASG = anterior superognathal, IG = inferognathal, PSG = posterior superognathal, dashed lines = sensory canal grooves.

is not rejected ($0.10 < P < 0.20$). An analysis of three samples (transects 1, 3, and 5, thus eliminating any potential geographic overlap of adjacent transects) does not lead to a rejection of the null hypothesis ($X^2 = 0.64$, d.f. = 2; $0.70 < P < 0.80$).

The log of dry weights versus log of body length for 59 extant sharks (taken from Bigelow and Schroeder, 1948) provided an estimated dry weight for *Dunkleosteus terrelli* (Figure 4). Dry weight for a 4.6 m (15 ft) *Dunkleosteus terrelli* is estimated at 665.0 kg (1466.3 lbs). A wet weight estimate is 36.6 kg (80.6 lbs; or using a continuous swimmer conversion factor, 17.3 kg (38.1 lbs)).

Discussion

Given the precautions concerning interpreting paleoecology based on a fragmentary fossil record (e.g., Elder, 1985; Elder and Smith, 1988; Allison et al., 1991), it is important to evaluate all available evidence. Elder and Smith (1988) presented a method to interpret fish ecology from taphonomic evidence. Using principles of information theory (Tasch, 1965) in their studies of fish taphonomy within lakes, they noted that taphonomic processes provide an informational trade-off. As information about an organism is lost during the taphonomic process, these processes themselves provide new information about the organism's physical and chemical environment and the post-mortem history of the organism. Taphonomy provides not only information on the environment of burial, but if explored fully, the post-mortem history may reveal details about the source of these organisms and their life habitat. Unlike a laboratory experiment where individual variables can be controlled, historical events require a thorough consideration of all taphonomic variables.

The fossil record for placoderms is meager, limiting evaluation of habitat and life history. Within the Appalachian Basin, *Dunkleosteus terrelli* is numerically the predominant Late Devonian vertebrate fossil. It is one of the best-described members of the fauna (Heintz, 1932) and is recognized easily due to its large size and distinctive osteology relative to the other large members of the fauna (e.g., the thin plates and unique morphology of *Titanichthys* clearly distinguish this taxon from *Dunkleosteus* within the Cleveland Member fauna). *Dunkleosteus terrelli* specimens range in estimated size from 25 cm to 6 m with some even smaller specimens questionably attributed to the species. This size range represents a wide range of age classes.

The available *Dunkleosteus terrelli* material housed within the Cleveland Museum of Natural History was collected over many decades. Peter A. Bungart (Hlavin, 1976) collected, from 1923 to 1946, the bulk of the material in the region of Cuyahoga and Lorain Counties in northern Ohio (Figure 3), diligently and meticulously recording all material associated with a single individual even when collecting continued over several years. This collection possibly represents the best Paleozoic material amenable to statistical analysis with the least amount of sampling bias.

Although questions remain concerning the origin of anoxic basins (Hoover, 1960, p. 31; Degens et al., 1986; Wignall, 1994; Schieber, 1998), a number of factors are common to the various hypotheses relating to the development of black shales such as the Cleveland Member, including: (1) minimal or lack of available oxygen (Hoover, 1960; Heckel, 1972; Degens and Ross, 1974; Brumsack and Thurow, 1986; Wignall, 1994; Allison et al., 1995); (2) presence of hydrogen sulfide representing a potential toxin (Hoover, 1960, p. 34; Heckel, 1972; Jannasch et al., 1974); (3) an unstable substrate consisting of fine sediments with high porosity (Keller, 1974); (4) water depths with low light or below the photic-zone (additionally, below wave base), and (5) limited or lack of trace fossils and bioturbation (bioturbation in the Cleveland Member is reported by Lewis, 1988, p. 25; Schieber, 2003, notes

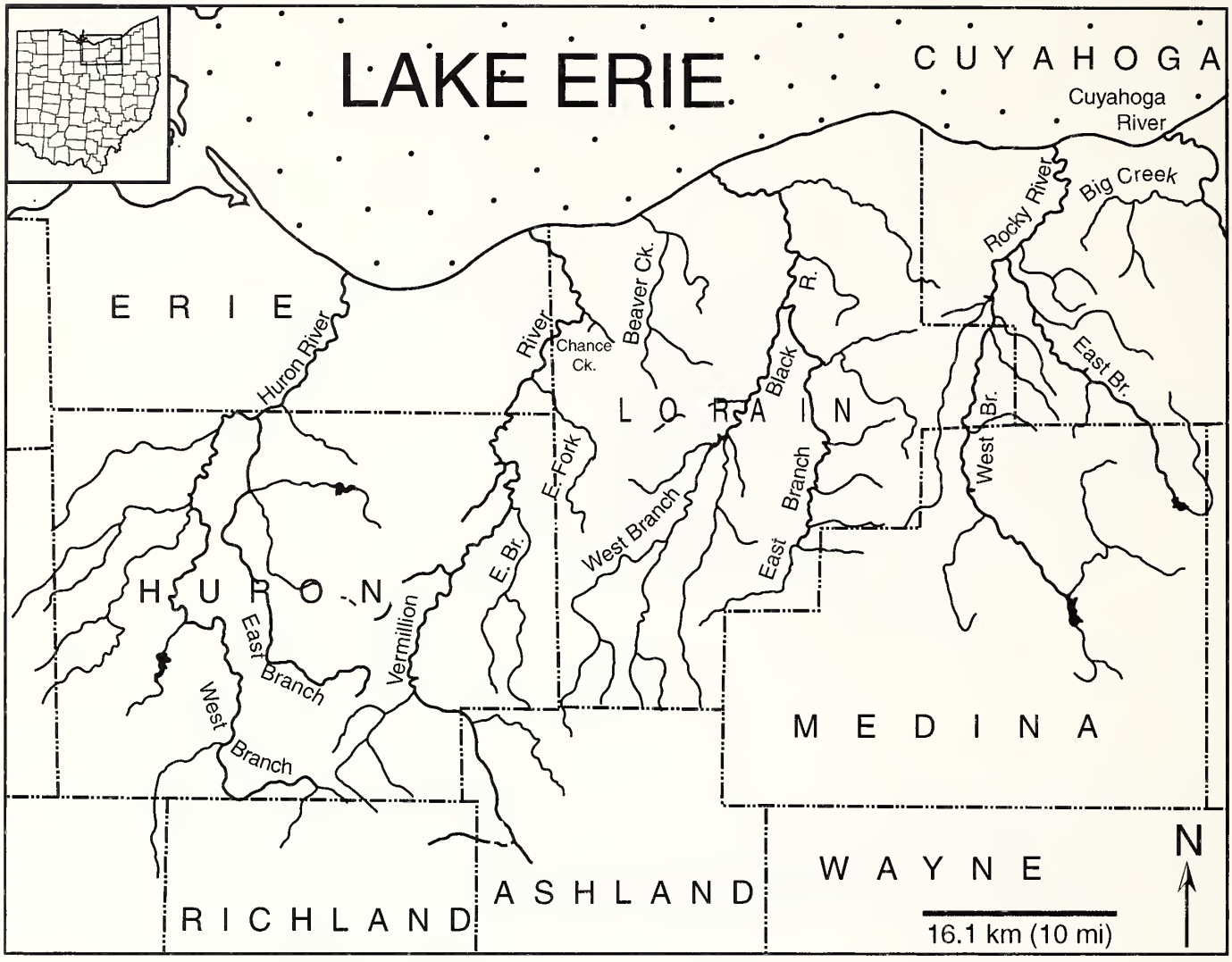

Figure 3. Drainage map of northern Ohio showing the seven river or creek drainages that provided specimens in the current study. Inset map of Ohio indicates the study area (box). Labels: counties, intermediate sized font; and creeks/rivers, small sized font. Compiled from Ohio Department of Natural Resources, Principal streams and their drainage areas (map), 1985, and U.S. Geological Survey Kipton, Ohio, 7.5-minute quadrangle topographic map, 1969.

the unrecognized presence of bioturbation in black shales; see Brett and Allison, 1998, for a review of paleontological approaches to interpreting the environment of deposition). The combined effects of the first four factors above clearly impact the potential for the establishment of a benthic community. Common to all models are anoxic pore waters (factor 1). What differs is whether anoxia extends from the sediment-water interface up into the water column. Published accounts of the benthic community associated with black shales (factor 5) range from a complete absence of benthic organisms (Hoover, 1960, p. 32, 42; Conant and Swanson, 1961, p. 56–62; Heckel, 1972; Hlavin, 1976; Allison et al., 1995, p. 100) to low diversity communities capable of tolerating the physical properties of the depositional environment (anoxic-dysoxic, stable or intermittent; hydrogen sulfide; depths potentially below the photic-zone; and unstable substrate; Hannibal et al., 2005). Detailed geochemical (e.g., degree of pyritization) and published sedimentological data for the Cleveland Member are limited, although recent studies of laterally equivalent black shales, other non-contemporaneous black shales, or modern examples provide useful analogues for the Cleveland Member (hopefully similar studies will be expanded to include the Cleveland Member).

Modern oxygen-minimum zones that intersect the sediment-water interface are known from numerous regions of high primary productivity, for example, the northwest Indian Ocean (Degens et al., 1986) and the Gulf of California (Brumsack and Thurow, 1986). However, there are only a few examples of potential analogues for stagnant foreland basins, including the Black Sea (Degens and Ross, 1974) and Norwegian fjords (Brumsack and Thurow, 1986). The Black Sea, a potential modern analogue to the ancient distal Appalachian Basin, is characterized by a reduced sedimentation rate (variable within the basin) and high sediment porosity with the sediments containing greater than or equal to 71% water by volume (Keller, 1974). Sedimentation occurs within an anoxic water column with toxic levels of hydrogen sulfide. The upper few millimeters of sediment

Table 1. Contingency tables ($r \times k$) for the *Dunkleosteus terrelli* specimens in the current study. Table for five river/creek drainage basins represents north-south transects paralleling the ancient Catskill shoreline. The critical X^2 value for alpha = 0.05 is 9.49; therefore, the null hypothesis is not rejected ($0.10 < P < 0.20$). Table for three samples (drainage basins) eliminates any potential geographic overlap of adjacent transects. The critical X^2 value for alpha = 0.05 is 5.99; therefore, the null hypothesis is not rejected ($0.70 < P < 0.80$). Calculations based on Equation 1. Abbreviations: *df*, degrees of freedom [$(r - 1)(k - 1)$]; E, calculated expected occurrences; O, observed occurrences; 1, Huron and Vermilion Rivers and Chance Creek; 2, Beaver Creek; 3, Black River; 4, Rocky River; and 5, Big Creek and Interstate-71.

Contingency table for five drainage basins											
Gnathals	**1-O**	**1-E**	**2-O**	**2-E**	**3-O**	**3-E**	**4-O**	**4-E**	**5-O**	**5-E**	**Total**
With	18	17.48	4	3.35	7	7.44	13	8.18	32	37.56	74
Without	29	29.52	5	5.65	13	12.56	9	13.82	69	63.44	125
Total	47	47.00	9	9.00	20	20.00	22	22.00	101	101.00	*N = 199*
O^2/E	18.54		4.78		6.59		20.66		27.26		
	28.49		4.42		13.45		5.86		75.04		
Σ	205.10										
$X^2 = \Sigma - N$	6.10										
df	4										
P value	$0.1 < P < 0.2$										
Contingency table for three drainage basins											
With	18	15.95			7	6.8			32	34.27	57
Without	29	31.05			13	20.66			69	66.73	111
Total	47	47			20	20			101	101.00	*N = 168*
O^2/E	20.32				7.22				29.88		
	27.08				12.78				71.34		
Σ	168.64										
$X^2 = \Sigma - N$	0.64										
df	2										
P value	$0.7 < P < 0.8$										

are unable to support even the remains of microorganisms. The next 30–60 cm are reported to have the consistency of a "slurry" (Keller, 1974, p. 333). Shear strength does not improve within the sediments until a depth of approximately 140 cm (Keller, 1974, fig. 2). Associated with the anoxic water column and presence of hydrogen sulfide is the formation and accumulation of iron sulfides (Berner, 1974; Rozanov et al., 1974). Neither the Black Sea or fjords (episutural basin of extreme depth or drowned glacial valley with restricted surface area, respectively) are truly representative of the large epicontinental basins of the Devonian; however, the muds deposited in these anoxic environments share the physical properties of sediments that potentially form black shales.

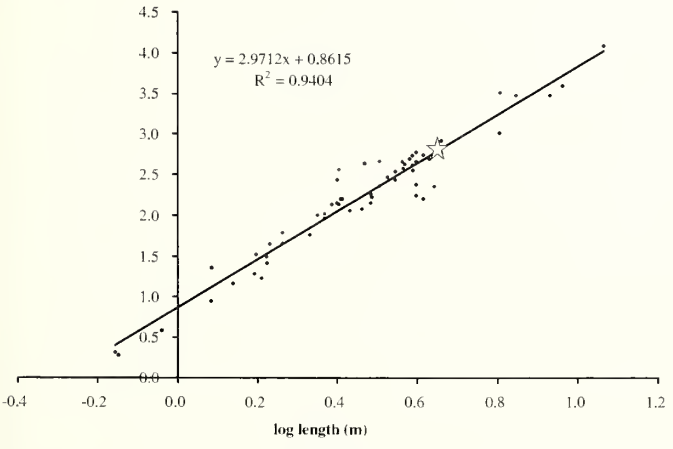

Figure 4. Plot of log dry weight versus log body length for extant North Atlantic sharks (circles). Estimated dry weight for *Dunkleosteus terrelli* of 665.0 kg (1466.3 lbs) for a body length of 4.6 m (15 ft) is indicated by a star.

The Cleveland Member (Nelson, 1955; Hoover, 1960; Mausser, 1982) is typical of black shales with a high organic content accumulated in an anoxic environment. The shale produces a petroliferous odor when freshly broken due to this organic content (Hoover, 1960, p. 23). Its composition of fine sediments, with little or no carbonates in the bulk of the shale (Mausser, 1982, p. 86; although discontinuous cone-in-cone and carbonate concretions are present), suggests an unstable high-porosity substrate at the time of deposition (estimated water content at the time of deposition for the Cleveland Member is 75–80%, J. Schieber, personal communication, 2004). The presence of disseminated pyrite (Mausser, 1982) throughout the formation indicates the presence of hydrogen sulfide at the time of deposition.

In northern Ohio, Upper Devonian Appalachian Basin rocks are exposed in a number of north-south river basins that drain into Lake Erie (Figure 3). These river basins represent a series of north-south transects that roughly parallel the ancient Catskill Delta (Figure 1B, C) thereby providing a series of proximal-to-distal samples within the black shales of the Appalachian Basin. The Cleveland Member represents the distal element of the basin facies that are laterally equivalent to the eastward slope deposits of the Chagrin Member (Figure 1D). This shoreward facies transition is a temporally repeated pattern within the Appalachian Basin as noted by Baird and Brett (1986) for the Genesee sequence of New York.

Evaluation of the paleogeographic distribution of *Dunkleosteus terrelli* provides two potential hypotheses: (H1) *D. terrelli* lived, died, and was preserved within the basin; (H2) *D. terrelli* lived and died elsewhere, but was transported into the basin where it was preserved. The paleogeography of *D. terrelli* is reflected in the nature and distribution of its remains within the Cleveland Member. Hypothesis 1 would suggest the possibility that remains of this species are either intact (no disarticulation due to post-

mortem transport or through other processes) or disarticulated (if disarticulated in transport then there should be no pattern suggesting an eastward source of remains from outside the deep basin). Hypothesis 2 requires transport of *D. terrelli* remains into the deep basin. Associated with the latter hypothesis would be a pattern reflecting the distance traveled from the source (e.g., more eomplete specimens proportionally found closer to the source or elements that disarticulate early in the taphonomic process found closer to the souree).

The remains of *Dunkleosteus terrelli* within the Cleveland Member are typically disarticulated with a variable number of plates missing (only 5.1% of the evaluated specimens possess over 25% of the dermal and perichondral bones). Elder (1985) and Elder and Smith (1988) noted three potential sources for the disarticulation and removal of organic remains in an aquatic environment: flotation, scavenging, or transport by currents (see also Allison et al., 1991). Within the distal Appalachian Basin, the latter two mechanisms have little or no influence on organic remains once they have settled to the bottom. Proposed mechanisms to account for anoxia and the deposition of black shales require an environment below wave base that may be further restricted from mixing by the presence of a density stratification (formation of a pycnocline; see Murphy et al., 2000, and Sageman et al., 2003, for alternative models for the formation of an anaerobic benthos). An anoxic environment (and presence of hydrogen sulfide in some models) would make the bottom unsuitable for macroscopic scavengers; however, that does not preclude scavenging upon floating carcasses within the water column. The presence of an unsuitable bottom habitat is supported in part by the limited or lack of bioturbation and trace fossils. Additionally there is little evidence for the presence of a diverse macroscopic infauna or epifauna, and no evidence for the presence of epibionts encrusting bones. Fossil sharks within the Cleveland Member often are found fully articulated with soft tissues preserved (Williams, 1990). These fossils have been reported from carbonate concretion zones in the shales of Big Creek and Interstate-71. This represents a sampling bias in that concretions are easily seen in profile, in contrast to flattened isolated specimens. Shark fossils are found from outside the concretion zones in westward deposits either associated with cone-in-cone deposits or isolated within the shale. The skeletons of these fishes consist of perichondrally ossified prismatic cartilage that is highly susceptible to mechanical damage and is destroyed easily by scavengers or currents.

The fine grain size of Cleveland Member sediments further suggests a relatively low energy depositional environment (Nelson, 1955; Mausser, 1982) and the absenee of currents sufficient to move the relatively large bones of *Dunkleosteus terrelli.* Additionally, there are no sedimentary structures (bedding features) suggesting the presence of higher energy bottom currents within the Cleveland Member. Sediment winnowing does occur, demonstrated by the presence of several isolated lag deposits (invertebrate thanatocoenoses, Hlavin, 1976; silty lags, J. Schieber, personal communication, 2004); however, winnowing tends to accumulate bone and pelagic invertebrates rather than remove them. The large and relatively heavy *Dunkleosteus terrelli* bones would preferentially remain within these deposits.

Flotation remains as the most plausible mechanism to account for the disarticulated remains of *Dunkleosteus terrelli.* Flotation could occur in fishes living within the basin or it may represent a mechanism for the transport of organisms into the basin.

Common to the patterns of disarticulation in both aquatic (Elder, 1985; Schäfer, 1972) and terrestrial (Hill, 1979; Weigelt, 1989) organisms is the loss of elements near sites of access by scavengers (microscopic and macroscopic). The oropharyngeal cavity represents such a site with scavenging activity in this region resulting in the disarticulation and potential loss of gnathal elements. In teleosts and arthrodires (Figure 2B, C) both upper and lower gnathal elements, which lack ossified connections to the axial skeleton, are lost. In contrast, within mammals where the maxillae and premaxillae are eonnected intimately with the skull, the dentaries alone are detached from the skull. Work by Elder (1985) and others (Schäfer, 1972; Hill, 1979; Smith and Elder, 1985; Elder and Smith, 1988) suggests that gnathal elements (dentaries only in mammals) in particular are lost early in the disarticulation process, thus presence of specimens with gnathal elements suggests a relatively short time of exposure to pre-burial taphonomic proeesses (including both transport and scavenging). In the case of *Dunkleosteus terrelli* within the Appalachian Basin, the presence of isolated gnathal plates suggests that floating carcasses may have dropped elements relatively close to the original life habitat.

Elder (1985), Smith and Elder (1985), and Elder and Smith (1988) documented the importance of water depth and temperature to the process of flotation. The physical principles outlined in the gas laws of Charles and Gay-Lusac ($k = V/T$) and Boyle ($k = PV$) clearly delineate limitations for the potential of an organism to float upon bacterial decomposition within finite ranges of water depth and temperature. Thus, the volume of accumulating decomposition gases within the tissues or body cavities to induce flotation will increase with warming (a latitudinal or climate factor) and decrease with depth (increased pressure). Elder (1985) suggested a limiting depth for flotation in a number of teleosts although her experimental work did not consider larger species or variable densities. She suggested that settling below a depth of 10 m even within tropical waters would severely limit or prevent flotation. In contrast, Allison et al. (1991) noted the calculated potential of flotation in whales up to a depth of 1200 m. Unlike the teleosts studied by Elder (1985), whale specimens may be nearly neutrally buoyant at the time of their settling to the bottom (some are positively buoyant and float at the time of death, representing an inherent static buoyancy, Allison et al., 1991).

The Appalachian Basin in the Late Devonian was located in the subtropics (30–35° S), suggesting moderate to warm water temperatures (17–18° C) based on oxygen isotopic data from brachiopods (Streel et al., 2000, fig. 30, p. 154). Several authors dispute the water depth within the open Appalachian Basin; however, all estimates are well within the computed depths of Allison et al. (1991) that are necessary for flotation (61.0–91.4 m, Nelson (1955); 30.5–45.7 m, Hlavin (1976); 50–100 m, Brett et al. (2003); up to 100 m using the depth limits, noted by Ferguson (1963), for *Lingula* found within the Cleveland Member; contrast these estimates with Schieber's (1998) estimate of 10–20 m for the Chattanooga Shale of Tennessee, although, the Chattanooga Shale is characterized by a number of lag deposits and erosional surfaces).

The presence of *Dunkleosteus terrelli* remains in the black shales of the Appalachian Basin can be explained either as a post-mortem accumulation of organisms that lived within the basin or a rain of parts falling from carcasses transported via flotation from aerated regions. The results of a Chi-squared statistical analysis of these fossils did not support the hypothesis that *D.*

terrelli was restricted to the shallow aerated eastern part of the basin and that its presence in the distal sediments was the result of carcasses floating into the basin (Table 1; $X^2 = 6.1$, d.f. = 4, $0.10 < P < 0.20$). In an additional analysis of non-adjacent transects (nos. 1, 3, and 5), the null hypothesis was not rejected ($X^2 = 0.64$, d.f. = 2, $0.70 < P < 0.80$). Non-rejection of the null hypothesis is consistent with a random distribution of *D. terrelli* within the basin, thus it is more likely that this speeies was a pelagic form (living and dying within the basin) and not an obligate bottom dweller (restricted to the eastern aerated shallower benthos, e.g., the basin slope represented by the Chagrin Member or more shoreward regions, Figure 1D).

Given our knowledge of the bottom habitat associated with black-shale formation, *Dunkleosteus terrelli* would have had to be a continuous swimmer. The paleontological, sedimentological, and geochemical evidence all suggest that the bottom environment was inhospitable; however, even if fishes could reach the bottom within the basin, the stability of the substrate to support the weight of these organisms would have proven to be a problem.

At present there are few estimates for the size or weight of *Dunkleosteus terrelli* (Heintz, 1932). The large amount of bone and concomitantly high body mass has led several researchers to conclude that *D. terrelli* must be a benthic form (e.g., Denison, 1978; although rejected by later authors, Heintz, 1932, considered *Dunkleosteus* to be an active swimmer and predator). Comparison of *Dunkleosteus terrelli* (using an adult length of 4.6 m (15 ft) to modern sharks (Figure 4) suggests a dry weight of approximately 665.0 kg (1466.3 lbs). Bigelow and Schroeder (1948) suggested that wet weight is 5.5% of dry weight in extant sharks (2.6% for free or continuous swimming forms). Using this estimate, the wet weight for *D. terrelli* can be calculated to be 36.6 kg (80.6 lbs; or using a free swimming estimate, 17.3 kg or 38.1 lbs). This represents a conservative estimate due to the lack of bone in sharks and the conversion to wet weight being based on organisms possessing lipids for static buoyancy. A wet weight of 36.6 kg (or 17.3 kg for continuous swimmers) would generate sufficient shear forces to permit the settling of *D. terrelli* into the substrate exposing it to the toxic properties of the sediments and potentially elogging the gills with fine silt (refer to Keller, 1974, p. 333–334, for estimates of shear strength in black muds). If *D. terrelli* lived within the basin it can be assumed that it did not rest on the bottom, but swam continuously.

A second point bearing upon the interpretation of placoderm lifestyles is their mode of locomotion. Placoderms apparently possessed a low profile and poorly supported heterocercal tail and have been interpreted to have swum using a sine-wave undulation of the body (Thomson, 1971; anguilliform locomotion of Lindsey, 1978). They have been compared to extant macrurid or chimaerid fishes (Stensiö, 1963, p. 13), which demonstrate a bottom-dwelling lifestyle. Although anguilliform locomotion may be considered a relatively inefficient form of locomotion (e.g., relative velocity between anguilliform and other forms of locomotion) it does not mean that anguilliform swimmers are not effective prolonged or continuous swimmers. One needs only to look at the migratory patterns of extant eels (*Anguilla anguilla*), which migrate between North America and Europe (McDowall, 1988) to reeognize this point. Although placoderms apparently never achieved some of the advanced forms of locomotion seen in modern teleosts (e.g., carangiform and thunniform locomotion, Lindsey, 1978), they did develop a number of locomotor adaptations associated with increased lift and reduced drag (Carr, 1995).

Conclusion

The taphonomic evidence did not support an interpretation of *Dunkleosteus terrelli* as an obligate benthic organism. A Chi-squared statistical analysis of the distribution for the remains of this species failed to support a restricted bottom-living hypothesis. *Dunkleosteus terrelli* was a free-swimming species living within the Appalachian Basin, which may help to explain its wide North American distribution (California to eastern United States; if synonymised with *D. marsaisi* (Lehman, 1954) from Morocco (Rücklin, 2002) the range would extend via the Rheic Ocean to east of the Old Red Sandstone Continent, Figure 1A). This interpretation is consistent with the analysis of Carr (1995), which noted the development of loeomotor specializations within pachyosteomorph arthrodires and was further supported by the preservation of relatively complete specimens or the distribution of elements lost early in the disarticulation process throughout the basin.

Potential objections to viewing placoderms as free-swimming organisms have included their possession of heavy body armor and an anguilliform form of locomotion. The distribution of *Dunkleosteus terrelli* remains in the Appalachian Basin is consistent with disarticulation due to localized post-mortem flotation. The presence of post-mortem flotation in a basin with published depth estimates ranging from 30 to 100 meters suggests an organism with some level of additional static buoyancy beyond inherent tissue buoyancy (refer to Allison et al., 1991). An interpretation of anguilliform locomotion does not necessarily imply an ineffective form of locomotion. It appears that an interpretation of bottom life is a consequence of the researcher's choice of extant analogue rather than any necessary correlation between lifestyle and form of locomotion.

The implications of this study are three-fold and form the basis of continuing work on the Cleveland Member fauna. Life within the basin raises questions concerning the: (1) reproductive strategy; (2) life history; and (3) static buoyancy in *Dunkleosteus terrelli.* An inhospitable bottom limits potential nesting sites. It is not possible at this time to determine whether this species was viviparous or oviparous; although, the presence of putative egg cases within the Cleveland Museum of Natural History collections (CMNH 8133–8136, 9461) raises some interesting questions. Further work is needed to provide information on the distribution of age classes for *D. terrelli* within the Appalachian Basin. Finally, the presence of disarticulation associated with flotation raises questions concerning static buoyancy in *D. terrelli.* Elder (1985) has pointed out the physical limits (depth and temperature) associated with flotation; however, Allison et al. (1991) have demonstrated that given sufficient static buoyancy, flotation may occur up to depths of 1200 m. The presence of air sacs in placoderms has been questioned (Denison, 1941, recognized the presence of air sacs in *Bothriolepis*, but did not consider them to be a feature of placoderms in general, although this interpretation has never been confirmed in other specimens of *Bothriolepis* or in any other placoderm taxa (D. Goujet, personal communication, 2004); Gardiner, 1984, considered air sacs to be a derived feature within Osteichthyes). However, the predominance of disarticulation associated with floating in *D. terrelli* strongly suggests the presence of a static buoyancy mechanism within this species (if not an air sac then potentially lipids as seen in chondrichthyans). Further work on taphonomic patterns and flotation within *D. terrelli* may help to shed light on these questions.

Acknowledgments

I would like to thank D. Goujet and G. R. Smith for their early reviews and the latter for discussions on taphonomy, R. Cox and D. Dunn for our many discussions, and C. Brett, J. Schieber, and D. Goujet for review of the final manuscript. Posthumous thanks and regards are expressed to M. E. Williams for our many discussions concerning the Cleveland Member fauna over a twenty-year period. Finally, I want to additionally thank D. Fisher, C. Gans, and P. D. Gingerich who provided encouragement and reviews on an early version of this work submitted in partial fulfillment of the requirements for a Doctor of Philosophy in Geological Sciences at The University of Michigan.

References

Allison, P. A., C. R. Smith, H. Kukert, J. W. Deming, and B. A. Bennett. 1991. Deep-water taphonomy of vertebrate carcasses: a whale skeleton in the bathyal Santa Catalina Basin. Paleobiology, 17:78–89.

Allison, P. A., P. B. Wignall, and C. E. Brett. 1995. Palaeo-oxygenation: effects and recognition, p. 97–112. *In* D. W. J. Bosence and P. A. Allison (eds.), Marine Palaeoenvironmental Analysis from Fossils. Geological Society Special Publication No. 83.

Baird, G. C., and C. E. Brett. 1986. Erosion on an anaerobic seafloor: significance of reworked pyrite deposits from the Devonian of New York State. Palaeogeography, Palaeoclimatology, Palaeoecology, 57:157–193.

Berner, R. A. 1974. Iron sulfides in Pleistocene deep Black Sea sediments and their paleo-oceanographic significance, p. 524–531. *In* E. T. Degens and D. A. Ross (eds.), The Black Sea—Geology, Chemistry, and Biology. American Association of Petroleum Geologists Memoir 20.

Bigelow, H. B., and W. C. Schroeder. 1948. Sharks, p. 59–546. *In* J. Tee-Van, C. M. Breder, S. F. Hildebrand, A. E. Parr, and W. C. Schroeder (eds.), Fishes of the Western North Atlantic, Lancelets, Cyclostomes, and Sharks. Sears Foundation for Marine Research, Memoir 1, Part 1. Yale University Press, New Haven.

Brett, C. E., and P. A. Allison. 1998. Paleontological approaches to the environmental interpretation of marine mudroeks, p. 302–349. *In* J. Schieber, W. Zimmerle, and P. S. Sethi (eds.), Shales and Mudstones, Vol. 1. E. Schweizebart'sche Verlagsbuchhandlung, Stuttgart.

Brett, C. E., and G. C. Baird. 1993. Taphonomic approaches to temporal resolution in stratigraphy: examples from Paleozoic marine mudrocks, p. 250–274. *In* S. M. Kidwell and A. K. Behrensmeyer (eds.), Taphonomic Approaches to Time Resolution in Fossil Assemblages. Paleontological Society Short Courses in Paleontology, No. 6.

Brett, C. E., A. H. Turner, P. I. McLaughlin, D. J. Over, G. W. Storrs, and G. C. Baird. 2003. Middle-Upper Devonian (Givetian-Famennian) bone/conodont beds from central Kentucky, USA: reworking and event condensation in the distal Acadian foreland basin. Courier Forschunginstitut Senckenberg, 242:125–139.

Brumsack, H.-J., and J. Thurow. 1986. The geochemical facies of black shales from the Cenomanian/Turonian boundary event (CTBE), p. 247–265. *In* E. T. Degens, P. A. Meyers, and S. C. Brassell (eds.), Biogeochemistry of Black Shales. Im Selbstverlag des Geologisch-Paläontologischen Institutes der Universität Hamburg, No. 60, Hamburg.

Carr, R. K. 1995. Placoderm diversity and evolution. VIIth International Symposium: Studies on Early Vertebrates. Bulletin du Muséum d'Histoire Naturelle, 17:85–125.

Carr, R. K. 1996. *Stenosteus angustopectus* sp. nov. from the Cleveland Shale (Famennian) of northern Ohio with a review of selenosteid (Placodermi) systematics. Kirtlandia, 49: 19–43.

Carr, R. K., and G. L. Jackson. 2010. The vertebrate fauna of the Cleveland Member (Famennian) of the Ohio Shale, Chapter 5. *In* J. T. Hannibal (ed.), Guide to the Geology and Paleontology of the Cleveland Member of the Ohio Shale. Ohio Geological Survey Guidebook 22.

Conant, L. C., and V. E. Swanson. 1961. Chattanooga Shale and related rocks of central Tennessee and nearby areas. U.S. Geological Survey Professional Paper 357. 91 p.

Degens, E. T., P. A. Meyers, and S. C. Brassell (eds.). 1986. Biogeochemistry of Black Shales. Im Selbstverlag des Geologisch-Paläontologisehen Institutes der Universität Hamburg, Hamburg. 421 p.

Degens, E. T., and D. A. Ross (eds.). 1974. The Blaek Sea—Geology, Chemistry, and Biology. American Association of Petroleum Geologists Memoir 20. 663 p.

Denison, R. H. 1941. The soft anatomy of *Bothriolepis*. Journal of Paleontology, 15:553–561.

Denison, R. H. 1978. Handbook of Paleoichthyology, Vol. 2, Placodermi. Gustav Fischer, Stuttgart. 128 p.

Denison, R. H. 1979. Handbook of Paleoichthyology, Vol. 5, Acanthodii. Gustav Fischer, Stuttgart. 62 p.

Dennis, K. D., and R. S. Miles. 1981. A pachyosteomorph arthrodire from Gogo, Western Australia. Zoological Journal of the Linnean Society, 73:213–258.

Elder, R. 1985. Principles of aquatic taphonomy with examples from the fossil record. Unpublished Ph.D. dissertation, University of Michigan, Ann Arbor. 351 p.

Elder, R. L., and G. R. Smith. 1988. Fish taphonomy and environmental inference in paleolimnology. Palaeogeography, Palaeoclimatology, Palaeoecology, 62:577–592.

Elliot, D. K., H. G. Johnson, R. Cloutier, R. K. Carr, and E. B. Daeschler. 2000. Middle and Late Devonian vertebrates of the western Old Red Sandstone Continent. Courier Forschunginstitut Senckenberg, 223:291–308.

Ettensohn, R. 1985. Controls on development of Catskill Delta complex basin-facies, p. 65–77. *In* W. L. Woodrow and W. D. Sevon (eds.), The Catskill Delta. Geological Society of America Special Paper 201.

Ferguson, L. 1963. The paleoecology of *Lingula squamiformes* Phillips during a Scottish Mississippian marine transgression. Journal of Paleontology, 37:669–681.

Gardiner, B. G. 1984. The relationships of the palaeoniscid fishes, a review based on new specimens of *Mimia* and *Moythomasia* from the Upper Devonian of Western Australia. Bulletin British Museum (Natural History), 37:173–428.

Hannibal, J. T., K. L. Gallup, L. E. Hulslander, E. F. Kennedy, C. A. Moglovkin, B. J. Olsen, M. V. Prarat, and J. A. Von Glahn. 2005. The black shale paradox: presumed pelagic, pseudoplanktonic, and burrowing and other benthic organisms preserved in the Cleveland Shale (Famennian), a "deep water" black shale deposited in anoxic conditions. Geological Society of America Abstracts with Programs, 37(2):4.

Heckel, P. H. 1972. Recognition of ancient shallow marine environments, p. 226–286. *In* J. K. Rigby and W. K. Hamblin (eds.), Recognition of Ancient Sedimentary Environments. Society of Economic Paleontologists and Mineralogists Special Publication 16.

Heintz, A. 1932. The structure of *Dinichthys*: a contribution to our knowledge of the Arthrodira. Bashford Dean Memorial Volume Archaic Fishes, 4:115–224.

Hill, A. 1979. Disarticulation and scattering of mammal skeletons. Paleobiology, 5:261–274.

Hlavin, W. J. 1976. Biostratigraphy of the Late Devonian black shales on the cratonal margin of the Appalachian geosyncline. Unpublished Ph.D. dissertation, Boston University. 211 p.

Hoover, K. V. 1960. Devonian–Mississippian shale sequence in Ohio. Ohio Division of Geologieal Survey Information Circular 27. 154 p.

Jannasch, H. W., H. G. Truper, and J. H. Tuttle. 1974. Microbial sulfur cycle in the Black Sea, p. 419–425. *In* E. T. Degens and D. A. Ross (eds.), The Black Sea—Geology, Chemistry, and Biology. American Association of Petroleum Geologists Memoir 20.

Keller, G. H. 1974. Mass physical properties of some western Black Sea sediments, p. 332–337. *In* E. T. Degens and D. A. Ross (eds.), The Black Sea—Geology, Chemistry, and Biology. American Association of Petroleum Geologists Memoir 20.

Lehman, J. P. 1954. Les Arthrodires du Maroc méridional (Tafilalet). 19th International Geological Congress, Algiers (1952), 19:123.

Lewis, T. L. 1988. Late Devonian and Early Mississippian distal basin-margin sedimentation of northern Ohio. Ohio Journal of Science, 88(1):23–39.

Lindsey, C. C. 1978. Form, function, and locomotory habits in fish, p. 1–100. *In* W. S. Hoar and D. J. Randall (eds.), Fish Physiology. Academie Press, New York.

Mausser, H. F. 1982. Stratigraphy and sedimentology of the Cleveland Shale (Devonian) in northeast Ohio. Unpublished master's thesis, Case Western Reserve University, Cleveland. 116 p.

McDowall, R. M. 1988. Diadromy in Fishes: Migrations between Freshwater and Marine Environments. Timber Press, Portland. 308 p.

Miles, R. S. 1969. Features of placoderm diversification and the evolution of the arthrodire feeding mechanism. Transactions of the Royal Society of Edinburgh, 68:123–170.

Miles, R. S., and T. S. Westoll. 1968. The placoderm fish *Coccosteus cuspidatus* Miller *ex* Agassiz from the Middle Old Red Sandstone of Scotland. Part 1, descriptive morphology. Transactions of the Royal Society of Edinburgh, 67:373–476.

Moy-Thomas, J. A., and R. S. Miles. 1971. Paleozoic Fishes. W. B. Saunders Company, Philadelphia. 259 p.

Murphy, A. E., B. B. Sageman, D. J. Hollander, T. W. Lyons, and C. E. Brett. 2000. Black shale deposition and faunal overturn in the Devonian Appalachian Basin: clastic starvation, seasonal water-column mixing, and efficient biolimiting nutrient recycling. Paleoceanography, 15(3):280–291.

Nelson, B. 1955. Mineralogy and stratigraphy of the pre-Berea sedimentary rocks exposed in northern Ohio. Unpublished Ph.D. dissertation, University of Illinois, Urbana-Champaign. 113 p.

Newberry, J. S. 1873. Descriptions of fossil fishes. Report of the Geological Survey of Ohio. Vol. 1, Pt. 2, Palaeontology, p. 245–355.

Rozanov, A. G., I. I. Volkov, and T. A. Yagodinskaya. 1974. Forms of iron in surface layer of Black Sea sediments, p. 532–541. *In* E. T. Degens and D. A. Ross (eds.), The Black Sea—Geology, Chemistry, and Biology. American Association of Petroleum Geologists Memoir 20.

Rücklin, M. 2002. New finds of placoderms from the Late Devonian of Morocco. 7th European Workshop on Vertebrate Palaeontology, Sibiu, Romania, Abstracts. 31 p.

Sageman, B. B., A. E. Murphy, J. P. Werne, C. A. Ver Straeten, D. J. Hollander, and T. W. Lyons. 2003. A tale of shales: the relative roles of production, decomposition, and dilution in the accumulation of organic-rich strata, Middle-Upper Devonian, Appalachian basin. Chemical Geology, 195:229–273.

Schäfer, W. 1972. Ecology and Palaeoecology of Marine Environments. Translated by I. Oertel. Oliver and Boyd, Edinburgh. 568 p.

Schieber, J. 1998. Sedimentary features indicating erosion, condensation, and hiatuses in the Chattanooga Shale of central Tennessee: relevance for sedimentary and stratigraphic evolution, p. 187–215. *In* J. Schieber, W. Zimmerle, and P. S. Sethi (eds.), Shales and Mudstones (Vol. 1). E. Schweizebart'sche Verlagsbuchhandlung, Stuttgart.

Schieber, J. 2003. Simple gifts and hidden treasures—implications of finding bioturbation and erosion surfaces in black shales. The Sedimentary Record, 1:4–8.

Seilacher, A. 1990. Taphonomy of Fossil-Lagerstätten, p. 266–270. *In* D. E. G. Briggs and P. R. Crowther (eds.), Palaeobiology: A Synthesis. Blackwell Scientific Publications, Oxford.

Siegel, S., and N. J. Castellan, Jr. 1988. Nonparametric Statistics for the Behavioral Sciences. McGraw-Hill Book Company, New York. 399 p.

Smith, G. R., and R. Elder. 1985. Environmental interpretation of burial and preservation of Clarkia fishes, p. 85–93. *In* C. J. Smiley (ed.), Late Cenozoic History of the Pacific Northwest. Pacific Division of the American Association for the Advancement of Science, California Academy of Science, San Francisco.

Stensiö, E. A. 1963. Anatomical studies on the arthrodiran head. Part I. Preface, geological and geographical distribution, the organization of the arthrodires, the anatomy of the head in the Dolichothoraci, Coccosteomorphi, and Pachyosteomorphi. Taxonomic appendix. Kungliga Svenska Vetenskapsakademiens, Handlingar, 9(2):1–419.

Streel, M., M. V. Caputo, S. Loboziak, and J. H. G. Melo. 2000. Late Frasnian-Famennian climates based on palynomorph analyses and the question of the Late Devonian glaciations. Earth-Science Reviews, 52:121–173.

Tasch, P. 1965. Communications theory and the fossil record of invertebrates. Transactions Kansas Academy of Science, 68: 322–329.

Thomson, K. S. 1971. The adaptation and evolution of early fishes. Quarterly Review of Biology, 46:139–166.

Webb, P. W. 1982. Locomotor patterns in the evolution of actinopterygian fishes. American Zoologist, 22:329–342.

Weigelt, J. 1989. Recent Vertebrate Carcasses and their Paleobiological Implications. Translated by J. Schaefer. University of Chicago Press, Chicago. 188 p.

Wignall, P. B. 1994. Black Shales. Clarendon Press, Oxford. 127 p.

Williams, M. E. 1990. Feeding behavior in Cleveland Shale fishes, p. 273–287. *In* A. J. Boucot, Evolutionary Paleobiology of Behavior and Coevolution. Elsevier, Amsterdam.

Woodrow, D. L., and W. D. Sevon (eds.). 1985. The Catskill Delta. Geological Society of America Special Paper 201. 246 p.

Zagger, G. W. 1995. Conodont biostratigraphy and sedimentology of the latest Devonian of northern Ohio. Unpublished master's thesis, Case Western Reserve University, Cleveland. 112 p.

KIRTLANDIA
The Cleveland Museum of Natural History

November 2010 *Number 57:46–52*

THE PHYLOGENETIC ORIGIN OF JAWS IN VERTEBRATES: DEVELOPMENTAL PLASTICITY AND HETEROCHRONY

JOHN A. LONG
Natural History Museum of Los Angeles County
900 Exposition Boulevard, Los Angeles, California 90007
jlong@nhm.org

BRIAN K. HALL
Department of Biology
Dalhousie University, Halifax, Nova Scotia, Canada B3H 4J1

KENNETH J. MCNAMARA
Department of Earth Sciences
University of Cambridge, Downing Street, Cambridge CB2 3EQ, United Kingdom

AND **MOYA M. SMITH**
MRC Centre for Developmental Neurobiology
Kings College London, London Bridge, EC19 RT, United Kingdom

ABSTRACT

The bearing that agnathans have on the origin of jawed vertebrates is one of the great unsolved problems in vertebrate phylogeny. Here we propose a mechanism for the evolution of jaws in vertebrates based on a combination of evidence from the fossil record and from experimental developmental biology. In chick embryos, osteogenesis can be evoked experimentally from scleral mesenchyme by the same mandibular epithelium that evokes osteogenesis in the jaws. Sclerotic bones appeared before jaws in vertebrate phylogeny and scleral ossicles and jaw skeletons are linked by shared developmental processes. As only one group of fossil agnathans—the Osteostraci—has ossified sclerotic bones, they alone possessed the inherent developmental potential to develop bone in the lower jaws and are also considered the most probable sister taxon to gnathostomes.

Introduction

Nineteenth-century anatomists recognized that, based on embryonic development, innervation and vascular patterns, vertebrate jaws were the serial homologues of the skeletal branchial arches posterior to them (Gegenbaur, 1872). However, the skeletal support for the gill arches in living agnathans and gnathostomes are positioned differently (lateral in the former and medial in the latter) and so have been considered non-homologous (Goodrich, 1930; Schaeffer and Thomson, 1980). Mallatt (1984, 1996) suggested that an ancestral pregnathostome fish had two sets of branchial skeletal supports, one medial and one lateral, with the medial set being the current situation in all gnathostomes, while the lateral set is seen in living agnathans. Janvier (1996a) proposed that the lateral gill-arch cartilages are primitive for all vertebrates as the only set. Recent work by Kimmel et al. (2001) on neural crest ectomesenchyme in the zebrafish *Danio rerio* supports the notion that the lateral set of gill-arch structures comprise the gill arches in gnathostomes, and that, consequently, there is no barrier to the hypothesis that jaw cartilages arose from such gill-arch support cartilages.

A review of gnathostome origins by Forey and Janvier (1993) stated that "the way in which jaws develop remains unknown." On the basis of new paleontological data others have challenged the canonical view that jaws evolved from modification of the anteriormost branchial arches (Maisey, 1986). A review by Smith and Coates (2000) has emphasized the difficulties of accepting this classic segmentalist theory, of repetition of similar branchial arches, either on the basis of the phylogenetic changes proposed from the paleontological data, or from the developmental data. Janvier (1998) has compared succinctly the currently accepted theory with an alternative model, namely the conversion of skeletal structures supporting the velar feeding apparatus in the living agnathan lampreys, to the lower jaw cartilage of gnathostomes. This velar apparatus is quite anterior and medial

to the branchial basket, and supplied by the same nerves and homologous muscles as the jaws of gnathostomes. Shigeru Kuratani and his colleagues (Kuratani et al., 1999, 2001; Kuratani, 2003a, 2003b, 2004) showed that the lips of lampreys are derived from non-homologous embryonic components (mesoderm derived cartilage). With respect to crest derived cartilage of gnathostome jaws, the timing of neural crest emigration for the mandibular stream, some of which contributes to the cartilages, is identical in lampreys and gnathostomes. It appears to us that cartilaginous and jointed jaws could evolve from the velar ectomesenchymal condensations as either or both medial and lateral parts (Johnels, 1948), as Janvier (1996a, 1996b) proposed, and not by co-option of those of the more caudal branchiomeric arches. The addition of dermal bone for attachment of feeding elements to an articulated joint is another, as yet unrecognized, step and one we here consider to have occurred through developmental plasticity and heterochrony. It has become apparent that the evolution of jaws is not an example of co-option of one structure adapted for one function to take over another, i.e., from respiration to feeding (Smith and Coates, 2000). Equally, it is not an example of a parallel co-option of molecular patterning mechanisms used for anteroposterior positional information in the hindbrain to patterning the branchial arches, as suggested by Raff (1996). Mandibular arch with Hox-negative mandibular arch patterning appears to be separate from patterning of the gill arches (Graham, 2001; Graham and Smith, 2001), also the mandibular arches derive the bulk of their neural crest mesenchyme cells from the cephalic region (a small contribution from the midbrain with most rostral hindbrain). Kuratani (2003) postulated that the evolution of the vertebrate jaw developed as a change in developmental program for the specification of crest cells. All this raises important unanswered questions, such as, how the upper and lower jaws are linked in their development and evolution, and whether other developmental modules are part of this developmental matrix. Once dissociated from the development and evolution of gill arches, the concept that part of the anterior visceral skeleton including an osteogenic module, articulated with part of the rostral chondrocranium, may contribute to the developmental process forming jaws, becomes a possibility.

Phylogenetic Relationships

Two different pieces of evidence support agnathan thelodonts as a group sharing significant characters with gnathostomes; one, on the basis of stomachs preserved in the fork-tailed thelodonts (Wilson and Caldwell, 1993, 1998), the other on the evidence that branchial denticle whorls are present in one thelodont, *Loganellia scotica* (Van der Bruggen and Janvier, 1993) and in sharks. This has been supported by further studies comparing the arrangement of these branchial denticles with those of the early shark, *Akmonistion* (Smith and Coates, 2000, 2001; previously cited as *Stethacanthus* sp. (Coates and Sequiera, 2001)). The proposal made by Smith and Coates is that these could be an early example of oropharyngeal denticles in an agnathan able to be transformed through evolution to tooth whorls, inferred to be a primitive character of gnathostome vertebrates. It is proposed that these denticle groups exhibit a prepattern for the dentition as it evolved onto the jaw margins (Smith and Coates, 1998, 2000). Although thelodonts are probably a paraphyletic group with respect to more advanced pregnathostomes and gnathostomes (Janvier, 1996b), thelodonts may also include sub-adult osteostracans (of which juveniles are unknown). This could provide an explanation for the apparent absence of teeth or specialized oropharyngeal denticles in the closest sister-group to jawed vertebrates, the osteostraeans. Clearly, there is a problem here with (secondary?) absence of toothlike denticles in those groups which may include incipient stages in early jaw evolution. However, a cladistic analysis (Donoghue et al., 2000) proposes thelodonts as a monophyletic group, as opposed to the paraphyletic group proposed by Janvier (1981, 1996b). However, we note that Donoghue et al. did not test for monophyly of thelodonts.

Other phylogenetic analyses (Janvier, 1981, 1984, 1985; Forey, 1984; Forey and Janvier, 1993) support the view that the Osteostraci share more synapomorphies with gnathostomes than with any other agnathan group. These analyses were done before the fork-tailed thelodonts were recognized as a group. Numerous morphological characters link (toothless) osteostracan agnathans to placoderms and crown-group gnathostomes (Forey and Janvier, 1993; Janvier, 1996b), and this robust arrangement cannot be rejected easily. The only systematically argued alternative, which places thelodonts *sensu lato* as the immediate gnathostome sister-group (Wilson and Caldwell, 1998) has much lower resolution and uses a smaller data set.

Smith and Coates (1998, 2000, 2001) accept the fact that no satisfactory explanation of this apparently edentate stretch of gnathostome phylogeny has yet been presented. The extinct agnathan groups Galeaspida and Pituriaspida (Young, 1991) are also potential alternative sister taxa to the Gnathostomata, but incomplete data on the jaws and branchial skeleton preclude discussion here. Both Pituriaspida and Osteostraci probably had paired pectoral fins (assumed to be present in Pituriaspida) due to the large pectoral fenestra in their dermal armour (Young, 1991). Similarly, Osteostraci have perichondral bone developed in the neurocranium (a feature shared with gnathostomes), although little is known of the structure of the tail and pectoral fin (if present) in this group. It should be noted that the stated absence of perichondral bone in Galespida (Wang et al., 2005) has challenged previous statements that it is present in the neurocranium and is used to support their position close to Gnathostomata (Young, 1991). While the paleontological data suggests that several of these groups may be sister-groups to the Gnathostomata, resolution of this problem using cladistic methodologies is equivocal; character states require polarity which in some cases cannot be determined without arbitrary character weighting, or more complete anatomical data from new fossil discoveries.

Developmental Processes

There is a developmental link between those mechanisms integral to initiation of the bony scleral ring of the eyes (Figure 1) to that of the cartilage and bone of the jaws, Meckel's cartilage, and dermal membrane bones (Hall, 1981, 2005). All three skeletal components develop from neural crest-derived mesenchyme dependent on, and sequential to, inductive interactions with embryonic epithelia. Membrane bones of the lower jaw arise following interaction with mandibular epithelium. Scleral bones in birds (we do not know the inductive signals in reptiles or fish) arise following induction from specialized epithelial papillae overlying the eye (Hall, 1981, 2005; Pinto and Hall, 1991).

As an alternative to this source of the signal, osteogenesis can be evoked from scleral mesenchyme by mandibular epithelium. In experimental studies of chick embryos, scleral mesenchyme will develop into sclerotic bones of the eye following contact with mandibular epithelium, i.e., the bones are recognizably scleral ossicle. The epithelium provides a signal that is sufficient to

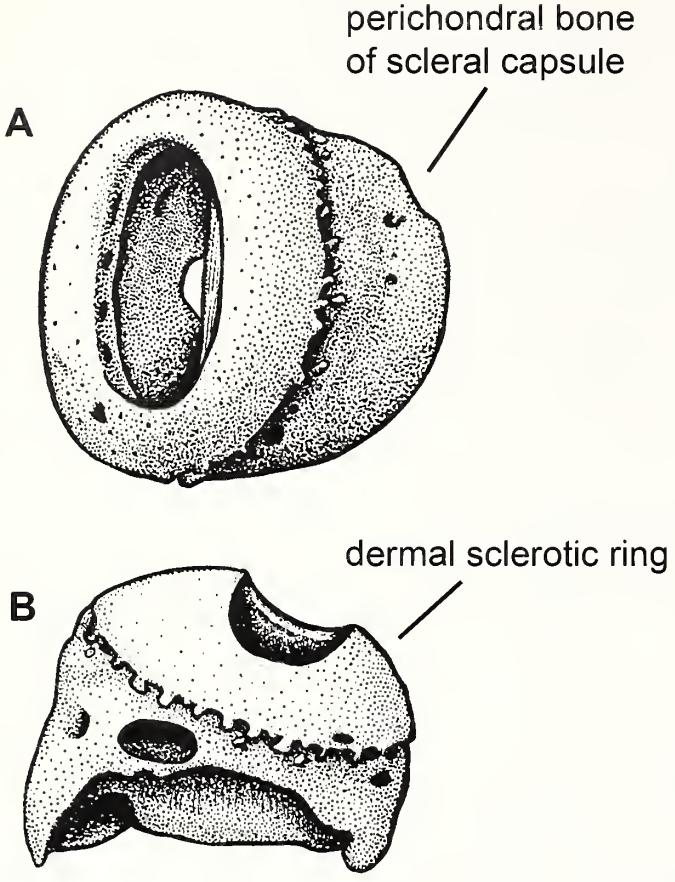

Figure 1. Fossilized sclerotic ring from the osteostracan *Trematapis mammillata* Patten, after Janvier (1985).

initiate differentiation, but morphogenesis is controlled by the mesenchyme (Hall, 1981, 1982, 1989). It follows from these observations that the formation of lower jaw bones, at least in chick embryos—the one taxon for which experimental evidence is available—uses the same class of inductive mechanisms as do scleral bones. This is a putative, shared, homologous developmental mechanism (Hall, 1995, 2003) providing a link between developmental mechanisms underlying scleral ossicles of the eye and those that initiate chondrogenesis and osteogenesis in the jaws.

We suggest that evolutionary origin of the lower jaws in the first fishes may have been developmentally interconneeted with the origins of sclerotic ring ossification. The scenario would be:

- neural crest cells migrate to surround the eye in a jawless vertebrate;
- neural crest cells migrate further ventrally and laterally as the primordia of the mandibular arch develop en route to jawed vertebrates;
- either inductively active epithelium migrated with neural crest cells as is known to occur in extant gnathostomes (Couly and Le Douarin, 1990); and/or
- mandibular arch neural crest cells interacted with adjacent epithelium to elicit inductive signaling (see Hall, 1992, for such a mechanism);
- bone was induced in the first lower jaws using the same developmental mechanism as evokes scleral bones, i.e., the evolutionary origin of the jaw skeleton is developmentally linked to initial ossification around the eyes.

Further, Couly et al. (2002) revealed that the interaction between the head ectoderm and oral endoderm leads to the patterning of the jaw cartilages in the chick embryo.

Studies from both heterochrony and paleontology support this scenario.

Heterochronic Processes

The role of heterochrony in the appearance of major evolutionary novelties has long been recognized. McKinney and McNamara (1991) suggested that heterochronic processes involving changes to the timing of onset of initiation and growth of structures (predisplacement and postdisplacement) at very early developmental stages may have played a role in the evolution of some higher taxa, a view reinforced by Richardson et al. (1997) and Richardson (1999).

Hall (1984) has demonstrated how the timing of production of Meckel's cartilage varies between classes of vertebrates. It forms earliest in development in birds, later in amphibians and cyclostomes, and even later still in mammals. Phylogenetically this can be interpreted as peramorphic predisplacement in birds, relative to amphibians and cyclostomes, but paedomorphic postdisplacement in mammals (see Hall, 2000). The analogy between this and the appearance of jaws and sclerotic rings in fishes in evolution is through a similar inductive tissue interaction. If both scleral and mandibular mesenchyme can form bone in response to mandibular oral epithelium in birds, and assuming similar tissue interactions in other taxa, then the timing of jaw initiation is likely to be earlier in osteostracans than in jawless fishes, such as cyclostomes. In heterochronic terms (McKinney and McNamara, 1991) predisplacement in the timing of migration of the neural crest cells may have been a critical factor in triggering bone formations in fishes.

MacDonald and Hall (2001) demonstrated that the timing of the epithelial-mesenchymal interactions responsible for the produetion of Meckel's cartilage varies between three inbred strains of mice, and that timing of the interactions correlates with timing of condensation of the cells that give rise to Meckel's cartilage. The significance of this study is threefold:

1. providing an experimental demonstration that heterochrony is an evolutionary mechanism;
2. demonstrating that timing changes can occur between closely related taxa;
3. demonstrating that such timing changes can occur in the relatively short number of generations required to establish the inbred lines.

Molecular studies indicate the classes of genes that are likely to be responsible for such heterochronic changes; the most likely candidates are *Bmp-2* and *-4, Msx-1*, and *Fgf-4* and *-8* (Barlow and Francis-West, 1997; Chen et al., 2000; Ferguson et al., 2000; MacDonald and Hall, 2001; Hall, 2005).

We would expect onset of ossification of mandibular bones to be controlled similarly. Indeed, recent studies on teleost fish are consistent with teleost scleral ossicles having a closer relationship to scleral cartilage than to the scleral ossicles of other vertebrate groups, to the point that teleost ossicles may not be homologous with scleral ossicles in birds but with scleral cartilage; for example, fish ossicles arising in scleral cartilage, and avian ossicles as

separate dermal ossifications (Franz-Odendall and Hall, 2006). If this was true for the earliest agnathans, i.e., if their scleral ossicles arose in relation to cartilage, then the link we propose between jaw and scleral skeletons becomes even stronger, especially as scleral cartilages in reptiles and birds are initiated following an inductive interaction between mesenchyme and pigmented retinal epithelium (Pinto and Hall, 1991; Hall, 2005).

Fyfe and Hall (1981) and Hall (1981) discuss mutants, such as scaleless (sc) that prevent epithelial papillae formation, and thus inhibit cell condensations and scleral bone formation. McAleese and Sawyer (1982) showed that because the scaleless gene is first expressed in the ectoderm and later in the mesenchyme, combining embryonic sc/sc ectoderm with +/+ mesenchyme of the same age results in a scaleless phenotype. However, recombining sc/sc ectoderm with mesenchyme from older embryos results in a scaled phenotype being produced. Thus, the timing of gene expression is critical to papilla formation. Consequently, skeletal elements that arise following epithelial-mesenchymal interactions (Meckel's cartilage, scleral, and mandibular bones; see previous paragraph) can be interpreted as occurring by pre- or postdisplacement of the time of expression of genes expressed in inductively active epithelia.

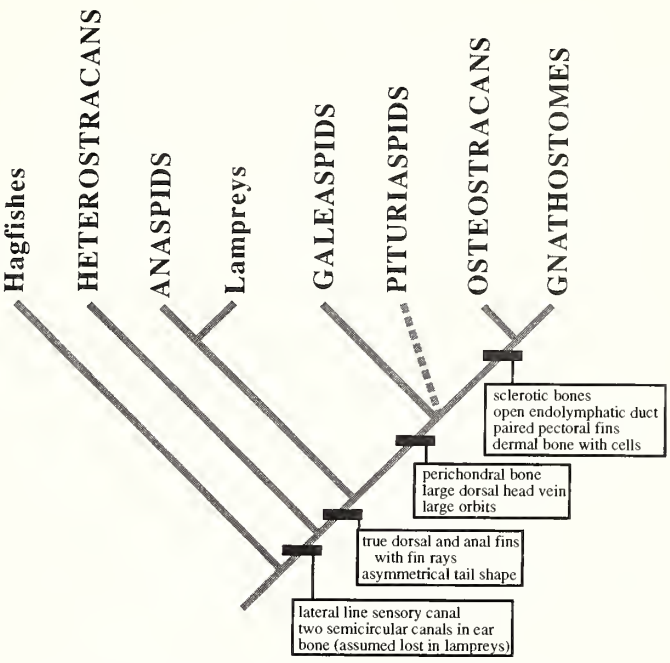

Figure 2. Preferred hypothesis of agnathan-gnathostome interrelationships based on the presence of scleral ossifications as inducers of jaw formation. Cladogram after Forey and Janvier (1984). Phylogenetic position of anaspids is unsure; they could alternatively be the sister-group to the node containing galeaspids and higher taxa (Janvier, 1975).

Paleontological Data

The presence of ossified sclerotic bones in fossil agnathan fishes has been demonstrated only in one group—the Osteostraci (e.g., Janvier, 1985, fig. 1). Osteostracans have been proposed as the most likely sister-group to gnathostomes; they share the presence of paired pectoral fins, open endolymphatic ducts, dermal bone with cells, and an epicercal tail with modified scale cover (Janvier, 1981, 1984, 1985; Forey, 1984; Forey and Janvier, 1993).

Maisey (1986, 1988) proposed a close relationship between anaspids and gnathostomes based on six characters. Some of these are shared or of uncertain distribution. However, stronger more reliable characters uniting gnathostomes with osteostracans have been proposed by more recent workers. The presence of circumorbital bones in anaspids is not seen to be homologous with the bony sclerotic plates seen in osteostracans and some basal gnathostomes as these are not as strongly interlocking as in sclerotic plates, nor do they share a well-ossified fundal surface to the ossified eye capsule, a feature seen on osteostracans and basal placoderms (Janvier, 1985; Long and Young, 1988).

Thelodonts, a group of fossil agnathans lacking armoured plates, have also been proposed as a possible closer relative to gnathostomes (Janvier, 1981; Wilson and Caldwell, 1998). However, based on many well-preserved specimens of *Phlebolepis* (Ritchie, 1968), *Turinia* (Turner, 1982), and the more recently described deep-bodied fork-tailed furcacaudiforms from Canada (Wilson and Caldwell, 1993, 1998), all of which have the orbital region of the head well-preserved, the sclerotic bones are clearly absent in thelodonts. Lack of this developmental potential to form dermal bones anywhere, including the sclera, may preclude the thelodonts from a position where they could transform into gnathostomes with bones in the jaws. This difficulty disappears, or at the very least is lessened, if agnathan scleral ossicles formed in association with scleral cartilage.

Sharks also lack bone (except in some specialized regions like the base of fin brushes, see Coates et al., 1998), but they always have jaws and teeth. As to the presence of scleral bones in basal chondrichthyans, the Devonian shark *Cladoselache* (Dean, 1909) and some other Cleveland Shale sharks (e.g., as in Williams, 1998), show enlarged dermal scales surrounding the orbit that may be homologous to other gnathostome scleral bones or to circumorbital bones. In placoderms, dermal scleral bones are often highly ornamented, similar to their elaborate body scales (e.g., *Murrindalaspis*, Long and Young, 1988; Young, 2008) providing support for the hypothesis that scleral bones might well have originated primarily from enlargement of the dermal scales around the eyes. Similar rings of ornamented denticles surround the eye in Cleveland Shale "*Ctenacanthus*" (Williams, 1998).

Developmental Interpretation

On the basis of the developmental link between scleral and mandibular bone, we propose that osteostracans are the most likely sister-group to gnathostomes (Figure 2). In all the earliest gnathostome groups, such as acanthothoracid placoderms, even the fundal surface of the sclerotic capsule may be perichondrally ossified (Long and Young, 1988). This condition is also partially developed in osteostracans (Figure 1), with bone developing as a separate membranous ossification site as well as forming subperiosteally in the scleral cartilage capsule and, as discussed above, appears to be the condition in teleosts.

The evolution of jaws may not be simply related to the functional significance of the structures themselves (i.e., to support teeth and improve feeding ability), but is almost certainly constrained by developmental controls. These involve the timing of neural crest cell migration and changes in the timing of regulatory molecules within the developmental modules. Many early agnathans had well-developed oral plates lining the ventral border of the mouth, providing them with an effective feeding mechanism that operated in a manner similar to a lower jaw (Janvier, 1974, 1985). In some osteostracans, like *Trematapsis*, an

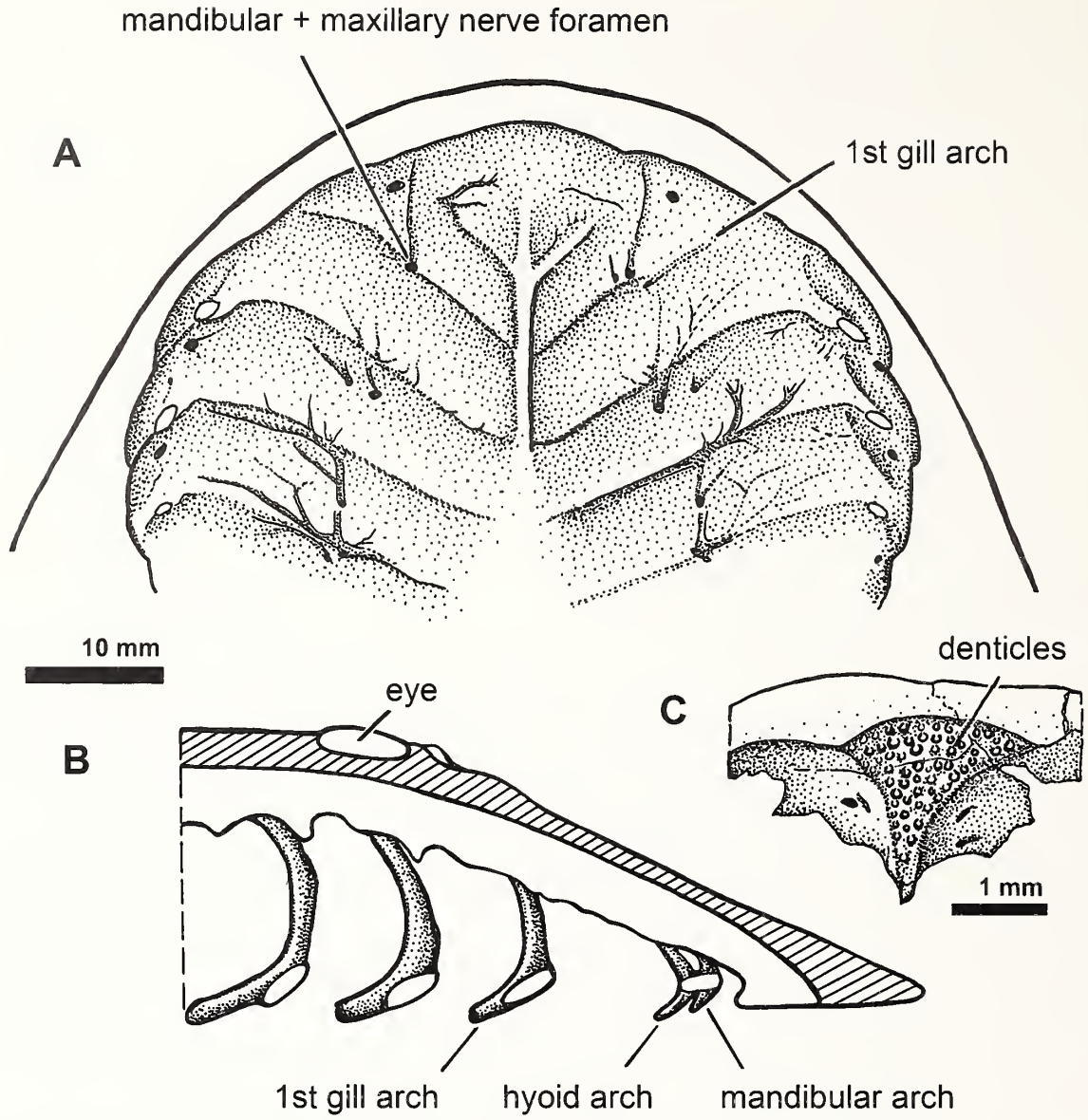

Figure 3. A, interpretation of orobranchial cavity in *Scolenaspis signata* (Wangsjo) from the Early Devonian of Spitzbergen with sagittal section (B) shown below, including attempted restoration of gill-arch elements. C, supraoral region of *Trematapis mammillata* Patten from the Late Silurian of Estonia and Gotland, Sweden, showing intrabuccal denticles. After Janvier (1985).

anterior median lamina covered by denticles was situated just inside the roof of the mouth (Janvier, 1985, fig. 17; shown here in Figure 3C). This implies that a ventral structure may have acted against this surface for food reduction, possibly a denticle covered rasping organ, based on the lamprey model of the piston cartilage and "toothed" plate.

The inside visceral surface of the dorsal shields of osteostracans shows both the impressions of branchial pouches and grooves for the cranial nerves supplying the muscles that are presumed to operate skeletal cartilages of the branchial arches. Janvier (1996a) has reinterpreted these nerves from the first reconstruction of Stensiö (1958) to show that the mandibular and maxillary branches of the trigeminal are relatively much more anterior than previously thought. The foramen for the mandibular and maxillary nerves (V) is visible on the first branchial ridge in *Scolenaspis* and in several other osteostracans (Janvier, 1985). Therefore, the branchial ridges of osteostracans situated close to the mouth margins may be homologous structures to the gnathostome jaws, and are topographically compatible with the quite anterior position of the velar cartilages in the lamprey. Moreover, the first two branchial pouches were situated well forward of the eyes (Figures 3A, 3B). Osteostracans presumably had cartilaginous gill-arch supports as shown by impressions of gill structures on the visceral surface of their shield. It is significant that these gill pouches are separate from the first two probable feeding arches. The developmental link between jaws and scleral formation is further emphasized by the fact that the ophthalmic nerve is also a branch of the fifth cranial nerve (as are the mandibular and maxillary nerves), serving to innervate the eyeball with small ciliary nerves.

Consequently, by small, but critical, changes to the timing of early developmental events, the evolution of the anterior

branchial arch elements to become primitive jaws did not necessitate large scale structural reorganization.

Acknowledgments

We thank the Raine Memorial Trust for provision of a Raine visiting Professorship to BKH to come to Western Australia, and K. Aplin, L. Budney, K. Campbell, T. Fedak, T. Franz-Odendaal, P. Janvier, J. Maisey, and G. Young for their helpful discussion of the work or for comments made on the submitted manuscript.

References

Barlow, A. J., and P. H. Francis-West. 1997. Ectopic application of recombinant BMP-2 and BMP-4 can change patterning of developing chick facial primordia. Development, 124:391–398.

Chen, Y., Y. Zhang, T. X. Jiang, A. J. Barlow, T. R. St. Armand, S. Heaney, P. H. Francis-West, C.-M. Chuong, and R. Mass. 2000. Conservation of early odontogenic signaling pathways in Aves. Proceedings of the National Academy of Sciences, U.S.A., 87:10040–10044.

Coates, M. I., I. J. Sansome, S. E. K. Sequeira, and M. M. Smith. 1998. Spines and tissues of ancient sharks. Nature, 396:729–730.

Coates, and Sequiera. 2001. A new stethacanthid chondrichthyan from the Lower Carboniferous of Bearsden, Scotland. Journal of Vertebrate Paleontology, 21:438–459.

Couly, G., S. Creuzet, S. Bennaceur, C. Vincent, and N. M. Le Douarin. 2002. Interactions between Hox-negative cephalic neural crest cells and the foregut endoderm in patterning facial skeleton in the vertebrate head. Development, 129:1061–1073.

Couly, G., and N. M. Le Douarin. 1990. Head morphogenesis in embryonic avian chimaeras: evidence for a segmental pattern in the ectoderm corresponding to the neuromeres. Development, 108:543–558.

Dean, B. 1909. Studies on fossil fishes (sharks, chimaeroids and arthrodires). Memoirs of the American Museum of Natural History, 5:211–287.

Donoghue, P. C. J., P. L. Forey, and R. J. Aldridge. 2000. Conodont affinity and chordate phylogeny. Biological Reviews, 75:191–251.

Ferguson, C. A., A. S. Tucker, and P. T. Sharpe. 2000. Temporospatial cell interactions regulating mandibular and maxillary arch patterning. Development, 127:403–412.

Forey, P. L. 1984. Yet more reflection on agnathan-gnathostome relationships. Journal of Vertebrate Paleontology, 4:330–343.

Forey, P. L., and P. Janvier. 1993. Agnathans and the origin of jawed vertebrates. Nature, 361:129–134.

Franz-Odendall, T. A., and B. K. Hall. 2006. Skeletal elements within teleost eyes and a discussion of their homology. Journal of Morphology, 267:1326–1337.

Fyfe, D. M., and B. K. Hall. 1981. A scanning electron microscopic study of the developing epithelial scleral papillae in the eye of the chick embryo. Journal of Morphology, 167:201 p.

Gegenbaur, C. 1872. Untersuchungen zur vergleichenden Anatomie der Wirbelthiere. III. Das Kopfskelet der Selachier. Engelman, Leipzig. 316 p.

Goodrich, E. S. 1930. Studies on the structure and development of vertebrates. Dover, New York. 837 p.

Graham, A. 2001. The development and evolution of the pharyngeal arches. Journal of Anatomy, 199:133–141.

Graham, A., and A. Smith. 2001. Patterning the pharyngeal arches. BioEssays, 23:54–61.

Hall, B. K. 1981. Specificity in the differentiation and morphogenesis of neural crest derived scleral ossicles and of the epithelial scleral papillae in the eye of the embryonic chick. Journal of Embryology and Experimental Morphology, 66:175–190.

Hall, B. K. 1982. How is mandibular growth controlled during development and evolution? Journal of Craniofacial Genetics and Developmental Biology, 2:45–49.

Hall, B. K. 1984. Developmental processes underlying heterochrony as an evolutionary mechanism. Canadian Journal of Zoology, 62:1–7.

Hall, B. K. 1989. Morphogenesis of the skeleton: epithelial or mesenchymal control? p. 198–201. *In* H. Splechtna and H. Hilgers (eds.), Trends in Vertebrate Morphology. Proceedings of the 2nd International Symposium on Vertebrate Morphology, Vienna, 1986. Fortschritte der Zoologie, 35. Fischer-Verlag, Stuttgart.

Hall, B. K. 1992. Cell-cell interactions in craniofacial growth and development, p. 261–267. *In* Z. Davidovitch (ed.), The Biological Mechanisms of Tooth Movement and Craniofacial Adaptation. EBSCO Media, Birmingham.

Hall, B. K. 1995. Homology and embryonic development. Evolutionary Biology, 28:1–37.

Hall, B. K. 2000. The evolution of the neural crest in vertebrates, p. 14. *In* L. Olsson and C.-O. Jacobsen (eds.), Regulatory Processes in Development. Wenner-Gren International series, Volume 76. Portland Press, London.

Hall, B. K. 2003. Descent with modification: the unity underlying homology and homoplasy as seen through an analysis of development and evolution. Biological Reviews of the Cambridge Philosophical Society, 78:409–433.

Hall, B. K. 2005. Bones and Cartilage: Developmental and Evolutionary Skeletal Biology. Elsevier/Academic Press, London. 760 p.

Janvier, P. 1974. The structure of the naso-hypophysial complex and the mouth in fossil and extant cyclostomes, with remarks on amphiaspiforms. Zoologica Scripta, 3:193–200.

Janvier, P. 1975. Les yeuxs des cyclostomes fossils et le probleme de l'origines des Myxinoides. Acta Zoologica, 56:1–9.

Janvier, P. 1981. The phylogeny of the craniate, with particular reference to the significance of fossil agnathans. Journal of Vertebrate Paleontology, 1:121–171.

Janvier, P. 1984. The relationships of the Osteostraci and the Galeaspida. Journal of Vertebrate Paleontology, 4:344–358.

Janvier, P. 1985. Les cephalaspides du Spitsberg: anatomie, phylogenie et systematique des osteostraces siluro-devoniens; revision des osteostraces de la Formation de Wood Bay (Devonien inferieur du Spitsberg). Cahiers de Paleontologie, C.N.R.S. edit., Paris. 244 p.

Janvier, P. 1996a. Early Vertebrates. Oxford University Press, Oxford. 326 p.

Janvier, P. 1996b. The dawn of the vertebrates: characters versus common ascent in the rise of current vertebrate phylogenies. Palaeontology, 39:259–287.

Janvier, P. 1998. Les vertebres avant le Silurien. Geobios, 30:931–950.

Johnels, A. G. 1948. On the development and morphology of the skeleton of the head of *Petromyzon*. Acta Zoologica, 70:139–279.

Kimmel, C. B., C. T. Miller, and R. Keynes. 2001. Neural crest patterning and the evolution of the jaw. Journal of Anatomy, 199:105–119.

Kuratani, S. 2003a. Evolution of the vertebrate jaw: homology and developmental constraints. Paleontological Research, 7:89–102.

Kuratani, S. 2003b. Evolutionary developmental biology and vertebrate head segmentation: a perspective from developmental constraint. Theory in Biosciences, 122:230–251.

Kuratani, S. 2004. Evolution of the vertebrate jaw: comparative embryology and molecular developmental biology reveal the factors behind evolutionary novelty. Journal of Anatomy, 205:335–347.

Kuratani, S., N. Horigome, and S. Hirano. 1999. Developmental morphology of the cephalic mesoderm and re-evaluation of segmental theories of the vertebrate head: evidence from embryos of an agnathan vertebrate, *Lampetrajaponica*. Developmental Biology, 210:381–400.

Kuratani, S., Y. Nobusada, N. Horigome, and Y. Shigetani. 2001. Embryology of the lamprey and evolution of the vertebrate jaw: insights from molecular and developmental perspectives. Philosophical Transactions of the Royal Society B, 356:15–32.

Long, J. A., and G. C. Young. 1988. Acanthothoracid remains from the Early Devonian of New South Wales, including a complete sclerotic capsule and pelvic girdle. Memoirs of the Australasian Association of Palaeontologists, 7:65–80.

MacDonald, M. E., and B. K. Hall. 2001. Altered timing of the extracellular-matrix-mediated epithelial-mesenchymal interaction that initiates mandibular skeletogenesis in three inbred strains of mice: development, heterochrony, and evolutionary change in morphology. Journal of Experimental Zoology, 291:258–273.

Maisey, J. 1986. Heads and tails: a chordate phylogeny. Cladistics, 2:201–256.

Maisey, J. 1988. Phylogeny of early vertebrate skeletal induction and ossification patterns. Evolutionary Biology, 22:1–36.

Mallatt, J. 1984. Early vertebrate evolution: pharyngeal structure and the origin of gnathostomes. Journal of Zoology London, 204:169–183.

Mallatt, J. 1996. Ventilation and the origin of jawed vertebrates: a new mouth. Zoological Journal of the Linnean Society, 117:329–404.

McAleese, S. R., and R. H. Sawyer. 1982. Avian scale development. IX. Scale formation by scaleless (sc/sc) epidermis under the influence of normal scale dermis. Developmental Biology, 89:493–502.

McKinney, M. L., and K. J. McNamara. 1991. Heterochrony: The Evolution of Ontogeny. Plenum Press, New York. 420 p.

Patterson, C. 1982. Morphological characters and homology, p. 21–74. *In* K. A. Joysey and A. E. Friday (eds.), Problems of Phylogenetic Reconstruction. Systematics Association Special Volume 21. Academic Press, London.

Pinto, C. B., and B. K. Hall. 1991. Towards an understanding of the epithelial requirement for osteogenesis in scleral mesenchyme of the embryonic chick. Journal of Experimental Zoology, 259:92–108.

Raff, R. A. 1996. The Shape of Life: Genes, Development, and the Evolution of Animal Form. University of Chicago Press, Chicago. 544 p.

Richardson, M. K. 1999. Vertebrate evolution: the developmental origins of adult variation. BioEssays, 21:604–613.

Richardson, M. K., J. Hanken, M. L. Gooneratne, C. Pieau, A. Raynaud, L. Selwood, and G. M. Wright. 1997. There is no highly conserved embryonic stages in the vertebrates: implications for current theories of evolution and development. Anatomy and Embryology, 196:91–106.

Ritchie, A. 1968. *Phlebolepis elegans* Pander, an Upper Silurian thelodont of Oesel, with remarks on the morphology of thelodonts, p. 81–88. *In* T. Orvig (ed.), Current Problems in Lower Vertebrate Phylogeny, Nobel Symposium, 4.

Schaeffer, B., and K. S. Thomson. 1980. Reflections on agnathan-gnathostome relationships, p. 19–33. *In* L. Jacobs (ed.), Aspects of vertebrate history. Essays in Honor of Edwin Harris Colbert. Museum of Northern Arizona Press, Flagstaff.

Smith, M. M., and M. I. Coates. 1998. Evolutionary origins of vertebrate dentitions: phylogenetic patterns and developmental evolution. European Journal of Oral Sciences, Supplement 1, 106:482–500.

Smith, M. M., and M. I. Coates. 2000. Evolutionary origins of teeth and jaws: developmental models and phylogenetic patterns, p. 133–151. *In* M. F. Teaford, M. M. Smith, and M. J. W. Ferguson (eds.), Development, Function and Evolution of Teeth. Cambridge University Press, Cambridge.

Smith, M. M., and M. I. Coates. 2001. The evolution of vertebrate dentitions: phylogenetic pattern and developmental models, p. 223–240. *In* P. E. Ahlberg (ed.), Major Events in Vertebrate Evolution. Taylor and Francis, London.

Stensiö, E. A. 1958. Les cyclostomes fossils ou ostracodermes, p. 173–425. *In* P. P. Grasse (ed.), Traite de Zoologie, 12(1). Masson, Paris.

Turner, S. 1982. A new articulated thelodont (Agnatha) from the Early Devonian of Britain. Palaeontology, 25:879–889.

Turner, S. 1991. Monophyly and interrelationships of the Thelodonti, p. 87–119. *In* M. M. Chang, Y. H. Liu, and G. R. Zhang (eds.), Early Vertebrates and Related Problems of Evolutionary Biology. Science Press, Beijing.

Van der Bruggen, W., and P. Janvier. 1993. Denticles in thelodonts. Nature, 364:107.

Wang, N.-Z., P. C. J. Donoghue, M. M. Smith, and I. J. Sansom. 2005. Histology of the galeaspid dermoskeleton and endoskeleton, and the origin and early evolution of the vertebrate cranial endoskeleton. Journal of Vertebrate Paleontology, 25:745–756.

Williams, M. E. 1998. A new specimen of *Tamiobatis vetustus* (Chondrichthyes, Ctenacanthoidea) from the Late Devonian Cleveland Shale of Ohio. Journal of Vertebrate Paleontology, 18:251–260.

Wilson, M. V. H., and M. W. Caldwell. 1993. New Silurian and Devonian fork-tailed 'thelodonts' are jawless vertebrates with stomachs and deep bodies. Nature, 361:442–444.

Wilson, M. V. H., and M. W. Caldwell. 1998. The Furcacaudiformes: a new order of jawless vertebrates with thelodont scales, based on articulated Silurian and Devonian fossils from northern Canada. Journal of Vertebrate Palaeontology, 18:10–29.

Wilson, M. V. H., and T. Marrs. 2004. Towards a phylogeny of the thelodonts, p. 95–108. *In* G. Arratia, R. Cloutier, and M. V. H. Wilson (eds.), Recent Advances in the Origin and Early Radiation of Vertebrates. Verlag Dr. Friedrich Pfeil, Munich.

Young, G. C. 1991. The first armoured agnathan vertebrates from the Devonian of Australia, p. 67–85. *In* M. M. Chang, Y. H. Liu, and G. R. Zhang (eds.), Early Vertebrates and Related Problems of Evolutionary Biology. Science Press, Beijing.

Young, G. C. 2008. Number and arrangement of extraocular muscles in primitive gnathostomes: evidence from extinct placoderm fishes. Biology Letters, 4:110–114.

KIRTLANDIA
The Cleveland Museum of Natural History

November 2010 *Number 57:53–60*

FUNCTIONAL AND ONTOGENETIC IMPLICATIONS OF BITE STRESS IN ARTHRODIRE PLACODERMS

ERIC SNIVELY
Mechanical Engineering, Russ College of Engineering and Technology
Ohio University, Athens, Ohio 45701
es180210@ohio.edu

PHILIP S. L. ANDERSON
Department of Earth Sciences, University of Bristol, Wills Memorial Building
Queen's Road, Bristol BS8 1RJ, United Kingdom

AND **MICHAEL J. RYAN**
Department of Vertebrate Paleontology
Cleveland Museum of Natural History, 1 Wade Oval Drive, Cleveland, Ohio 44106

ABSTRACT

Arthrodires were predatory vertebrates of the Devonian seas, with simple lower jaws conducible to examination of feeding across growth, evolution, and local diversity. 2D finite element analyses (FEA) of arthrodire mandibles (scaled to equivalent length and force, and checked against a 3D control), and a new method of stress integration, enable extensive comparisons of bite stress. FEA indicates that juveniles of Cleveland Member *Dunkleosteus terrelli* had robust mandibles, and could shear into tough prey tissues similarly to adults. Low mandible rotational inertias of some Gogo Formation arthrodires suggest rapid jaw depression for suction feeding, whereas others had low mandible stress suggesting greater bite force. These results point to high trophic diversity of Gogo arthrodires in their reef habitats, and high predatory competence of young *Dunkleosteus*.

Introduction

Arthrodire placoderms were successful Late Devonian predators, as open marine forms recorded in the North American Cleveland Member of the Ohio Shale (Figure 1A–C) and as reef dwellers (Figure 1E–J) preserved in the Gogo Formation of Australia (Playford, 1980; Jaminski et al., 1998; Long and Trinajstik, 2010). The diversity of arthrodires and the simplicity of their lower jaws (consisting of a posterior blade and anterior dental regions: Anderson, 2008) have elicited productive characterizations of feeding in these basal gnathostomes (Carr, 1995; Anderson, 2008, 2009; Anderson and Westneat, 2007, 2009). Anderson (2008, 2009) applied geometric morphometrics, moment arm analysis, and jaw second moments of area to explore morphological and functional variation in feeding arthrodires. Anderson and Westneat (2007, 2009) examined more dynamic functions with musculoskeletal kinematic modeling of jaws in *Dunkleosteus terrelli*. Further studies have extended the kinematic modeling to other arthrodires (Anderson, 2010).

We introduce two additional methods to elicit hypotheses and to evaluate the functional performance of arthrodire jaws. Finite element (FE) analysis is common for estimating stresses and strains in skull elements (Ross, 2005; Rayfield, 2007, and references in each). Across surfaces or within modeled bones, histograms of stress at sampled points (nodes in an FE model) are valuable for comparing structural performance in different taxa (Slater et al., 2009; Tseng, 2009; Tseng and Binder, 2009). We use curve fitting and simple differential equations to graph and compare stresses across hundreds of points. This method facilitates higher-resolution evaluation of stresses than histograms of only a few points and simplifies comparisons of stress magnitude in given regions of a mandible.

Rotational inertias (*RI*) of their mandibles influenced how quickly arthrodires could open their jaws and are a reasonable inverse indicator of suction-feeding performance. Suction feeding in gnathostomes is effective with rapid expansion of the oral cavity, hypothesized for large arthrodires by Anderson and Westneat (2009). For a given abductive (jaw opening) torque τ_j, a lower rotational inertia of the lower jaw will increase its angular acceleration α_j, rate of opening, and effectiveness of suction feeding. Although low *RI* of inferognathals does not confirm suction feeding to the exclusion of other mechanisms, *RI* is one measure of biomechanical performance for deriving such hypotheses of feeding style.

Phylogenetic, functional, and morphological aspects of arthrodire feeding style are more thoroughly explored elsewhere (Anderson, 2008, 2009, 2010; Anderson and Westneat, 2007). We focus here on the utility of our methods for exploring such

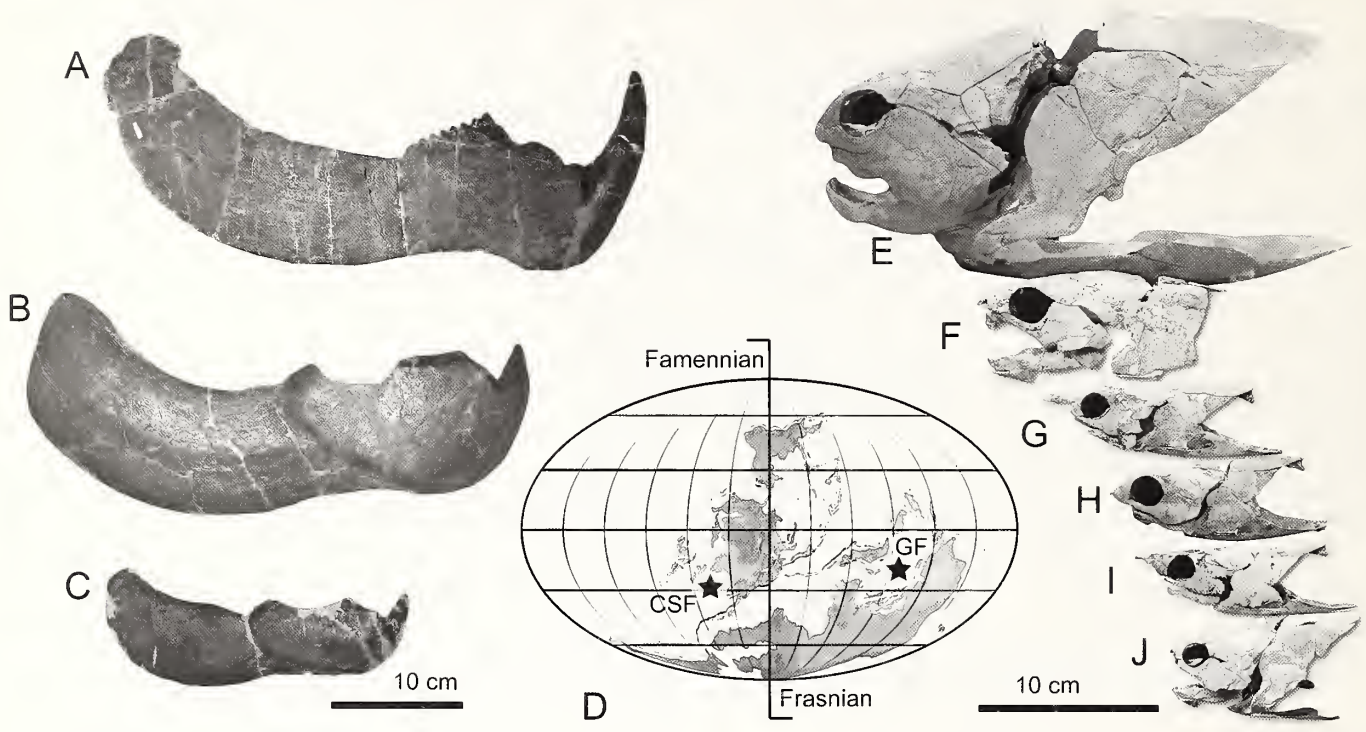

Figure 1. Arthrodire specimens analyzed for this study. Inferognathals of A, *Gorgonichthys clarki* (CMNH) and B, C, adult and juvenile *Dunkleosteus terrelli* (CMNH) from the Cleveland Member (CSF = Cleveland Shale Formation, superseded). D, Paleomap of the late Devonian (after Blakey, 2010) showing locations of Cleveland Member and Gogo Formation habitats. E, *Eastmanosteus calliaspis*. F, *Incisoscutum sarahae*. G, *Fallacosteus turnarae*. H, *Latocamuris coulthardi*. I, *Camuropiscis concinnus*. J, *Mcnamaraspis kaprios*. Note similar mandible shapes in *Dunkleostens*, *Gorgonichthys*, and *Eastmanostens*, and the relative slenderness of the blade and large size of the anterior cusp in *Gorgonichthys* compared with those of *Dunkleosteus*.

questions and to test three hypotheses of feeding ontogeny and function. Some large *Dunkleostens terrelli* inferognathals appear more gracile than smaller ones, yet more robust than the inferognathals of their large contemporary, *Gorgonichthys clarki*. The deep lower jaw in small *Dunkleostens* specimens suggests that such individuals had lower inferognathal stresses than large adult *Dunkleosteus* per unit bite force and jaw length (hypothesis 1). Mandibles of *Gorgonichthys* are predicted to have the highest relative stress.

Mandibles of Gogo Formation arthrodires vary more than those of large predaceous forms from the Cleveland Member. The basal pachyosteomorph *Eastmanostns* (Carr, 1991; Anderson, 2009) has a long, tall dental region, and Anderson (2009) quantitatively identified it as a potential generalist feeder. At the other pole of mandible shape is the mandible of the coccosteomorph *Camuropiscis*, which has a slender anterior portion and a deep posterior blade. These shape differences and second moments of area of the jaws (Anderson, 2009) suggest two hypotheses. One hypothesis is that *Eastmanosteus* had lower stress in the anterior portion of the mandible per unit jaw length than in other Gogo taxa (hypothesis 2), indicating greater bite force. The other hypothesis is that the slender anterior portion of the mandible in *Camuropiscis* indicates that it had lower rotational inertia than in the other examined Gogo arthrodire mandibles (hypothesis 3), contributing to rapid expansion of the jaws and potentially effective suction feeding on small prey.

In this paper the abbreviation CMNH designates the Cleveland Museum of Natural History.

Materials and Methods

Finite element models

We constructed sagittal representations of the inferognathals after the methods of Rayfield (2004), Shychoski (2006), and Snively and Cox (2008). Point-by-point tracings of the jaws in lateral view (scaled to their original size) were saved as DXF coordinates and imported into Comsol Multiphysics for meshing and application of material properties. For comparability we scaled the models to the same length of 300 mm. (Scaling them to same surface area [Dumont et al., 2009] is better for performance comparisons, but would have given forms with a tall dental region a greater advantage, and tested hypotheses 1 and 2 less stringently.) FE meshes consisted of approximately 20,000 triangle elements for each model. Because material properties of semidentine are unknown, we assigned uniform properties to the dental region and blade of each inferognathal (density = 1850 kg/m^3, elastic modulus = 20 GPa, Poisson's ratio = 0.3). These are realistic properties for dentine and dense compact bone without extensive Haversian reworking (a common histology for placoderm lower jaws: Mark Wilson, personal communication, 2010).

Forces and constraints

For FE comparisons of the Gogo Formation and Cleveland Member arthrodires and respective comparisons within these faunas, we applied equivalent forces and constraints to all 300-mm models. These were 300 N of adductor muscle force and 100 N force at the anterior cusp or equivalent position in

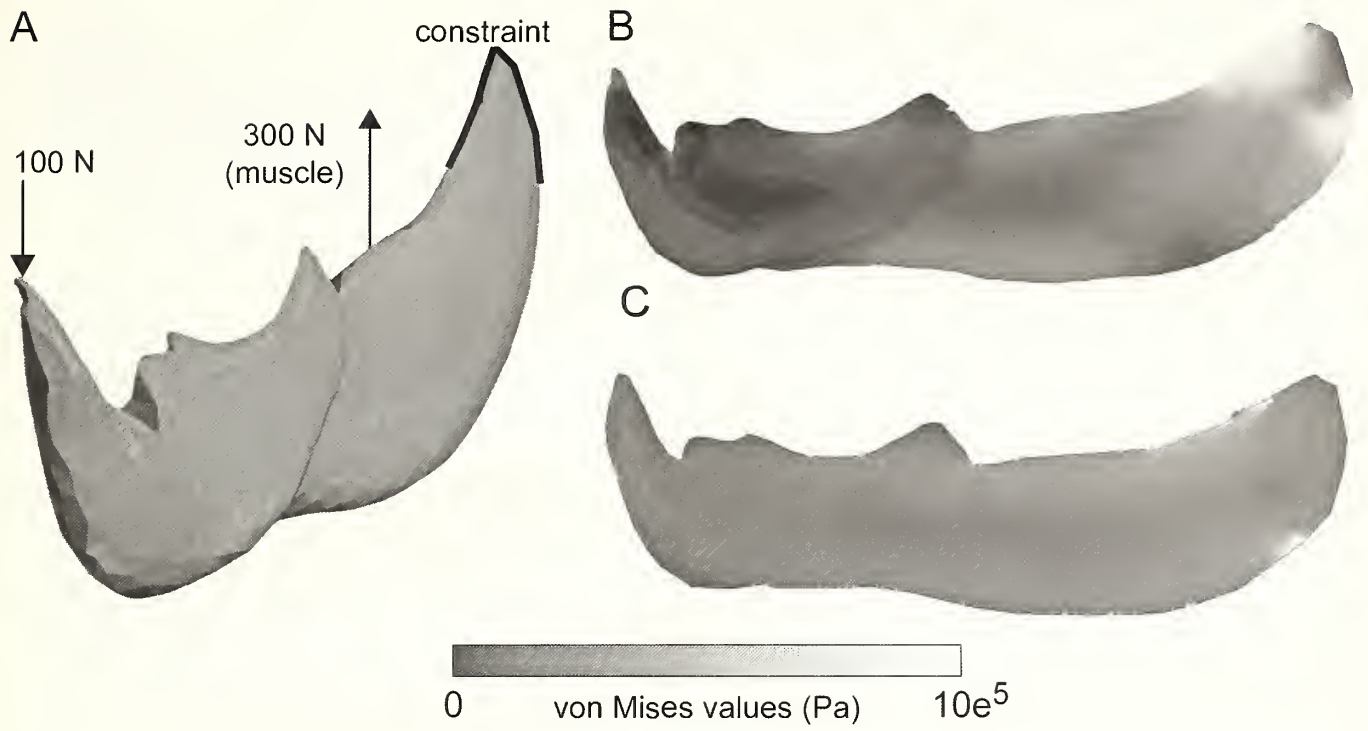

Figure 2. 2- and 3D finite element inferognathal models of *Dunkleosteus terrelli* experience similar von Mises stresses, supporting the use of 2D vs. 3D models for comparisons of the blade region. Bite force (100 N) is applied to the anterior cusp, and muscle force (300 N) to the middle of the blade. A, 3D model in oblique view. B, 3D model in lateral view. C, 2D projection model. Higher stresses occur in the 3D model at the point of force application, but stress magnitudes and distribution are nearly identical in the blade regions.

specimens that lack this structure (Figure 2A). To allow the jaws to deform and to prevent free rotation, all models were constrained at the jaw joint along the posterior periphery of the lower jaw. We did not constrain the specimens at the bite point to ensure that the structures could deform at this position.

3D-control FEA for 2D models

We assessed the realism of sagittal 2D models against a 3D model of a *Dunkleosteus* inferognathal (Figure 2). Several specimens were CT scanned at Canada Diagnostics Centre (Calgary, Alberta). Scan data of one inferognathal (CMNH 7069) was converted to an FE model with 40,000 elements with Mimics (Materialise), using methods of Wroe et al. (2007), Arbour and Snively (2009), and Bell et al. (2009). Equivalent forces, properties, and constraints were then applied to 2- and 3D representations.

Stress comparisons

Von Mises stress (a sum of stress principal components at nodes) was used for visualizing stress distribution and assessing structural performance of the jaws. Von Mises is a good index of relative proximity to yield stress, and its distribution parallels that of strain energy density (Bell et al., 2009). Because it does not yield strict values for compression and tension, von Mises facilitates fine-scaled, visual comparisons of regional stress using a grayscale color palette.

We compared von Mises stress quantitatively by determining equations of best fit for stresses along regions of jaws and by plotting and integrating the equations; areas under the curves gave indices of total stress. We drew transects in Multiphysics where relatively high stress occurred in the jaws: the dental region for Gogo arthrodires and the dorsal region of the blade in *Dunkleostens* and *Gorgonichthys*. Results for 200 points along the transects were exported into Microsoft Excel as readings of radial position versus stress. We used Excel to calculate lines of best-fit, high-degree exponential functions that are only meaningful within the positional bounds of the transects. These became functions F of differential equations of the change of stress (S) versus position (p).

$$F(S) = \frac{dS}{dp}$$

Total stress was evaluated by solving the definite integral for $F(S)$ from the starting position ($p = 1$) to the endpoint of the transect ($p = n$; in this case $n = 200$).

$$\sum S = \int_{1}^{n} c_{(x)}p^{x} \ldots + c_{(x=1)}p^{0}$$

Here "c" represents coefficients, and "x" the degrees of the terms for each position. This method complements the common graphical representation of stress versus position, by giving comparative values for total stress while sampling stress at many more positions.

Relative rotational inertias

Our methods for calculating relative *RI* were similar to those of Henderson and Snively (2003), but with simplified segment masses. We scaled inferognathals of *Camuropiscis*, *Eastmanosteus*, *Fallacosteus*, *Latocamuris*, *Incisoscutum*, and *Mcnamaraspis* to

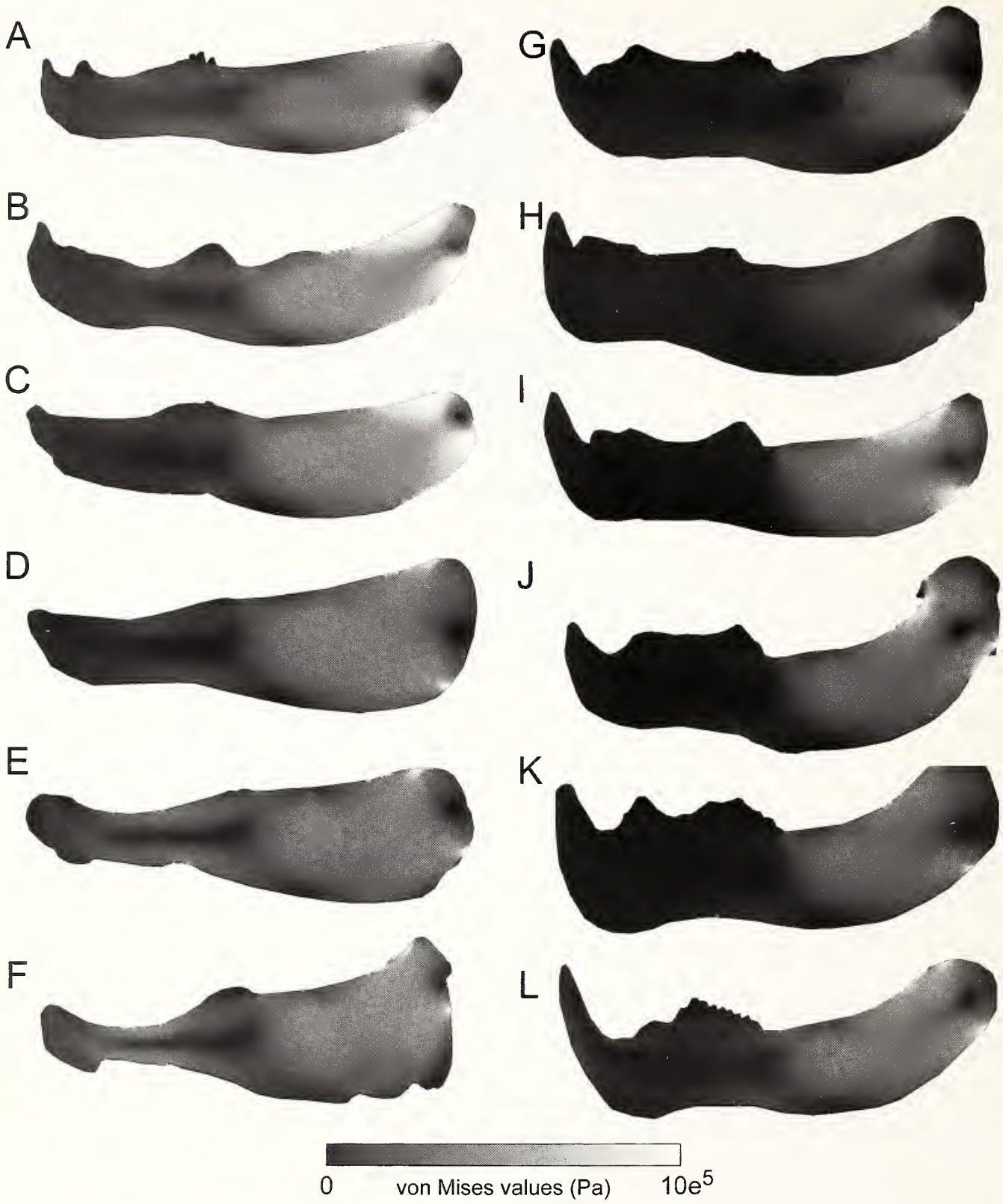

Figure 3. Stress magnitudes and distributions in examined arthrodire inferognathals, with all specimens scaled to 30 cm. Increasing von Mises stresses are color coded from dark (lowest) to white (highest). A–F are Gogo Formation specimens. A, *Mcnamaraspis kaprios*. B, *Eastmanosteus calliaspis*. C, *Incisoscutum sarahae*. D, *Latocamuris coulthardi*. E, *Fallacosteus turnarae*. F, *Camuropiscis concinnus*. G–J, *Dunkleosteus terrelli*, from smallest (20 cm) to largest (55 cm) original lengths. K, *Dunkleosteus terrelli* specimen with posterior blade restored; estimated length 65 cm. L, *Gorgonichthys clarki*, approximately 42 cm. Stresses increase in the region anterior to the blade in A–F and in the dorsal part of the blade of Cleveland Member arthrodires; stresses are generally higher in originally larger specimens.

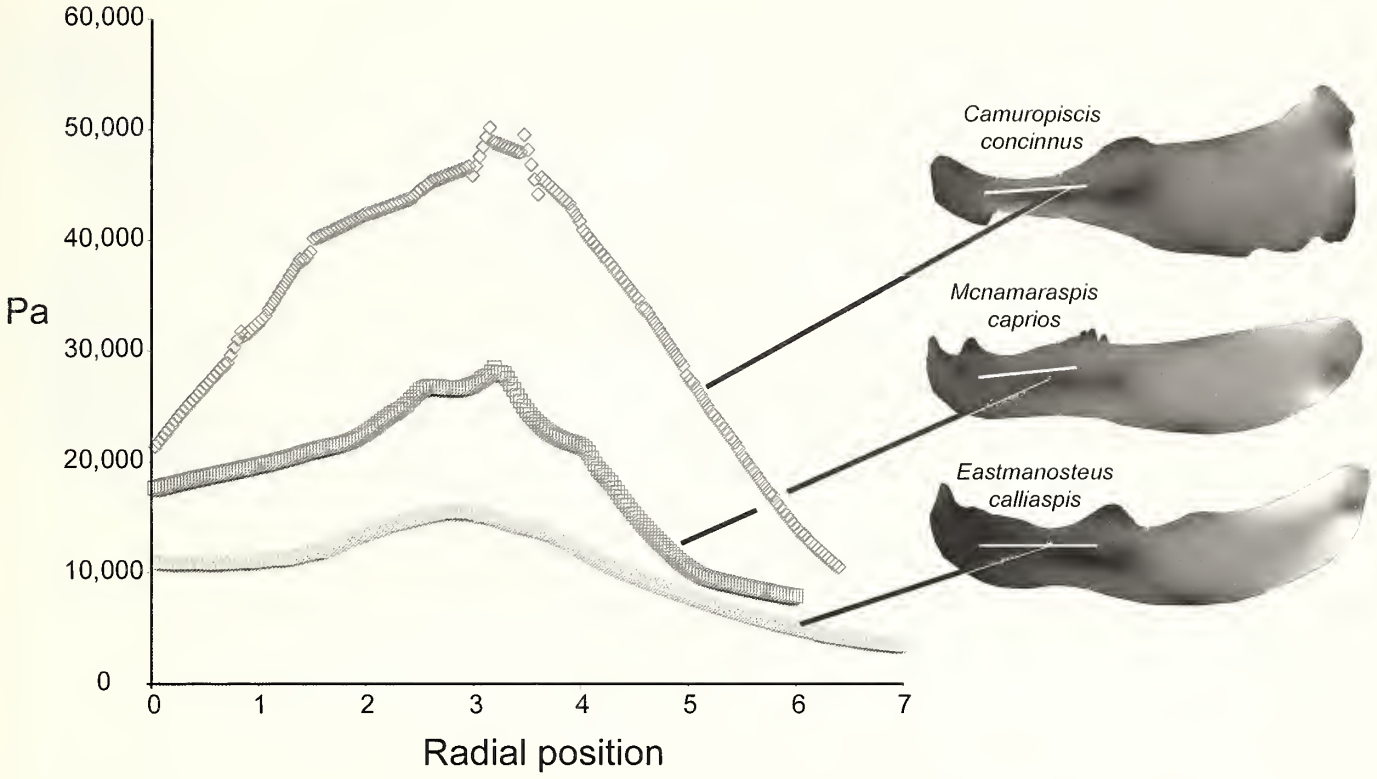

Figure 4. Integrated mandible stresses in three Gogo Formation arthrodires, graphing von Mises stresses in an anterior transect of each mandible (Pa) as a function of radial position within the transect. All specimens are scaled to 300 mm in length. The *Camuropiscis* mandible experienced much higher anterior stresses than the others.

3 cm in length with the same assumed thickness, and divided them anteroposteriorly into 17 segments. *RI*s were then calculated by adding segment *RI*s using the parallel axis theorem (Henderson and Snively, 2003)

$$RI = \sum m_i r_i^2$$

in which m_i is the mass of a segment, and r_i is its distance from the center of rotation (in this case the jaw joint). Because each segment has the same length and width, its height becomes a proxy for mass.

Results

Patterns of von Mises values

Comparing 2- and 3D models is informative about interpreting 2D results (2D models are not strictly validated, which in FEA requires checking results against physical displacements). 3D and 2D models of a *Dunkleosteus* inferognathal show similar stress distributions in the blade region and in the ventral portion of the dental region (Figure 2). However, higher stress occurs at the point of force application (the anterior-cusp tip) on the 3D model. This verifies that comparative interpretations of stress in the 2D models posterior to the dental region, and even in the ventral part of the dental region itself, gives the same basic pattern as the 3D models. The results suggest that stresses will be higher than indicated in the 2D models along pointed structures and cutting edges of the jaws, even though the 2D models represent "thin" sagittal slices.

Stress magnitudes vary substantially with shape and region in arthrodire mandibles scaled to the same lengths and forces (Figure 3). Stresses are biologically interpretable away from the highest values, which occur at transitions between constrained and unconstrained regions (Saint-Venant's principle: Cook, 1995). All inferognathals experience comparatively high yet diffuse stresses in the blades (post-dental regions), ventral to where muscle forces are applied. Muscle-induced stresses appear lower in blades of Cleveland Member forms than in Gogo Formation specimens, except in a large gracile *Dunkleosteus* (Figure 3G) and the *Gorgonichthys* specimen (Figure 3L). The dental portions behave like cantilevered beams, with central regions of lower stress approximating a neutral axis. Stresses are higher in the dental regions of the Gogo Formation arthrodires (Figure 3A–F) than in *Dunkleosteus* and *Gorgonichthys* specimens from the Cleveland Member (Figure 3G–L). Dental-region stresses increase from forms categorized functionally as "generalists" and "choppers" (e.g. *Mcnamaraspis* and *Dunkleosteus*) to "biters" (*Camuropiscis*; Anderson, 2008).

Integrated stress and relative rotational inertias

For anterior transects of Gogo specimens (Figure 4), integrated stress diminishes from 212,020 Pa for *Camuropiscis concinnus* to 114,569 Pa for *Mcnamaraspis caprios*, and to 66,682 Pa in *Eastmanosteus calliaspis*. The *Camuropiscis* mandible experienced twice the peak stress as in *Mcnamaraspis*, and four times that of *Eastmanosteus*. Von Mises values along the mandible blade in Cleveland Member arthrodires are higher than in the dental regions of the Gogo Formation forms. Integrated stresses for the

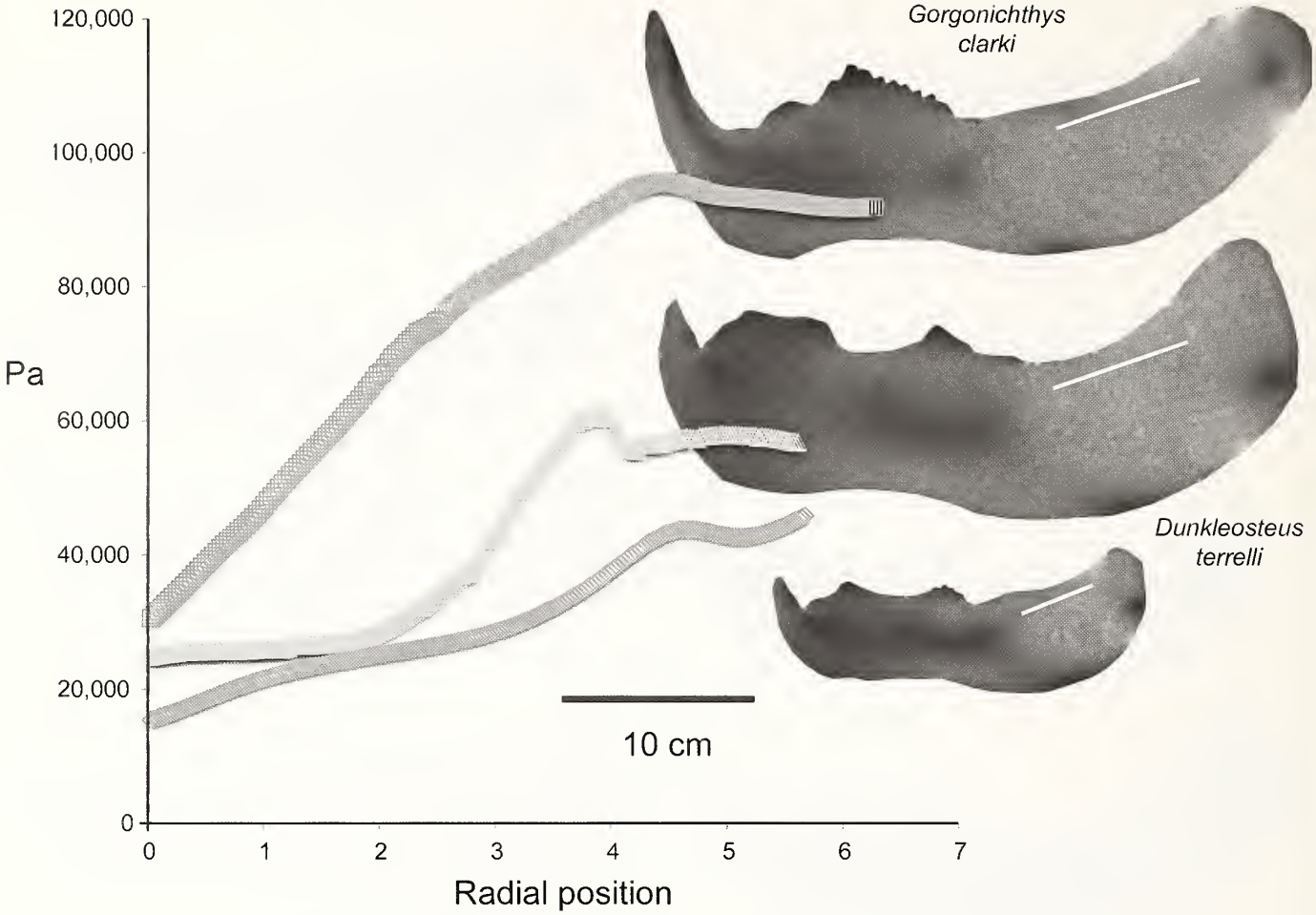

Figure 5. Integrated mandible stresses in Cleveland Member arthrodires, graphing von Mises stresses (Pa) in the dorsal portion of each blade as a function radial position. Specimens are scaled to 300 mm each. White lines across the specimens indicate transects of stress results.

Cleveland Member forms (Figure 5) are 444,841 Pa (445 kPa) in the large *Gorgonichthys clarki*, 260 kPa in the adult *Dunkleosteus terrelli*, and 118 kPa in the juvenile.

Relative rotational inertias for Gogo arthrodires are listed in Table 1. *Mcnamaraspis* and *Eastmanosteus* have the highest relative *RI*s (22–23), 16–20% higher than in *Camuropiscis*, which has the lowest *RI*. *Latocamuris* and *Fallacosteus* also have comparatively low *RI*s. Most of the specimens were of similar absolute size (Figure 1), and the relative *RI*s reflect absolute quantities. *Eastmanosteus* is much larger than the others, and the high relative *RI* of its mandible indicates a much higher inertia in life.

Table 1. Relative rotational inertias ($RI = \sum m_i r_i^2$) of representative Gogo arthrodires. "Mass" (m_i) is represented by the height of a given slice i, with equivalent thicknesses for all slices in all specimens.

Taxon	Relative *RI*
Camuropiscis	19.00
Eastmanosteus	22.06
Incisoscutum	20.09
Mcnamaraspis	22.81
Fallacosteus	19.60
Latocamuris	19.92

Discussion

Finite-element results for the Cleveland Member arthrodires suggest lower stresses in juvenile *Dunkleosteus* for a given jaw length (corroborating hypothesis 1), and relatively high stresses in *Gorgonichthys*. Lower relative stress in juvenile *Dunkleosteus* indicates the ability to accommodate high bite force, analogous to the adults which applied among the highest known bite forces (Anderson and Westneat, 2009). Indeed this pattern suggests slight negative allometry in *Dunkleosteus* bite force. The juveniles were likely able to shear into resistant prey tissues when biting, similarly to the adults but on a smaller scale, and to hunt a broader range of prey types than might be predicted from their smaller size. This contrasts with the condition common in tetrapods, including lizards and carnivorous dinosaurs (Rieppel, 1979; Currie, 2003; Therrien et al., 2005; Shychoski and Snively, 2008), in which the lower jaws of juveniles are more gracile than in adults. Using morphometrics (Anderson, 2008) and biomechanical studies of extant and fossil forms, we can test whether changes in *Dunkleosteus* bite force, through ontogeny and its available prey spectrum, are unusual among aquatic gnathostomes. In some cases the effects of both geometry and material properties can be assessed, as in white sharks whose jaws accrue additional layers of stiff calcified cartilage (Dingurkas et al., 1991), but may change overall shape isometrically as they grow.

Among the more diverse Gogo Formation arthrodires, finite element and rotational inertia results parallel Anderson's (2008, 2009) morphometric characterizations, yet complement possible feeding modes for *Fallacosteus* and *Camuropiscis*. As expected, *Mcnamaraspis* and *Eastmanosteus* (a generalist) have lower relative stress in and posterior to the dental region than *Camuropiscis* (a biter/grazer). High stress in this gracile region of *Camuropiscis* inferognathals suggests jaws well-suited to fine procurement and manipulation of prey, yet less suited to hard bites than in other arthrodires, despite flat anterior biting surfaces and a deep posterior mandible suggestive of durophagy.

Deep posterior and shallow anterior portions of the inferognathals in *Camuropiscis*, *Latocamuris*, and *Fallacosteus* imparted low sagittal rotational inertias about the jaw joint. This would have enabled rapid opening of the jaws, especially when coupled with high levels of kinematic transmission calculated for these groups from four-bar linkage models (Anderson, 2010). Rapid jaw abduction suggests effective suction feeding and rapid ingestion of prey. Biomechanical indicators of suction feeding do not falsify reef grazing or other means of procuring prey in *Camuropiscis* (including ingestion and crushing of crustaceans: Anderson, 2009). Instead, they offer an alternative hypothesis and/or complementary feeding mechanism open to further testing. In this and other cases, consideration of the role and function of articular cartilage will greatly aid kinematic and structural parsing of arthrodire feeding variation (R. K. Carr, personal communication, 2008).

These studies are ultimately important for understanding trophic radiations among gnathostomes. The Gogo Formation was laid down in a reef setting. Reefs today harbor high diversity and disparity of trophic niches (Anderson, 2008). Have reefs consistently been centers of niche variety for 400 Ma, and has the complexity of jaw mechanisms (lower in arthrodires and higher in derived teleosts) governed magnitudes of speciation and divergence? Did negative allometry of jaw stress in *Dunkleosteus* lead to niche partitioning by size more than mechanics? How common and effective are isometric and allometric mandible growth as contributors to functional performance and ecological diversity? With spectacular preservation and simple lower jaws, arthrodires are among the first and best groups for grounding such questions.

Acknowledgments

We thank G. Jackson and D. Chapman (CMNH), and L. Hwang (Comsol Inc.) for technical assistance, and D. Henderson (Royal Tyrrell Museum) for discussion. Thoughtful reviews by S. Cumbaa and C. McHenry and feedback from J. Long, R. Carr, and E. Rayfield was invaluable. We also thank G. Jackson (CMNH), R. Jones (Australian Museum), and J. Long and K. McNamara (Western Australian Museum) for access to specimens. Funding was provided by CMNH, the Jurassic Foundation, Alberta Ingenuity, Russ College of Engineering (Ohio University), and the Canada Foundation for Innovation (awards to P. Currie and M. Caldwell). Students of Villanova University (Biology 7970) tested our finite element protocols. This is publication no. 2 of TGICEA, Villanova University.

References

Anderson, P. S. L. 2008. Shape variation between arthrodire morphotypes indicates possible feeding niches. Journal of Vertebrate Paleontology, 28:961–969.

Anderson, P. S. L. 2009. Biomechanics, functional patterns, and disparity in Late Devonian arthrodires. Paleobiology, 35: 312–342.

Anderson, P. S. L. 2010. Using linkage models to explore skull kinematic diversity and functional convergence in arthrodire placoderms. Journal of Morphology, 271:990–1005.

Anderson, P. S. L., and M. W. Westneat. 2007. Feeding mechanics and bite force modeling of the skull of *Dunkleosteus terrelli*, an ancient apex predator. Biology Letters, 3:76–79.

Anderson, P. S. L., and M. W. Westneat. 2009. A biomechanical model of feeding kinematics for *Dunkleosteus terrelli* (Arthrodira, Placodermi). Paleobiology, 35:251–269.

Arbour, V. M., and E. Snively. 2009. Biomechanics and function of the tail club in ankylosaurid dinosaurs. The Anatomical Record, 292:1412–1426.

Bell, P. R., E. Snively, and L. Shychoski. 2009. A comparison of the jaw mechanics in hadrosaurid and ceratopsid dinosaurs using finite element analysis. The Anatomical Record, 292: 1338–1351.

Blakey, R. C. 2010. Global Paleogeography. Accessed March 31, 2010. <http://jan.ucc.nau.edu/~rcb7/globaltext2.html>

Carr, R. K. 1991. Reanalysis of *Heintzichthys gouldii* (Newberry), an aspinothoracid arthrodire (Placodermi) from the Famennian of northern Ohio, with a review of brachythoracid systematics. Zoological Journal of the Linnean Society, 103:349–390.

Carr, R. K. 1995. Placoderm diversity and evolution. *In* M. Arsenault, H. Lelievre, and P. Janvier (eds.), Studies on early vertebrates. (VIIth International Symposium, 1991, Miguasha Parc, Quebec.) Bulletin du Museum National d'Histoire Naturelle, Paris, 4e série, C 17(1–4):85–125.

Cook, R. D. 1995. Finite Element Modeling for Stress Analysis. John Wiley & Sons, New York. 320 p.

Currie, P. J. 2003. Allometric growth in tyrannosaurids (Dinosauria: Theropoda) from the Upper Cretaceous of North America. Canadian Journal of Earth Sciences, 40:651–665.

Dingerkus, G., B. Seret, and E. Guilbert. 1991. Multiple prismatic calcium phosphate layers in the jaws of present-day sharks (Chondrichthyes; Selachii). Experientia, 47:38–40.

Dumont, E. R., I. R. Grosse, and G. J. Slater. 2009. Requirements for comparing the performance of finite element models of biological structures. Journal of Theoretical Biology, 256: 96–103.

Henderson, D. M., and E. Snively. 2003. *Tyrannosaurus* en pointe: allometry minimized rotational inertia of large carnivorous dinosaurs. Proceedings of the Royal Society B, Biology Letters, 271:S57–S60.

Jaminski, J., T. J. Algeo, J. B. Maynard, and J. C. Hower. 1998. Climatic origin of dm-scale compositional cyclicity in the Cleveland Member of the Ohio Shale (Upper Devonian), Central Appalachian Basin, U.S.A, p. 217–242. *In* J. Schieber, W. Zimmerle, and P. S. Sethi (eds.), Shales and Mudstones. I. E. Schweizerbart'sche Verlagsbuchhandlung, Stuttgart.

Long, J. A., and K. Trinajstik. 2010. The Late Gogo Formation Lägerstatte of Western Australia: exceptional early vertebrate preservation and diversity. Annual Review of Earth and Planetary Sciences, 38:255–279.

Playford, P. E. 1980. Devonian "Great Barrier Reef" of the Canning Basin, Western Australia. American Association of Petroleum Geologists Bulletin, 64:814–840.

Rayfield, E. J. 2004. Cranial mechanics and feeding in *Tyrannosaurus rex*. Proceedings of the Royal Society of London B, 271:1451–1459.

Rayfield, E. J. 2007. Finite element analysis and understanding the biomechanics and evolution of living and fossil organisms. Annual Review of Earth and Planetary Sciences, 35:541–576.

Rieppel, O., and L. Labhardt. 1979. Mandibular mechanics of *Varanus niloticus*. Herpetologica, 35:158–163.

Ross, C. F. 2005. Finite element analysis in vertebrate biomechanics. Anatomical Record, 283:253–258.

Shychoski, L. 2006. A geometric morphometric and finite element analysis investigating tyrannosauroid phylogeny and ontogeny emphasizing the biomechanical implications of scale. Unpublished M.Sc. thesis, University of Bristol, Bristol, England. 125 p.

Shychoski, L., and E. Snively. 2008. Ecological implications of tyrannosaurid lower jaw ontogeny, biomechanical scaling, and bite function. Journal of Vertebrate Paleontology, 28(Supplement to 3):142A.

Slater, G. J., E. R. Dumont, and B. Van Valkenburgh. 2009. Implications of predatory specialization for cranial form and function in canids. Journal of Zoology, 278:181–188.

Snively, E., and A. Cox. 2008. Structural mechanics of pachycephalosaur crania permitted head-butting behavior. Palaeontologia Electronica 11, Issue 1, 3A. 17 p. Accessed March 31, 2010. <http://palaeo-electronica.org/2008_1/140/index.html>

Therrien, F., D. M. Henderson, and C. B. Ruff. 2005. Bite me: biomechanical models of theropod mandibles and implications for feeding behavior, p. 179–237. *In* K. Carpenter (ed.), The Carnivorous Dinosaurs. Indiana University Press, Bloomington.

Tseng, Z. J. 2009. Cranial function in a late Miocene *Dinocrucuta gigantea* (Mammalia: Carnivora) revealed by comparative finite element analysis. Biological Journal of the Linnean Society, 96:51–67.

Tseng, Z. J., and W. J. Binder. 2009. Mandibular biomechanics of *Crocuta crocuta*, *Canis lupus*, and the late Miocene *Dinocrocuta gigantea* (Carnivora, Mammalia). Zoological Journal of the Linnean Society, 158:683–696.

Wroe, S., K. Moreno, P. Clausen, C. McHenry, and D. Cunroe. 2007. High-resolution three dimensional computer simulation of hominid cranial mechanics. Anatomical Record, 290: 1248–1255.

KIRTLANDIA
The Cleveland Museum of Natural History

November 2010 *Number 57:61–81*

THE CLEVELAND TYRANNOSAUR SKULL (*NANOTYRANNUS* OR *TYRANNOSAURUS*): NEW FINDINGS BASED ON CT SCANNING, WITH SPECIAL REFERENCE TO THE BRAINCASE

LAWRENCE M. WITMER AND RYAN C. RIDGELY
Department of Biomedical Sciences, College of Osteopathic Medicine
Ohio University, Athens, Ohio 45701
witmerL@ohio.edu

ABSTRACT

The Cleveland Museum of Natural History's skull of a small tyrannosaurid theropod dinosaur (CMNH 7541) collected from the Hell Creek Formation has sparked controversy, with competing hypotheses suggesting that it represents a separate taxon of dwarf tyrannosaurid (*Nanotyrannus lancensis*), a juvenile specimen of *Tyrannosaurus rex* (the only other acknowledged Hell Creek tyrannosaurid), or a compromise position (a juvenile *Nanotyrannus*). Beyond this controversy, CMNH 7541 holds importance because of the anatomical information that such a well preserved skull can provide, and it is in this context that we have sought to probe the structure of the braincase region (e.g., pneumatic sinuses, cranial nerve foramina), as well as other regions of the skull. We subjected the skull to computed x-ray tomography (CT scanning), followed by computer analysis and 3D visualization. The braincase and a number of other bones (e.g., vomer, quadrate, quadratojugal, palatine, mandible) were digitally "extracted" from the CT datasets. Although the new findings strongly confirm the long-held view that CMNH 7541 pertains to a tyrannosaurid, the mosaic of charaeters it presents makes finer taxonomic assignment difficult. For example, some characters support affinities with *T. rex*, yet other characters argue for a much more basal position. The key question that awaits resolution is whether the differences observed can be attributed to juvenility, and such resolution will require information from new, as yet unpublished specimens. Nevertheless, some of the differences seen in CMNH 7541 (e.g., the pattern of pneumatic foramina in the basicranium) are highly divergent and are harder to attribute to ontogeny. Among other findings, we report here thin, laminar structures within the main nasal airway that are interpretable as being respiratory turbinates, which have potential implications for metabolic physiology.

Introduction

The Cleveland Museum of Natural History (CMNH), in a 1942 expedition led by David H. Dunkle, collected an isolated skull of a tyrannosaurid theropod dinosaur from the Hell Creek Formation (Late Maastrichtian, Cretaceous) of southeastern Montana. This skull (CMNH 7541) was described by Gilmore (1946) as a new species of *Gorgosaurus*, *G. lancensis*. Since its discovery, CMNH 7541 has attracted considerable attention, primarily because of its small size. With a length of only about 570 mm, it was—and remains—one of the smallest skulls known for definitive tyrannosaurids; for comparison, the skulls of adult *Tyrannosaurus rex* can exceed 1300 mm. Given its small size, some workers (e.g., Rozhdestvensky, 1965) suggested that CMNH 7541 might pertain to a juvenile of a known species, presumably *T. rex*, the only other definitively known Hell Creek tyrannosaurid. Russell (1970), however, later supported Gilmore's assignment of adult status to the skull, as well as its referral to *Gorgosaurus* (a name that Russell regarded as a junior synonym of *Albertosaurus*).

In 1988, the results of a collaborative project by R. T. Bakker, the late Cleveland Museum of Natural History curator Michael Williams (to whom this issue of *Kirtlandia* is dedicated), and P. J. Currie were published (Bakker et al., 1988). This article suggested that not only was CMNH 7541 an adult skull, but also the skull of a new genus and species of dwarfed tyrannosaur that was only very distantly related to *Tyrannosaurus rex*. Thus, *Nanotyrannus lancensis* and "pygmy tyrants" entered the lexicon of dinosaurs. Nevertheless, doubts lingered and others suggested that CMNH 7541 might be in fact a juvenile *T. rex* (Carpenter, 1992). In 1999, T. D. Carr published a major article documenting the juvenile features of CMNH 7541 and identifying a number of derived features that suggested that CMNH 7541 pertains to a young *T. rex* (Carr, 1999; see also Carr and Williamson, 2004; Carr et al., 2005). Carr's work has been very influential, such that many

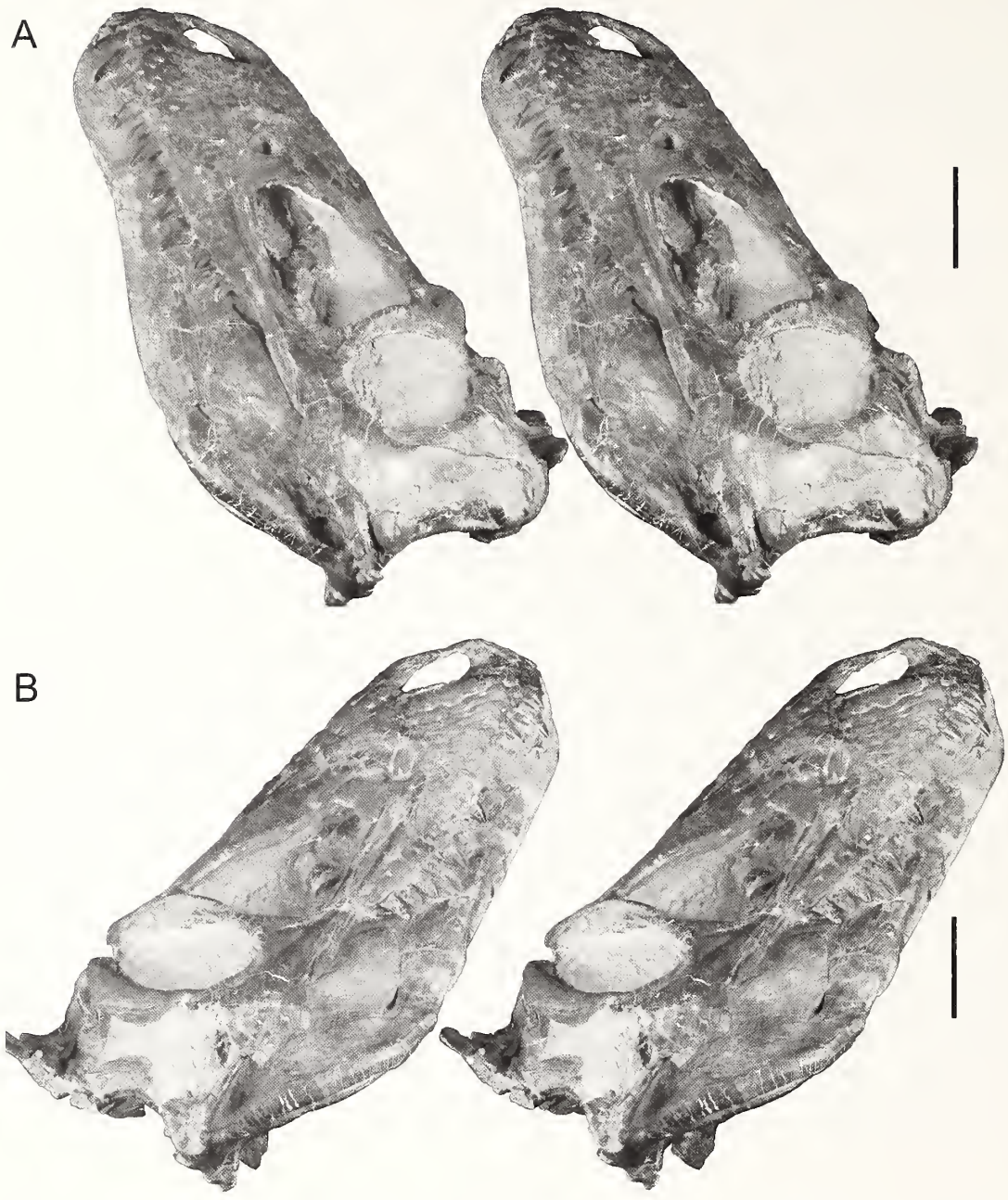

Figure 1. Cleveland tyrannosaur skull, CMNH 7541. Stereophotographs of skull in A, left lateral view; B, right lateral view. Orientations reflect posture with lateral semicircular canal horizontal. Scale bars equal 10 cm.

workers regard CMNH 7541 as a juvenile *T. rex* (Holtz, 2001, 2004; Brochu, 2003; Paul, 2008; Brusatte et al., 2009). However, although he accepted the juvenile status of the skull, Currie (2003a, b; Currie et al., 2003) regarded *Nanotyrannus lancensis* as a valid taxon, albeit very closely related to *T. rex*. Recently, P. Larson (2008) has emerged as a vocal advocate for the validity of *N. lancensis*, even referring several other specimens to this species.

Thus, the Cleveland Museum tyrannosaur skull has had a somewhat tortured systematic history, starting out as a gorgosaur (Gilmore, 1946; Russell, 1970), then becoming its own genus (*Nanotyrannus*) that was placed as the most basal tyrannosaurid (Bakker et al., 1988), then becoming a juvenile *T. rex* (Carr, 1999; Holtz, 2001, 2004; Brochu, 2003; Carr and Williamson, 2004; Carr et al., 2005; Brusatte et al., 2009), and then becoming a juvenile that grew up into a distinct *Nanotyrannus*, yet placed as the sister-group to *T. rex* (Currie 2003a, b; Currie et al., 2003). Resolution of this issue is important because, on the one hand, if CMNH 7541 is a juvenile *T. rex*, then there may remain just a single Late Maastrichtian tyrannosaur species in western North America. Moreover, it would mean that ontogenetic studies of *T. rex* would be on a much sounder footing, because most other juvenile or subadult *T. rex* skulls are less complete than CMNH 7541 (Carr and Williamson, 2004). On the other hand, if *Nanotyrannus* is valid, then we have a greater diversity of tyrannosaurs, but less information about ontogeny.

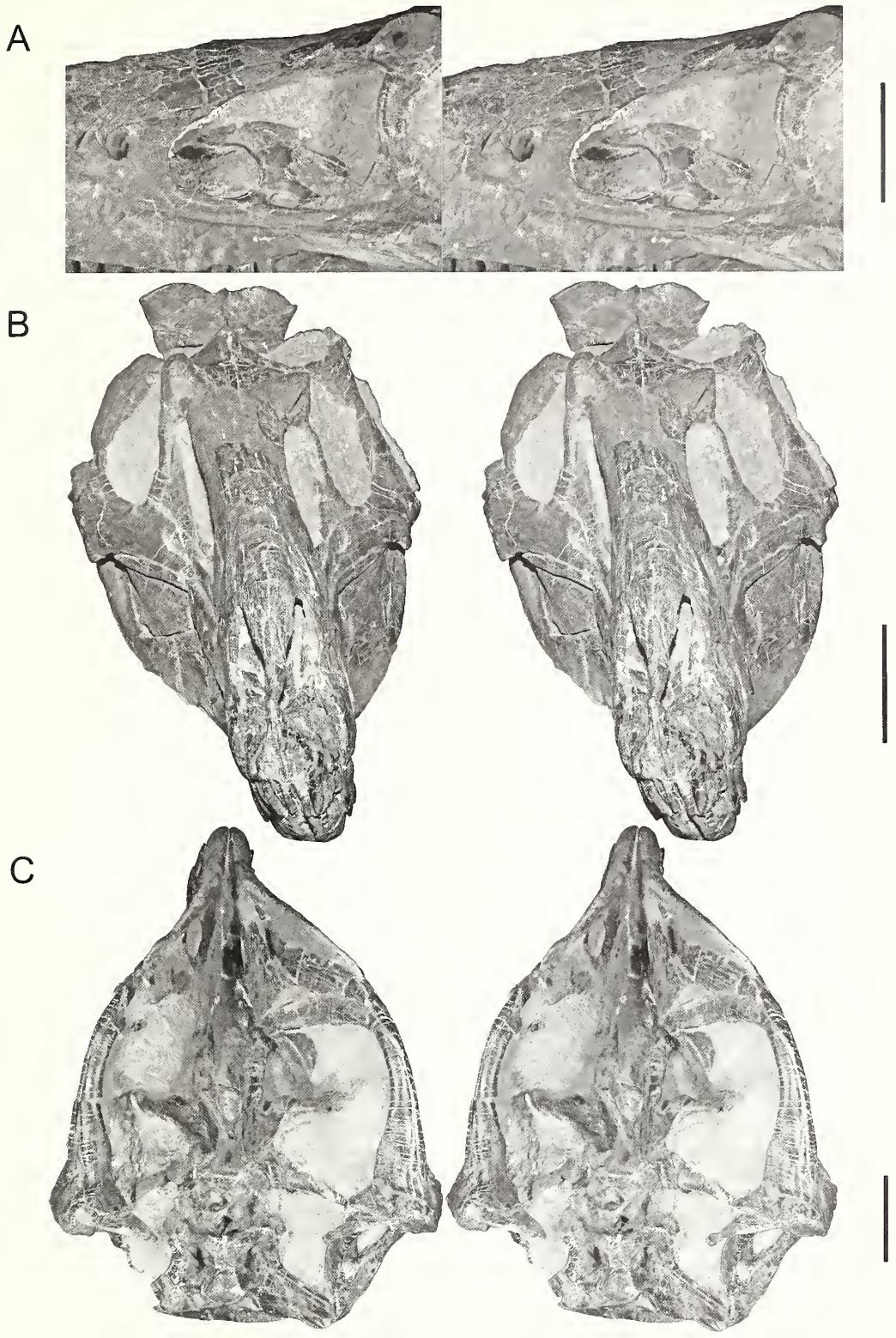

Figure 2. Cleveland tyrannosaur skull, CMNH 7541. Stereophotographs of A, close-up of left antorbital region; B, skull in rostral view; C, skull in ventral view. Orientations reflect posture with lateral semicircular canal horizontal. Scale bars equal 10 cm.

Our interest in the Cleveland skull, however, did not arise from this interesting and important systematic controversy. Our studies of CMNH 7541 are part of a larger study of the evolution of the brain and ear regions of dinosaurs and other archosaurs (Witmer et al., 2003; Sampson and Witmer, 2007; Sereno et al., 2007; Witmer and Ridgely, 2008a, b, 2009; Witmer et al., 2008). Tyrannosaurs are often regarded (particularly in public venues) as having expanded brains and heightened sensory apparatuses

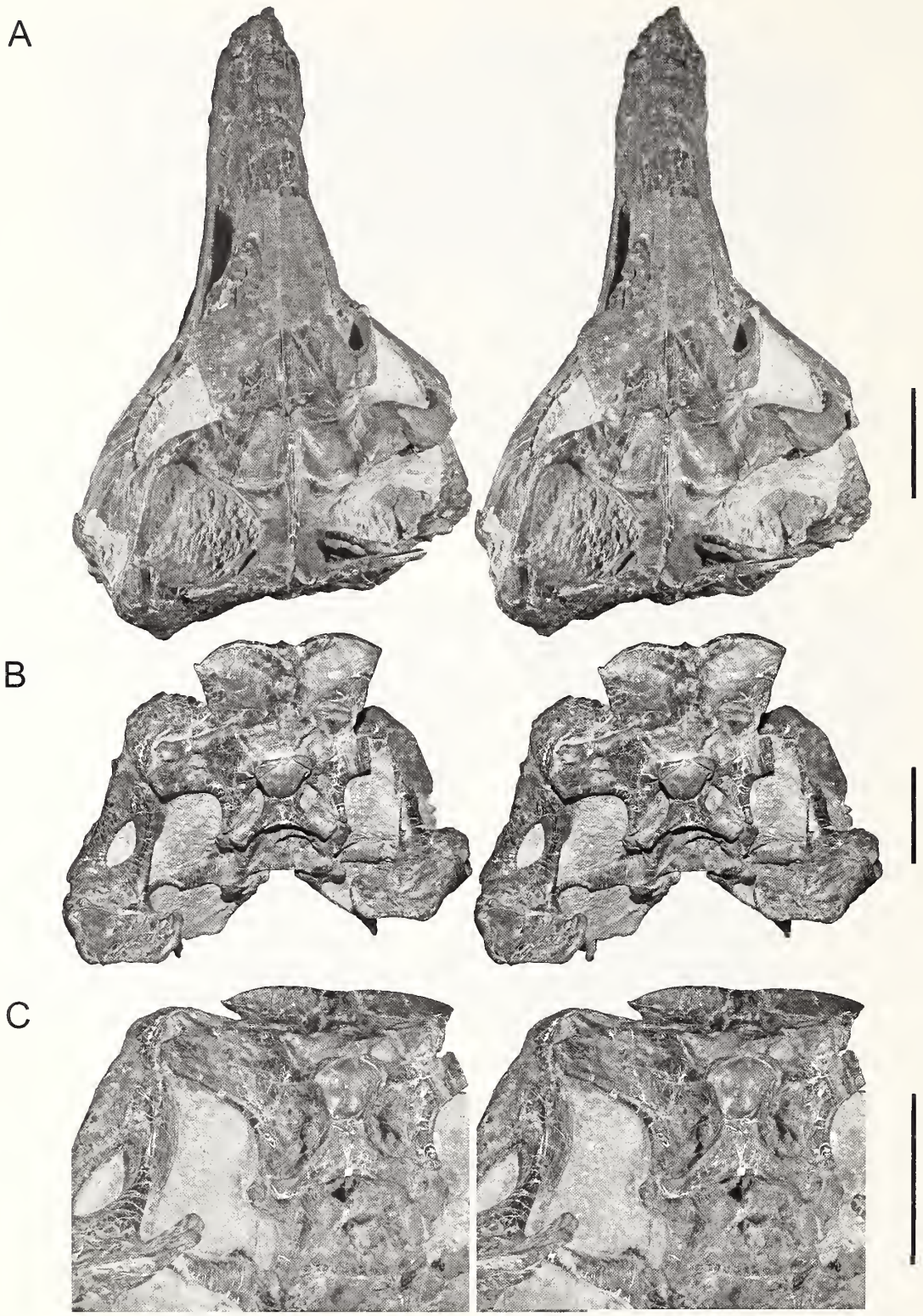

Figure 3. Cleveland tyrannosaur skull, CMNH 7541. Stereophotographs of A, skull in dorsal view; B, skull in caudal view; C, close-up of cranial base in ventral view. Orientations reflect posture with lateral semicircular canal horizontal. Scale bars equal 10 cm.

(Bakker et al., 1988; Horner and Lessem, 1993; Brochu, 2000, 2003; Witmer et al., 2008; Witmer and Ridgely, 2009; Zelenitsky et al., 2009). Study of CMNH 7541 has helped shaped this perception, with early computed x-ray tomographic (CT) scans suggesting that the animal "combined the eyes and brain of an eagle with the snout and hearing of a wolf" (Bakker, 1992, p. 60). The goal of our project was to probe braincase structure of the Cleveland skull using CT data and to reconstruct the brain cavity (cerebral endocast), inner and middle ear anatomy, and general patterns of cranial blood flow, and compare these findings with

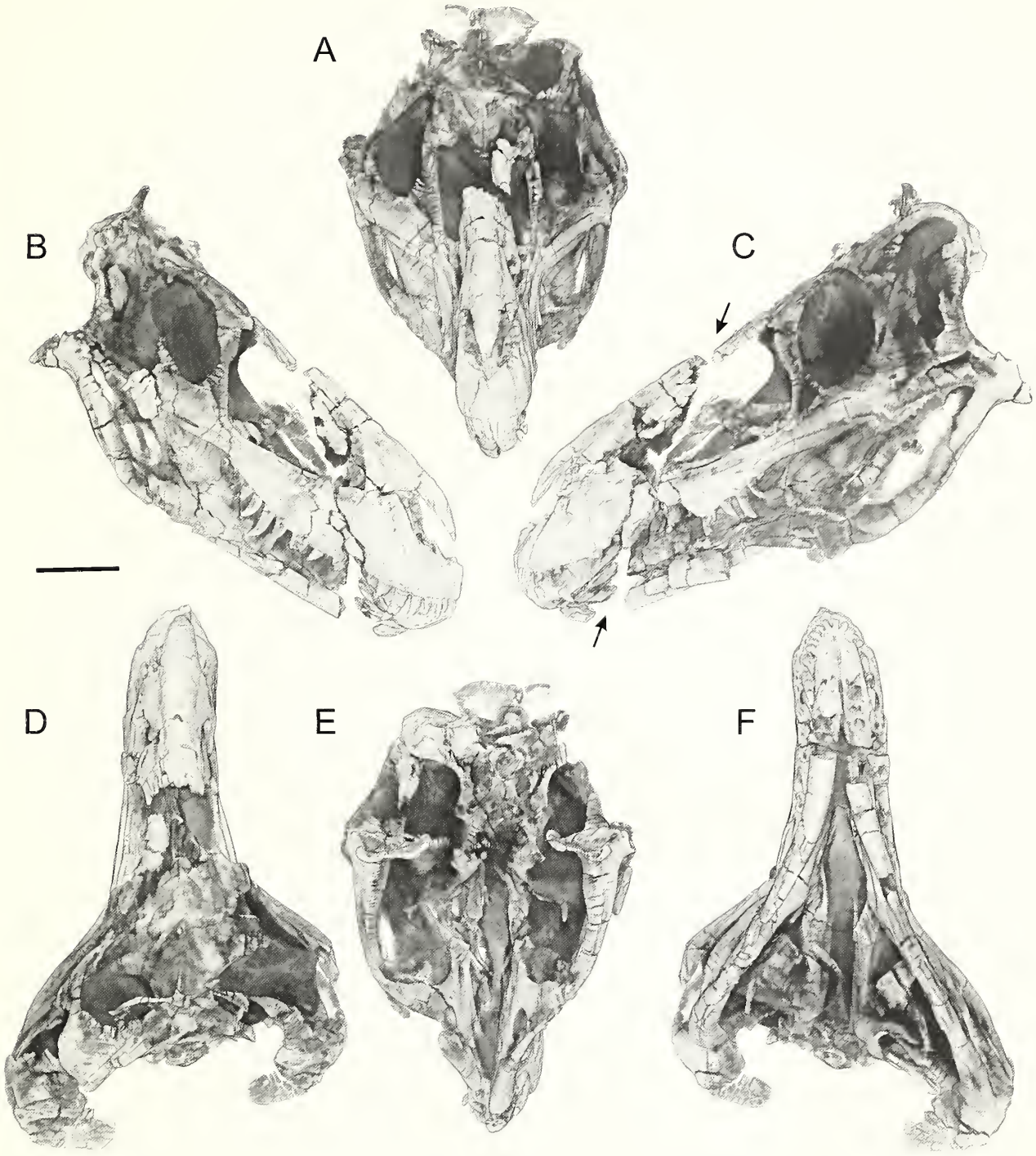

Figure 4. Cleveland tyrannosaur skull, CMNH 7541. Volume renderings of the skull derived from the CT data in A, rostral view; B, right lateral view; C, left lateral view; D, dorsal view; E, caudal view; F, ventral view. Densities corresponding to plaster have been excluded, revealing the extent of plaster restoration. Arrows in C indicate the transverse oblique plane of fracture that the specimen experienced prior to restoration. Scale bar equals 10 cm.

similar findings from other tyrannosaurs and other theropods in general. Michael Williams was to be a collaborator on the project, but passed away before the work began. Some of the results of the project are presented here and others (e.g., a comparative analysis of the brain endocast) are presented in a companion article (Witmer and Ridgely, 2009).

The present article, in particular, presents some details on braincase structure and patterns of paratympanic pneumaticity in CMNH 7541. We also will present some findings on other areas of the skull that might have bearing on the systematic issues raised above, because we recognize that resolution of the controversy impacts any conclusions (e.g., intraspecific/ontogenetic versus

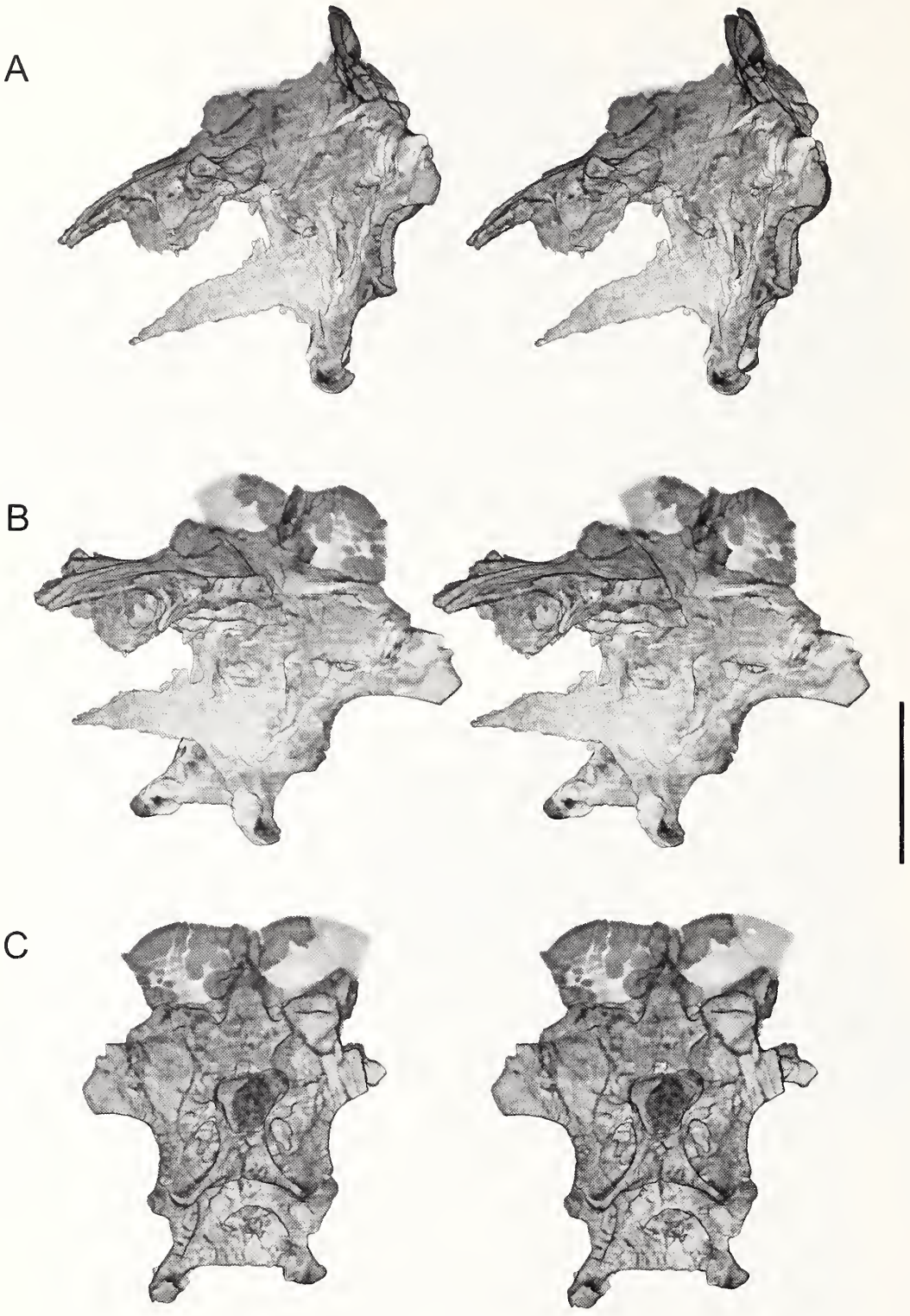

Figure 5. Cleveland tyrannosaur skull, CMNH 7541. Volume renderings (stereopairs) of digitally extracted braincase derived from CT data in A, left lateral; B, left rostroventrolateral; C, caudal views. Figure 6A–C provides corresponding labeled views. Scale bar equals 10 cm.

interspecific/taxonomic variation). Some of these issues are explored in the Discussion. We also take the opportunity to provide some high quality stereophotographs of the specimen with the hope that they will help other workers sort out the critical systematic issues. A critical new find that has bearing on the interpretation and taxonomic status of the Cleveland skull was the discovery in 2001 of a relatively complete skeleton of a tyrannosaurid by the Burpee Museum of Natural History (BMR

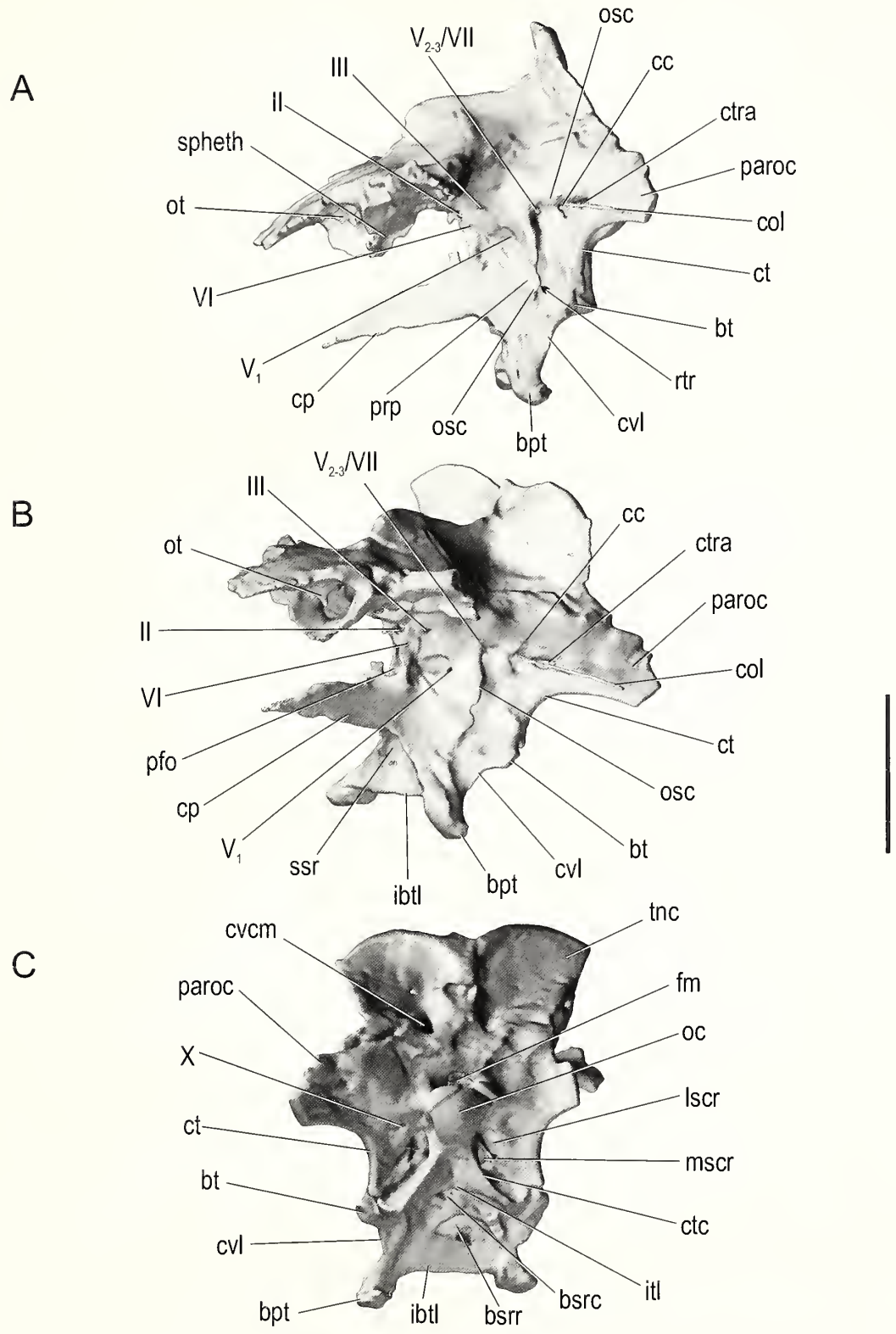

Figure 6. Cleveland tyrannosaur skull, CMNH 7541. Surface renderings of digitally extracted braincase derived from CT data in A, left lateral; B, left rostroventrolateral; C, caudal views. Figure 5A–C shows corresponding stereopairs of volume renderings. Scale bar equals 10 cm. See Appendix for abbreviations.

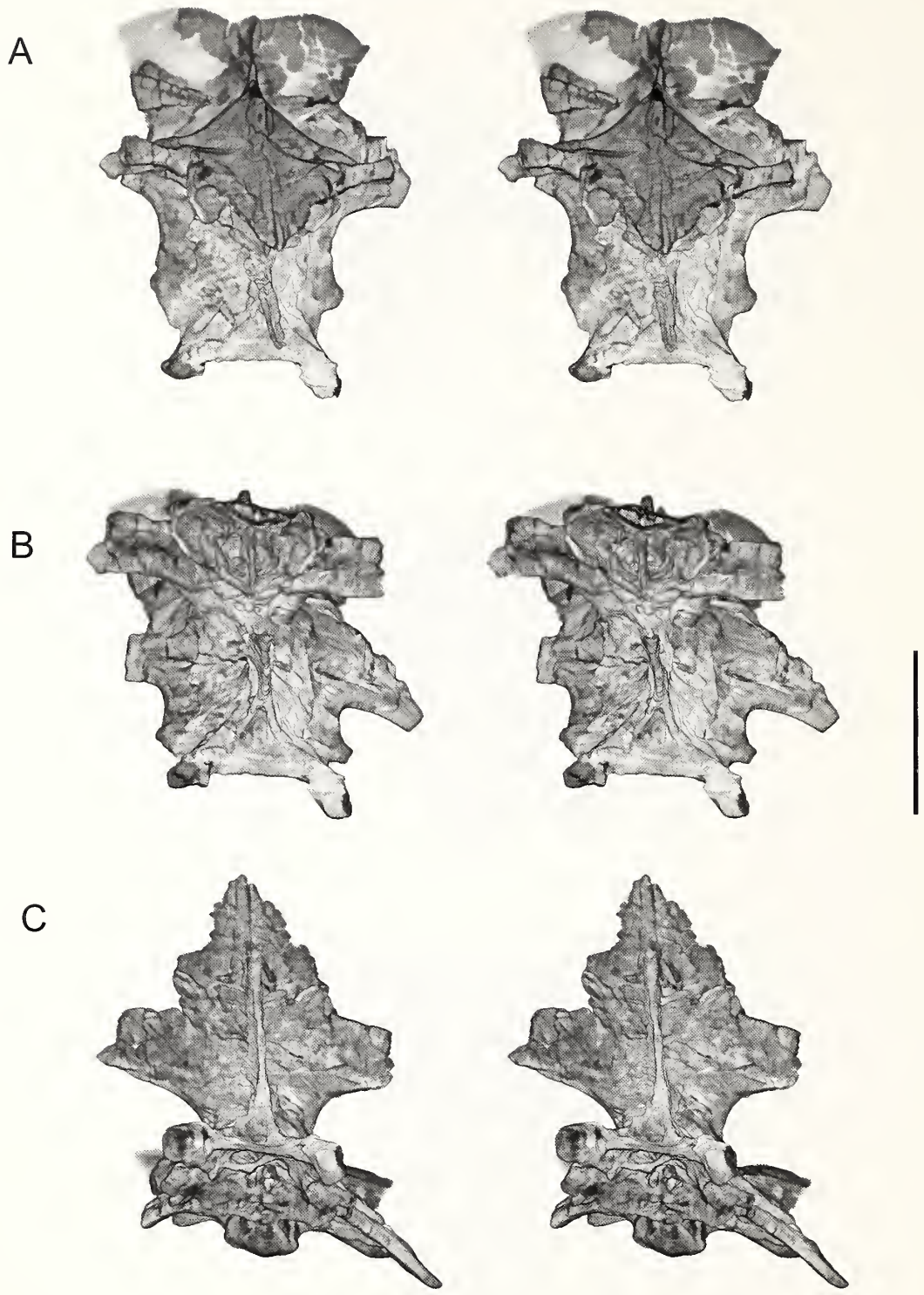

Figure 7. Cleveland tyrannosaur skull, CMNH 7541. Volume renderings (stereopairs) of digitally extraeted braincase derived from CT data in A, rostral; B, rostroventral; C, ventral views. Figure 8A–C provides corresponding labeled views. Scale bar equals 10 cm.

P2002.4.1) that closely resembles CMNH 7541 in many ways (Henderson and Harrison, 2008) and which is generally thought to represent a similar ontogenetic age of the same species (P. Larson, 2008). Remarkably, this otherwise very complete specimen lacks the braincase, and so the Cleveland skull remains critical in this regard, but comparisons to BMR P2002.4.1 are made here where relevant.

Materials and Methods

The primary specimen used in this study was CMNH 7541, a nearly complete skull of a probably juvenile tyrannosaurid, collected from the Hell Creek Formation of Carter County, Montana (see Gilmore, 1946, for collection details and geological setting). A variety of other tyrannosaurid specimens were studied in connection with this project (for a full listing,

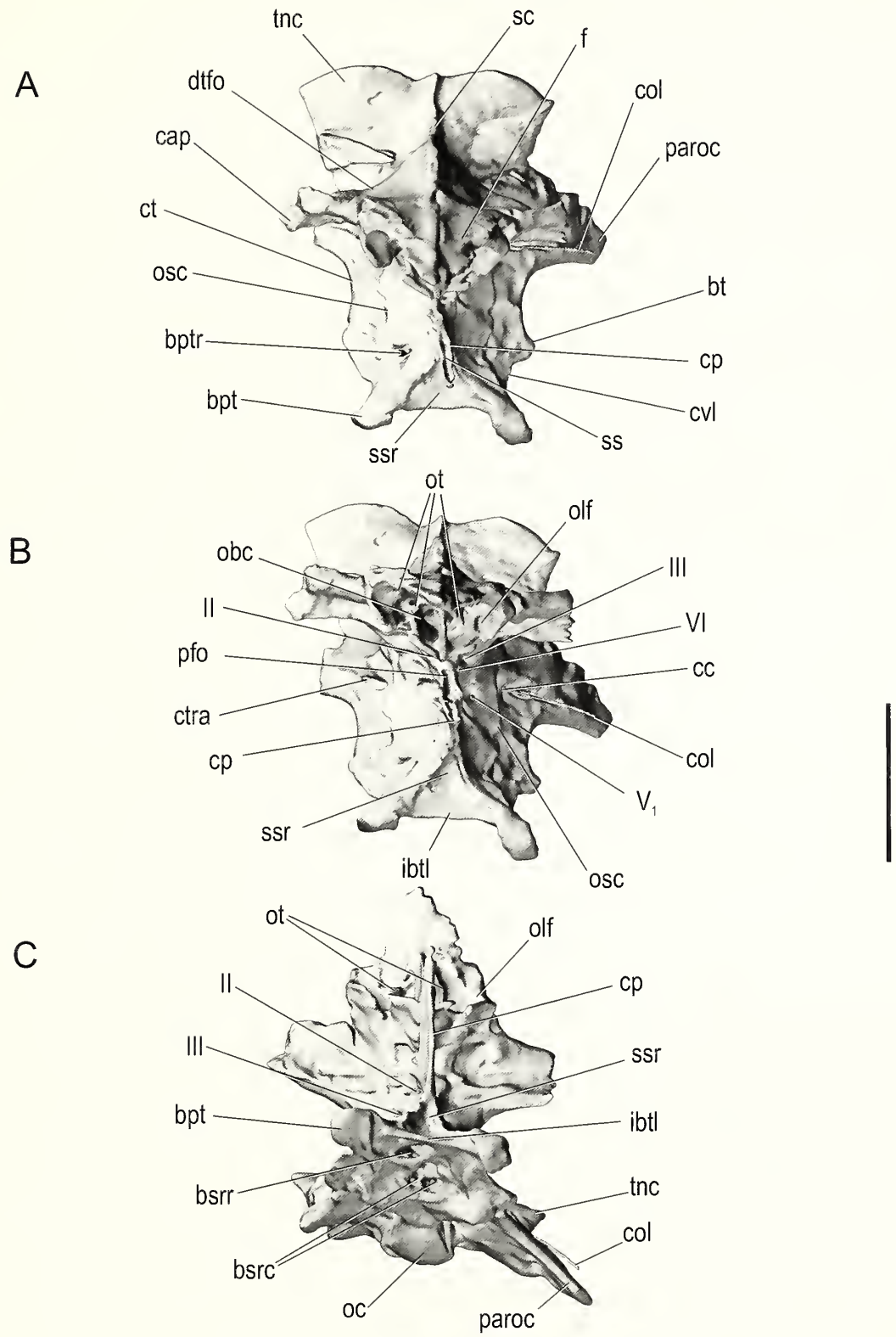

Figure 8. Cleveland tyrannosaur skull, CMNH 7541. Surface renderings of digitally extracted braincase derived from CT data in A, rostral; B, rostroventral; C, ventral views. Figure 7A–C shows corresponding stereopairs of volume renderings. Scale bar equals 10 cm. See Appendix for abbreviations.

see Witmer and Ridgely, 2009). In addition to general observation, the major tool used in this study was CT scanning (computed x-ray tomography), followed by 3D analysis and visualization. CMNH 7541 has been CT scanned no fewer than three times.

The first scans were done in 1990 on a medical scanner at a Toronto hospital, in the presence of Michael Williams, Andrew Leitch, and Robert T. Bakker (Bakker, 1992). Scanning details have not been published, but results were presented in a popular article by Bakker (1992), who reconstructed the brain cavity and, within the nasal cavity, an elongate turbinate. The same CT data were used later by J. A. Ruben to refute the finding of respiratory turbinates in this skull (Ruben, 1996; Ruben et al., 1996, 1997).

The Cleveland skull was scanned for the second time in 1998 at the Boeing Rocketdyne CT Lab in California under the auspices of the Cleveland Museum of Natural History with funding from the Field Museum of Natural History. The skull was scanned at a slice thickness of 1 mm with slices in the horizontal plane, yielding 300 slices; voxel sizes were 0.4042 × 0.4042 × 1.0 mm. As part of the collaboration with M. Williams, the Cleveland Museum of Natural History provided Witmer with the full 16-bit dataset from these scans.

In hopes of revealing aspects of anatomy that are unclear in the Boeing dataset, the skull was scanned for the third time in 2005 at O'Bleness Memorial Hospital, Athens, Ohio, on a General Electric LightSpeed Ultra MultiSlice CT scanner equipped with the Extended Hounsfield option, which enhances the ability to resolve details from dense objects such as fossils. Because the Boeing dataset was derived from scans of the skull in the horizontal plane, the x-rays had to pass through the full length of the skull, which ean produce artifacts. Thus, we scanned the skull axially, which minimized the amount of material the x-rays had to penetrate. The full skull was scanned helically with a slice thickness of 1.25 mm at 140 kV and 300 mA, yielding 483 slices and voxel sizes of 0.082 × 0.082 × 1.25 mm. The skull was then scanned again, this time focusing on the braincase, tightening the field of view and extending from the caudal end of the skull through the orbits and ending rostrally just in front of the lacrimals' jugal processes; slice thickness was 625 microns (0.625 mm) at 140 kV and 170 mA, yielding 385 slices and voxel sizes of 0.049 × 0.049 × 0.625 mm. No CT scan is free from artifact, and both the Boeing and Athens datasets have their advantages and disadvantages. Ultimately, much of the work presented here is based on a composite "super-dataset" created by registering and combining the Boeing and multiple Athens datasets.

Viewing, analysis, and visualization of the scan data were done using Amira 3.1.1 and 4.2 (Mercury-TGS, Chelmsford, MA) on 32- and 64-bit Windows XP PCs equipped with nVidia Quadro FX graphics cards and 2–8 GB of RAM. Structures of interest were highlighted (segmented) using Amira's segmentation tools and visualized either in isolation or combined with other structures or the whole skull. Both surfaces and volumes were generated, and these served as the basis for most of the illustrations in this artiele. Additional information, such as interactive movies and 3D PDFs, are available on the authors' website: www.ohio.edu/witmerlab.

Museum abbreviations used in this paper are: AMNH, American Museum of Natural History, New York City, New York; BMR, Burpee Museum of Natural History, Rockford, Illinois; CMNH, Cleveland Museum of Natural History, Cleveland, Ohio; FMNH, Field Museum of Natural History, Chicago, Illinois; MOR, Museum of the Rockies, Bozeman, Montana; OMNH, Oklahoma Museum of Natural History, Norman, Oklahoma; ROM, Royal Ontario Museum, Toronto, Ontario; and TMP, Royal Tyrrell Museum of Palaeontology, Drumheller, Alberta.

Results

CMNH 7541 has been the subject of at least three major anatomical studies (Gilmore, 1946; Bakker et al., 1988; Carr, 1999), and thus there is no need for in-depth anatomical description here. Instead, our intent is to focus on a few areas that have not been adequately discussed in print and that are revealed by the CT scan data. It is also our intent to capitalize on the new-found visualization capabilities provided by the new imaging technologies and software, and so we emphasize illustration over text (in the spirit of the old adage of a picture being worth a thousand words).

General attributes

Figures 1–3 provide stereophotographs of the skull in several views, showing not just bony structure but also the amount of matrix remaining in the skull and, to a certain extent, the amount of plaster restoration. Plaster is relatively low density and homogenous and is easily identified and removed in volume renderings of the CT data. Figure 4 presents views of the skull with the plaster (and some regions of thin matrix) dropped out. Examination of Figure 4 reveals that the snout had been fractured along an oblique transverse plane running caudodorsally to rostroventrally (arrows in Figure 4C) such that, when repaired and restored in plaster (quite expertly, it may be said), much of the central parts of the nasal and antorbital cavities wound up being largely plaster.

Braincase

The braincase of CMNH 7541 is visible in dorsal, caudal, and ventral views in the actual (physical) specimen (Figures 2D–E, 3A–C), but the other surfaces are obscured by matrix and other bones. To more easily compare the braincase to those of other theropods, the braincase of CMNH 7541 was digitally "disarticulated" along sutures and then extracted so that it could be viewed in isolation (Figures 5–8). The general conformation of the braincase is fairly similar to those of other tyrannosaurs in having a well developed otosphenoidal crest (= crista prootica) running from the otoccipital bone caudally and arching rostrally and then ventrally on the prootic, laterosphenoid, and basisphenoid bones (Figure 6B). Tucked ventrally or caudoventrally below the margin of the otosphenoidal crest, from caudal to rostral, are the caudal tympanic recess aperture, columellar reeess (with the columella [= stapes] in place in the fenestra vestibuli), the maxillomandibular and facial foramina (for CN V_{2-3} and CN VII, respectively), the rostral tympanic recess, and eerebral carotid foramen. As in other tyrannosaurids, the facial foramen opens so close to the maxillomandibular foramen that the two essentially share an aperture laterally (Witmer et al., 2008; Witmer and Ridgely, 2009; Brusatte et al., 2009).

As in other tyrannosaurids, perhaps all coelurosaurs, and many tetanurans (Sampson and Witmer, 2007; Witmer and Ridgely, 2009), the ophthalmic nerve (CN V_1) exits the laterosphenoid rostrally via its own foramen. Another attribute shared with other tyrannosaurids is the almost complete ossification of the front of the braincase, with orbitosphenoid and sphenethmoid ossifications contacting their fellows in the midline and enclosing foramina for the olfactory bulbs and tracts, optie nerves (CN

II), oculomotor nerves (CN III), and abducens nerves (CN VI) (Figures 6, 8). The sphenethmoid is particularly significant because it preserves details relating to the olfactory apparatus. The sphenethmoid itself is divided by a midline osseous septum (mesethmoid), which in life would have separated the rostral terminations of the olfactory tracts (i.e., the olfactory bulbs), as described for other theropods (Sampson and Witmer, 2007; Ali et al., 2008; Witmer and Ridgely, 2009). Lateral to the region of the olfactory bulbs are a series of thin bony laminae descending from the roof of the sphenethmoid and possibly also the frontal (Figures 6A, B; 7B, C; 8). These laminae are external to the neural domain and would be within the nasal cavity, and thus these laminae are best interpreted as olfactory turbinates that would have supported the sensory olfactory epithelium, as observed in extant taxa. The olfactory apparatus indeed seems well developed in CMNH 7541, which is consistent with its large olfactory bulbs, as well as with the large bulbs and expansive nasal olfactory regions seen in other tyrannosaurs (Witmer et al., 2008; Witmer and Ridgely, 2009).

CMNH 7541 shares with other tyrannosauroids modestly-sized but widely-spaced basal tubera (Bakker et al., 1988; Carr, 1999; Currie et al., 2003; Li et al., 2010), yet it retains strong basipterygoid processes. Likewise, all tyrannosaurids, including CMNH 7541, share extensive pneumaticity associated with the middle ear and pharynx (rostral and caudal tympanic recesses, basisphenoid recesses, subcondylar recess, subsellar recess; Witmer, 1997b; Witmer and Ridgely, 2009; see below).

Despite the similarities with other tyrannosaurids noted above, CMNH 7541 displays a number of noteworthy differences. For example, the cultriform process (parasphenoid rostrum) is relatively low and straight (Figures 5A, 6A), rather than, as in most other tyrannosaurids (Russell, 1970; Carr, 1999; Brochu, 2003; Currie, 2003b), having a strongly arched ventral margin that sweeps dorsally before leveling off parallel to the frontals. This may relate to CMNH 7541 having a relatively smaller subsellar recess (a ventral pneumatic chamber in the base of the cultriform process; Figures 6B, 9) relative to other tyrannosaurids. Among tyrannosaurids, the conformation of the cultriform process and subsellar recess is most similar to that of *Gorgosaurus* (Witmer and Ridgely, 2009) and *Alioramus* (Brusatte et al., 2009). Another difference is that CMNH 7541 has a much less projecting preotic pendant (Figure 6A), whereas in other tyrannosaurids it is a large and rugose structure associated with the otosphenoidal crest (Holliday and Witmer, 2008; Witmer and Ridgely, 2009); its weak development in CMNH 7541 may relate to the small size of the animal.

Other differences relate to the location of the vagus foramen (CN X) on the occiput and to the structure of the subcondylar recesses of the basicranium. In most other tyrannosaurids (certainly *T. rex*), the vagus foramen (CN X) is located medially in the caudal surface of the otoccipital within a paracondylar pocket or recess adjacent to the occipital condyle. In CMNH 7541, however, the vagus foramen is located more laterally (Figure 6C), in a position more typical of other coelurosaurs.

Ornithomimids, all tyrannosaurids (although apparently not the tyrannosauroid *Xiongguanlong*; Li et al., 2010), and potentially even some non-coelurosaurs (Sampson and Witmer, 2007) have subcondylar recesses (lateral and medial), which are pneumatic recesses located ventral to the occipital condyle and which excavate the basioccipital and otoccipital in the region above the basal tubera. Furthermore, in most tyrannosaurids, there are pneumatic apertures in the floor of the recess leading into chambers within the basioccipital and otoccipital (Currie, 2003b; Witmer and Ridgely, 2009). The subcondylar recesses of CMNH 7541 differ from those of *T. rex*. In the former, the recesses as a whole are deeper and the basioccipital and otoccipital pneumatic apertures (leading into the medial and lateral subcondylar sinuses, respectively) are much closer together (essentially adjacent to each other and within a shared fossa; see Figures 5C, 6C, 9). Related to this difference is that the ventromedial wall of the subcondylar recess (the condylotuberal crest; Figures 5C, 6C, 9) is much stronger in CMNH 7541 than in specimens of *T. rex*. Taken together, the subcondylar region of CMNH 7541 is more primitive than that of *T. rex* and is intermediate between the latter and more basal tyrannosaurids (e.g., *Gorgosaurus*, ROM 1247; *Daspletosaurus*, FMNH PR308; see Witmer and Ridgely, 2009) and even more basal theropods (e.g., *Acrocanthosaurus*, OMNH 10146).

Other workers (e.g., Gilmore, 1946; Bakker et al., 1988) have pointed out the divergent nature of the apertures within the basisphenoid pneumatic recess of CMNH 7541, but 3D visualization of the pneumatic sinuses helps clarify the situation in comparison to other tyrannosaurids. In general, the basisphenoid recess of CMNH 7541 more closely resembles that of *Gorgosaurus* and *Daspletosaurus* in having a longer rostrocaudal distance between the intertuberal and interbasipterygoid laminae (= basituberal and basipterygoid webs, respectively, of Bakker et al., 1988; see Figures 5–8), whereas in *T. rex* these two laminae are quite closely appressed (Witmer and Ridgely, 2009). However, what makes CMNH 7541 so divergent is the pattern of apertures within the basisphenoid recess. As preserved (Figures 3C, 6C), there are three asymmetrical apertures, unlike any other known theropod. When traced dorsally into the pneumatic sinuses using the CT data, the caudal two apertures can be seen to represent a pair (even if they are not fully bilaterally symmetrical) because they expand into paired (i.e., left and right) sinuses (the caudal basisphenoid sinuses; Figures 8C, 9) that lead into the basioccipital and communicate on either side of the occiput with the medial subcondylar recesses. Expansion of the basisphenoid recess into sinuses within the basioccipital is fairly common in theropods generally, although the pattern of apertures in CMNH 7541 is unique.

The third and most rostral aperture within the basisphenoid recess has been difficult to interpret. Other tyrannosaurids have a rostral pair of foramina (left and right) in the interbasipterygoid lamina that lead into pneumatic chambers within the basisphenoid (Russell, 1970; Bakker et al., 1988; Witmer, 1997b; Currie, 2003b; Witmer and Ridgely, 2009). Tracing the seemingly single aperture in CMNH 7541 in the CT data reveals that the aperture branches dorsally into essentially left and right sinuses (the rostral basisphenoid sinuses) that expand within the basisphenoid and eventually communicate with the rostral tympanic recesses on their respective sides (Figures 7C, 8C, 9). As a result, it would seem that the pair of foramina in the interbasipterygoid lamina of other tyrannosaurids is present in CMNH 7541, but that the two apertures share a common fossa that is diverted towards the right side somewhat. Thus in sum, we are proposing that the basisphenoid pneumatic sinuses are fundamentally similar to those of other tyrannosaurids, albeit highly modified. Gilmore (1946, p. 10) explained this unusual and asymmetric morphology as representing "an unhealthy condition of the bone," but there is no overt sign of pathology in this region.

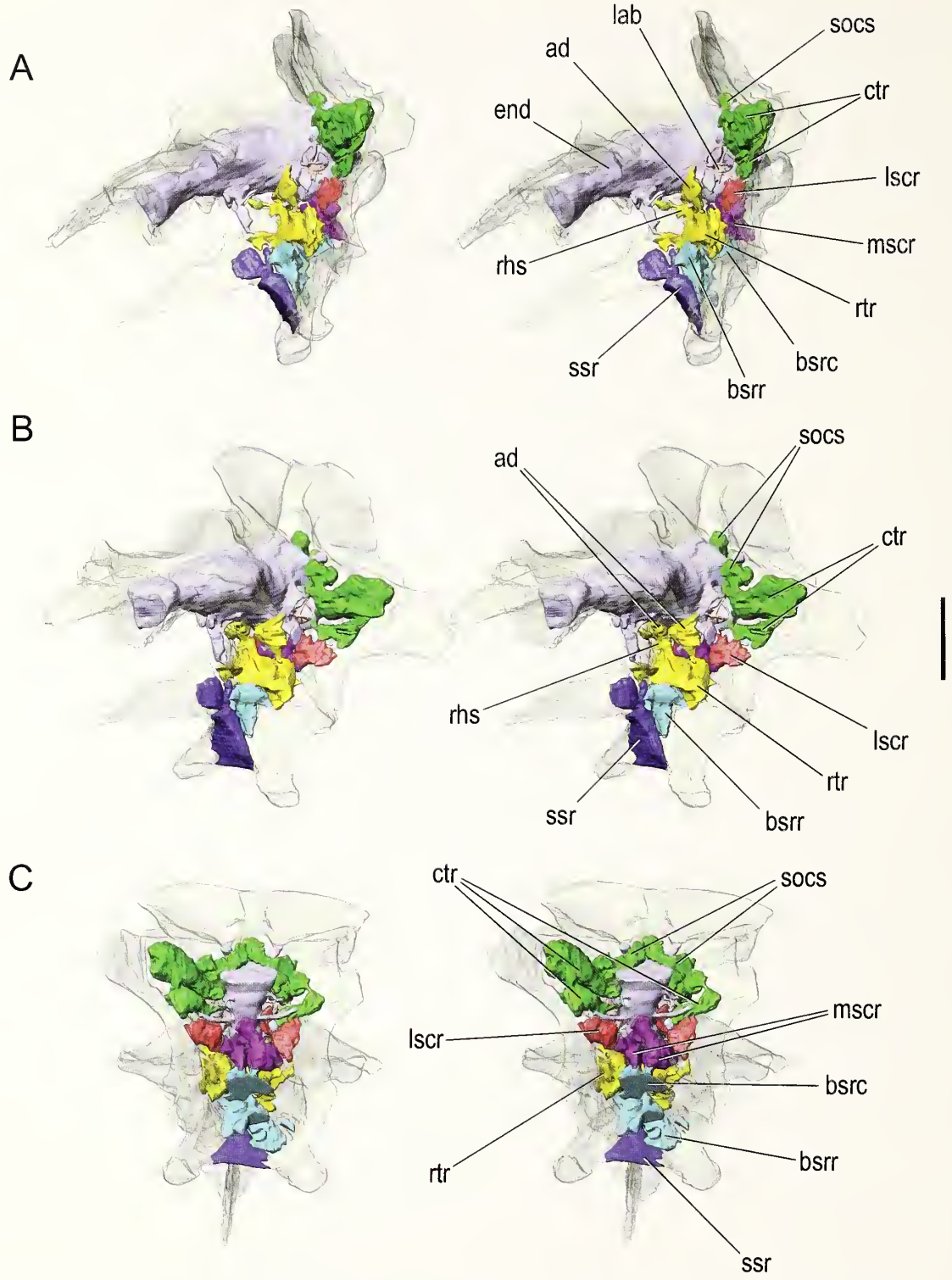

Figure 9. Cleveland tyrannosaur skull, CMNH 7541. Surface renderings of digitally extracted braincase derived from CT data, made partially transparent to reveal brain endocast (light blue) and internal pneumatic sinuses, in A, left lateral; B, left rostroventrolateral; C, caudoventral views. Scale bar equals 10 cm. See Appendix for abbreviations.

Pneumatic sinuses of the braincase

The pneumatic recesses of CMNH 7541 have been touched on above, but they will receive fuller treatment here in that they have been reconstructed in three dimensions using the CT-scan data (Figure 9). As noted, there is a clear aperture leading into the caudal tympanic recess, and, as in most other coelurosaurs (Witmer, 1997b), the aperture is located in the base of the paroccipital process adjacent to the columellar recess and bounded by the prootic and opisthotic. In CMNH 7541, the caudal tympanic recess expands within the paroccipital process,

giving off two diverticula, one ventrally and the other dorsally. The ventral diverticulum enters the crista tuberalis (= basioccipital wing of the otoccipital, descending ventral root of the paroccipital process of Bakker et al., 1988) where it is broadly confluent with the lateral subcondylar recess. Despite this confluence, the cavity within the crista tuberalis of CMNH 7541 clearly derives as a primary diverticulum of the lateral subcondylar reeess, because, in other tyrannosaurids (e.g., *T. rex*, *Gorgosaurus*), the communication between the two pneumatic spaces is slight to nonexistent, and it is the lateral subcondylar sinus that occupies the crista tuberalis (Witmer and Ridgely, 2009). The dorsal diverticulum certainly derives as an outgrowth of the caudal tympanic recess and forms a series of interconnecting chambers medially within the otoccipital and supraoccipital and laterally within the paroccipital process (Figure 9), as in other tyrannosaurids and indeed most other coelurosaurs (Witmer, 1997b; Witmer and Ridgely, 2009). There may be a tenuous communication between contralateral recesses within the supraoccipital but not the broad communication observed in *T. rex* and *Gorgosaurus*.

The rostral tympanic recess is located, again fairly typically, in the region where the cerebral carotid artery enters the braincase under shelter of the otosphenoidal crest, that is, in the area where the basisphenoid, prootic, and laterosphenoid contact each other (Figure 9). The rostral tympanic recess expands within the basisphenoid where it communicates with both the rostral and caudal basisphenoid sinuses, but more broadly with the rostral basisphenoid sinus. The rostral tympanic recess has a major dorsal diverticulum (the aseending diverticulum; Figure 9A, B) that leads into the substance of the laterosphenoid bone, occupying the region between the canals for the ophthalmic nerve (CN V_1) rostrally and maxillomandibular nerve (CN V_{2-3}) caudally. The connection between the ascending diverticulum and the rostral tympanic recess is very narrow. The ascending diverticulum is present in *Gorgosaurus* but is usually absent (or very rudimentary) in adult *T. rex* and *Dapletosaurus* (Witmer and Ridgely, 2009), which could be a legitimate, systematically informative difference. However, a newly discovered, very young skull of *Tarbosaurus* (just 29 cm total skull length; Tsuihiji et al., 2007, in review) displays a well developed ascending diverticulum of the rostral tympanic recess; although we lack comparable CT data for adult *Tarbosaurus*, if we assume that *Tarbosaurus* resembled adult *T. rex*, ontogenetic loss of the ascending diverticulum in tyrannosaurines remains a possibility.

The rostral tympanic recess has another, more medial, diverticulum (the retrohypophyseal sinus, Figure 9A, B) that extends dorsomedially within the clivus of the basisphenoid just caudal to the hypophyseal (pituitary) fossa. This sinus represents a contralateral communication of the left and right rostral tympanic recesses, and has been found in all the tyrannosaurids studied here (Witmer and Ridgely, 2009). In CMNH 7541, the retrohypophyseal sinus itself sends a small median diverticulum between the paired abducens (CN VI) canals.

The sinuses associated with the basisphenoid reeess have been mentioned above in connection with their external apertures. Given the asymmetry of their bony apertures, it is not surprising that the sinuses themselves are quite asymmetrical, much more so than the caudal and rostral tympanic recesses and their associated diverticula. The caudal basisphenoid sinuses expand dorsally and somewhat caudally, passing through the basioccipital, as noted above, to become broadly confluent with the medial subcondylar recess on the occiput (Figure 9). The caudal basisphenoid sinus has some communication with the rostral tympanic recess (more so on the left side). The rostral basisphenoid sinuses expand dorsally and rostrally within the basisphenoid. Interestingly, although the shared aperture of the two rostral basisphenoid sinuses within the recess is shifted to the right side, the left sinus is larger and more broadly communicates with the rostral tympanic recess (Figure 9). This asymmetry could be natural but some small amount of postmortem crushing cannot be ruled out, as the right side of the braincase is generally not as well preserved as is the left side.

The subsellar recess is located rostral to the interbasipterygoid lamina at the ventral base of the cultriform process (Figure 9). The subsellar recess is relatively small in comparison to that of *T. rex* and *Daspletosaurus* but is similar in size to that of some juvenile *Gorgosaurus* specimens (e.g., ROM 1247). There are no pneumatic foramina within the subsellar recess on CMNH 7541.

On the right side of CMNH 7541, but not the left, there is an aperture in the basisphenoid bone just dorsal to the base of the basipterygoid process. The aperture is surrounded by a shallow fossa, and these features can be regarded as a basipterygoid recess (Chure and Madsen, 1996; Witmer, 1997b). The aperture leads into a sinus (the basipterygoid sinus) that ascends dorsally within the basisphenoid. Its communications with other sinuses in the basisphenoid are slight to nonexistent, although it does appear to breach the interbasipterygoid lamina within the basisphenoid recess, where, if so, it would then communicate with the air sinus located there. The basipterygoid process itself is not pneumatized.

Finally, the subcondylar recesses open into a pneumatic fossa on the occiput below the occipital condyle (Witmer, 1997b) and have been mentioned above in connection with pneumatic apertures located in the otoccipital and basioccipital within the fossa (Figure 9C). Carr (1999) and Currie (2003b) both regarded the fossa for the subcondylar recesses of CMNH 7541 as shallow, but to our eyes it seems intermediate between the deep recess of young *Gorgosaurus* specimens (ROM 1247) and the very shallow recess of mature specimens of *T. rex* (e.g., AMNH 5027, AMNH 5117, FMNH PR2081; see Witmer and Ridgely, 2009). As noted above, the otoccipital aperture of the lateral subcondylar recess expands into a sinus within the crista tuberalis (where it communicates with the caudal tympanic recess), whereas the basioccipital aperture leads to the medial subcondylar sinus that communicates with the caudal basisphenoid sinus. The medial subcondylar sinus does not pneumatize the occipital condyle but just the very base of the neck, as Osborn (1912) showed for *T. rex* (AMNH 5029; see also Witmer and Ridgely, 2009).

Thus in summary, CMNH 7541 has an extensively pneumatized braincase, with clearly identifiable rostral and caudal tympanic recesses, a series of basisphenoid sinuses arising rostrally and caudally from the basisphenoid recess, medial and lateral subcondylar recesses, a small subsellar recess, and, on one side only, a basipterygoid recess. Virtually all of these sinuses communicate broadly with adjacent sinuses. The two tympanic recesses are clearly derived from the middle ear sac (as their names imply), but the basisphenoid and subsellar recesses may derive from a separate median pharyngeal system (Witmer, 1997b). Likewise, although the subcondylar recesses could be tympanic in origin, it is not possible to rule out pneumatization via a cervical pulmonary diverticulum (Witmer, 1997b; Witmer and Ridgely, 2009).

Columella (= stapes)

The columella is clearly preserved in natural position on the left side (Figure 6A, B; 8A, B). It is a very delicate element, extending from the fenestra vestibuli within the columellar recess,

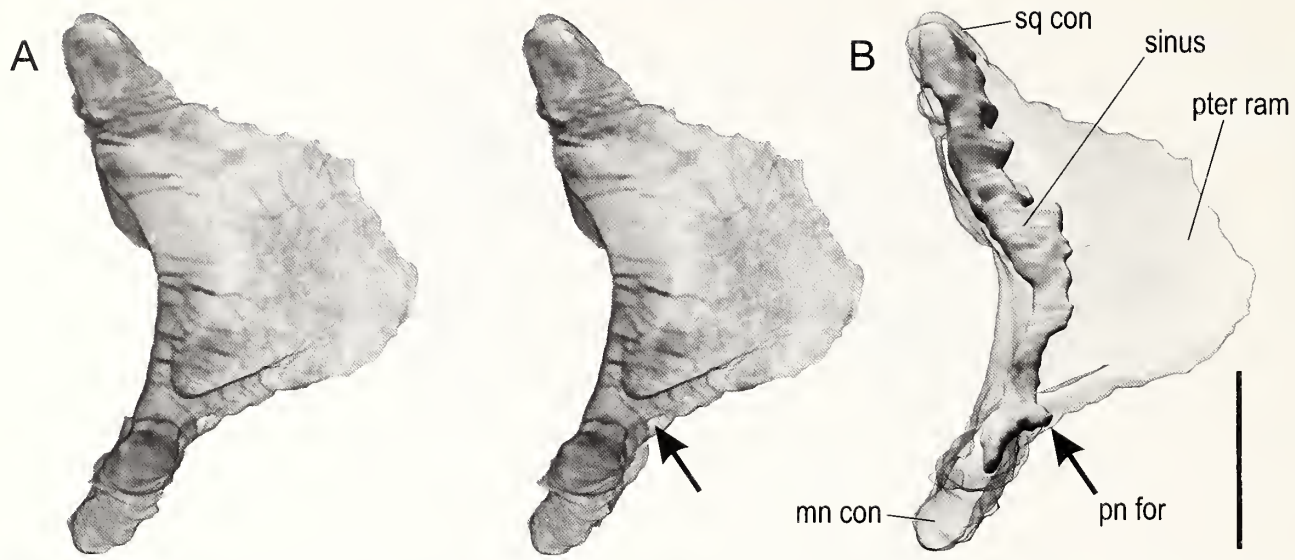

Figure 10. Cleveland tyrannosaur skull, CMNH 7541. Volume (A) and surface (B) renderings of digitally extracted left quadrate derived from CT data in medial view. Volume renderings (A) are stereopairs; arrow points to the pneumatic foramen. Surface rendering (B) is partially transparent to reveal the internal pneumatic sinus. Scale bar equals 5 cm. See Appendix for abbreviations.

passing along the paroccipital process below the otosphenoidal crest, to end laterally just caudomedial to the dorsal head of the quadrate. The columella is only about 1.4 mm in diameter, yet is 71.7 mm in length. The length is probably an underestimate in that the lateral tip is exposed in the actual fossil, and it is unknown how much was lost in collection, preparation, etc. The fact that the columella is preserved in situ and is straight suggests that the braincase region as a whole has not undergone significant deformation.

Quadrate and its pneumaticity

The left quadrate was digitally extracted from the full CT dataset to examine and illustrate the position of its pneumatic aperture (Figure 10). Although a taxonomic difference in position of this foramen has not been noted previously, the quadrate pneumatic foramen of albertosaurines (*Gorgosaurus*: AMNH 5363; *Albertosaurus*: TMP 81.10.1; see also Currie, 2003b, p. 200) is in a slightly different position than in *Daspletosaurus* (FMNH PR 308) and *Tyrannosaurus* (FMNH PR2081). In the former, the pneumatic foramen is directed more medially, whereas in the latter group the crest of bone above the foramen on the quadrate's pterygoid ramus is much stronger and diverts the pneumatic foramen to a more rostral position such that it no longer directly faces the tympanic cavity. In CMNH 7541, the quadrate pneumatic foramen again has more of an intermediate position (Figure 10). The foramen itself is relatively small in CMNH 7541. BMR P2002.4.1 is very similar in these regards. The quadrate pneumatic sinus in CMNH 7541 is somewhat better preserved on the right side (not illustrated in Figure 10), but on both sides the sinus extends essentially the full height of the element (Figure 10B).

Quadratojugal and its pneumaticity

The quadratojugal is preserved on only the left side of CMNH 7541, and even here the bone is fractured and displaced such that its jugal process remains in articulation with the jugal, whereas its squamosal process has been shifted dorsally and rostrally. The most significant attribute of the quadratojugal is the peculiar foramen in its lateral surface within the ventral apex of the lateral fossa. BMR P2002.4.1 shows a virtually identical foramen, but such a foramen is absent in adult *T. rex* and has not been reported in other tyrannosaurids, other than a small foramen in a specimen of *Gorgosaurus* sp. reported by P. Larson (2008). Although only rarely noted in print (e.g., P. Larson, 2008), some tyrannosaur workers have wondered if this difference supports the validity of the taxon *Nanotyrannus lancensis*. To clarify the anatomy, we examined this foramen in the CT dataset and digitally extracted the bone for visualization (Figure 11). The foramen is almost certainly a pneumatic foramen, expanding into a blind cavity within the substance of the bone. The cavity has no medial outlets, only the lateral aperture. This also would tend to indicate that the lateral quadratojugal fossa is a pneumatic fossa, most likely associated with the middle ear. Although it remains possible that presence of this quadratojugal pneumatic foramen is a juvenile feature of *T. rex* that was lost later in ontogeny, the very young skull of *Tarbosaurus* described by Tsuihiji et al. (2007; in review) lacks such a foramen, as do adult *Tarbosaurus* quadratojugals, suggesting that presence and then loss of the pneumatic foramen was not a general ontogenetic sequence of tyrannosaurines.

Palatine bone and its pneumaticity

The left palatine bone of CMNH 7541 also was digitally extracted (Figure 12). The bone is a fairly typical tyrannosaurid palatine. The bone is pneumatic as in other tyrannosaurids and some other theropods (Witmer, 1997a, b; Witmer and Ridgely, 2008b) with two pneumatic foramina plainly visible on the actual skull (Figure 2A). When examined with CT, however, it can be seen that the two pneumatic sinuses within the bone do not communicate but instead form separate chambers. Although the vomeropterygoid process is fully pneumatized (Figure 12B), the bone is not strongly inflated, as seen in many *T. rex* specimens (e.g.,

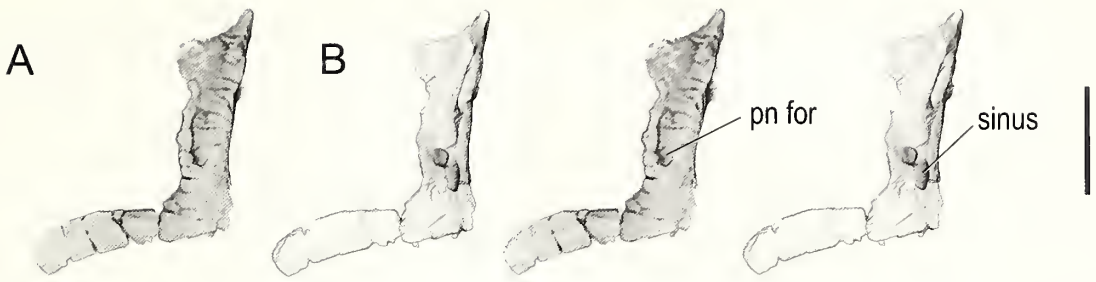

Figure 11. Cleveland tyrannosaur skull, CMNH 7541. Volume (A) and surface (B) renderings of digitally extracted left quadratojugal derived from CT data in lateral view. Both sets are stereopairs. Surface rendering (B) is partially transparent to reveal the internal pneumatic sinus. In the actual specimen, the jugal process was displaced relative to the rest of the bone, but has been digitally reattached here. Scale bar equals 5 cm. See Appendix for abbreviations.

FMNH PR2081, MOR 008). In general, the palatine of BMR P2002.4.1 has a similar conformation with a large pneumatic aperture caudally, but, unlike CMNH 7541, the rostral pneumatic feature does not breach the bone and so is a fossa, not a foramen.

Vomer

The shape of the rostral end of the vomer is an important character in tyrannosaurid systematics, with basal tyrannosauroids and albertosaurines (*Gorgosaurus* and *Albertosaurus*) retaining the primitive condition of a narrow, "lanceolate" vomer and tyrannosaurines (*Daspletosaurus*, *Tarbosaurus*, *Tyrannosaurus*) having a derived, laterally expanded, diamond-shaped vomer (Holtz, 2001, 2004; Currie et al., 2003; Li et al., 2010). The vomer of CMNH 7541 is almost completely enclosed in matrix, with just the caudalmost portion exposed within the antorbital cavity (Figures 1A, 2A). So, to shed light on the systematically important end of the bone, we digitally extracted the vomer for visualization (Figure 13). The vomer of CMNH 7541 has the primitive condition, with a narrow rostral end. In fact, the rostralmost tip has the further primitive attribute of forking to contact the palatal processes of the maxilla and premaxilla. Overall, the vomer is a fairly typical non-tyrannosaurine theropod vomer with a dorsal sulcus and a ventral keel. The vomer of BMR P2002.4.1 is again almost identical to that of CMNH 7541. A valid question is whether this morphology is truly primitive or just reflective of an early ontogenetic stage that would transform later in life to the definitive adult tyrannosaurine condition (i.e., *T. rex*). In this context, the very young *Tarbosaurus* specimen described by Tsuihiji et al. (2007; in review) is significant in having a rostrally narrow vomer similar to those of CMNH 7541 and BMR P2002.4.1, suggesting that indeed a lanceolate vomer can ontogenetically transform into a diamond-shaped vomer. That said, if CMNH 7541 pertains to a juvenile *T. rex*, then the rate of transformation would have had to have been markedly different in *T. rex* and *Tarbosaurus* in that an unnumbered juvenile *Tarbosaurus* skull (only about 27% larger than CMNH 7541) already has a diamond-shaped vomer.

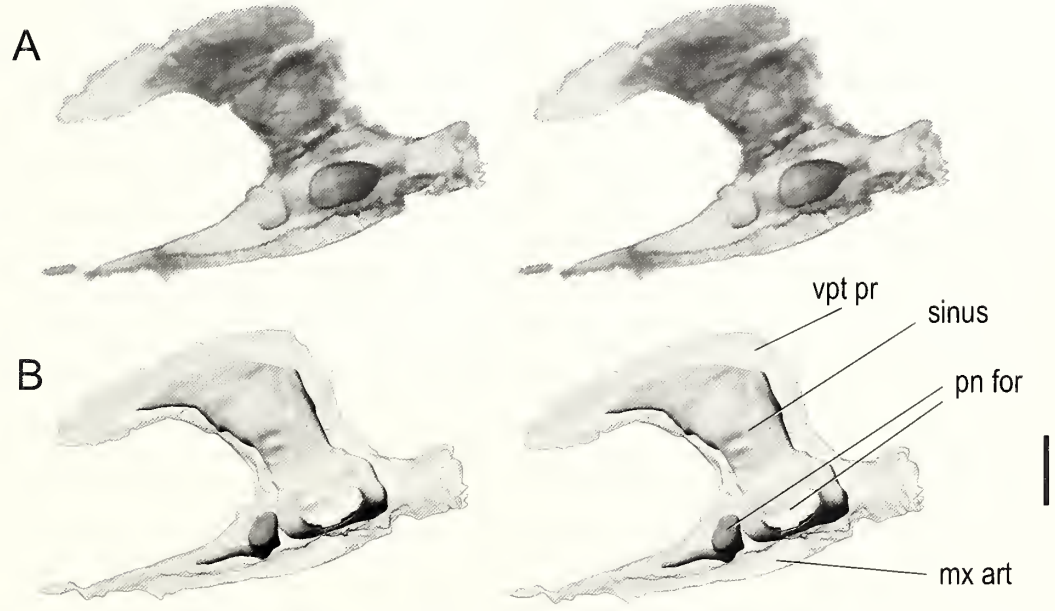

Figure 12. Cleveland tyrannosaur skull, CMNH 7541. Volume (A) and surface (B) renderings of digitally extracted left palatine derived from CT data in lateral view. Both sets are stereopairs. Surface rendering (B) is partially transparent to reveal the internal pneumatic sinuses; note that the two sinuses do not communicate. Scale bar equals 2 cm. See Appendix for abbreviations.

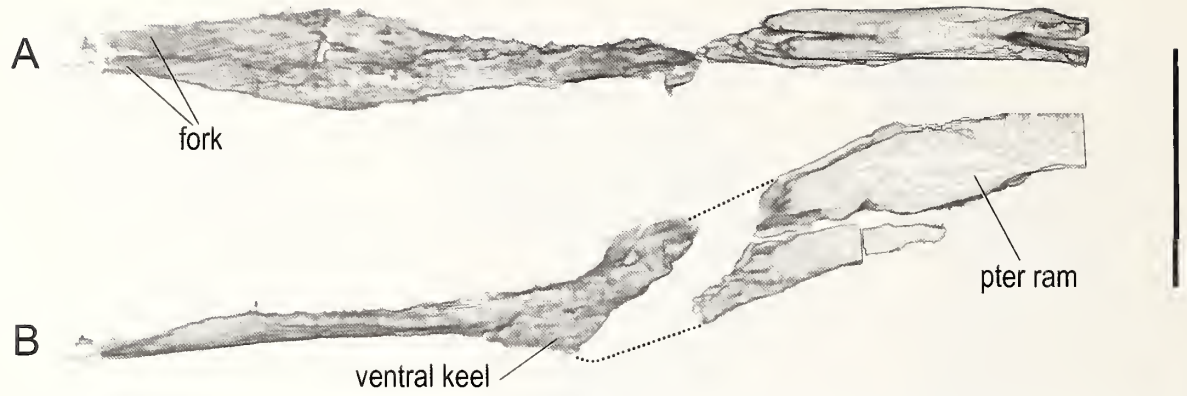

Figure 13. Cleveland tyrannosaur skull, CMNH 7541. Volume renderings of digitally extracted vomer derived from CT data in A, dorsal; B, left lateral views. Note that rostral portion of the bone is primitive in being lanceolate and forked. Dotted lines represent restored portions in the area corresponding to the transverse oblique plane of fracture (see Figure 4C). Scale bar equals 5 cm. See Appendix for abbreviations.

Possible respiratory turbinates

Respiratory turbinates in amniotes have received a great deal of attention because of their potential role in debates on dinosaur metabolic status (Bakker, 1992; Ruben, 1996; Ruben et al., 1996, 1997). The idea promoted by J. A. Ruben (1995) is that respiratory turbinates may be mandatory in endothermic animals to help mitigate the effects of respiratory evaporative water loss that would result from the high lung-ventilation rates characteristic of endotherms. As mentioned above, CT scanning of CMNH 7541 has been a major player in this debate. Bakker (1992) reconstructed a large scrolled turbinate within the snout of this animal, but, given that the reconstruction was published in a popular magazine (*Discover*), no details were given. Later Ruben and his team (1996, 1997) argued (using the same scan data) that no turbinates were present, and that, moreover, the airway was too small to house turbinates.

Unfortunately, CMNH 7541 is not the best specimen on which to base a debate, because so much of the snout is damaged and reconstructed with plaster. As noted above, clear *olfactory* turbinates are present far caudally (Figures 5–8); they are immediately adjacent to the olfactory bulb fossa and could not have functioned as respiratory turbinates because they are well out of the main nasal airstream (see Witmer and Ridgely, 2008b, 2009). Rostral to the olfactory turbinates is a large segment of matrix in which no ossified or calcified (i.e., fossilized) turbinate-like structures can be seen, and rostral to this is a large plaster-reconstructed area (in association with the oblique transverse fracture mentioned earlier; see Figure 4B, C). Ironically, this large region is the area in which Bakker (1992, p. 61) reconstructed his turbinates.

Our new scanning of CMNH 7541, however, has identified structures within the rostral portion of the snout—in front of the region where Bakker (1992) reconstructed a turbinate and behind the region where Ruben et al. (1996) showed turbinates to be lacking—that may be interpreted as being respiratory turbinates (Figure 14). The structures in question are located in the main nasal airway above the maxillary antra (which themselves are largely reconstructed in plaster). These structures form a series of thin, but moderately dense laminae visible within undistorted matrix that are associated with both the nasal and the maxilla and project into the nasal airway. There are some regions of symmetry, and some elements that can even be tentatively regarded as "scrolls" (Figure 14). The density of these putative turbinates is less than the adjacent nasal and maxilla but more than the surrounding matrix. Whether or not these moderate density values reflect calcification of cartilaginous structures or just very thin bone is difficult to determine. Certainly, they are positioned appropriately to be turbinates with a respiratory function in that they are within the portion of the main nasal airway between the naris and choana.

Mandible

The two mandibles are preserved in full occlusion with the skull, and so, although many details of the mandible can be seen (Figures 1–3), details of the tooth-bearing portions are not easily observed. Thus, obtaining information on the common comparative metric of number of tooth positions had been impossible for CMNH 7541. To remedy this situation, we digitally extracted the right mandible because the dental region is better preserved (Figure 15). CMNH 7541 has at least 16 relatively clear tooth positions, which is similar to BMR P2002.4.1, which has 16 or 17 (P. Larson, 2008). For comparison, Holtz (2004, p. 119) provided a range among tyrannosaurids of 18 in *Alectrosaurus* and 11 in *T. rex*. Hurum and Sabath (2003, p. 187) reported 12–14 dentary tooth positions in *T. rex* and 14–15 in *Tarbosaurus*. Russell (1970) reported 15–16 for *Daspletosaurus*. Thus, CMNH 7541 is fully within the range of Tyrannosauridae, but does not overlap *T. rex*. Significantly, Tsuihiji et al. (2007; in review) reported the exact same range of dentary tooth positions (14–15) in a very young specimen of *Tarbosaurus* as Hurum and Sabath (2003) reported for adult *Tarbosaurus*, suggesting no ontogenetic change in tooth counts in this species that is so closely related to *T. rex*, and thus diminishing the case for CMNH 7541 being a young *T. rex*.

Discussion

The preceding sections have sought to provide anatomical details of the Cleveland tyrannosaur skull (CMNH 7541) that have not been previously widely available (or available at all). CT scanning—and, more significantly, 3D visualization of the CT scan data—has yielded a new look at this famous fossil. For many workers, the systematic question is paramount, but it is obvious that the ontogenetic question is inextricably linked to any

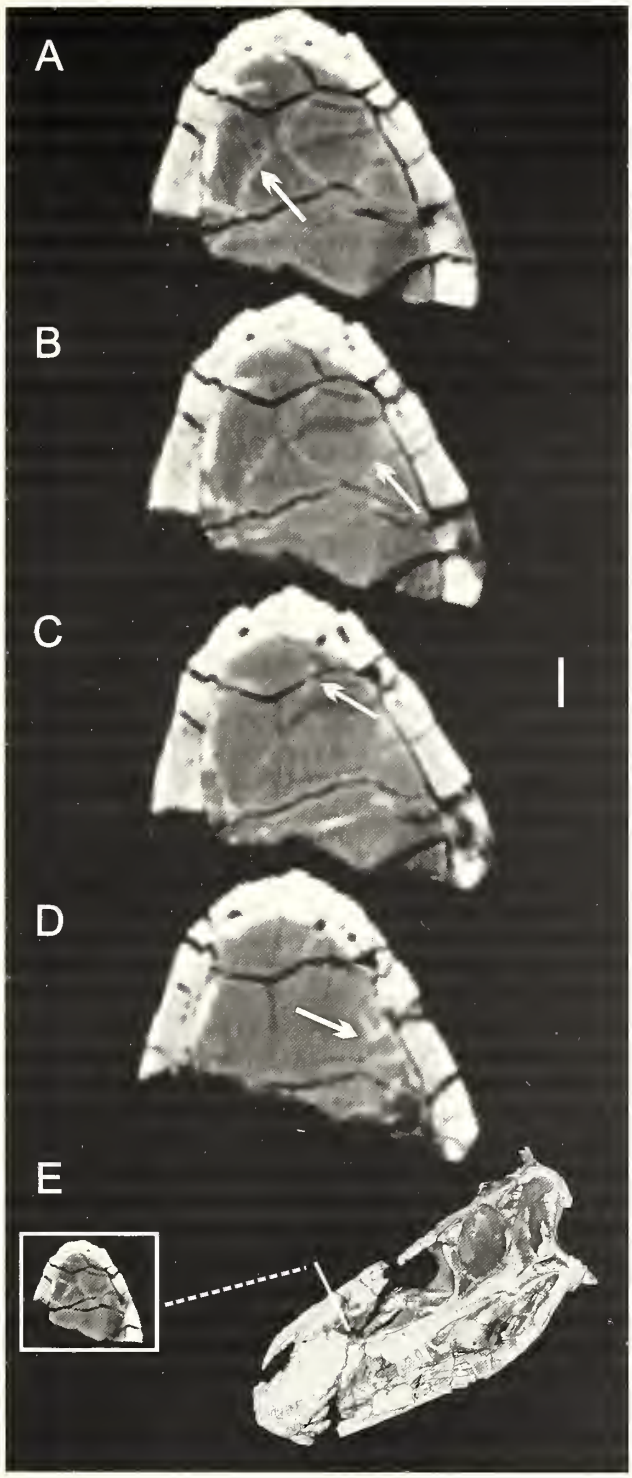

Figure 14. Cleveland tyrannosaur skull, CMNH 7541. A–D, progressively more caudal CT slices through the snout at the position shown in E, showing structures interpretable as respiratory turbinates (arrows). Note that some symmetry is preserved in A and B. In C, a structure (arrow) can be seen to cross a crack. D shows a series of structures associated with the maxilla. Scale bar equals 1 cm.

systematic outcome. That is, are the differences observed in CMNH 7541 attributable to its apparent young age or to it being a different taxon or both? Some of the different ideas were presented in the Introduction, and no firm resolution is offered here, in part because other data pertinent to this debate have yet to be published. Most significant is the discovery of a skull and associated partial postcranium (BMR P2002.4.1) of an animal that is very similar to CMNH 7541 and which will be critical in providing information from the postcranial skeleton that could be relevant to the systematic question. Moreover, there are other, still unpublished skulls of young and juvenile tyrannosaurids (Tsuihiji et al., 2007; in review; N. Larson, 2008; Carr and Williamson, 2010) that can shed light on patterns of ontogenetic transformation and help with discrimination of primitive versus juvenile characters. Other unpublished, clearly adult specimens have raised the prospect of there being species of tyrannosaurids in the Hell Creek other than *T. rex* (N. Larson, 2008; P. Larson, 2008). The question in this case would be, do these specimens display attributes of CMNH 7541 that might indicate that they are adult *Nanotyrannus lancensis*? Until these new specimens are analyzed and published, the status of CMNH 7541 must remain uncertain.

Having said that, the foregoing discussions have revealed an interesting suite of apparently derived attributes observed in CMNH 7541 that might suggest that it represents a taxon separate from *T. rex*. For example, the patterns of pneumatic sinuses and their bony apertures in the braincase are quite distinct from other tyrannosaurids. Although pneumatic sinuses certainly can change ontogenetically (Witmer, 1990, 1997a, b; Witmer and Ridgely, 2008b; and references therein), most of the changes in later ontogeny of most taxa pertain to expansion, contraction, and/or communication of sinuses and not to the basic pattern of bony apertures. For example, *Gorgosaurus* and *Tyrannosaurus* are more similar to each other in their patterns of basicranial pneumatic foramina than either is to the highly asymmetrical apertures of CMNH 7541, and there is no evidence to suggest that either of the two named taxa went through an ontogenetic stage resembling CMNH 7541. Likewise, the broad communication of the caudal tympanic recess and lateral subcondylar recess in CMNH 7541 is unique among tyrannosaurs sampled thus far. To these apparent apomorphies can be added the findings from the brain endocast of CMNH 7541(Witmer and Ridgely, 2009), such as the rostrally offset pituitary fossa and orbital cranial nerve canals, as well as the strongly downturned endocast and skull as a whole, as indicated by the orientation of the lateral semicircular canal of the inner ear.

Although many workers have been struck by the *T. rex*-like temporal expansion of CMNH 7541, this derived character is coupled with a series of primitive attributes, such as the narrow and lanceolate vomer, the uncompressed basisphenoid recess, the pattern of pneumatic apertures in the subcondylar recess, the strength of the condylotuberal crest, the low cultriform process and small subsellar recess, the laterally positioned vagus foramen, and the high number of dentary tooth positions. Although the possibility cannot be ruled out, it seems hard to believe that the animal pertaining to CMNH 7541 would have ontogenetically transformed all of these attributes (both primitive and derived) and grown up to be a typical member of *Tyrannosaurus rex*. CMNH 7541 does not pertain to a hatchling, but rather a fairly mature ("teenage") animal, though perhaps not yet in the exponential stage of growth (in the sense of Erickson et al., 2004), and thus it is hard to envision such major morphological

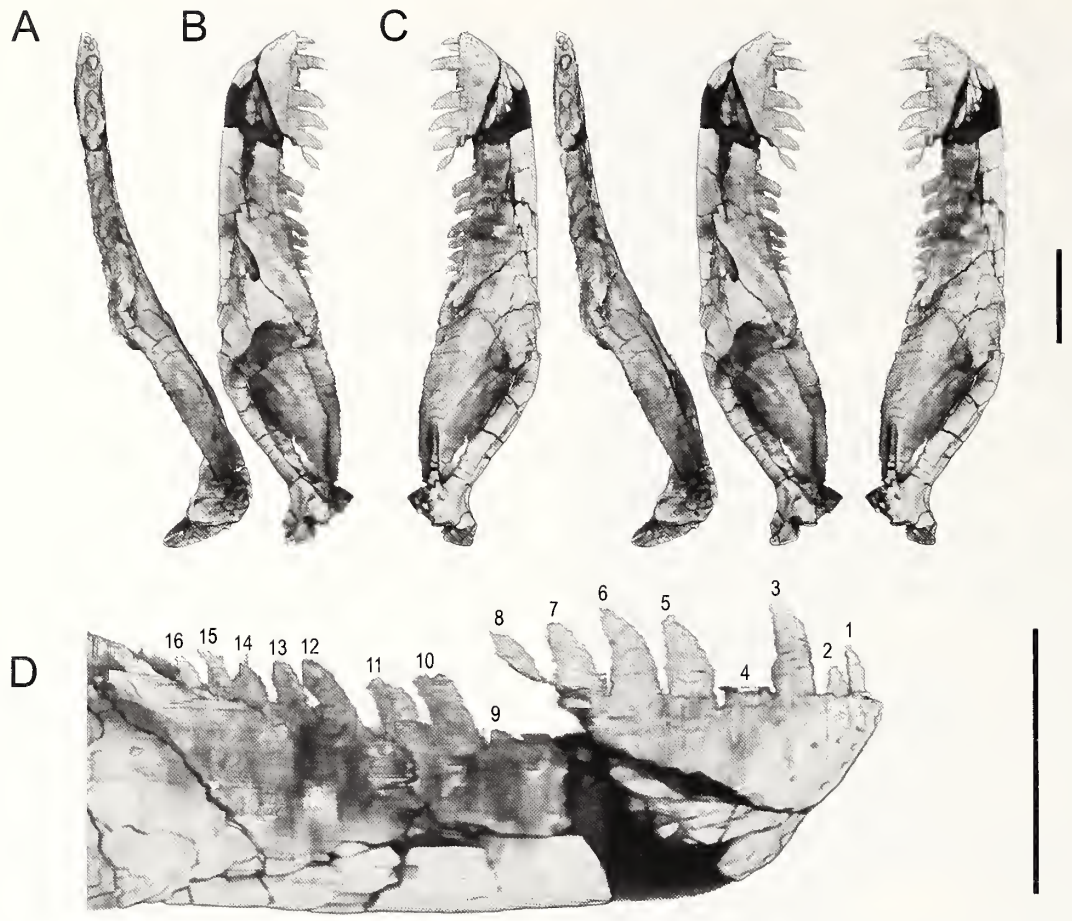

Figure 15. Cleveland tyrannosaur skull, CMNH 7541. Volume renderings of digitally extracted right mandible derived from CT data in A, dorsal; B, medial; C, lateral views. A–C are stereopairs. D, close-up of mandible in lateral view; numbers correspond to tooth positions, of whieh there are 16. Scale bars equal 10 cm.

changes. Certainly, significant morphological changes can take place in animals at nearly adult age, as Sampson (1999, 2001; see also Sampson et al., 1997) showed for ceratopsids in which many of the attributes relating to sexual display develop at essentially adult body sizes (see also Horner and Goodwin, 2006, 2009). Obviously, few if any of the features listed above for CMNH 7541 are of the type that would either be recruited for sexual display or are even remotely related to secondary sexual characteristics. We (Witmer and Ridgely, 2009) previously evaluated in some detail other means of explaining our findings, such as diagenetic distortion or pathology, but neither explanation is compelling. That said, we recognize that some aspects of CMNH 7541 are unusual enough that its being simply aberrant may always remain possible, which is why we have never stated definitively that it is not a juvenile *T. rex*. Ultimately, until the known but unpublished specimens are fully analyzed, we regard the taxonomic status of CMNH 7541 to be an open question, being either a separate taxon (*Nanotyrannus lancensis*) or a juvenile *Tyrannosaurus rex*.

Finally, given the finding here of structures interpretable as respiratory turbinates, it is tempting to make broader claims about metabolic physiology and endothermy. We hesitate to do so, because the skull has only a small area well enough preserved to make such assessments, and we would prefer to be able to sample more widely within the nasal cavity. Nevertheless, taking our data at face value, it is difficult to explain the laminar structures within the nasal airway as anything else. They are not artifacts of the CT scanning process, nor are they sedimentary structures. In fact, such structures are found nowhere else in the entire dataset. Assuming that they are indeed real structures projecting into the nasal airway and covered with moist mucosal respiratory epithelium, it is hard to imagine how they would *not* function as counter-current heat exchangers, precisely as postulated by Ruben and colleagues (1996, 1997). Whether or not these structures are indeed causally associated osteological correlates of endothermy or whether these supposed turbinates are extensive enough to have the effect posited by Ruben et al. (1996) is harder to say, but certainly it now seems unreasonable to argue that such structures are absent in dinosaurs.

Acknowledgments

We give posthumous thanks to Michael Williams for agreeing to the studies conducted here and regret that his passing did not allow him to participate. We thank the Cleveland Museum of Natural History and B. Latimer, M. Ryan, B. Redmond, and G. Jaekson for loan of CMNH 7541 and for allowing it to be CT scanned yet again. We are grateful to H. Rockhold and O'Bleness Memorial Hospital in Athens, Ohio, for providing access to their top-notch scanning serviees which provided us with an excellent

new dataset. We thank the Cleveland Museum for providing aceess to the existing Boeing CT dataset. We thank M. Henderson for sharing unpublished information on the Burpee Museum of Natural History tyrannosaur specimen. We thank T. Tsuihiji and M. Watabe for allowing us to participate in the CT scanning and analysis of the juvenile *Tarbosaurus* skull. For fruitful discussion, we thank J. Bourke, C. Brochu, S. Brusatte, T. Carr, P. Currie, J. Daniel, D. Dufeau, M. Henderson, T. Hieronymus, C. Holliday, J. Horner, T. Holtz, G. Hurlburt, J. Hurum, M. Lamanna, P. Larson, P. Makovicky, P. Manning, A. Martiny, R. Molnar, W. Porter, O. Rauhut, M. Ryan, S. Sampson, P. Sereno, E. Snively, K. Stevens, F. Therrien, T. Tsuihiji, and D. Zelenitsky among many others. We thank M. Ryan and J. Hannibal for comments that greatly improved the manuscript. We thank the Ohio Supercomputer Center for their support. Funding was provided by the National Science Foundation (IBN-0343744 and IOB-0517257) and the Ohio University College of Osteopathic Medicine.

References

Ali, F., D. K. Zelenitsky, F. Therrien, and D. B. Weishampel. 2008. Homology of the "ethmoid complex" of tyrannosaurids and its implications for the reconstruction of the olfactory apparatus of non-avian theropods. Journal of Vertebrate Paleontology, 28:123–133.

Bakker, R. T. 1992. Inside the head of a tiny *T. rex*. Discover, 13:58–69.

Bakker, R. T., M. Williams, and P. J. Currie. 1988. *Nanotyrannus*, a new genus of pygmy tyrannosaur, from the latest Cretaceous of Montana. Hunteria, 1:1–30.

Brochu, C. A. 2000. A digitally rendered endocast for *Tyrannosaurus rex*. Journal of Vertebrate Paleontology, 20:1–6.

Brochu, C. A. 2003. Osteology of *Tyrannosaurus rex*: insights from a nearly complete skeleton and high-resolution computed tomographic analysis of the skull. Society of Vertebrate Paleontology Memoir, 7:1–140.

Brusatte, S. L., T. D. Carr, G. M. Erickson, G. S. Bever, and M. A. Norell. 2009. A long-snouted, multihorned tyrannosaurid from the Late Cretaceous of Mongolia. Proceedings of the National Academy of Sciences, 106:17261–17266.

Carpenter, K. 1992. Tyrannosaurids (Dinosauria) of Asia and North America, p. 250–268. *In* N. J. Mateer and C. Pei-Ji (eds.), Aspects of Nonmarine Cretaceous Geology. China Ocean Press, Beijing.

Carr, T. D. 1999. Craniofacial ontogeny in tyrannosaurid dinosaurs (Dinosauria, Coelurosauria). Journal of Vertebrate Paleontology, 19:497–520.

Carr, T. D., and T. E. Williamson. 2004. Diversity of late Maastrichtian Tyrannosauridae (Dinosauria, Theropoda) from western North America. Zoological Journal of the Linnean Society, 142:479–523.

Carr, T. D., and T. E. Williamson. 2010. *Bistahieversor sealeyi*, gen. et sp. nov., a new tyrannosauroid from New Mexico and the origin of deep snouts in Tyrannosauroidea. Journal of Vertebrate Paleontology, 30:1–16.

Carr, T. D., T. E. Williamson, and D. R. Schwimmer. 2005. A new genus and species of tyrannosauroid from the Late Cretaceous (Middle Campanian) Demopolis Formation of Alabama. Journal of Vertebrate Paleontology, 25:119–143.

Chure, D. J., and J. H. Madsen. 1996. Variation in aspects of the tympanic pneumatic system in a population of *Allosaurus fragilis* from the Morrison Formation (Upper Jurassic). Journal of Vertebrate Paleontology, 16:63–66.

Currie, P. J. 2003a. Allometric growth in tyrannosaurids (Dinosauria: Theropoda) from the Upper Cretaceous of North America and Asia. Canadian Journal of Earth Sciences, 40:661–665.

Currie, P. J. 2003b. Cranial anatomy of tyrannosaurid dinosaurs from the Late Cretaceous of Alberta, Canada. Acta Palaeontologica Polonica, 48:191–226.

Currie, P. J., J. H. Hurum, and K. Sabath. 2003. Skull structure and evolution in tyrannosaurid dinosaurs. Acta Palaeontologica Polonica, 48:227–234.

Erickson, G. M., P. J. Makovicky, P. J. Currie, M. A. Norell, S. A. Yerby, and C. A. Brochu. 2004. Gigantism and comparative life-history parameters of tyrannosaurid dinosaurs. Nature, 430:772–775.

Gilmore, C. W. 1946. A new carnivorous dinosaur from the Lance formation of Montana. Smithsonian Miscellaneous Collections, 106:1–19.

Henderson, M. D., and W. H. Harrison. 2008. Taphonomy and environment of deposition of a juvenile tyrannosaurid skeleton from the Hell Creek Formation (latest Maastrichtian) of southeastern Montana, p. 82–90. *In* P. L. Larson and K. Carpenter (eds.), *Tyrannosaurus rex*, the Tyrant King. Indiana University Press, Bloomington.

Holliday, C. M., and L. M. Witmer. 2008. Cranial kinesis in dinosaurs: intracranial joints, protractor muscles, and their significance for cranial evolution and function in diapsids. Journal of Vertebrate Paleontology, 28:1073–1088.

Holtz, T. R. 2001. The phylogeny and taxonomy of the Tyrannosauridae, p. 64–83. *In* D. H. Tanke and K. Carpenter (eds.), Mesozoic Vertebrate Life. Indiana University Press, Bloomington.

Holtz, T. R. 2004. Tyrannosauroidea, p. 111–136. *In* D. B. Weishampel, P. Dodson, and H. Osmólska (eds.), The Dinosauria. University of California Press, Berkeley.

Horner, J. R., and D. Lessem. 1993. The complete *T. rex*. Simon and Schuster, New York. 239 p.

Horner, J. R., and M. B. Goodwin. 2006. Major cranial changes during *Triceratops* ontogeny. Proceedings of the Royal Society B, 273:2757–2761.

Horner, J. R., and M. B. Goodwin. 2009. Extreme cranial ontogeny in the Upper Cretaceous dinosaur *Pachycephalosaurus*. PLoS ONE, 4(10), e7626. doi:10.1371/journal.pone.0007626.

Hurum, J. H., and K. Sabath. 2003. Giant theropod dinosaurs from Asia and North America: skulls of *Tarbosaurus bataar* and *Tyrannosaurus rex* compared. Acta Palaeontologica Polonica, 48:161–190.

Larson, N. L. 2008. One hundred years of *Tyrannosaurus rex*: the skeletons, p. 1–61. *In* P. L. Larson and K. Carpenter (eds.), *Tyrannosaurus rex*, the Tyrant King. Indiana University Press, Bloomington.

Larson, P. L. 2008. Variation and sexual dimorphism in *Tyrannosaurus rex*, p. 102–128. *In* P. L. Larson and K. Carpenter (eds.), *Tyrannosaurus rex*, the Tyrant King. Indiana University Press, Bloomington.

Li, D., M. A. Norell, K.-Q. Gao, N. D. Smith, and P. J. Makovicky. 2010. A longirostrine tyrannosauroid from the Early Cretaceous of China. Proceedings of the Royal Society B, 277:183–190.

Osborn, H. F. 1912. Crania of *Tyrannosaurus* and *Allosaurus*. Memoirs of the American Museum of Natural History, 1:1–30.

Paul, G. P. 2008. The extreme lifestyles and habits of the gigantic tyrannosaurid superpredators of the Late Cretaceous of North America and Asia, p. 306–352. *In* P. L. Larson and K. Carpenter (eds.), *Tyrannosaurus rex*, the Tyrant King. Indiana University Press, Bloomington.

Rozhdestvensky, A. K. 1965. Growth changes in Asian dinosaurs and some problems of their taxonomy [in Russian]. Paleontological Journal, 3:95–109.

Ruben, J. 1995. The evolution of endothermy in mammals and birds: from physiology to fossils. Annual Review of Physiology, 57:69–95.

Ruben, J. 1996. Evolution of endothermy in mammals, birds, and their ancestors, p. 347–376. *In* I. A. Johnston and A. F. Bennett (eds.), Animals and Temperature. Cambridge University Press, Cambridge.

Ruben, J. A., W. J. Hillenius, N. R. Geist, A. Leitch, T. D. Jones, P. J. Currie, J. R. Horner, and G. Espe III. 1996. The metabolic status of some Late Cretaceous dinosaurs. Science, 273:1204–1207.

Ruben, J. A., W. J. Hillenius, A. Leitch, N. R. Geist, and T. D. Jones. 1997. New insights into the metabolic physiology of dinosaurs, p. 505–518. *In* J. O. Farlow and M. K. Brett-Surman (eds.), The Complete Dinosaur. Purdue University Press, Ashland.

Russell, D. A. 1970. Tyrannosaurs from the Late Cretaceous of western Canada. National Museums of Canada Publications in Paleontology, 1:1–34.

Sampson, S. D. 1999. Sex and destiny: the role of mating signals in speciation and macroevolution. Historical Biology, 13:173–197.

Sampson, S. D. 2001. Speculations on the socioecology of ceratopsid dinosaurs (Ornithischia: Neoceratopsia), p. 263–276. *In* D. Tanke and K. Carpenter (eds.), Mesozoic Vertebrate Life. Indiana University Press, Bloomington.

Sampson, S. D., and L. M. Witmer. 2007. Craniofacial anatomy of *Majungasaurus crenatissimus* (Theropoda: Abelisauridae) from the Late Cretaceous of Madagascar. Society of Vertebrate Paleontology Memoir, 8:32–102.

Sampson, S. D., M. J. Ryan, and D. H. Tanke. 1997. Craniofacial ontogeny in centrosaurine dinosaurs (Ornithischia: Ceratopsidae): taxonomic and behavioral implications. Zoological Journal of the Linnean Society, 221:293–337.

Sereno, P. C., J. A. Wilson, L. M. Witmer, J. A. Whitlock, A. Maga, O. Ide, and T. Rowe. 2007. Structural extremes in a Cretaceous dinosaur. PLoS ONE, 2(11), e1230. doi:10.1371/journal.pone.0001230.

Tsuihiji, T., M. Watabe, L. M. Witmer, T. Tsubamoto, and K. Tsogtbaatar. 2007. A juvenile skeleton of *Tarbosaurus* with a nearly complete skull and its implications for ontogenetic change in tyrannosaurids. Journal of Vertebrate Paleontology, 27(Supplement to 3), 160A.

Tsuihiji, T., M. Watabe, K. Tsogtbaatar, T. Tsubamoto, R. Barsbold, S. Suzuki, A. H. Lee, R. C. Ridgely, Y. Kawahara, and L. M. Witmer. In review. Cranial osteology of a juvenile specimen of *Tarbosaurus bataar* from the Nemegt Formation (Upper Cretaceous) of Bugin Tsav, Mongolia. Journal of Vertebrate Paleontology.

Witmer, L. M. 1990. The craniofacial air sac system of Mesozoic birds (Aves). Zoological Journal of the Linnean Society, 100:327–378.

Witmer, L. M. 1997a. The evolution of the antorbital cavity of archosaurs: a study in soft-tissue reconstruction in the fossil record with an analysis of the function of pneumaticity. Society of Vertebrate Paleontology Memoir, 3:1–73.

Witmer, L. M. 1997b. Craniofacial air sinus systems, p. 151–159. *In* P. J. Currie and K. Padian (eds.), Encyclopedia of Dinosaurs. Academic Press, New York.

Witmer, L. M., and R. C. Ridgely. 2008a. Structure of the brain cavity and inner ear of the centrosaurine ceratopsid *Pachyrhinosaurus* based on CT scanning and 3D visualization, p. 117–144. *In* P. J. Currie, W. Langston, Jr., and D. H. Tanke (eds.), A New Horned Dinosaur from an Upper Cretaceous Bone Bed in Alberta. National Research Council of Canada Monograph Series, Ottawa.

Witmer, L. M., and R. C. Ridgely. 2008b. The paranasal air sinuses of predatory and armored dinosaurs (Archosauria: Theropoda and Ankylosauria) and their contribution to cephalic architecture. Anatomical Record, 291:1362–1388.

Witmer, L. M., and R. C. Ridgely. 2009. New insights into the brain, braincase, and ear region of tyrannosaurs, with implications for sensory organization and behavior. Anatomical Record, 292:1266–1296.

Witmer, L. M., S. Chatterjee, J. W. Franzosa, and T. Rowe. 2003. Neuroanatomy of flying reptiles and implications for flight, posture, and behavior. Nature, 425:950–953.

Witmer, L. M., R. C. Ridgely, D. L. Dufeau, and M. C. Semones. 2008. Using CT to peer into the past: 3D visualization of the brain and ear regions of birds, crocodiles, and nonavian dinosaurs, p. 67–87. *In* H. Endo and R. Frey (eds.), Anatomical Imaging: Towards a New Morphology. Springer-Verlag, Tokyo.

Zelenitsky, D. K., F. Therrien, and Y. Kobayashi. 2009. Olfactory acuity in theropods: palaeobiological and evolutionary implications. Proceedings of the Royal Society B, 276:667–673.

Appendix. Key to abbreviations.

II	foramen for optic nerve (cranial nerve II)
III	foramen for oculomotor nerve (cranial nerve III)
V_1	foramen for ophthalmic nerve (cranial nerve V_1)
V_{2-3}/VII	common external opening in braincase for maxillomandibular and facial nerve canals
VI	foramen for abducens nerve (cranial nerve VI)
X	foramen for vagus nerve (cranial nerve X)
ad	ascending diverticulum of rostral tympanic recess
bpt	basipterygoid process of basisphenoid
bptr	basipterygoid process pneumatic recess
bsrc	basisphenoid recess, caudal
bsrr	basisphenoid recess, rostral
bt	basal tuber
cap	capitate process of laterosphenoid
cc	columellar recess
col	columella auris (= stapes)
cp	cultriform process (= parasphenoid rostum)
ctc	rista tuberalis of otoccipital
ctc	crista condylotuberalis of basioccipital, running between occipital condylar neck and basal tuber
ctr	caudal tympanic recess
ctra	caudal tympanic recess, aperture
cvcm	caudal middle cerebral vein foramen
cvl	crista ventrolateralis of basisphenoid, running between basal tuber and basipterygoid process
dtfo	dorsotemporal fossa
end	brain endocast
f	frontal bone
fm	foramen magnum
ibtl	interbasipterygoidal lamina of basisphenoid, running between basipterygoid processes
itl	intertuberal lamina of basisphenoid/basioccipital, running between basal tubera
lab	endosseous labyrinth
lscr	lateral subcondylar recess
mn con	mandibular condyle of quadrate
mx art	maxillary articular surface of palatine
mscr	medial subcondylar recess
obc	olfactory bulb cavity
oc	occipital condyle of basioccipital
olf	olfactory chamber of frontal
osc	otosphenoidal crest
ot	olfactory turbinates within olfactory chamber
paroc	paroccipital process of otoccipital (fused exoccipital + opisthotic)
pfo	pituitary (hypophyseal) fossa
pn for	pneumatic foramen
prp	preotic pendant
pter ram	pterygoid ramus of quadrate or vomer
rhs	retrohypophyseal pneumatic sinus
rtr	rostral tympanic recess
sc	sagittal crest
socs	sinus in supraoccipital from caudal tympanic recess
spheth	sphenethmoid ossification
sq con	squamosal condyle of quadrate
ss	sulcus septalis on cultriform process (for cartilaginous septum)
ssr	subsellar recess
tnc	transverse nuchal crest on parietal
vpt pr	vomeroterygoid process of palatine

KIRTLANDIA
The Cleveland Museum of Natural History

November 2010 *Number 57:82–86*

EVIDENCE FOR DECLINE IN THE UNIONIDAE OF THE EAST BRANCH ROCKY RIVER, OHIO

DANIEL A. GOUCH, MARK S. LYONS, AND ROBERT A. KREBS
Department of Biological, Geological, and Environmental Sciences
Cleveland State University, Cleveland, Ohio 44115-2406
r.krebs@csuohio.edu

ABSTRACT

A survey of freshwater mussels (Mollusca: Bivalvia: Unionidae) was conducted for the East Branch Rocky River, Ohio, during the summer of 2006. Development in this watershed is moderate though rapidly expanding, particularly in the upstream reaches. Perhaps as a consequence, a preliminary search failed to reveal any live mussels in the river in 2003. The present report is of an extensive survey covering 21 two-hour timed searches for live mussels and shells combined with visual assessments of disturbance and tests for water quality at each site. All searches were visual or by feeling for mussels embedded in the stream bottom where visibility was poor. These surveys produced only 34 live animals and 287 empty shells, which included live specimens of *Lampsilis radiata luteola*, *Lasmigona costata*, *Lasmigona compressa*, and *Strophitus undulatus* as well as fresh shells of *Pyganodon grandis*. The few sites that contained live animals and fresh shells were isolated, while worn shells were distributed more evenly throughout the river, suggesting a wider distribution of mussels in the past. Present water quality appeared good, and, therefore, the relatively low density and spatial isolation of unionids may reflect local geomorphologic factors combined with historic and current land usage.

Introduction

Headwater streams often determine water quality downstream, yet these smaller tributaries tend to be neglected in surveys of mussels (Mollusca: Bivalvia: Unionidae) due to their predicted lower species diversity and absence of rare species. However, as development continues to expand outward from many Great Lakes coastal cities, the less disturbed headwater regions are coming under greater pressure from anthropogenic changes, including channeling and increased proportions of impervious surfaces in the watershed, that greatly alter the flow dynamics (Dunne and Leopold, 1978, p. 693–704). Streams with high levels of impervious surface-cover exhibit marked degradation in both biological (Yoder et al., 1999) and hydrological (Booth and Jackson, 1997) health and integrity. The East Branch Rocky River is one such small stream and contains some of the most rapidly expanding urban areas in all of northeastern Ohio (Clapham, 2003). It is the smaller of two main branches of the Rocky River, which drains 752 km^2 west and southwest of Cleveland, Ohio. The East Branch Rocky River drains 213 km^2 of the Rocky River's upper reaches.

Freshwater mussels play an important role in lotic ecosystems (Vaughn et al., 2004). As benthic, burrowing filter-feeders, unionids remove great quantities of suspended particulate organic matter from the water column. Mussels also directly influence benthic communities as they burrow through sediment, depositing feces and pseudo-feces (Vaughn et al., 2001), while enhancing the rate of nitrate release from the substrate (Matisoff et al., 1985). This trophic role makes mussels highly sensitive to pollutants and habitat destruction. As a consequence, unionid mussels are perhaps the most threatened family of organisms worldwide, with perhaps 70% of species extinct, endangered, or threatened (Bogan, 1993; Williams et al., 1993). With their depletion the characteristics of many small streams have surely changed.

Because high mussel abundance is a characteristic of clear, undisturbed streams, such as Ohio's Grand River (Huehner et al., 2005), stream quality can be assessed not only by the presence of unionid mussels, but by the proportion of pollution sensitive versus more tolerant species that compose the mussel community (Metcalfe-Smith et al., 2003; Staton et al., 2003; McRae et al., 2004). A marked reduction in unionid diversity is an early indication that water quality has been degraded, and as such, they make excellent biological indicators of long- and short-term stream health, especially where historical data on mussel populations are available. Here we provide a detailed survey of unionids in the East Branch Rocky River and compare the distribution and abundance of mussels to standard chemical assessments of water quality in the stream, to a site-speeific analysis of anthropogenic alteration (Lyons et al., 2007), and to past and present diversity throughout the Rocky River (Krebs and Rundo, 2005).

Materials and Methods

To survey the East Branch Rocky River for the Unionidae, 21 sites were chosen based on access and spatial distribution

throughout the watershed in order to cover as much of the river as extensively as possible. A semi-quantitative approach of timed searches was applied due to its cost-effectiveness when a stream is largely wadable (Strayer et al., 1996). All surveys were conducted visually where possible, and by feel in areas with low visibility. Effort was standardized at two hours per site, which also made results comparable to those completed in the Rocky River main stem and West Branch Rocky River (Krebs and Rundo, 2005).

Appropriate habitats within the stream as well as the immediate adjacent floodplain were searched for both live animals and dead (shell) specimens. Live unionids were identified using Watters (1995) and immediately returned to the stream substrate. No effort was made to "bury" or otherwise conceal the returned mussels. Large fragments, individual valves, and whole, recently dead, shell specimens were collected for identification and storage by site as voucher specimens at Cleveland State University.

To examine site-specific anthropogenic effects, we applied a simple urbanization rating scale from Lyons et al. (2007). At each site, seven visible factors typically associated with a human presence were recorded and assessed on a rating scale from 0 to 3, where a score of zero indicated little to no human effects and a score of three denoted extreme modification of the river: (1) the presence of buildings; (2) presence of roads visible through the riparian zone; (3) breadth and condition of the riparian zone; (4) condition of the stream bank; (5) presence of dams or spillways; (6) occurrence of erosion; and (7) the quantity of human litter in the river. This measure of urbanization, which ranges from 0–21, is largely qualitative across sites, but it is easily applied to describe relative site-specific changes along the length of a river. Site-specific characteristics appear to be more important for predicting the presence of mussels than are many regional scale analyses (Poole and Downing, 2004).

Water chemistry measurements were taken throughout the watershed on multiple dates that spanned low, moderate, and high flow regimes throughout the summer of 2006. These results were then averaged over the collection dates for comparison to the mussel survey results. At each site, measurements of water temperature, dissolved oxygen (DO) and oxygen saturation (O_2%), specific conductivity, pH, salinity, and oxidation-reduction potential (redox) were made using an Orion 250A pH/conductivity meter for pH and redox, a YSI Inc. model DO200 meter to estimate DO, O_2%, and temperature, and a YSI Inc. model 85 meter for specific conductivity and salinity. All measurements were taken via external probes suspended as near to the substrate as possible, taking care not to disturb the surrounding benthic sediment particularly upstream of the testing location. Each meter was calibrated according to manufacturer's instructions on each day that tests were performed. Before and after each measurement, the probes were thoroughly rinsed with de-ionized water.

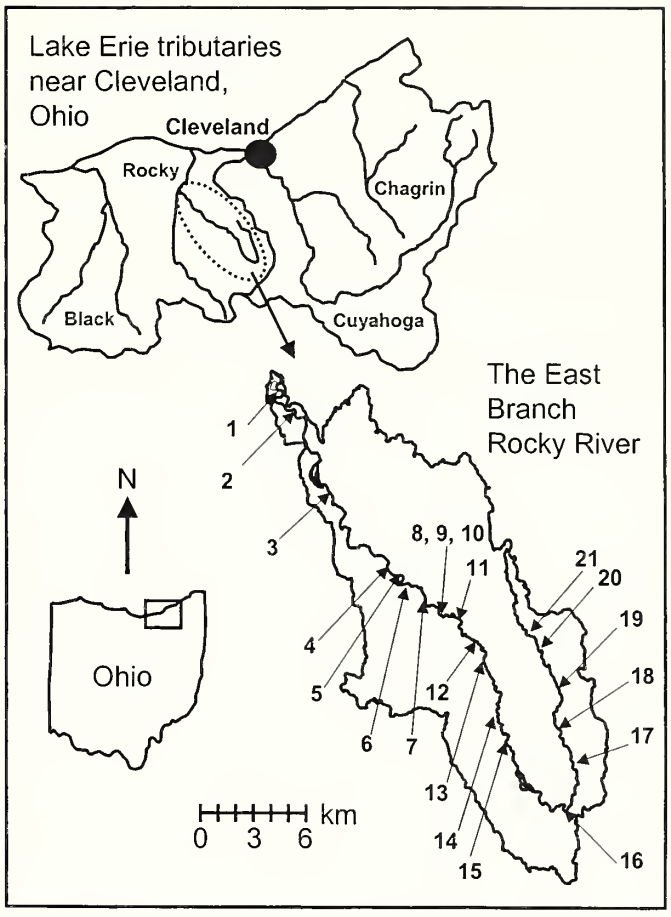

Figure 1. Map showing the larger streams around Cleveland, Ohio, and the location of the East Branch Rocky River watershed. Numerals indicate sampling sites for mussels.

Results

Surveys

The extensive surveys that spanned 21 sites yielded just 34 live individuals, although 287 shell specimens were collected. Four taxa were found alive in the stream: 26 *Lampsilis radiata luteola* (Lamarck, 1819), four *Lasmigona compressa* (Lea, 1829), three *Strophitus undulatus* (Say, 1817), and one *Lasmigona costata* (Rafinesque, 1820). A fifth species, *Pyganodon grandis* (Say, 1828), was represented only as shells in the river. As this species prefers lentic environments (Watters, 1995, p. 31), the 53 shells, many in fresh condition, may derive from impounded small tributary streams, as observed when a pond downstream of site 19 was purposely drained to reclaim land at a girl scout camp, Camp Jane Crowell. The pond was found to have been densely and apparently exclusively populated with *P. grandis*.

Suitable habitat for unionid mussels appeared limited in the East Branch Rocky River. Live individuals were found only at 5 sites: 8, 9, 10, 13, and 20 (Figure 1). Of these, sites 8–10 contained the most mussels (n = 26, with 21 in site 9 alone), and these sites composed a small continuous stretch of the stream such that the site-8 survey ended at the site-9 start point, and so on. Of the other eight individuals, five occurred at site 13 located within and below a public golf course in a stretch of the stream with major bank modification. Three live *S. undulatus* were found at site 20, a headwater region that was only recently developed.

Not only were live individuals very restricted in distribution, fresh shells were similarly found only where mussels occurred alive, with the exception of *P. grandis* already mentioned. Worn shells, however, were scattered along the river, but were not found at sites 19 and 21, the latter of which may be an ephemeral component of the headwaters. The frequency of shells basically followed that for live mussels in the stream, with 186 *Lampsilis radiata luteola*, 38 *Strophitus undulatus*, nine *Lasmigona compressa*, and a single fresh *Lasmigona costata* at the same site where one live individual was found. Weathered shells found per site more or less increased the further downstream we surveyed until

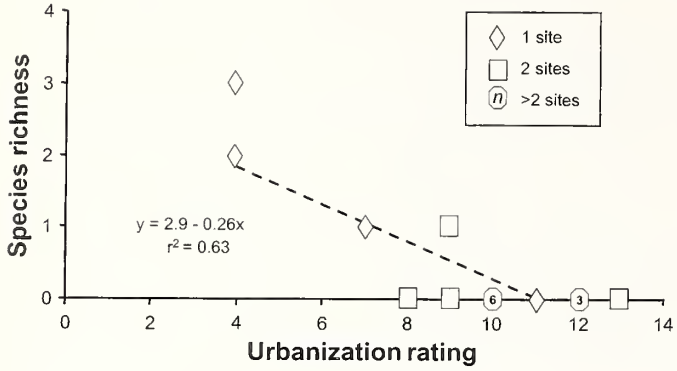

Figure 2. Simple linear regression for urbanization score versus species richness as indicated by the actual number of species observed living at a particular site. Species richness at each site was assumed to be an independent unit. Diamonds demarcate a single datum, squares are two overlapping data points, and octagons indicate overlapping data of three or six sites as labeled.

just below site 8, where the East Branch Rocky River becomes heavily urbanized, and shell numbers of any condition dropped off. The paucity of shells at site 7, when many were found in sites 8–10, suggests they are not washed far downstream, and therefore the number of mussels and their range has almost certainly declined.

Water quality and urbanization

Mean temperatures were generally moderate and stable for the length of the stream, which is characterized as a warm water habitat: the low temperature site (site 17) averaged 21.2 (SD ± 2.3) °C and the warmest (sites 1 and 2) were 24.1 (SD ± 3.1) °C, with a trend towards increasing temperatures as we sampled downstream. Salinity readings were virtually identical across sample locations (0.2–0.3 ppm), while relative conductivity ranged from a minimum of 349.5 µS/L at site 21 to a maximum of 567.5 µS/L at site 4. Oxygen redox potential ranged from −35.3 (site 13) to −78.3 (site 1), and measurements of the closely related pH ranged from 7.60 (site 13) to 8.23 (site 1). Oxygen levels were also generally good throughout, with a low of 5.9 ppm (67.2% saturation) at site 5 and a high of 8.3 ppm (93.6% saturation) at site 17.

While the condition of the water appeared good, visual assessments of each site suggested extensive urban impacts. The mean urbanization value was 9.5 using a site specific scale. Only at two sites were scores less than five, and overall, this simple metric explained over 60% of the variation in species diversity within the East Branch Rocky River (Figure 2).

Discussion

The extremely small population of unionids remaining in the East Branch Rocky River cannot be attributed to just the drainage area of this watershed. With extensive surveys covering 21 sites, only 34 live animals and 287 mostly worn shell specimens were recovered. These numbers are low when compared with similar efforts applied in the West Branch Rocky River (182 alive and nearly 600 shells of 11 different species), and even in the lower Rocky River, which has faced urbanization impacts longer than the East Branch, unionids within a short stretch of stream are more abundant (Krebs and Rundo, 2005). With the exception of *L. compressa*, the species present in the watershed all are common in the region, but because *Lasmigona* spp. may require clean habitat, their abundance may be dwindling regionally (Tevesz et al., 2002; Lyons et al., 2007). Oddly, one *L. costata* found constituted a new stream record, but of a remnant population.

Clearly, the fauna of the East Branch Rocky River is experiencing an unfortunate, but common, outcome of urban sprawl. With habitat declining, the extant unionid community is completely isolated and compressed to short stretches of the river. Any event that contributes to local extirpation will not be balanced by colonization, and changes to the fauna become unidirectional towards loss. Few previous collections were ever made for the East Branch Rocky River, limiting what can be said of change, although the Ohio State University Museum of Biological Diversity on-line data base (Watters and Cramer, 2008) lists three additional species from the East Branch Rocky River not found in the present survey: *Anodontoides ferussacianus* (Lea, 1834), *Toxolasma parvum* (Barnes, 1823), and *Utterbackia imbecillis* (Say, 1829). A shell of *U. imbecillis* was also found by Krebs and Rundo (2005), and *U. imbecillis* and *T. parvum* may persist within impounded tributaries (Smith et al., 2002). However, *A. ferussacianus*, which is regionally common in clean headwater streams, is probably extirpated from the East Branch Rocky River.

Even the much more diverse West Branch Rocky River has lost diversity within the last century. Specimens of *Alasmidonta marginata* (Say, 1818), *Amblema plicata* (Say, 1817), and *Pleurobema sintoxia* (Rafinesque, 1820), which are described as requiring clean-water (Watters, 1995; Metcalfe-Smith et al., 2000, 2003), are listed in the Cleveland Museum of Natural History holdings for the Rocky River (Heiser et al., 2002; an updated list of holdings is available from R. A. Krebs or from Tom Pucci, Cleveland Museum of Natural History).

The East Branch Rocky River changes both in chemistry and in velocity along its length, leading to conditions that destabilize the substrate and that create a chemical environment outside of that optimal for mussels. The headwaters are located in glaciated Appalachian highlands where they feed a stream flowing south, eventually to a drift filled pre-glacial valley (Hubbard and Champion, 1925). There, the stream makes a U-turn to the north, entering the lake and till plains of Lake Erie, and it generally follows the ancient river valley northwestward where it widens considerably in places as it cuts through glacial-valley and alluvial sediment, and in other places is bounded by steep shale and sandstone walls (Cushing and others, 1931, Plate 20; Ohio Environmental Protection Ageney, 1993). Throughout this region, the East Branch Rocky River is considered a high-gradient stream, averaging 3.1 m of elevation loss per kilometer in length (Ohio Environmental Protection Agency, 1999). The geological setting explains the noticeable increase in pH and associated rise in redox potential, as shales tend to exhibit a high cation exchange and buffering capacity. In places the river flows over bedrock rather than buried-valley and alluvial sediment. Changes in gradient related to substrate composition can increase current velocity, creating conditions for higher shear stress, which reduce mussel abundance (Gangloff and Feminella, 2007).

Throughout the East Branch Rocky River, water quality appears not to be a prohibitive factor limiting unionid mussels (Ohio Environmental Protection Agency, 1993, 1999). Several wastewater treatment plants, which are potential sources of episodic water quality impairment, have been removed or upgraded, and only three plants continue to discharge treated

effluent into the East Branch Rocky River or its tributaries (Ohio Environmental Protection Agency, 1999). However, as expected in an urban stream, there is a general trend towards human impacts downstream (Paul and Meyer, 2001), as indicated by site specific analyses. Mussels were present whenever impact scores were < 5, but no live mussels occurred when scores were > 10; higher scores tended to occur downstream. This trend corresponded with results for Ohio's Black River, just west of the Rocky River (Lyons et al., 2007).

Therefore, given a long stretch of sediment-poor bedrock in the lower stretches of the East Branch Rocky River, and several high dams creating man-made impoundments, the few areas of higher quality habitat will remain separated from other reaches of the watershed where mussels are abundant.

Acknowledgments

Our research was supported by a Research Experiences for Undergraduates (DBI 0243878) award from NSF to M. Walton at Cleveland State University (CSU), and by an Established Full-time Faculty Research Development award to R.A.K. by CSU. We thank D. Petit for permission to work in the Cleveland Metroparks, T. Watters for access to the Ohio State University Museum of Biological Diversity collections, J. Keiper for access to the collections of the Cleveland Museum of Natural History, and K. Bradley for alerting us to the drained pond at Camp Jane Crowell. Unionid shells were collected under Wild Animal permit no. 194 for 2006 from the Ohio Department of Natural Resources.

References

Bogan, A. E. 1993. Freshwater bivalve extinctions (Mollusca: Unionidae): a search for causes. American Zoologist, 33:599–609.

Booth, D. B., and C. R. Jackson. 1997. Urbanization of aquatic systems: degradation thresholds, stormwater detection, and the limits of mitigation. Journal of American Water Resource Associations, 33:1077–1090.

Clapham, W. B., Jr. 2003. Continuum-based classification of remotely sensed imagery to describe urban sprawl on a watershed scale. Remote Sensing of the Environment, 86:322–340.

Cushing, H. P., Frank Leverett, and F. R. Van Horn. 1931. Geology and mineral resources of the Cleveland District, Ohio: U.S. Geological Survey Bulletin 818, 138 p.

Dunne, T., and L. B. Leopold. 1978. Water in Environmental Planning. Freeman, New York. 818 p.

Gangloff, M. M., and J. W. Feminella. 2007. Stream channel geomorphology influences mussel abundance in southern Appalachian streams, USA. Freshwater Biology, 52:64–74.

Heiser, J. D., R. Bowers, and J. B. Keiper. 2002. List of freshwater mussels (Unionoida) at the Cleveland Museum of Natural History. Kirtlandia, 53:27–34.

Hubbard, G. D., and M. M. Champion. 1925. History of five river valleys. Ohio Journal of Science, 25:74–84.

Huehner, M. K., R. A. Krebs, G. Zimmerman, and M. Mejia. 2005. The unionid mussel fauna of northeastern Ohio's Grand River. Ohio Journal of Science, 105:57–62.

Krebs, R. A., and L. J. Rundo. 2005. Diversity of the Unionidae in the Rocky River, Ohio. Journal of Freshwater Ecology, 20:603–608.

Lyons, M. S., R. A. Krebs, J. P. Holt, L. J. Rundo, and W. Zawiski. 2007. Assessing causes of change in the freshwater mussels (Bivalvia: Unionidae) in the Black River, Ohio. American Midland Naturalist, 158:1–15.

Matisoff, G., J. B. Fisher, and S. Matis. 1985. Effect of microinvertebrates on the exchange of solutes between sediments and freshwater. Hydrobiologia, 122:19–33.

McRae, S. E., J. D. Allan, and J. B. Burch. 2004. Reach- and catchment-scale determinants of the distribution of freshwater mussels (Bivalvia:Unionidae) in south-eastern Michigan, USA. Freshwater Biology, 49:127–142.

Metcalfe-Smith, J. L., J. Di Maio, S. K. Staton, and S. De Solla. 2003. Status of the freshwater mussel communities of the Sydenham River, Ontario, Canada. American Midland Naturalist, 150:37–50.

Metcalfe-Smith, J. L., G. L. Mackie, J. Di Maio, and S. K. Staton. 2000. Changes over time in the diversity and distribution of freshwater mussels (Unionidae) in the Grand River, Southwestern Ontario. Journal of Great Lakes Research, 26:445–459.

Ohio Environmental Protection Agency. 1993. 1993 Biological and Water Quality Study of the Rocky River and Selected Tributaries: Summit, Lorain, Medina and Cuyahoga Counties, Ohio. OEPA Technical Report MAS/1993-8-3, 115 p.

Ohio Environmental Protection Agency. 1999. 1997 Biological and Water Quality Study of the Rocky River and Selected Tributaries: Summit, Lorain, Medina and Cuyahoga Counties, Ohio. OEPA Technical Report MAS/1998-12-3, 89 p.

Paul, M. J., and J. L. Meyer. 2001. Streams in the urban landscape. Annual Review of Ecology and Systematics, 32:333–365.

Poole, K. E., and J. A. Downing. 2004. Relationship of declining mussel biodiversity to stream-reach and watershed characteristics in an agricultural landscape. Journal of the North American Benthological Society, 23:114–125.

Smith, D. C., M. A. Gates, R. A. Krebs, and M. J. S. Tevesz. 2002. A survey of freshwater mussels (Unionidae) and other mollusks in the Cuyahoga Valley National Park. Ohio Biological Survey Miscellaneous Contribution No. 8, 31 p.

Staton, S. K., A. Dextrase, J. L. Metcalfe-Smith, J. Di Maio, M. Nelson, J. Parish, B. Kilgour, and E. Holm. 2003. Status and trends of Ontario's Sydenham River ecosystem in relation to aquatic species at risk. Environmental Monitoring and Assessment, 88:283–310.

Strayer, D. L., S. Claypool, and S. J. Sprague. 1996. Assessing unionid populations with quadrats and timed searches, p. 163–169. *In* K. S. Cummings, A. C. Buchanan, and L. M. Koch (eds.), Conservation and management of freshwater mussels II: initiatives for the future. Proceedings of a UMRCC symposium, 16–18 October 1995, St. Louis, Missouri. Upper Mississippi River Conservation Committee, Rock Island, Illinois.

Tevesz, M. J. S., L. Rundo, R. A. Krebs, B. G. Redmond, and A. S. Dufresne. 2002. Changes in the freshwater mussel (Mollusca: Bivalvia) fauna of the Cuyahoga River, Ohio, since late prehistory. Kirtlandia, 53:13–18.

Vaughn, C. C., and C. C. Hakencamp. 2001. The functional role of burrowing bivalves in freshwater ecosystems. Freshwater Biology, 46:1431–1446.

Vaughn, C. C., K. B. Gido, and D. E. Spooner. 2004. Ecosystem processes performed by unionid mussels in stream mesocosms: species roles and effects of abundance. Hydrobiologia, 527:35–47.

Watters, G. T. 1995. A Guide to the Freshwater Mussels of Ohio, 3rd ed. Ohio Division of Wildlife, Department of Natural Resources, Columbus, Ohio. 122 p.

Watters, G. T., and J. Cramer. 2008. The Ohio State University Division of Molluscs. http://www.biosci.ohio-state.edu/~molluscs/OSUM2/.

Williams, J. D., M. L. Warren, Jr., K. S. Cummings, J. L. Harris, and R. J. Neves. 1993. Conservation status of freshwater mussels of the United States and Canada. Fisheries, 18:6–22.

Yoder, C. O., R. J. Miltner, and D. White. 1999. Assessing the status of aquatic life designated uses in urban and suburban watersheds. p. 16–28. *In* A. Everson, S. Minamyer, J. Dye, P. Heimbrock, and S. Wilson (eds.), Proceedings of the National Conference on Retrofit Opportunities for Water Resource Protection in Urban Environments, EPA/625/R-99/002.

KIRTLANDIA

The Scientific Publication of The Cleveland Museum of Natural History

Instructions For Authors

Authors are invited to submit manuscripts on topics that are within The Cleveland Museum of Natural History's sphere of interest. These include manuscripts on: archaeology, botany, cultural and physical anthropology, conservation, ecology, evolution, geology, paleontology, systematics, and zoology. Specimen-based research, especially that based on Cleveland Museum of Natural History specimens, is most welcome. All manuscripts and correspondence regarding manuscripts should be directed to Editor, *Kirtlandia,* at: The Cleveland Museum of Natural History, 1 Wade Oval Drive, Cleveland, Ohio 44106-1796, USA.

Submit three copies of the manuscript, double-spaced on 8.5 x 11.0 inch (21.5 x 28 cm), or similar sized, paper, with only one space after each period. Abstracts should be concise and convey the main points and conclusions of the paper. Main headings should be centered and bold. Headings, as well as citations in text and in the references, should follow the style used in the most recent issue of the journal. Long tables should be submitted as appendices.

Citations should be cited in text as follows: Krebs (1994) or (Krebs, 1994); Krebs et al. (2002) or (Krebs et al., 2002); Teraguchi and Lublin (1999) or (Teraguchi and Lublin, 1999). If specific details from a book or article are cited, or if material is quoted or paraphrased, provide page citations as in these examples: (Miller, 1989, p. 261), or Teraguchi and Lublin (1995, p. 4–5). References should be cited in the text in chronological order, e.g.: Krebs, 1994; Teraguchi and Lublin, 1999; Krebs et al., 2002.

Tables should be concise and convey information not repeated in text. Use tabs in the word processor to create tables. Do not use spread-sheets such as Excel or Access or databases to create tables. Figures are to be black and white, and high quality, meaning 600 dpi for grayscale images (photographs) and 600 dpi for bitmap lineart (maps, illustrations, etc). High quality TIF images submitted electronically can be used with approval by the editor. All figures are to be numbered sequentially and referenced in the text (e.g., Figure 1, Figure 2, etc.). Subfigures are indicated alphabetically, and labeled as A, B, C, etc. Figure legends should be written following the style below (example refers to a two-part figure):

Figure 1. Tubercled blossom, *Epioblasma torulosa torulosa* (Rafinesque, 1820), currently extirpated from Ohio; A, shell exterior; B, shell interior. Scale bar equals 1 cm.

Italicize genus and species names, and give species authority and year of description when species are first mentioned in the text. If a long table or appendix of taxa is presented, authorities and years may be excluded from the text but must be reported in the table. For papers dealing with systematics, give the original reference describing the taxa presented. Unless a large number of taxa are noted, list the works naming species in the references at the end of your manuscript.

Instructions on preparation of the final copy of the manuscript will be provided upon acceptance. Page charges and reprint charges will be determined by the editor. The final software for the final submission of a paper must be on a PC-compatible CD in a current version of MS-Word (MS Office).

References

Krebs, C. J. 1994. Ecology: The Experimental Analysis of Distribution and Abundance. Fourth Edition. Harper Collins, New York. 801 p.

Krebs, R. A., H. M. Griffith, and M. J. S. Tevesz. 2002. A study of the Unionidae of Tinkers Creek, Ohio. Kirtlandia, 53:9–25.

Miller, B. B. 1989. Screen-washing unconsolidated sediments for small macrofossils, p. 260–263. *In* R. M. Feldmann, R. E. Chapman, and J. T. Hannibal (eds.), Paleotechniques. Paleontological Society Special Publication, No. 4.

Teraguchi, S. E., and K. J. Lublin. 1999. Checklist of the moths of Pallister State Nature Preserve, Ashtabula County, Ohio (1988–1992) with analyses of abundance. Kirtlandia, 51:3–18.

Cleveland Museum of NATURAL HISTORY